

Appendix K The Performance – Flood Wall and Levee Performance Analysis

K1 Soil Data Report – 17th Street Canal

Introduction

This is an interim data report detailing the data collected by the Interagency Performance Evaluation Task Force (IPET) to support the analysis of the I-wall section that breached at the 17th Street canal as a result of Hurricane Katrina on August 29, 2005. The location of the 17th Street canal is shown in Figure K1-1. The site of the breach, located on the east bank near the north end of the canal, is also noted on Figure K1-1.

The data will be used in the Floodwall and Levee Performance Analysis task as part of its effort to determine how the flood protection structures performed in the face of the forces to which they were subjected by Hurricane Katrina, and to compare this performance with the design intent, the actual as-built condition, and observed performance. This effort includes understanding why certain structures failed catastrophically and why others did not. The effort will determine, in detail, how the levees and floodwalls performed during Hurricane Katrina. The studies being conducted under this effort involve compiling available information concerning the as-built conditions of the levees and floodwalls, and eye-witness accounts of their performance during the hurricane to establish the underlying set of facts; performing field investigations, including mapping and soil borings to determine post-failure conditions; performing laboratory tests to determine properties of soils and structural materials for use in analyses of performance; developing analytical models in the form of cross sections at areas where breaches occurred and areas where the levees and floodwalls were stable; and performing limit equilibrium and soil-structure interaction analyses to develop a full understanding of the performance of the levees and floodwalls and to provide guidance for future design analyses. These studies will be documented in a series of reports. The series of reports will start with data reports detailing the data collected on the site conditions at 17th Street canal, London Avenue canal, Orleans canal, and Inner Harbor Navigation canal, as noted on Figure K1-1.

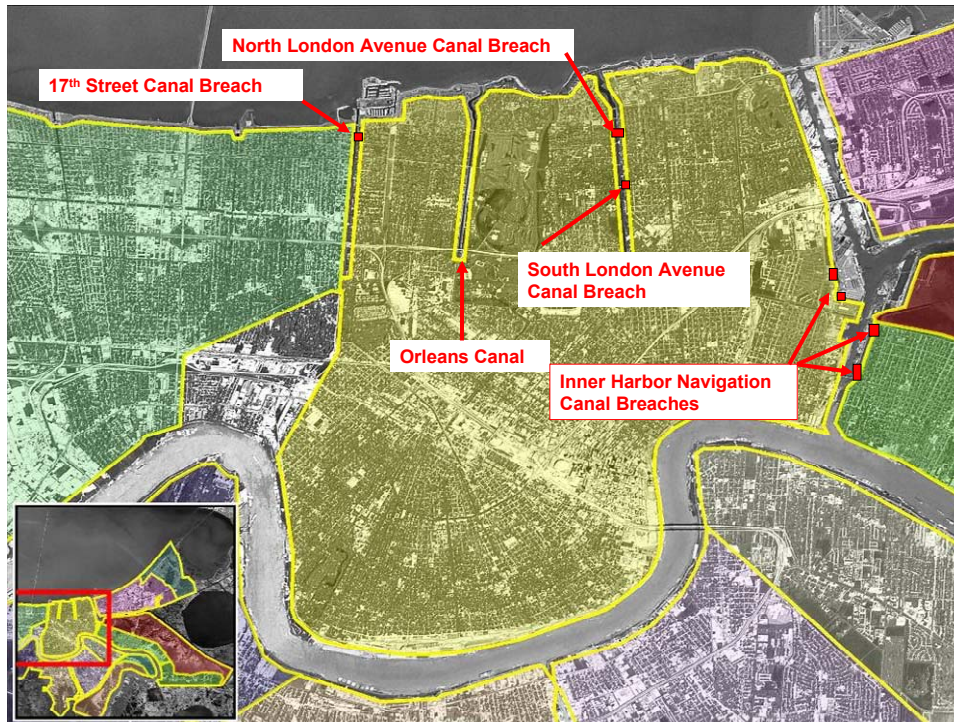


Figure K1-1. Location of Orleans Parish canals.

The key data obtained for the breach site and documented as part of this report include:

- a. Geology of the area.
- b. Description of soil stratigraphy.
- c. Representative pre-Katrina cross section through the breach area.
- d. Soil undrained shear strength profiles.

These data were obtained from a variety of sources, including the project's General Design Memorandum, design documents, and surveys prepared prior to Katrina. In addition, this report contains information obtained from field and laboratory investigations and surveys conducted after the Hurricane Katrina event. This report was prepared with the intent to provide numerical and physical modelers with the information needed to build their models.

Geology

Introduction

Before examining the individual failure areas at the 17th Street canal, a review of the geology is presented to familiarize the reader with the broader context of the geology of the delta plain, its stratigraphy, and the soils comprising the foundations at the different failure areas. For comparison purposes, the general geology of the 17th Street, Orleans, and London Avenue canals levee breaches is reviewed. The geology of the New Orleans area has been determined from detailed mapping studies of the Louisiana Coastal Plain (LCP), from a review of the published literature, from data collection activities at each of the failure sites by an IPET study team, and from an evaluation of preexisting and recently drilled engineering borings from each of the failure areas.

Previous Studies

A review of the past geologic literature from the New Orleans area identifies the US Army Corps of Engineers (USACE) as being actively involved with much of the regional and focused geologic studies that have been performed in the eastern LCP or deltaic plain (Dunbar and others, 1994 and 1995; Dunbar, Torrey, and Wakeley, 1999; Fisk, 1944; Kemp and Michel, 1967; Kolb, Smith, and Silva, 1975; Kolb, 1964; Kolb and Van Lopik, 1958a and 1958b; Kolb and Schultz, 1954; Kolb and Saucier, 1982; May and others, 1984; Michel, 1967; Saucier, 1963, 1984, and 1994; and Schultz and Kolb, 1950). Many of these studies and associated geologic maps are available from a USACE-sponsored website on the geology of the Lower Mississippi Valley that is accessible to the public at lmvmapping.erd.c.usace.army.mil.

Geologic History and Principal Physiographic Features of the New Orleans Area

To better understand the soils beneath the 17th Street, Orleans, and London Avenue canals, and the engineering properties of these soils, a brief summary of the geologic history of the New Orleans area is presented. Detailed descriptions of the geologic history are presented in Saucier (1964 and 1994); Kolb, Smith, and Silva (1975); Kolb and Saucier (1982); and Kolb and Van Lopik (1958).

The geology and stratigraphy of the New Orleans area are young in terms of its age. Generally, sediments comprising the New Orleans area are less than 7,000 years old. Formation of the present day New Orleans began with the rise in global sea level, beginning about 12,000 to 15,000 years before the present. The rise in sea level was caused by melting of continental glaciers in the Northern Hemisphere and the release of ice-bound water to the oceans. At the maximum extent of continental glaciation, eustatic sea level was approximately 300 ft (~100 m) lower than the present level. In addition, the ancestral coastal shoreline was much farther south of its current location, probably near the edge of the continental shelf.

The underlying Pleistocene surface throughout much of coastal Louisiana was subaerial, and exposed to oxidation, weathering, and erosion. These conditions led to the development of a well-developed drainage network across its surface, and created a distinct soil horizon in terms of its engineering properties. The Pleistocene horizon is easily recognizable in borings because of its distinct physical properties as compared to the overlying Holocene fill (i.e., oxidized color, stiffer consistency, higher shear strength, lower water content, and other physical properties.). The axis of the main valley or entrenchment of the Mississippi River was located west of New Orleans, in the vicinity of present day Morgan City, LA (Figure K1-2). Consequently, development of the early Holocene deltas was concentrated near the axis of Mississippi entrenchment when sea level rise began to stabilize sometime between 5,000 to 7,000 years before the present. New Orleans is located on the eastern edge of this buried entrenchment or alluvial valley.

The Pleistocene surface in the New Orleans area is variable, but generally ranges between 50 and 75 ft below sea level as determined from detailed mapping and examination of boring data (Kolb and Van Lopik 1958; Kolb, Smith, and Silva 1974; Saucier 1994; and Dunbar and others 1994 and 1995). Various sea level curves for the Louisiana coast are presented and discussed in Kolb, Smith, and Silva (1975) and Tornquist and Gonzalez (2002). These curves generally indicate that sea level transgression in the New Orleans area generally occurred between 6,000 to 9,000 years before the present, based on the mapped depths to the top of the Pleistocene surface.

As the rate of the sea level rise declined and stabilized, it led to the development of five, short-lived delta complexes across the Louisiana coast by deposition of Mississippi River sediments (Figure K1-2). Individual delta complexes are composed of numerous, branching distributary channels. These channels transport and deposit fluvial sediments along the margin of the delta and build land seaward into shallow coastal water. Distributary channels from the St. Bernard delta are responsible for filling the shallow Gulf waters in the greater New Orleans area (Frazier 1967).

Bayou Sauvage is a major distributary involved in the filling of the shallow Gulf waters in the New Orleans area (Figure K1-3). This channel extends eastward from the Mississippi River and is composed of Bayous Metairie, Gentilly (or Gentilly Ridge), and Sauvage. Natural levees of this distributary channel form a pronounced physiographic feature in the northern New Orleans area (Figure K1-3). Similarly, Mississippi River's natural levees are some of the highest land elevations found in New Orleans, and these were the first areas to be settled by the early inhabitants in the 1700s. Distributary channels in New Orleans are pronounced physiographic features, and are associated with the St. Bernard delta complex as determined from radiocarbon dating of organic sediments (Frazier, 1967; Kolb and Van Lopik 1958; McFarlan 1961; Britsch and Dunbar 1999; and Smith, Dunbar, and Britsch 1986).

Equally important to the development and filling history of the New Orleans area is the presence of a buried, barrier beach ridge which formed approximately 4,500 to 5,000 years before the present. This beach extends northeast in the subsurface along the southern shore of Lake Ponchartrain (Figure K1-4). Sea

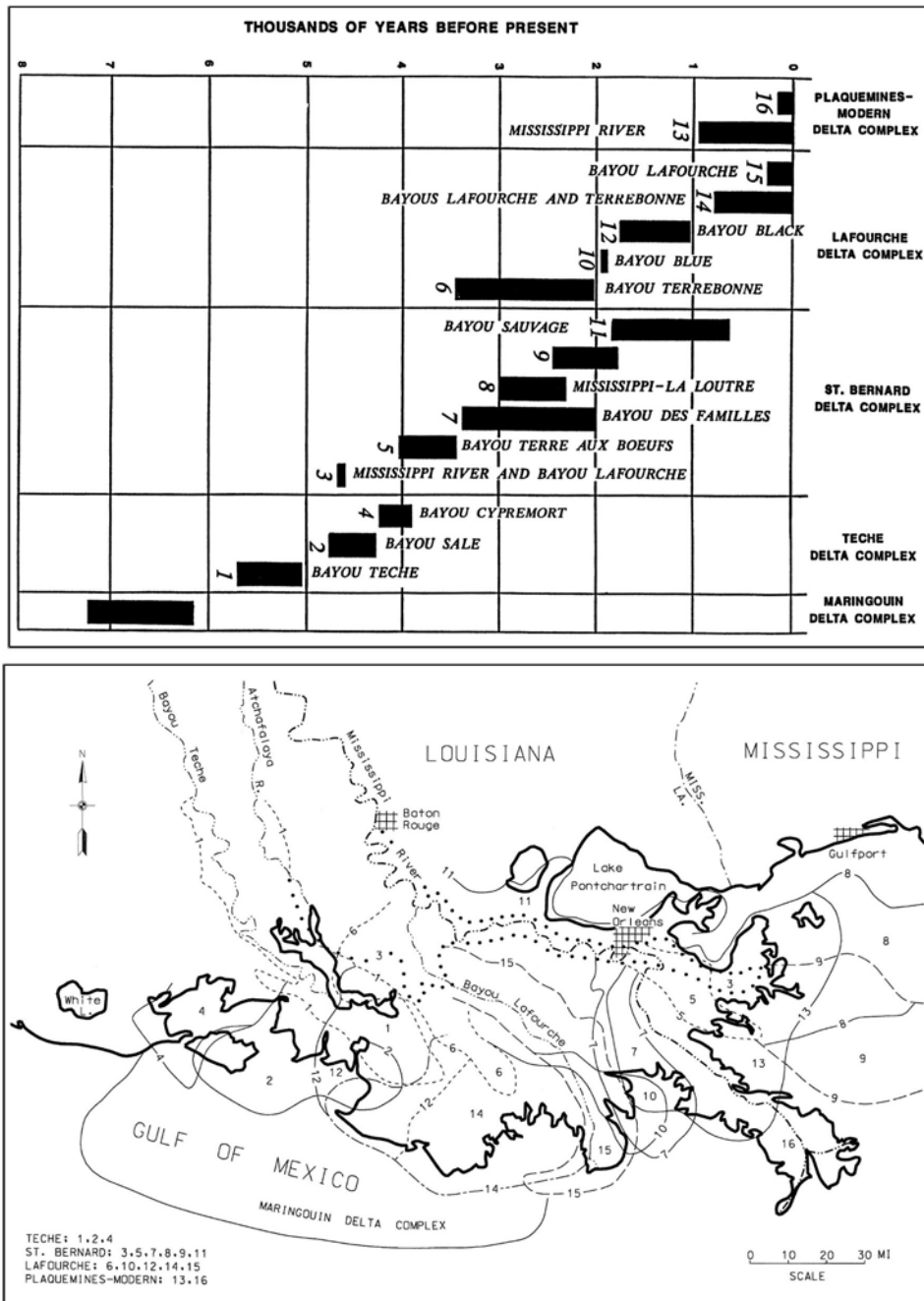


Figure K1-2. Location and approximate chronology of the Mississippi River Deltas, major distributary channels are numbered, note Bayou Sauvage (No. 11) which extends across the New Orleans area and forms the Bayou Metairie/Gentilly Ridge (after Frazier, 1967). Morgan City, LA, located along axis of maximum Mississippi River entrenchment.

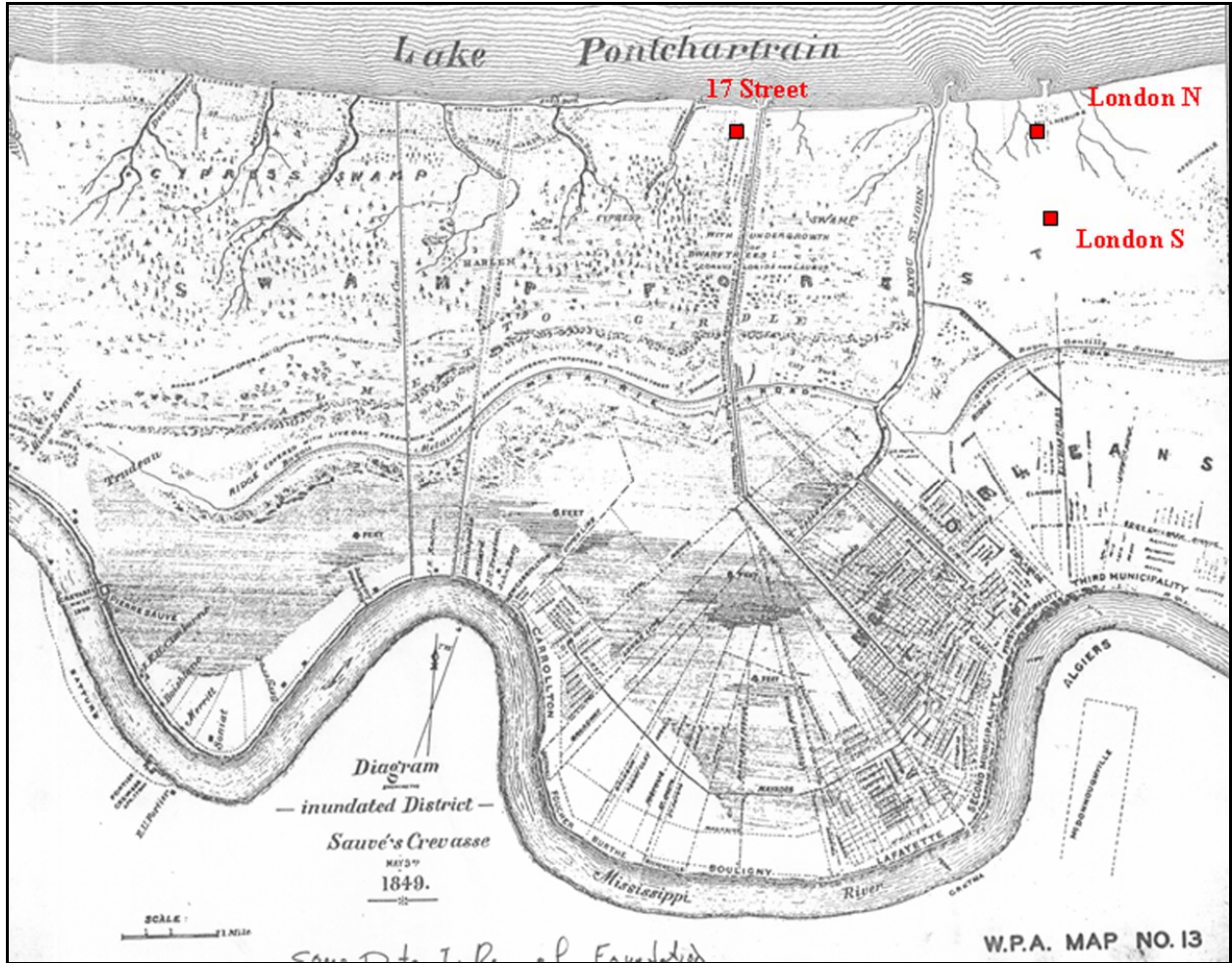


Figure K1-3. New Orleans area map from 1849 showing city limits and topography. Note the location of Bayous Metairie and Gentilly (i.e., Bayou Sauvage) and the identified cypress swamp north of the city at this time (Work Projects Administration 1943).

level was 10 to 15 ft lower than the current level when the beach ridge formed. A stable sea level permitted sandy sediments from the Pearl River to the east to be concentrated by longshore drift, and formed a sandy spit or barrier beach complex in the New Orleans area as shown by Figure K1-3 (Saucier 1994).

The presence of the barrier beach affected sedimentation patterns and the subsequent locations for advancing distributary channels in the New Orleans area. The beach complex likely prevented the Mississippi River and later St. Bernard distributaries from completely filling Lake Pontchartrain with sediment. Consequently, foundation soils beneath the 17th Street, Orleans, and London Avenue canal breaches are affected by their proximity to the buried beach complex. As shown by Figure K1-4, the breach at the 17th Street canal is located on the protected or land side of the beach ridge, while both of the London canal breaches are located over the thickest part or axis of this ridge complex. The beach ridge cuts across the Orleans canal with the north portion on the landside and south portion over the axis of this ridge complex.

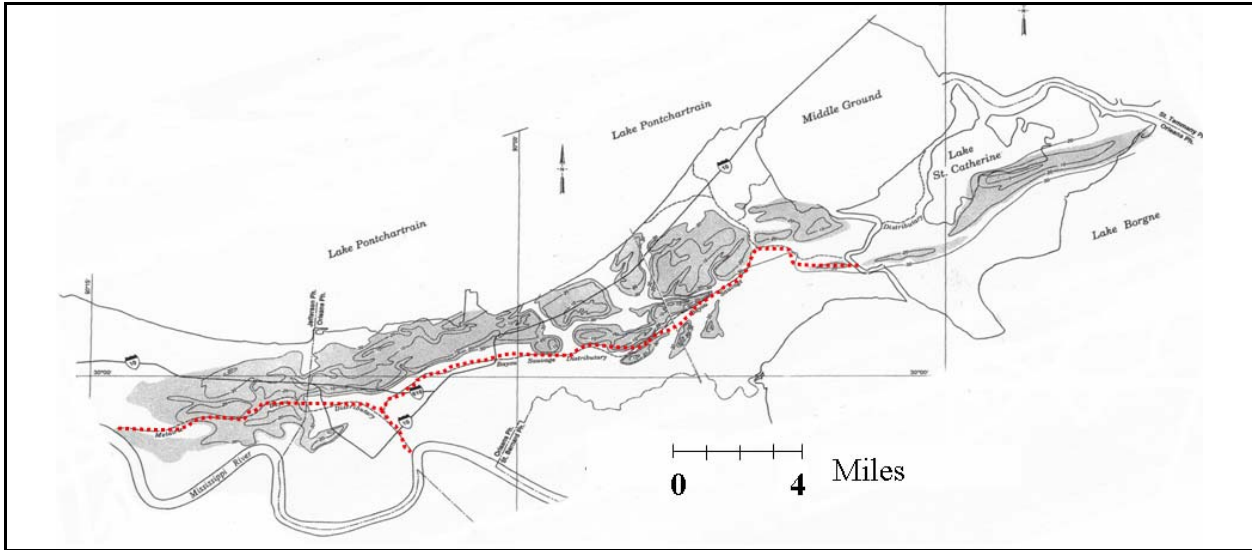


Figure K1-4a. Pine Island buried beach complex in the New Orleans Area (from Saucier 1994). Course of Bayou Sauvage (i.e., Bayous Metairie and Gentilly) identified in red. Note the presence of the barrier beach prevented this distributary course from extending northward into present day Lake Ponchartrain and filling the lake. Canal breaches are identified in blue with 17th Street breach behind the thickest part of the beach ridge, while both the London North and South breaches are on the axis of the barrier. See Figure K1-3b for close-up of canal areas.

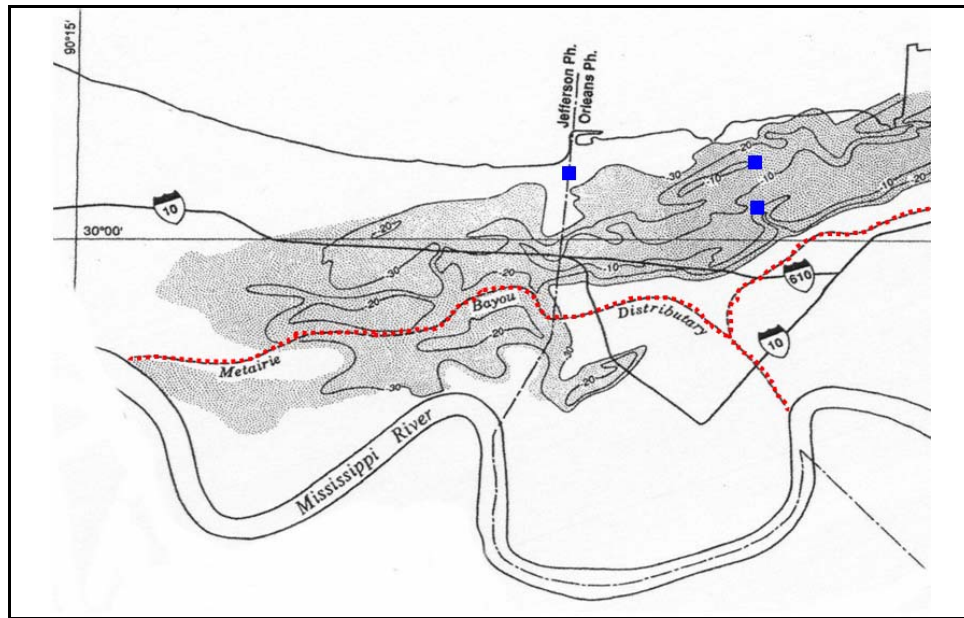


Figure K1-4b. Close-up view of the buried beach ridge, and the locations of the canal breaches to the buried beach (after Saucier 1994). The 17th Street breach is located behind the axis of the beach ridge while the London Canal breaches are located on the axis of the ridge. Bayou Metairie is identified in red and forms the Bayou Sauvage distributary course (No. 11) in Figure K1-2

Surface and Subsurface Geology of the New Orleans Area

A geologic map of the New Orleans area is presented in Figure K1-5 and identifies the major environments of deposition at the surface in the vicinity of the 17th Street, Orleans, and London Avenue canals. Located on the surface of the New Orleans area are natural levee and point bar deposits adjacent to the Mississippi River, abandoned distributary courses (Bayou Sauvage-Metairie north of the Mississippi River and Bayou des Familles south of the Mississippi River, respectively), and extensive marsh-swamp deposits at the surface (see also Figure K1-3). Land reclamation occurred in the 1920's along the shore of Lake Ponchartrain by dredging, and this area is identified as spoil deposits.

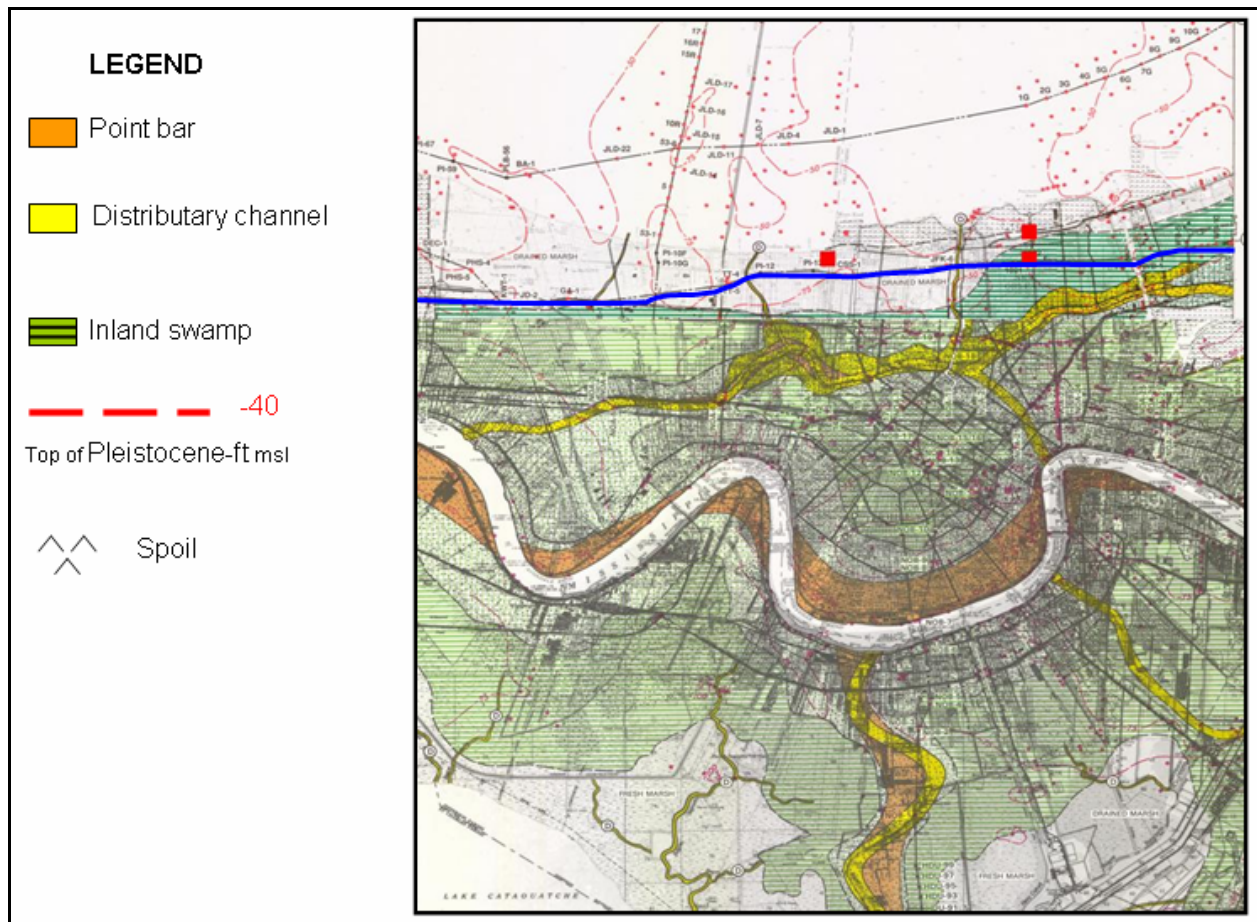


Figure K1-5. Geology map of the New Orleans and Spanish Fort Quadrangles showing the distribution of environments at surface. Elevation of the Pleistocene surface shown in red along with borings used to map this surface. Cross-section C-C' in blue extends through 17th Street and London Canal Areas (areas identified in red). See website lmvmapping.erd.c.usace.army.mil for nearby maps and other cross-sections identified. Portion of cross-section C-C' above is presented as Figure K1-6 (from Dunbar and others 1994 and 1995)

A portion of cross-section C-C from the Spanish Fort Quadrangle is presented as Figure K1-6 to identify the general subsurface stratigraphy beneath the 17th Street and London canal breaches. Boring data from this section

identify distinct depositional environments in the subsurface that are stacked vertically and form a stratigraphic record of the filling history during the Holocene period. Major stratigraphic units in the subsurface, beginning with the oldest, include the Pleistocene (older fluvial and deltaic deposits), bay sound/estuarine, relic beach (Pine Island Beach ridge) lacustrine/interdistributary, and marsh/swamp deposits. A summary description of the different depositional environments in the New Orleans area is presented in Appendix A (from Dunbar, Torrey, and Wakeley, 1999). Additionally, detailed descriptions of the different depositional environments are contained in Saucier (1994), Kolb (1962), and Kolb and Van Lopik (1958).

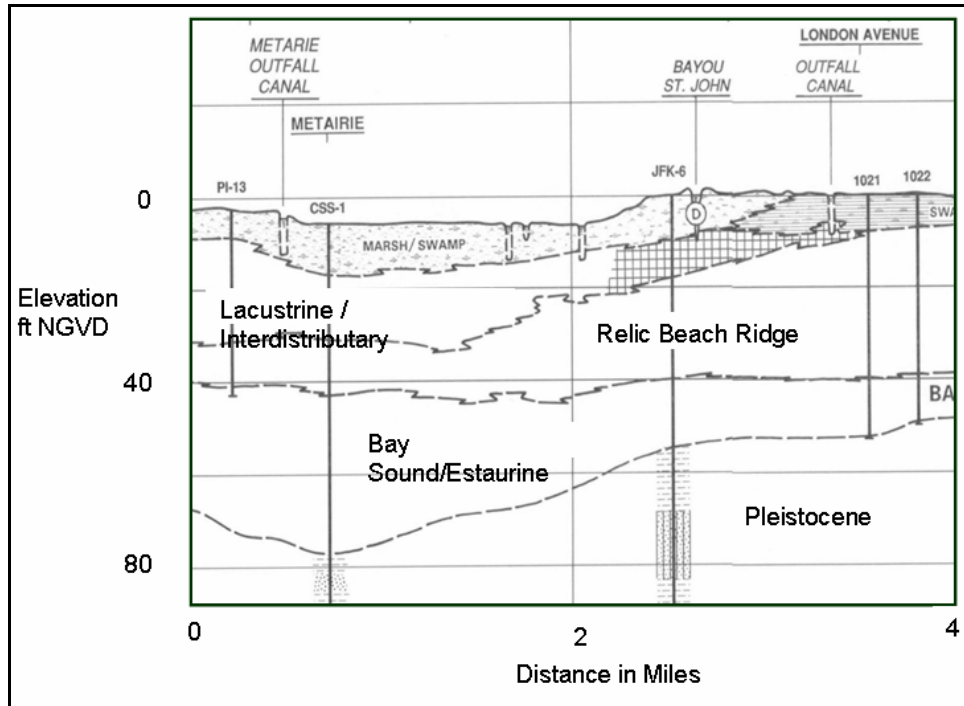


Figure K1-6. Portion of cross section C-C” from the Spanish Fort Quadrangle which extends through the 17th and London Canal breaches and identifies the stratigraphic environments in the subsurface (from Dunbar and others 1995)

Besides mapping the horizontal and vertical limits of the various environments of deposition, relationships between these environments and key engineering properties of the respective soils have been developed. These relationships have been tabulated and are published in Kolb (1962), Montgomery (1974), and Saucier (1994). A summary of these engineering relationships is presented in Appendix A. Similarly, relationships have been developed from the engineering properties and laboratory soil test data from 17th Street, Orleans, and London Avenue canals. These data are presented in later sections of this summary as related to discussions of their engineering significance.

Geologic information from the New Orleans area helped the IPET focus its investigation and collection of data for the 17th Street, Orleans, and London Avenue canal breaches. An understanding of the geology was an important first

step to systematically collecting and evaluating stratigraphic and engineering data from these breach areas.

Development of Cross Sections

Pre-Katrina Sections

A significant amount of information was obtained from General Design Memorandum No. 20 – 17th Street Outfall Canal – Volume 1 (GDM No. 20) in the development of pre-Katrina cross sections. This document was completed in March 1990 in preparation for upgrading the New Orleans levee system to provide increased flood protection against a stronger revised design hurricane.

Figures K1-7 and K1-8 show longitudinal profiles of the east and west bank levees of the northern half of the 17th Street Outfall canal, respectively. These figures, obtained from GDM No. 20, show boring locations and the soil types obtained during the explorations for the project upgrade. It is noted that odd numbered borings are located on the west bank, and even numbered borings are located on the east bank. Noted on the figures is the location of the breach site which is situated on the east bank of the canal between Stations 560+50 and 564+50.

A more detailed representation of the soil stratigraphy profile along the centerline in the breach area is shown in Figure K1-9. This profile was constructed using additional soil data acquired during the post-Katrina soil exploration conducted during September through October 2006. The additional borings included B1, B2, B3, B4, B5, NO-1-05U, and NO-2-05U. A plan view showing the locations of both old and new borings is shown in Figure K1-10. The new borings were needed because only the two old borings, B62 and B64 (reported in GDM No. 20), were in the immediate vicinity of the breach. The new borings extended the depth of the investigation in this area from approximately Elevation -50 ft NGVD to Elevation -115 ft NGVD. Additionally, data from cone penetration testing, from the new exploration program, were used to supplement soil data from the old and new borings and refine the stratigraphy in the breach area. Since the levee was destroyed in the breach area during the storm, the new borings, B1 through B4, were drilled from a barge in the canal and were offset from the centerline. Data acquired from these borings were projected back to the centerline in an effort to improve the interpretation of the stratigraphy.

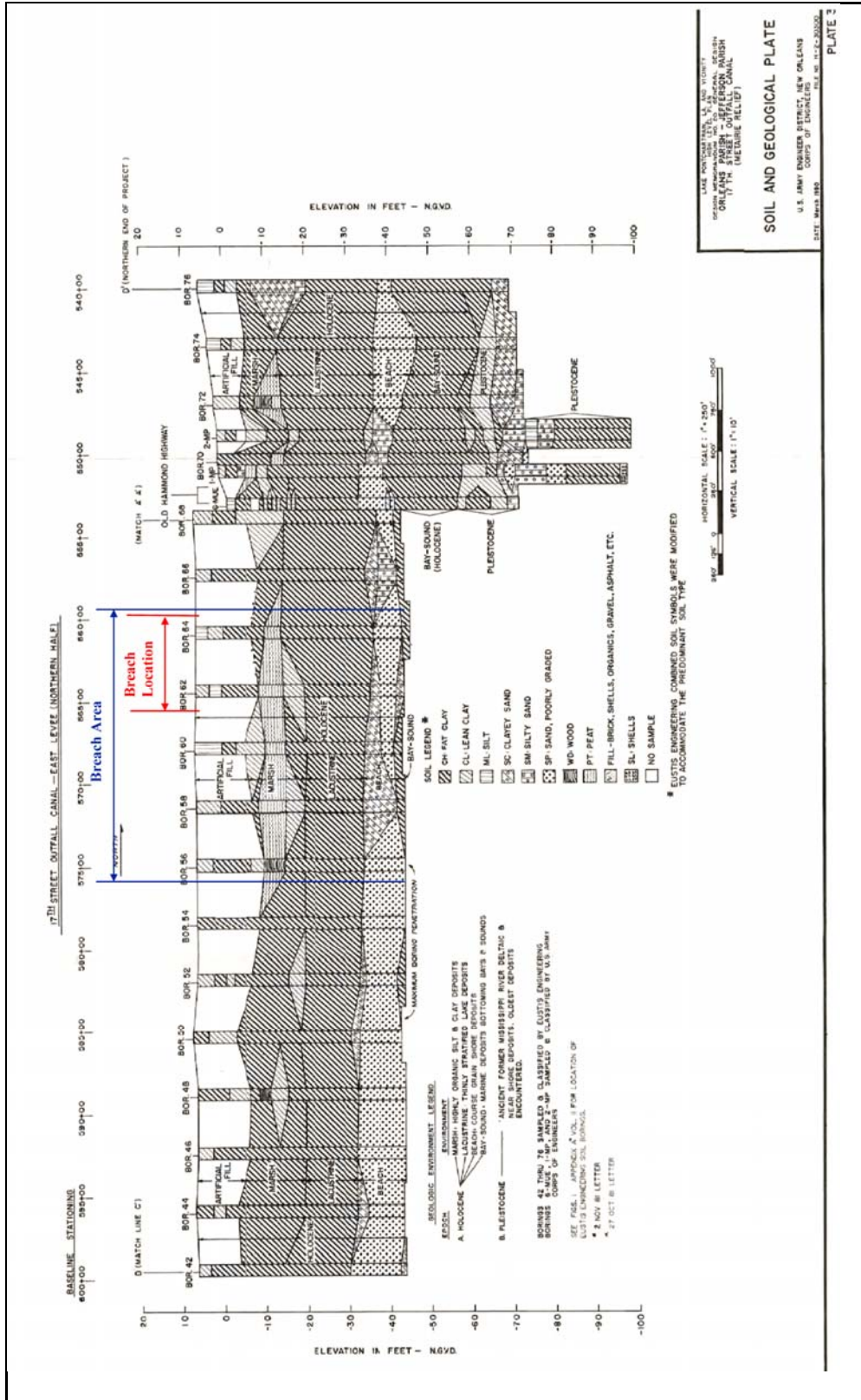


Figure K1-7. Geological Profile showing Breach Area (East Levee)

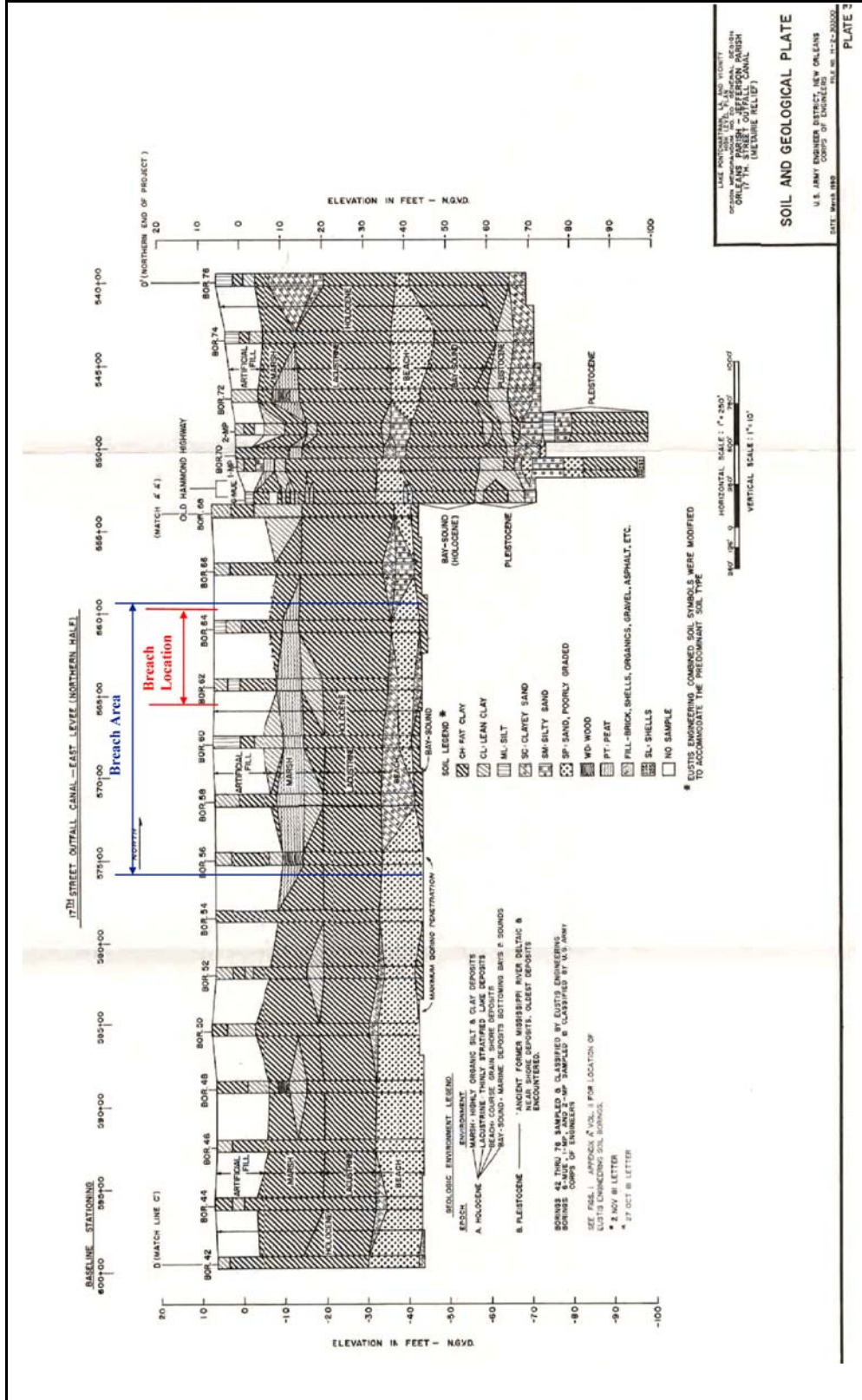


Figure K1-8. Geological Profile showing Breach Area (West Levee)



Figure K1-10. Boring and CPT Location Map

The information presented on Figure K1-9 yielded the following interpretation of the subsurface stratigraphy in the breach area. The subsurface in the breach area was simplified into six basic groups of soil types over the depth of the investigation:

| Layer | Approximate Elevation of Top of Layer, ft (NGVD) | Approximate Elevation of Bottom of Layer (NGVD) | Soil Type | Consistency |
|--|---|--|-------------------------------------|--------------------|
| Embankment | 6.5 | -10 | Clayey (CL's and CH) | Stiff |
| Marsh | -10 | -15 | Organic/Peat | Very Soft |
| Lacustrine | -15 | -35 | Clays (CH) | Very Soft |
| Beach Sand | -35 | -45 | Sand | |
| Bay Sound/Estuarine | -45 | -75 | Clayey (CH) | Stiff to V. Stiff |
| Pleistocene (Undifferentiated) Prairie Formation | -75 | | Clays – Generally CH with some sand | Stiff |

An additional word about the Marsh deposit may be useful. The marsh is represented as an organic soil and a peat-type material. Examination of the drilling logs suggests that since wood was encountered at the top part of the layer, this layer may be more fibrous near the top and more amorphous at the bottom of the layer. Further investigation of the peat layer may be necessary to better quantify the differences between the top and bottom of the layer.

Transverse Cross Sections through the Breach Site

Three representative transverse cross sections through the levee breach site were prepared from the data at hand. These three sections were developed from Station 8+30, Station 10+00, and Station 11+50. Station 8+30 is the most northerly station of the three. These cross sections were prepared with the intent that they represent the conditions that existed *immediately before* the arrival of Katrina. Data from a pre-Katrina airborne LIDAR (Light Detection and Ranging) survey on the New Orleans Levee System that was conducted during the year 2000 were used to improve the surface topography in the breach area from that presented in the GDM No. 20 and the design documents. The LIDAR data is the best data available for establishing the cross sections before Katrina, because accurate ground survey data were not available during the preparation of this report. The surveys generate points of X, Y, and Z data that are accurate to the nearest foot. A typical LIDAR section is shown in Figure K1-10. The LIDAR surveys were particularly useful in establishing the levee dimensions, slope, and toe elevations on the protected side of the floodwall. Unfortunately, the LIDAR system cannot penetrate through water, so it was not possible to use this technology to acquire the ground topography in the canal. A hydrographic survey was obtained *immediately after* Katrina, on August 31, 2006, to obtain the surface elevations of the canal between the floodwalls on the east and west banks. The data obtained from the hydrographic surveys are reflected in the cross-sections described in the next paragraph.

The three representative cross sections for Station 8+30, Station 10+00, and Station 11+50 are shown in Figures K1-11, K1-12, and K1-13, respectively. Three sections were prepared because the levee dimensions are variable in the

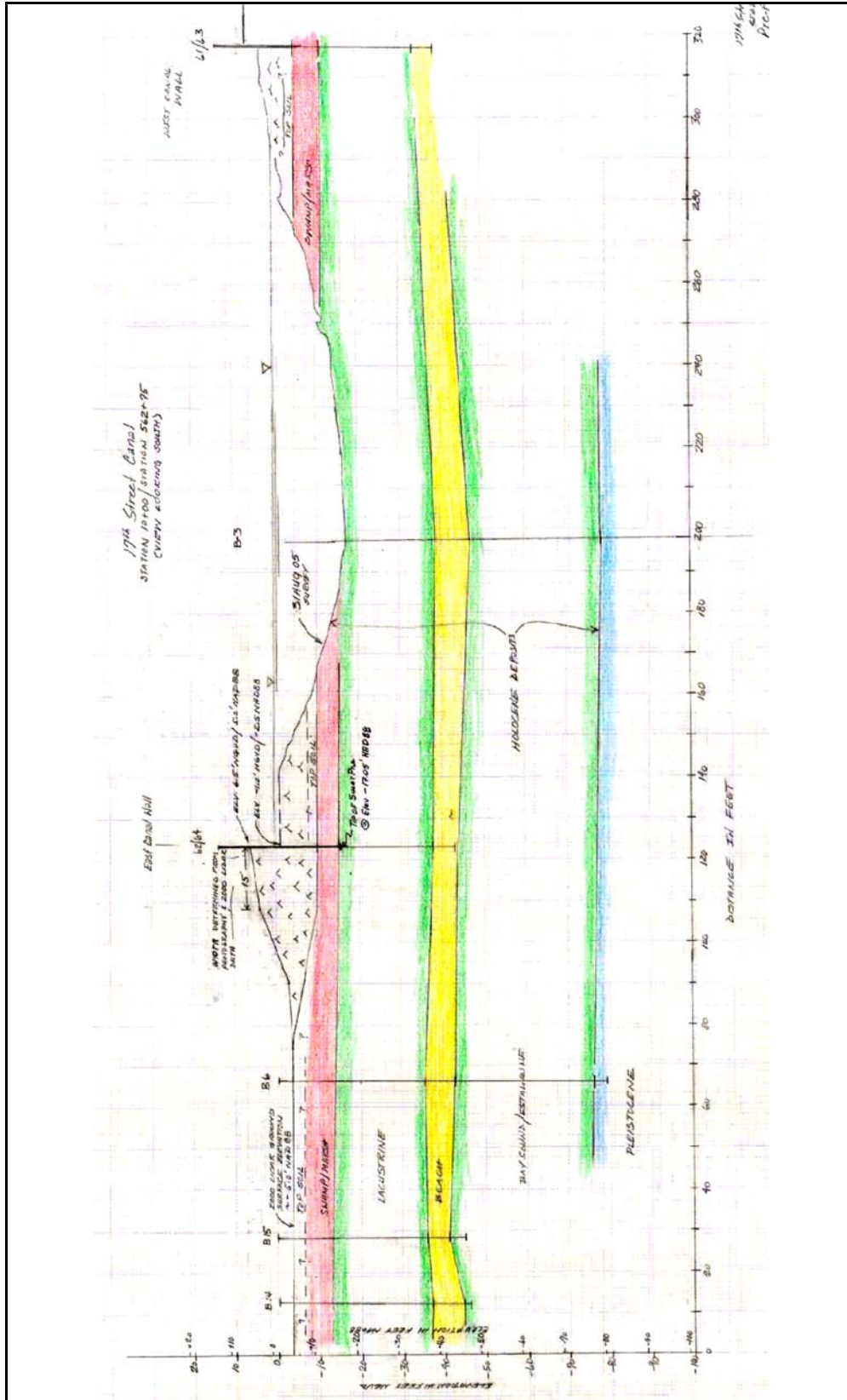


Figure K1-12. Prefailure Cross-Section at Sta 10+00 (New Stationing)/ Sta. 562+75 (GDM Stationing)

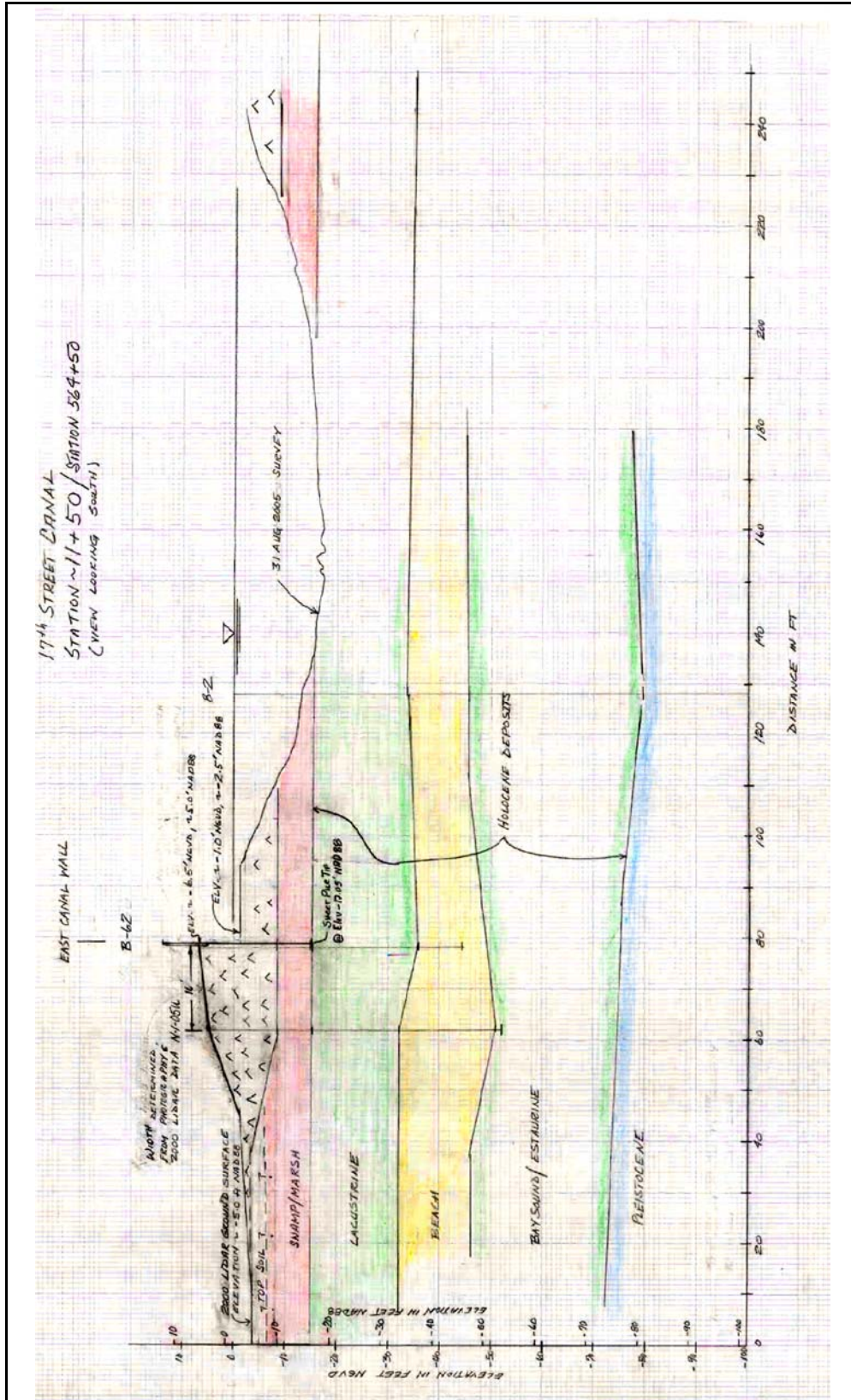


Figure K1-13. Prefailure Cross-Section at Sta. 11+50 (New Stationing) / Sta. 564+50 (GDM Stationing) (Note: Most scour occurred near this station)

breach area on the east bank. Each cross section shows the conditions across the entire canal from the west bank to the east bank where the breach site is located. A degree of interpretation was necessary, particularly pertaining to the east bank protected side, to complete the cross sections because of the lack of soil boring data in this area. Thus, the marsh/peat layer was interpreted to be thinner under the centerline of the levee than at the toe due to consolidation from the surcharge caused by the weight of the levee. Also, an interpretation was made to include a 2- to 3-ft layer of topsoil over the top of the peat in this area. This effect may be cultural in nature because the protected side of the east bank was located in a residential area with houses having well-kept lawns.

It is also noted that the levee cross section at Station 11+50, the southernmost section of the three and shown in Figure K1-13, is the location where the post-Katrina surveys showed that the most scour occurred while water was flowing through the breach.

Uncertainties

Many uncertainties pertaining to the subsurface in the breach area will be difficult, if not impossible, to resolve because the levee in this area was destroyed and drastically changed due to emergency relief efforts. There was a lack of subsurface information on the protected side of the levee during the 1990 levee raising project described in GDM No. 20. There are efforts planned by the IPET to obtain more information in the vicinity immediately north and south of the breach area to better define soil strengths and thickness of the top soil and peat layers.

Soil Properties

Introduction

The following is a summary of the current soil data available in the breach area of the 17th Street canal. The soil's data for the breach include all borings and cone penetrometer tests (CPT) in the breach area. This area was chosen because the geology and soil types are very similar to the soil types and geology found at the breach area. The breach area and breach location are shown in Figure K1-7. In addition, some soil data from the west levee will be used for the breach area because of similar geology and soil types. This area is shown in Figure K1-8.

The stratigraphy in the breach area is divided into Levee Embankment, Marsh Stratum, Lacustrine Stratum, and Beach Sand Stratum. The data for each stratum are presented below. These data consist of GDM borings, new borings (taken in 2005), and CPTs. Testing is not complete on all of the samples from new borings. In addition, field vane shear tests and CPTs are scheduled to occur in the next couple of weeks, which will provide more data in the breach area.

Levee Embankment

Data on the levee embankment consist of five borings shown in the 1990 General Design Memorandum (GDM) and four cone penetrometer tests (CPT). Of the five GDM borings, four borings collected 3-in. (diameter) undisturbed samples, and one boring collected 5-in. (diameter) undisturbed samples. From the 3-in. samples, four unconfined compression (UC) tests were performed, and five one-point unconsolidated-undrained triaxial compression tests (UU-1), confined at existing overburden pressure, were performed. From the 5-in. samples, four one-point unconsolidated-undrained triaxial compression tests (UU-1), confined at existing overburden pressure, were performed. From these laboratory tests, moisture content and wet unit weights were determined. The moisture contents (%w) in the breach area are shown in Figure K1-14. In addition, these moisture content data were also plotted (Figure K1-15) with the moisture content data collected for the entire east levee on the canal. Also, the moisture content data for the entire west levee on the canal are shown in Figure K1-16.

The wet unit weight data in the breach area are shown in Figure K1-17. Wet unit weight data from the breach area plotted with wet unit weight data for the entire east levee are shown in Figure K1-18. Wet unit weight for the entire west levee on the canal is shown in Figure K1-19.

The undrained shear strength determined from the laboratory tests conducted on samples in the breach area is shown in Figure K1-20. Interpretation of the undrained shear strength from the CPTs using Mayne's method is plotted with laboratory test results in Figure K1-21. Interpretation of the undrained shear strength from the CPTs using the bearing capacity equation ($N_k=15$) is plotted with laboratory test results in Figure K1-22. These interpretations were provided by Dr. Thomas Brandon (Virginia Tech). Undrained shear strength data in the breach area plotted with undrained shear strength data for the entire east levee are shown in Figure K1-23. Undrained shear strength data for the entire west levee are shown in Figure K1-24.

Marsh Stratum

The data for the marsh stratum will be divided into two groups: Data on the marsh stratum under the levee embankment, and data on the marsh stratum at the toe of the levee.

Under the Levee Embankment

Data on the marsh stratum under the levee embankment consist of five borings shown in the 1990 General Design Memorandum (GDM) and four cone penetrometer tests (CPT) taken on the east levee. Of the five GDM borings, four borings collected 3-in. (diameter) undisturbed samples and one boring collected 5-in (diameter) undisturbed samples. From the 3-in. samples, five unconfined compression (UC) tests were performed. From the 5-in. samples, no shear strength data were available. From these laboratory tests, moisture content and wet unit weights were determined. The moisture contents (%w) in the breach

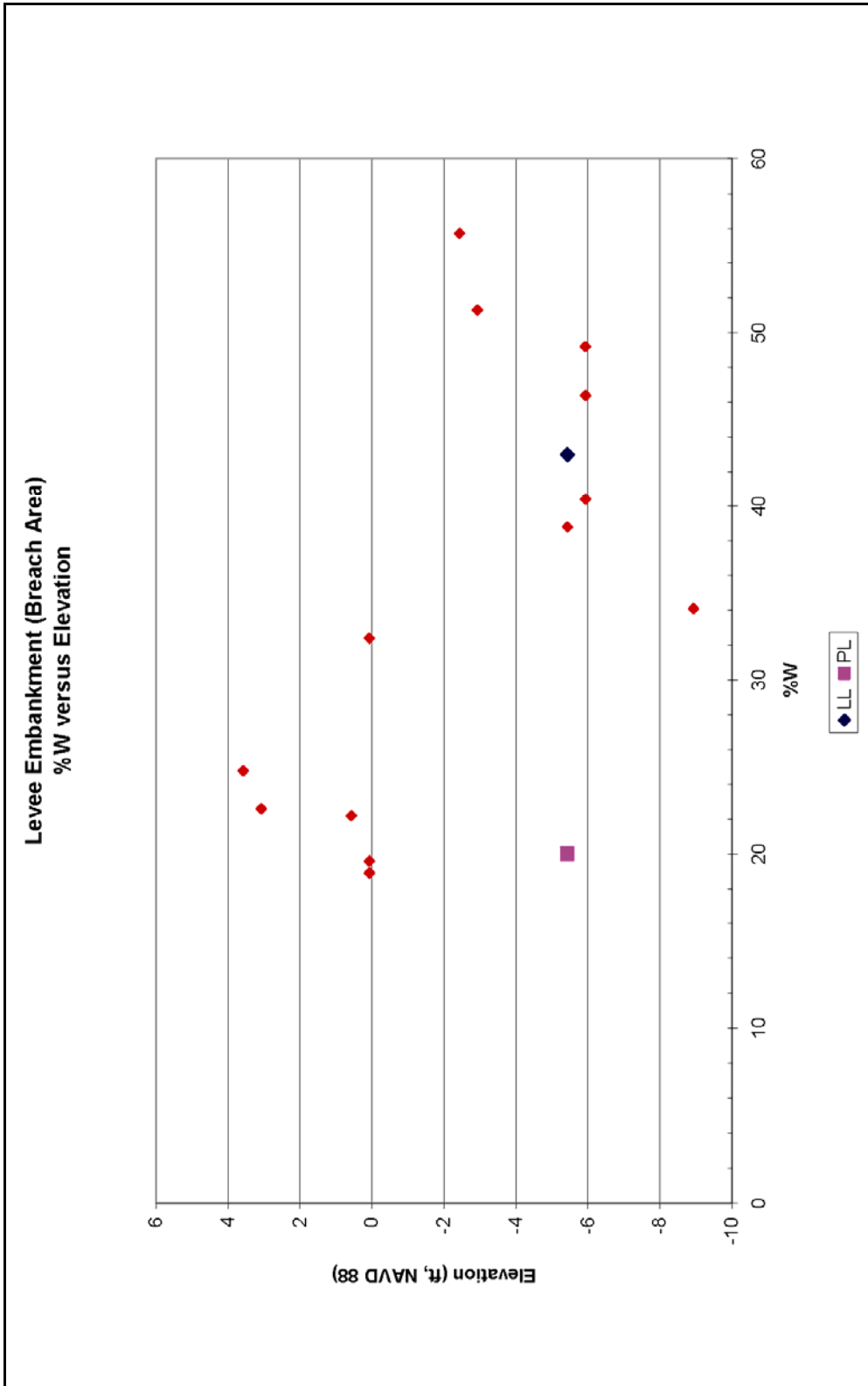


Figure K1-14. Levee Embankment (Breach Area), %w versus Elevation

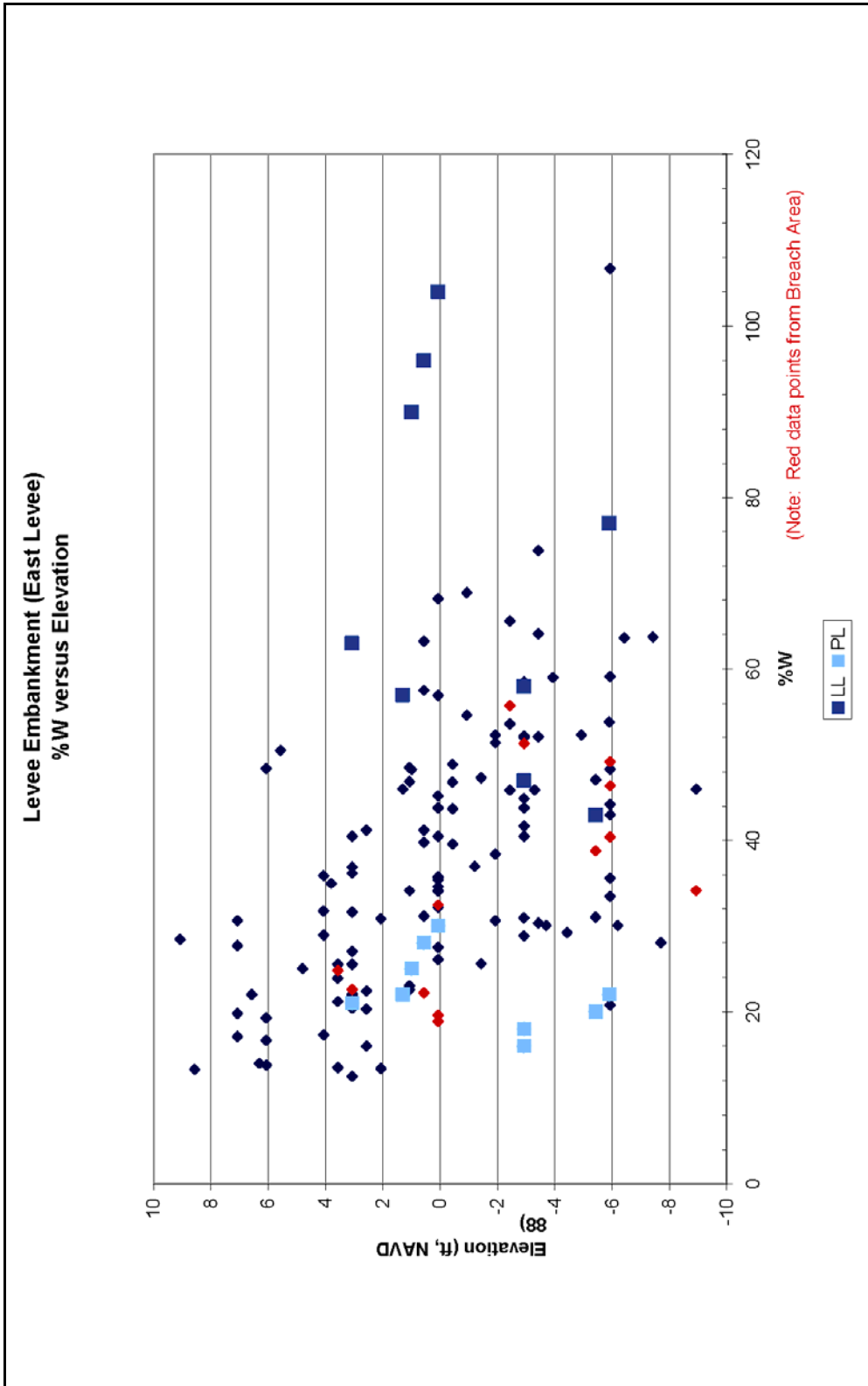
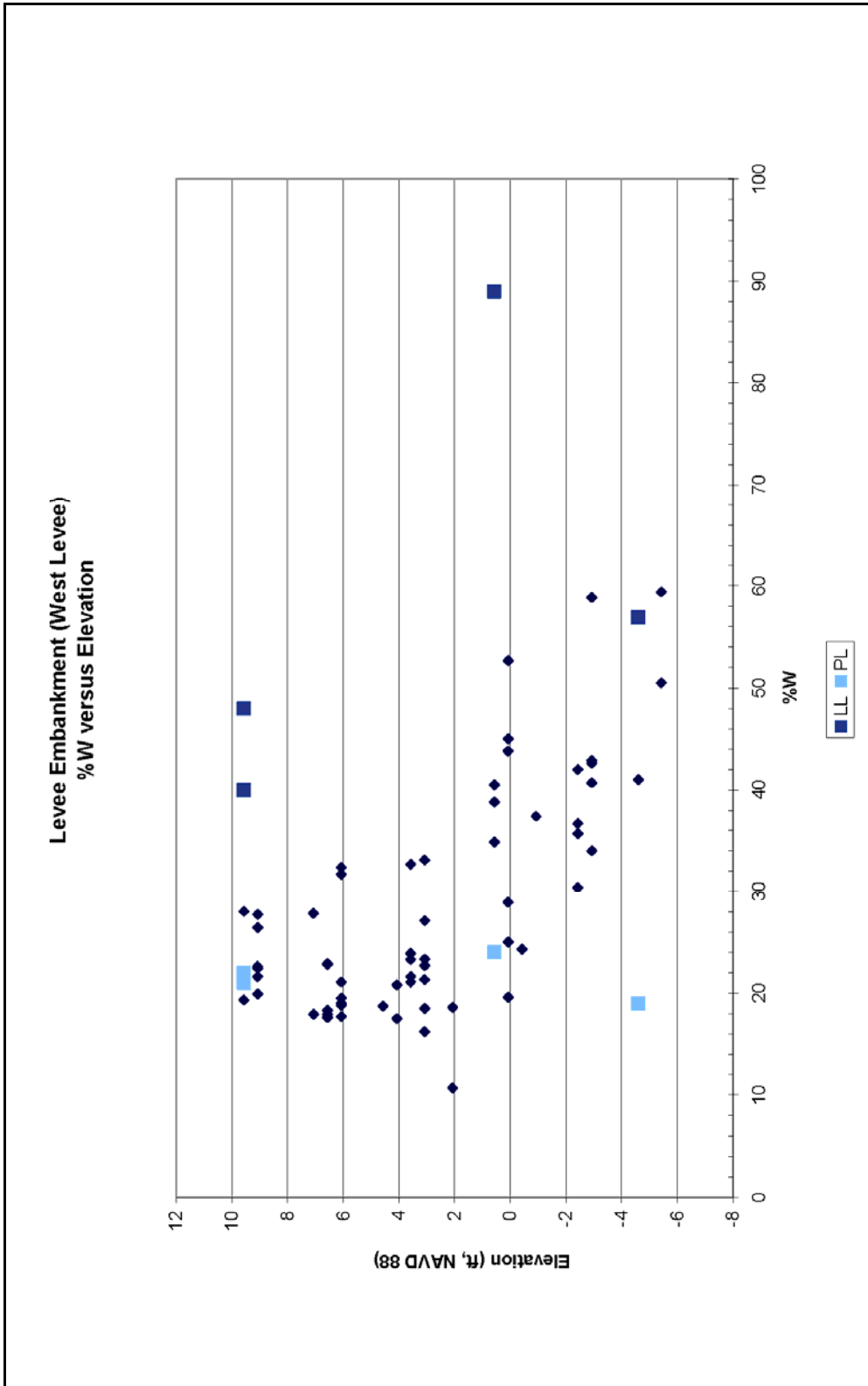


Figure K1-15. Levee Embankment (East Levee), %w versus Elevation



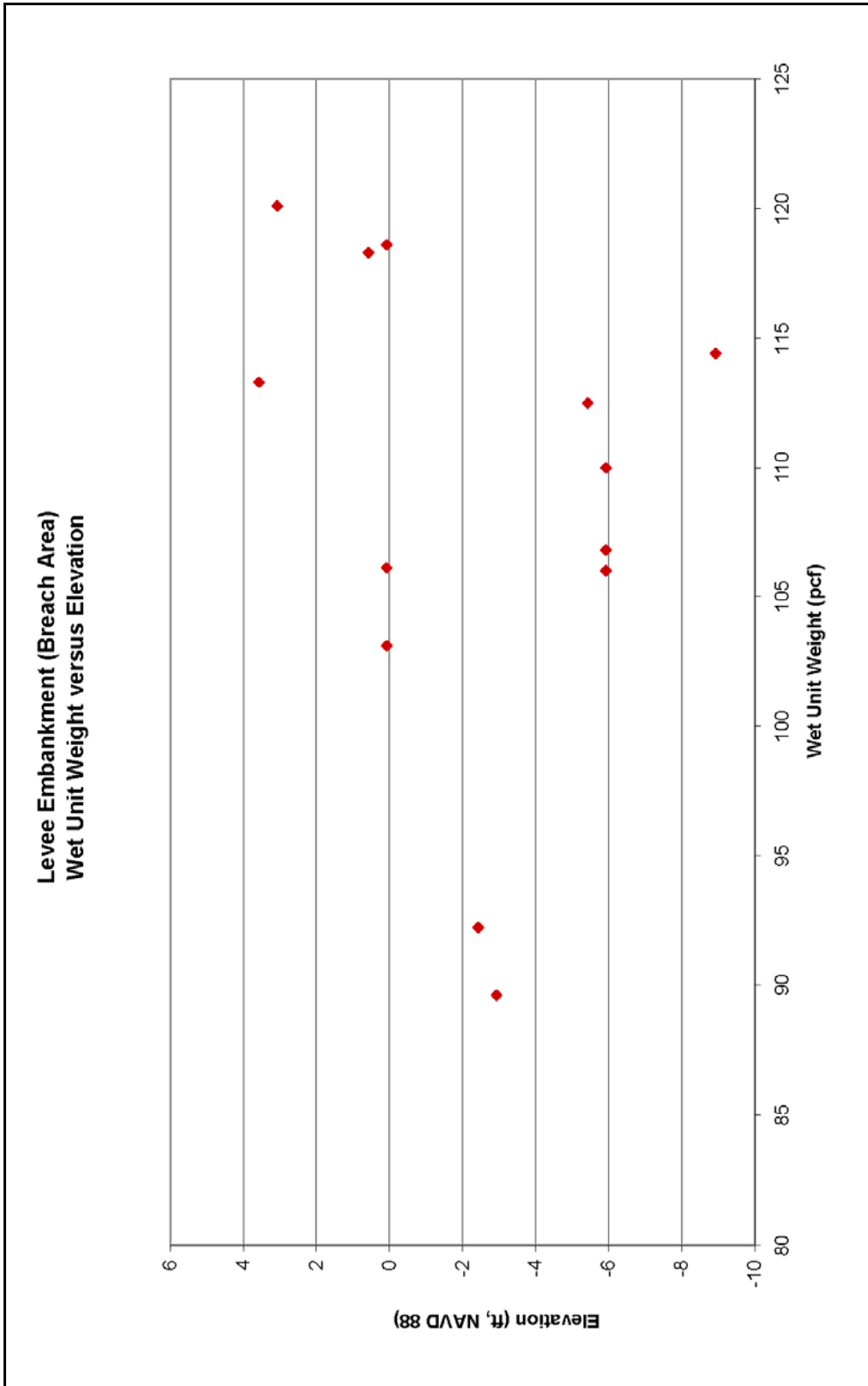


Figure K1-17. Levee Embankment (Breach Area), Wet Unit Weight versus Elevation

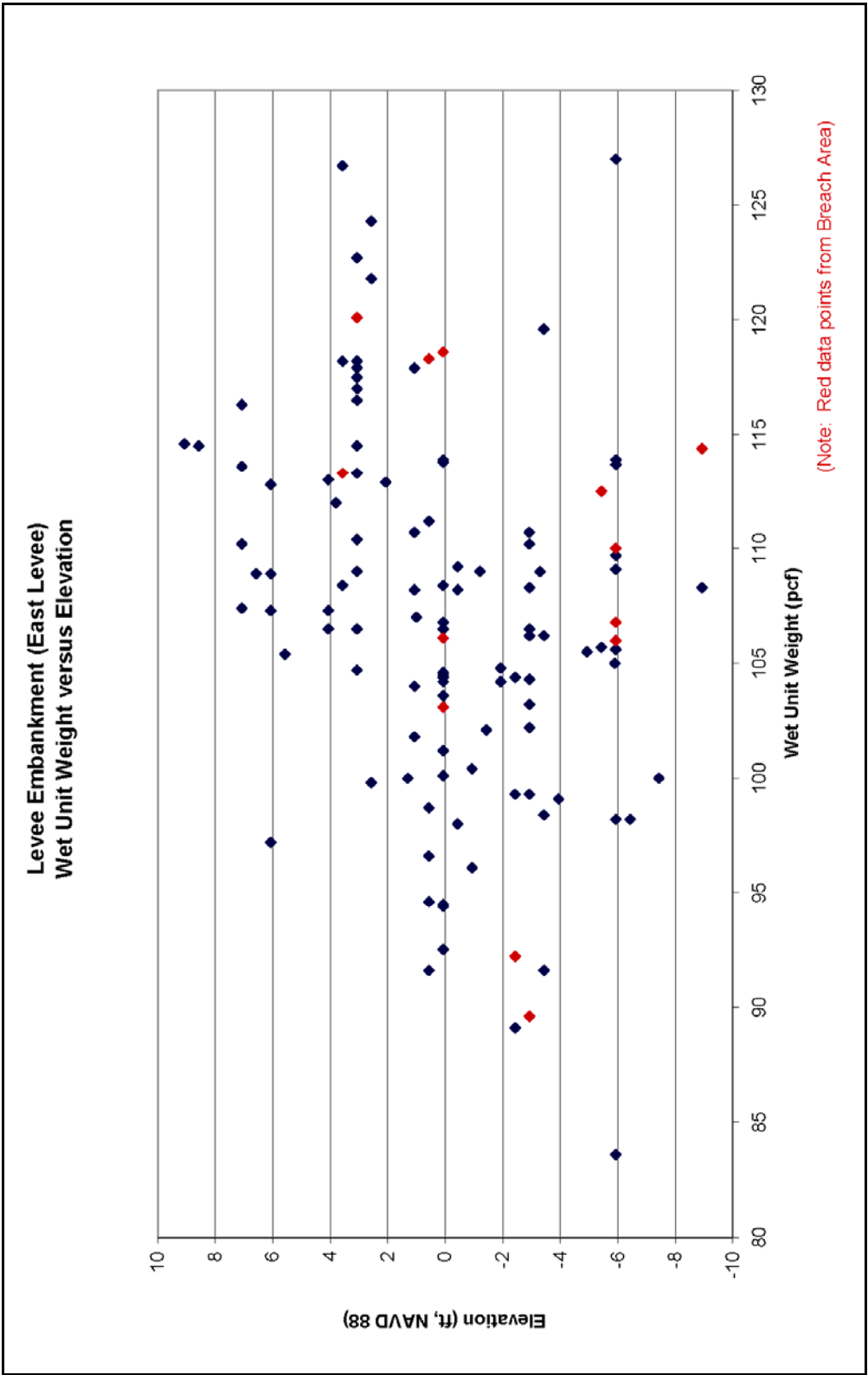


Figure K1-18. Levee Embankment (East Levee), Wet Unit Weight versus Elevation

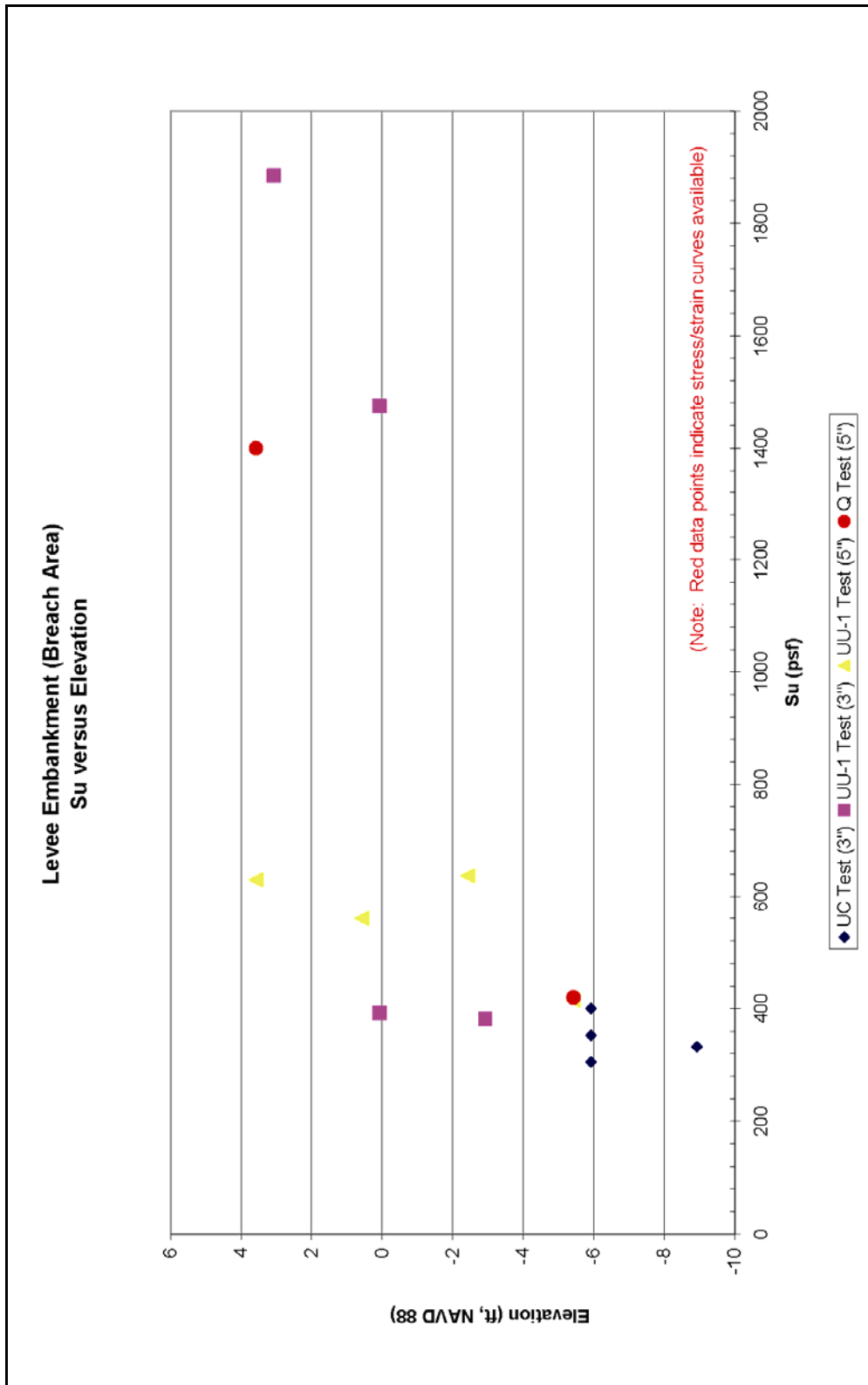


Figure K1-20. Levee Embankment (Breach Area), Su versus Elevation

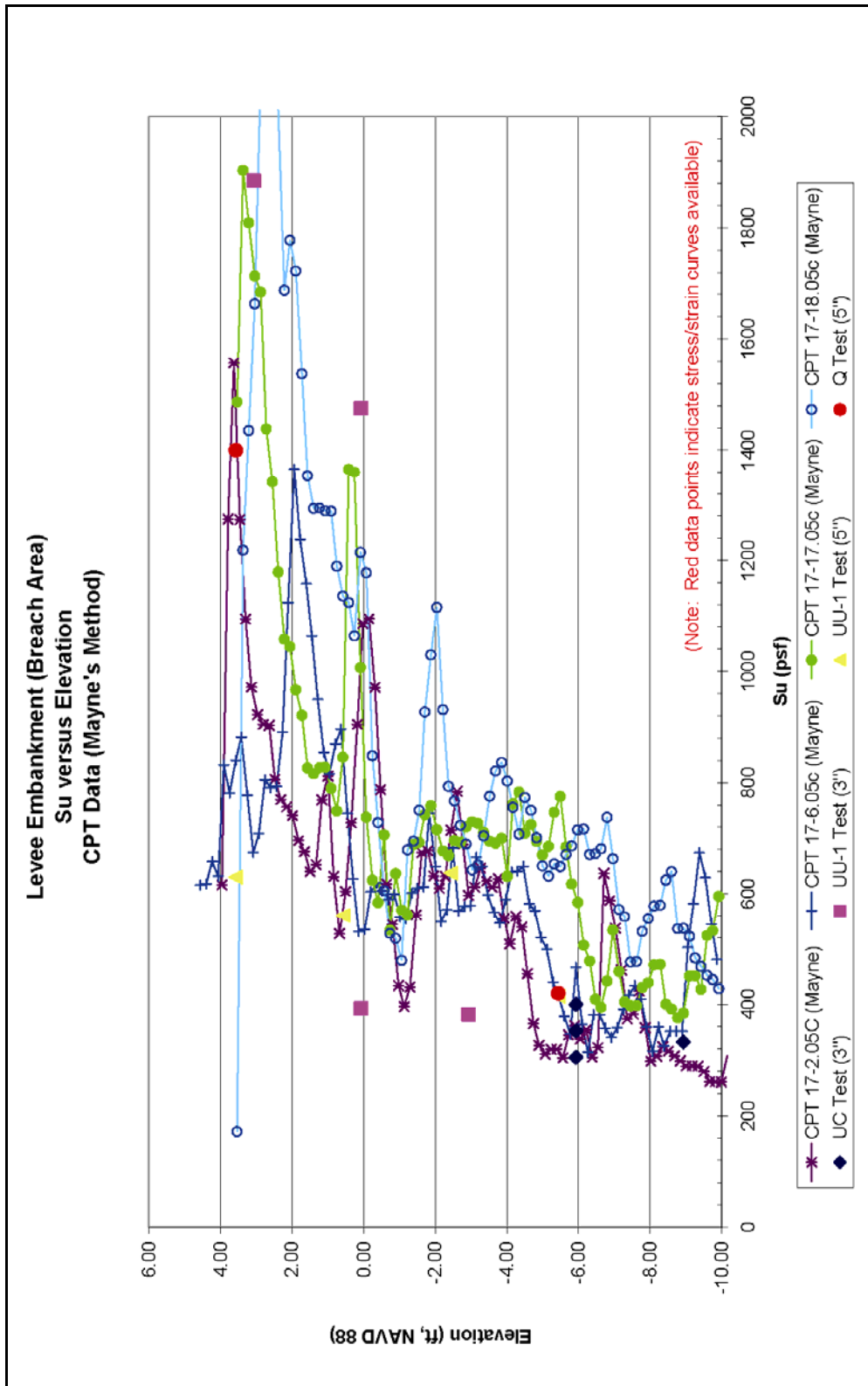


Figure K1-21. Levee Embankment, Su versus Elevation (CPT Data – Mayne's Method)

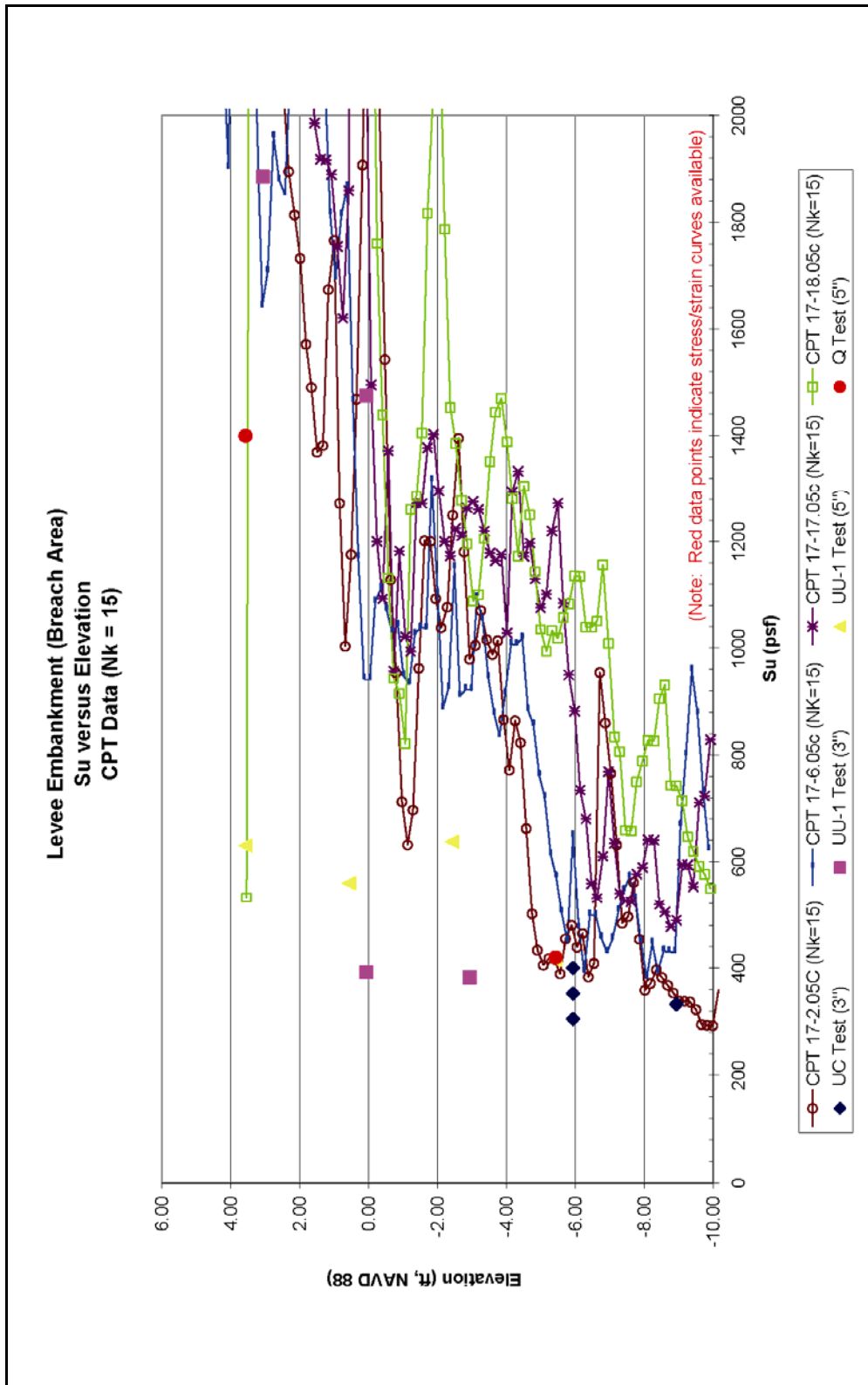


Figure K1-22. Levee Embankment (Breach Area), Su versus Elevation (CPT Data – Nk=15)

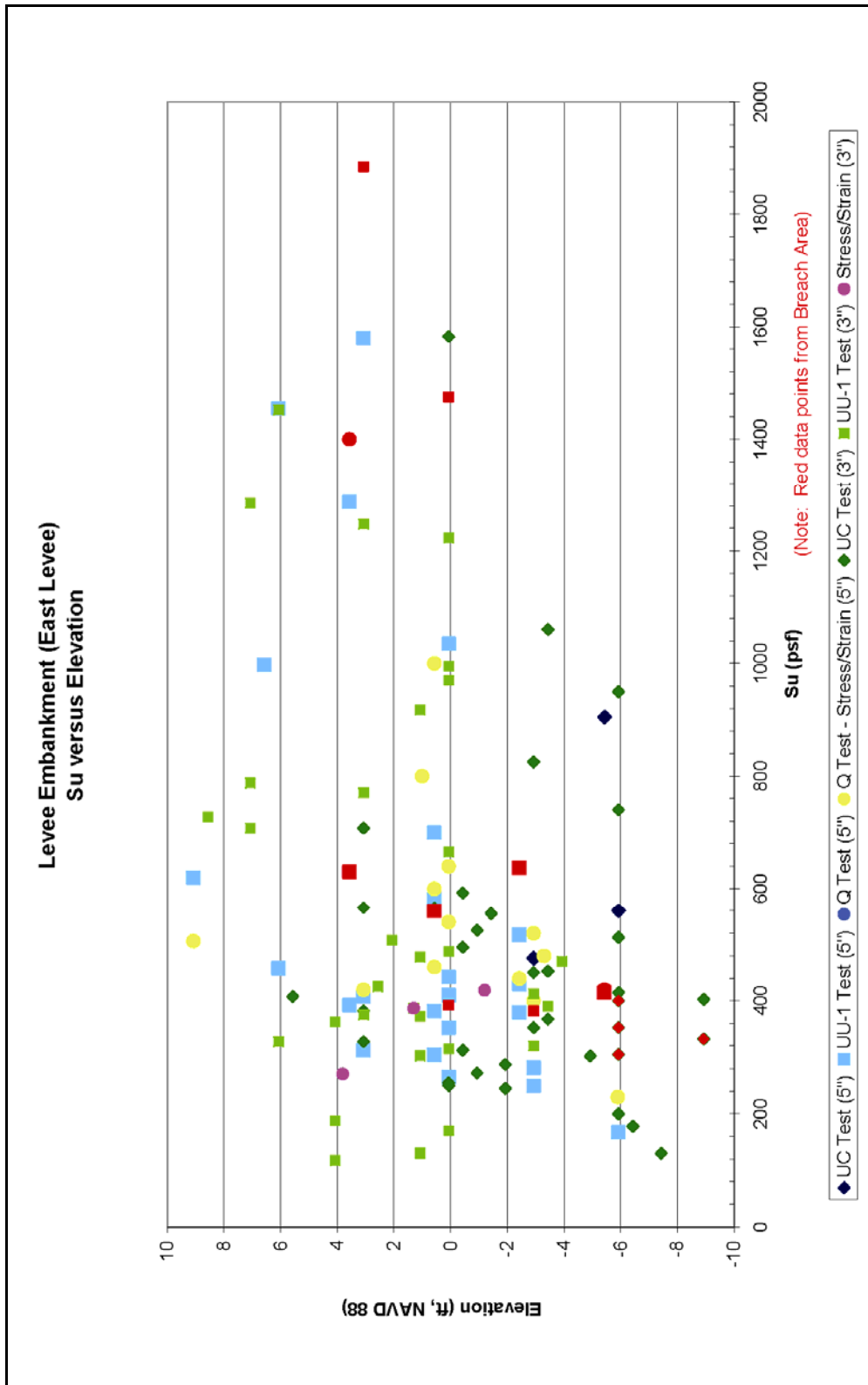


Figure K1-23. Levee Embankment (East Levee), Su versus Elevation

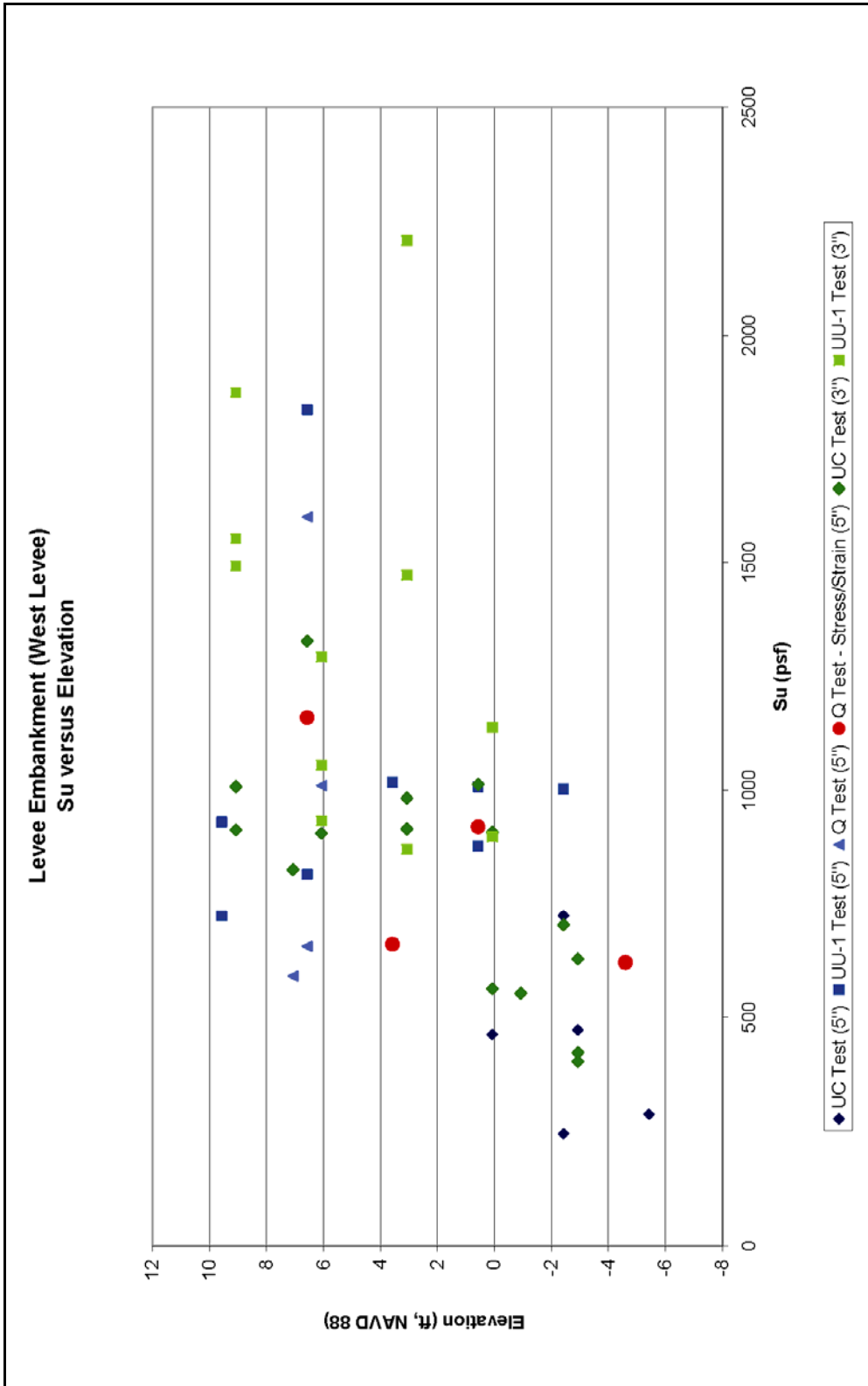


Figure K1-24. Levee Embankment (West Levee), Su versus Elevation

area are shown in Figure K1-25. In addition, this moisture content data were also plotted (Figure K1-26) with the moisture content data collected for the entire east levee on the canal. Also, the moisture content data for the entire west levee on the canal are shown in Figure K1-27.

The wet unit weight data in the breach area are shown in Figure K1-28. Wet unit weight data from the breach area plotted with wet unit weight data for the entire east levee are shown in Figure K1-29. Wet unit weight for the entire west levee on the canal are shown in Figure K1-30.

The undrained shear strength determined from the laboratory tests conducted on samples in the breach area is shown in Figure K1-31. Interpretation of the undrained shear strength from the CPTs using Mayne's method is plotted with laboratory test results in Figure K1-32. Interpretation of the undrained shear strength from the CPTs using the bearing capacity equation ($N_k=15$) is plotted with laboratory test results in Figure K1-33. These interpretations were provided by Dr. Thomas Brandon (Virginia Tech). Undrained shear strength data in the breach area plotted with undrained shear strength data for the entire east levee are shown in Figure K1-34. Undrained shear strength data for the entire west levee are shown in Figure K1-35.

At the Toe of Embankment

Data on the marsh stratum under the toe of the levee embankment consist of five borings taken in 2005 on the protected side, four borings taken in 2005 on the canal side, three borings on the west levee toe shown in the 1990 GDM. Of the borings on the protected side of the east levee, four borings collected 5-in. (diameter) undisturbed samples, and one boring collected 3-in. (diameter) undisturbed samples. Of the borings on the canal side of the east levee, three borings collected 5-in. (diameter) undisturbed samples, and one boring collected 3-in. (diameter) undisturbed samples. Of the three GDM borings taken on the protected side of the west levee, two borings collected 3-in. (diameter) samples, and one boring collected 5-in. (diameter) undisturbed samples. From the 3-in. samples, four unconfined compression (UC) tests were performed, and two one-point unconsolidated-undrained triaxial compression tests (UU-1), confined at existing overburden pressure, were performed. From the 5-in. samples, 14 UC tests were performed, and six unconsolidated-undrained triaxial compression tests (Q) were performed. From these laboratory tests, moisture content and wet unit weights were determined. The moisture contents (%w) in the breach area are shown in Figure K1-36. In addition, this moisture content data were also plotted (Figure K1-37) with the moisture content data collected for the entire east levee on the canal. Also, the moisture content data for the entire west levee on the canal are shown in Figure K1-38.

The wet unit weight data in the breach area are shown in Figure K1-39. Wet unit weight data from the breach area plotted with wet unit weight data for the entire east levee are shown in Figure K1-40. Wet unit weight for the entire west levee on the canal is shown in Figure K1-41.

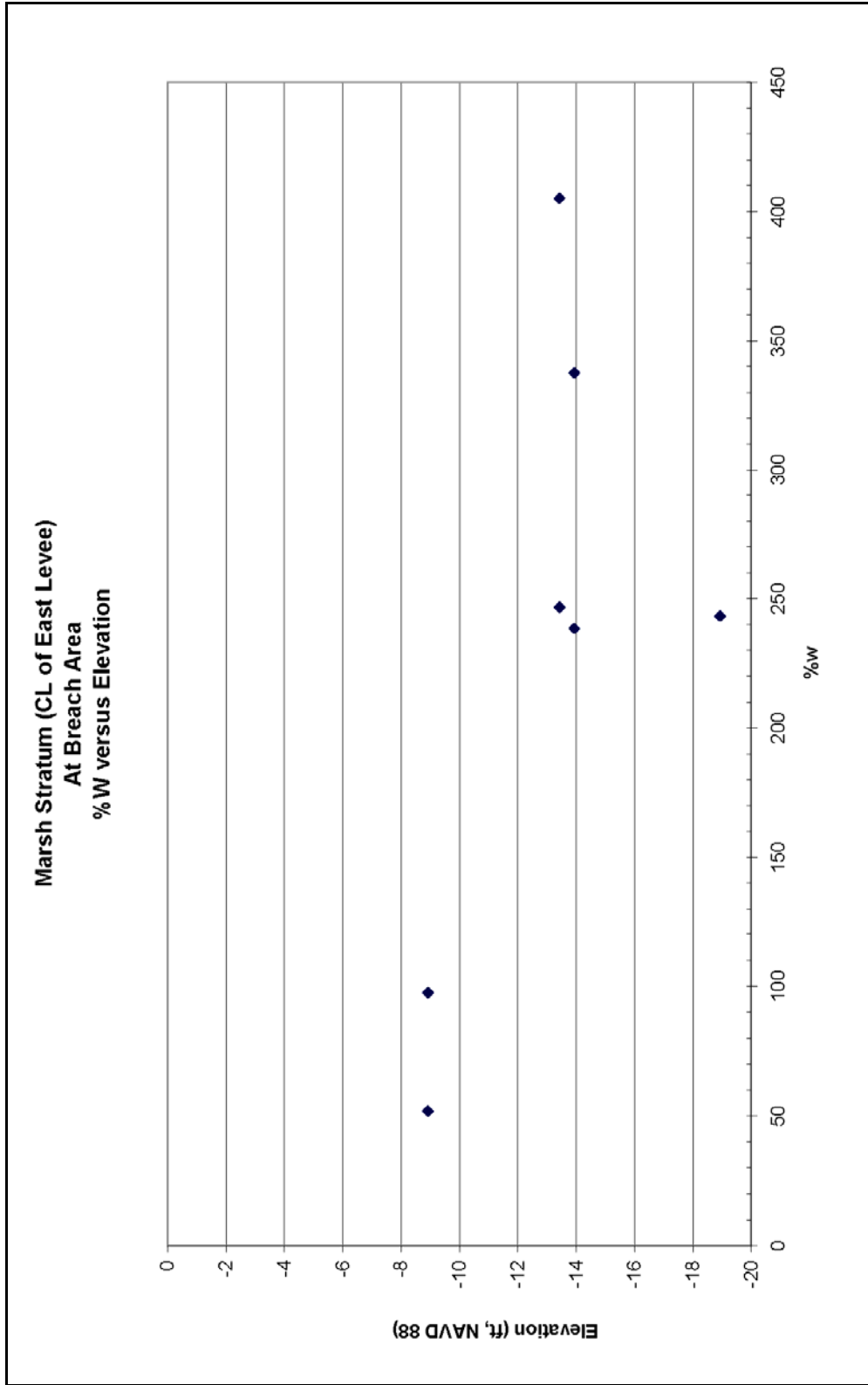


Figure K1-25. Marsh Stratum (CL of East Levee – At Breach Area), %w versus Elevation

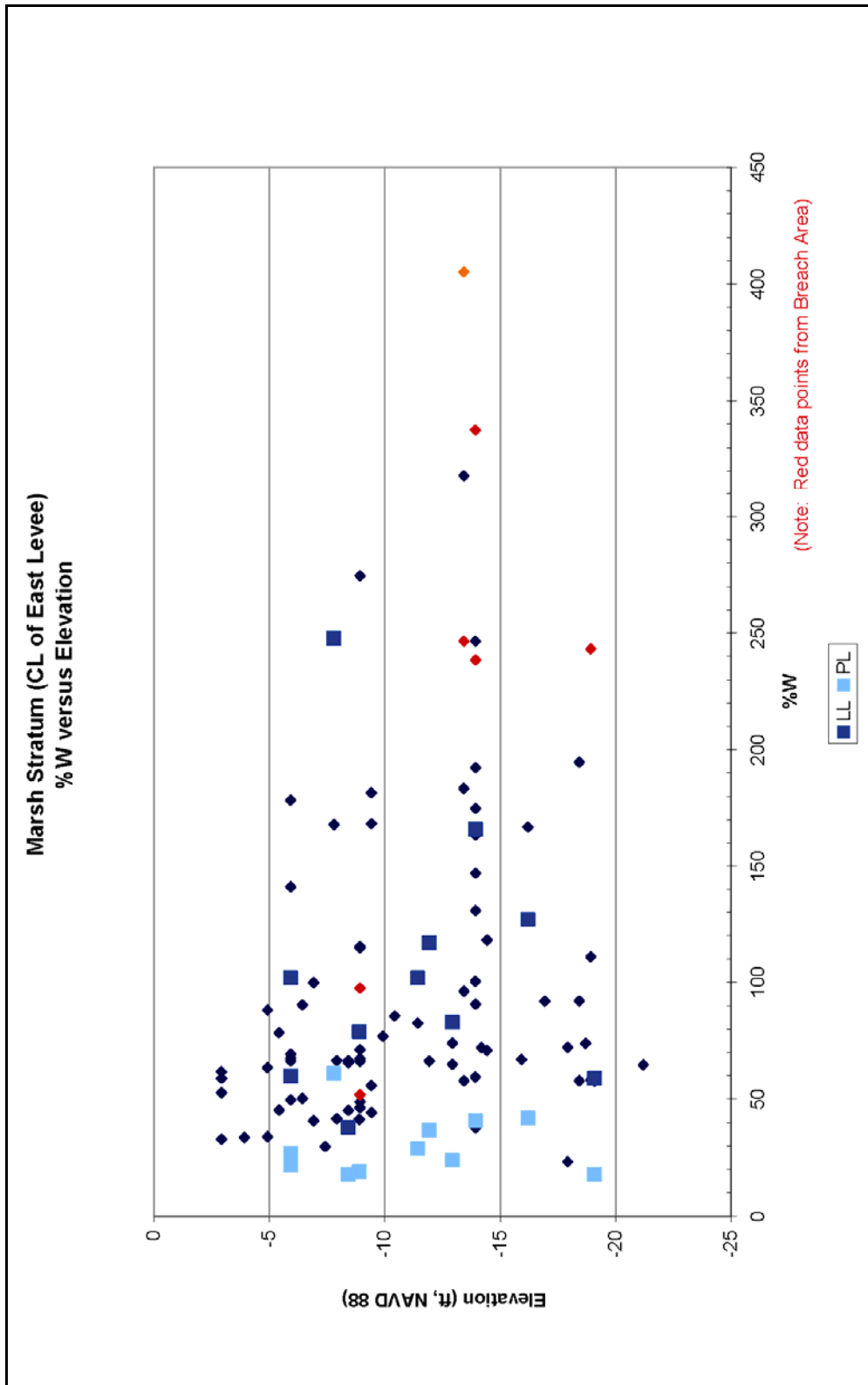


Figure K1-26. Marsh Stratum (CL of East Levee), %W versus Elevation

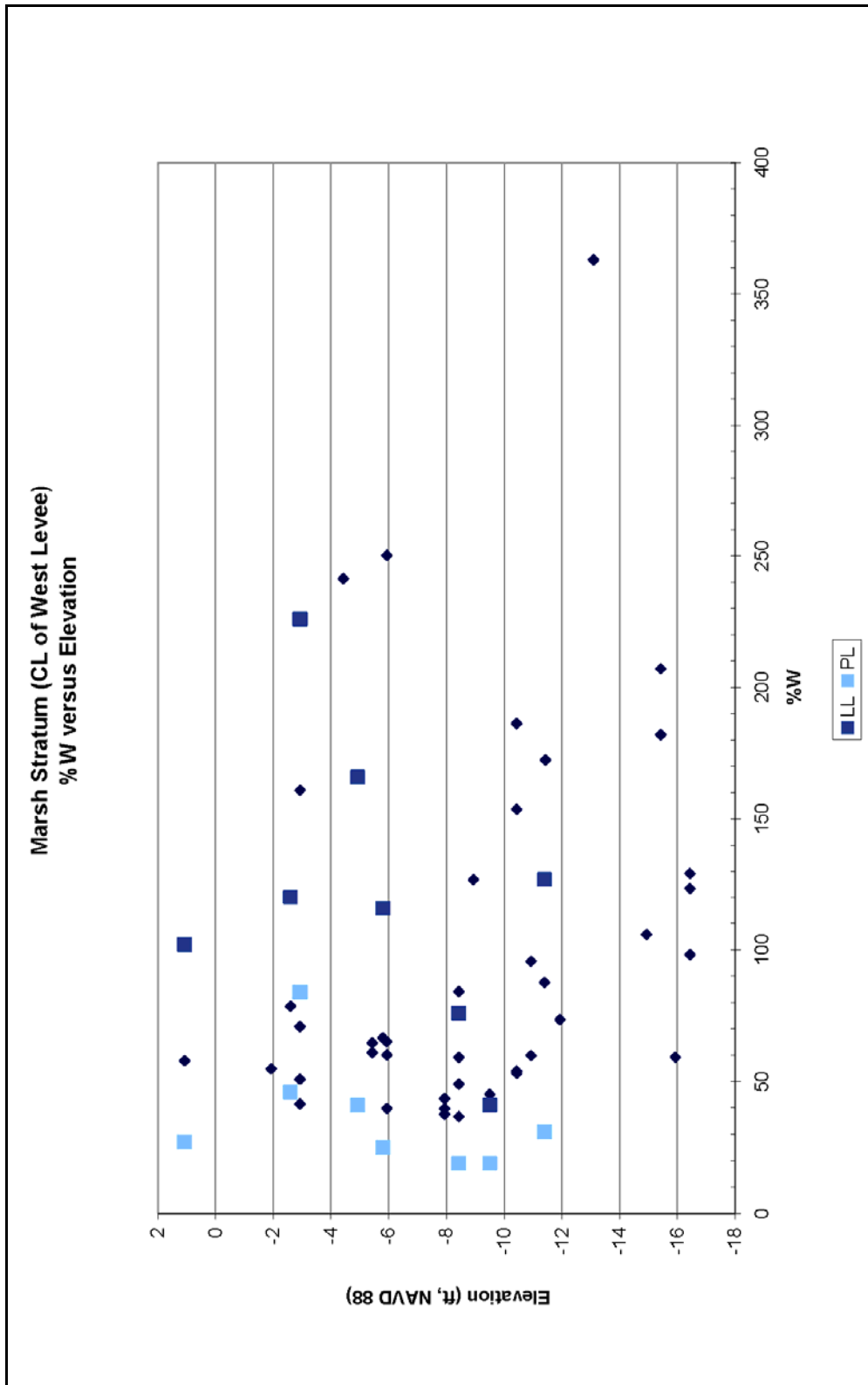


Figure K1-27. Marsh Stratum (CL of West Levee), %w versus Elevation

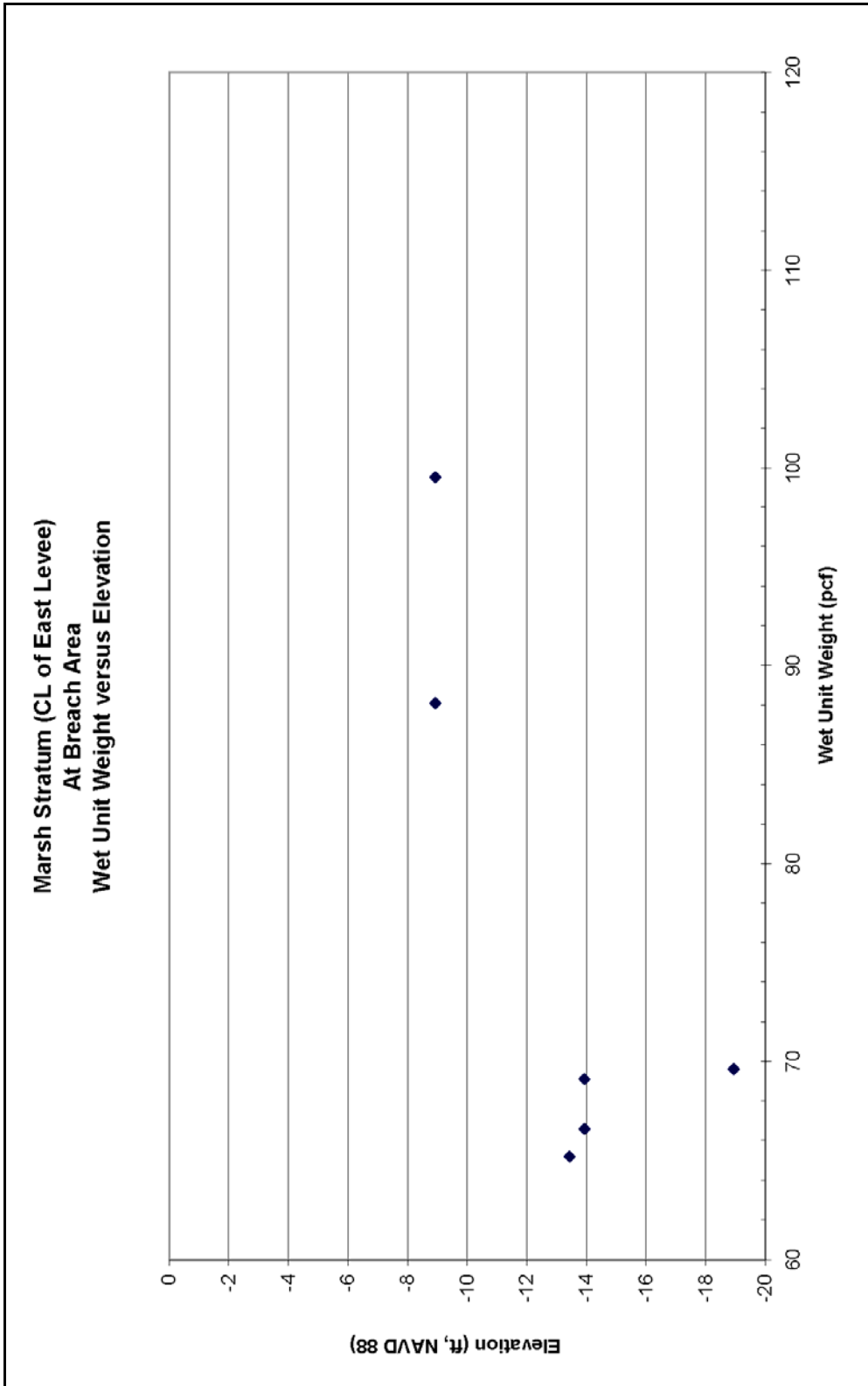
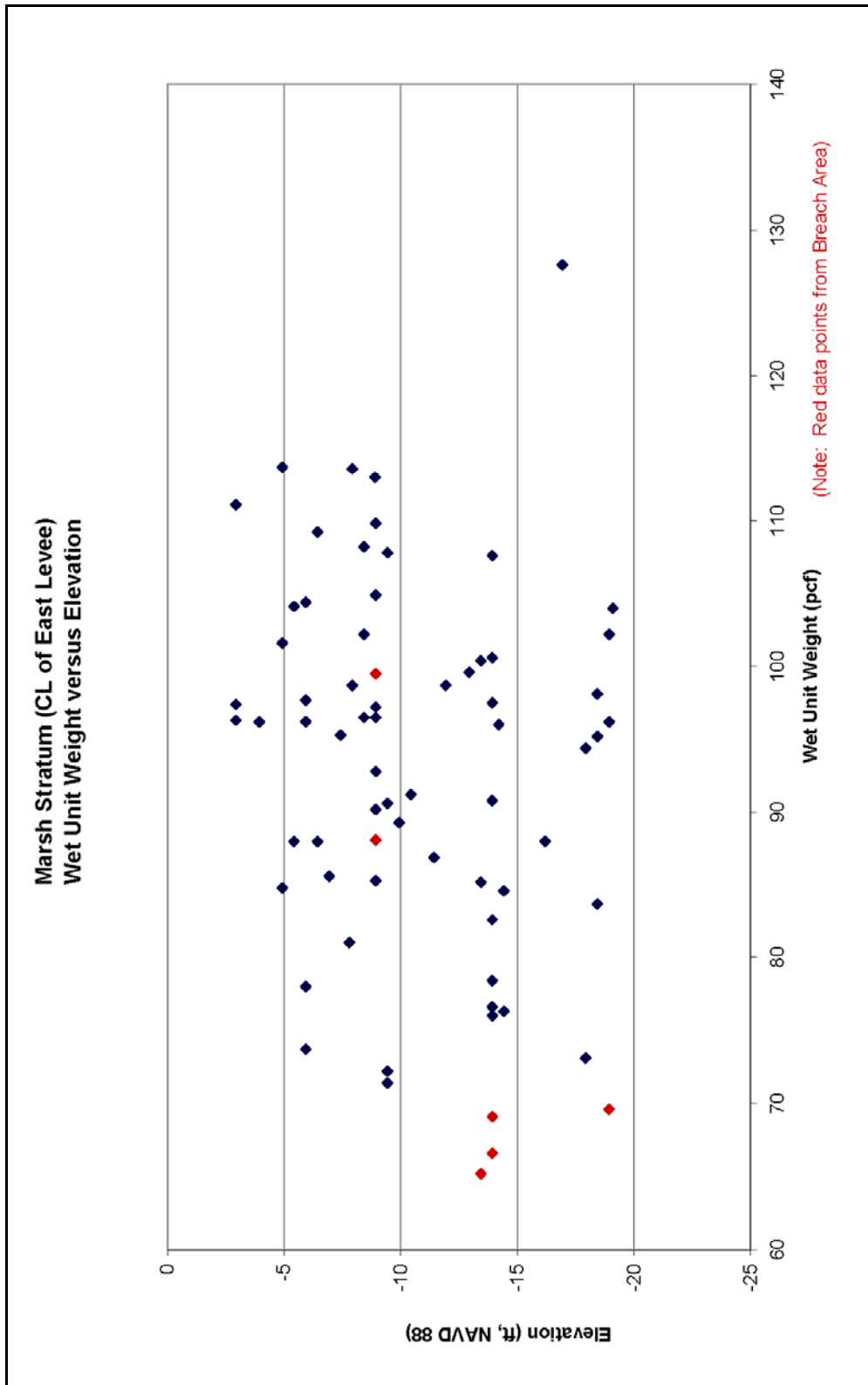


Figure K1-28. Marsh Stratum (CL of East Levee – At Breach Area), Wet Unit Weight versus Elevation



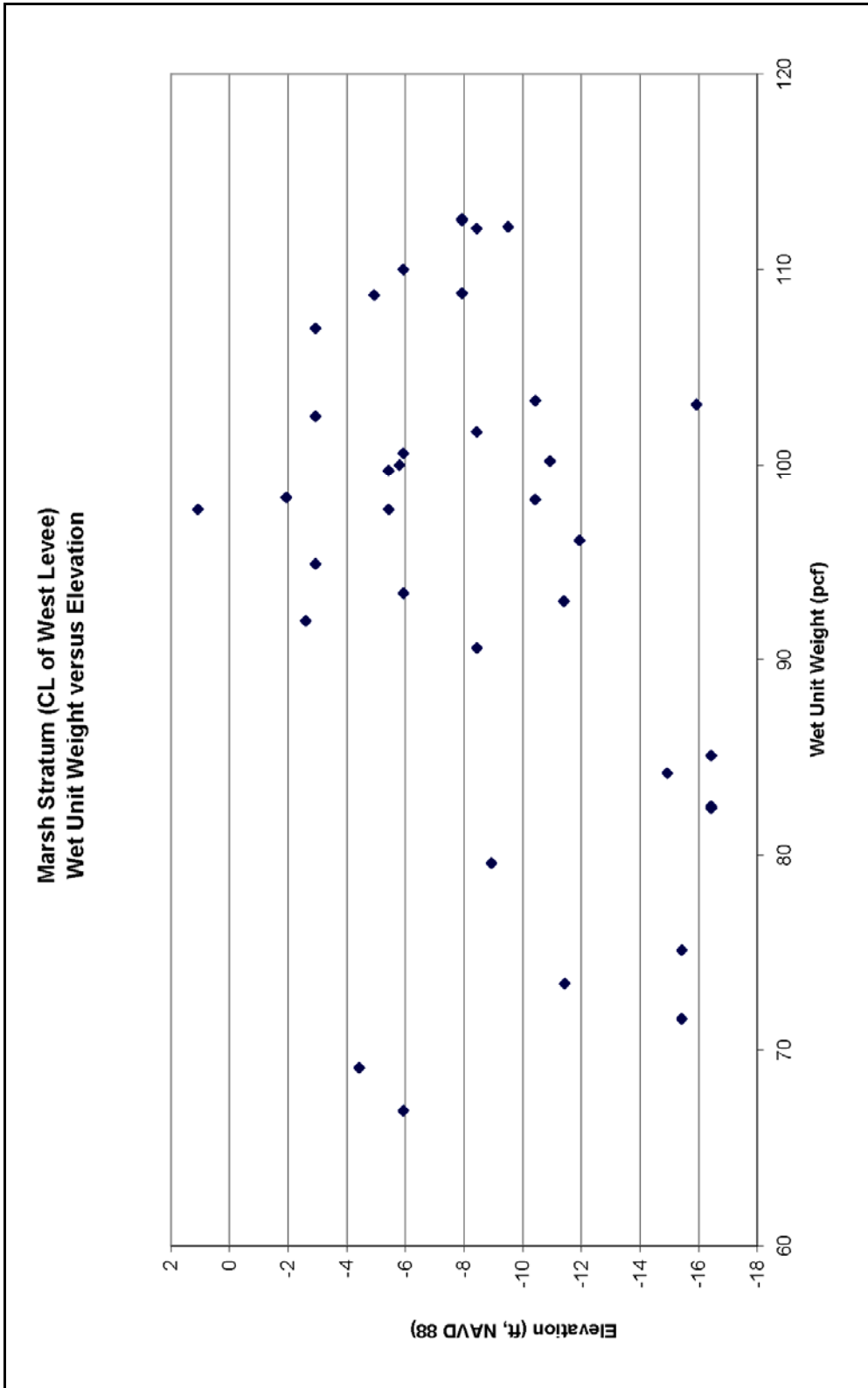


Figure K1-30. Marsh Stratum (CL of West Levee), Wet Unit Weight versus Elevation

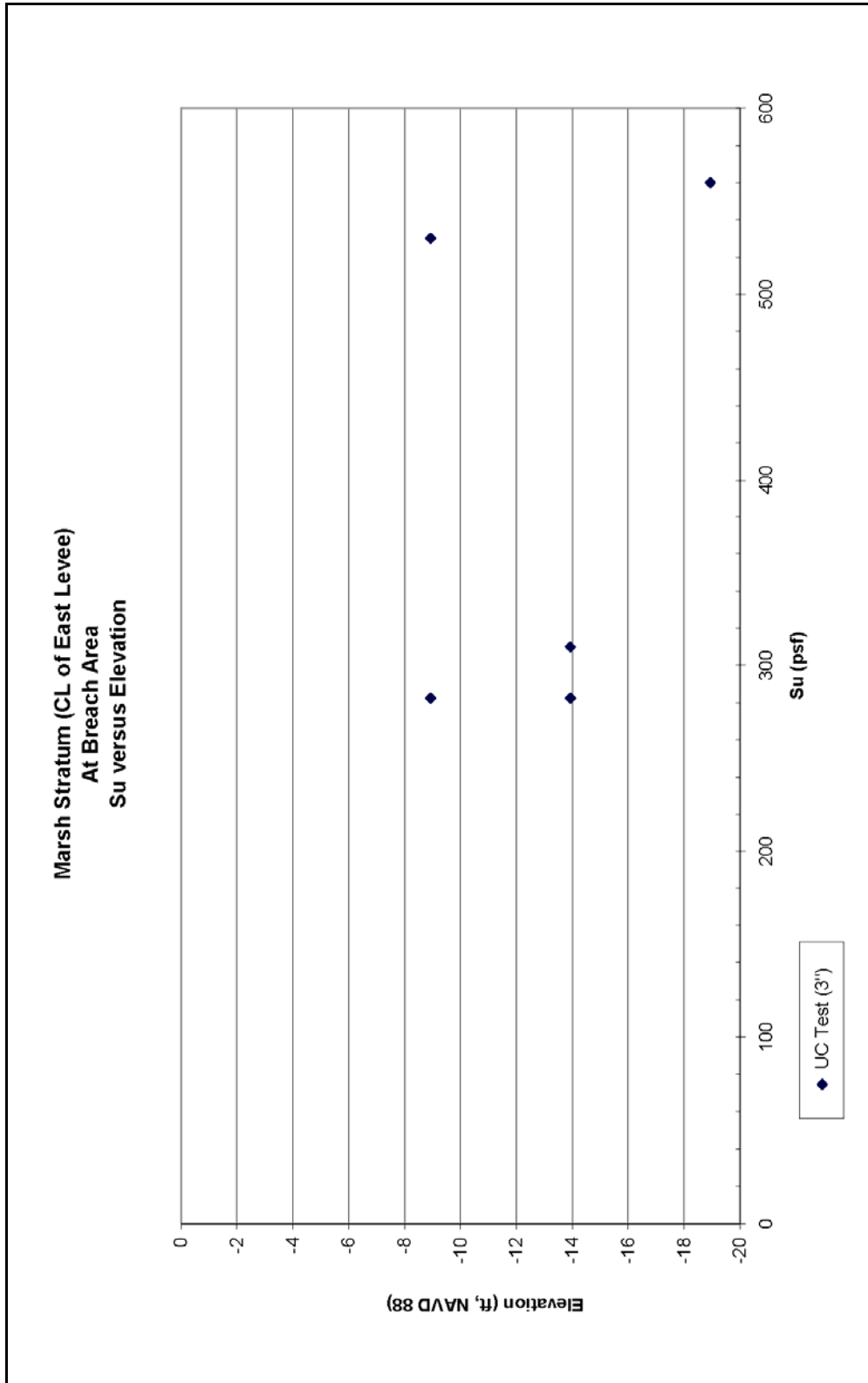


Figure K1-31. Marsh Stratum (CL of East Levee – At Breach Area), Su versus Elevation

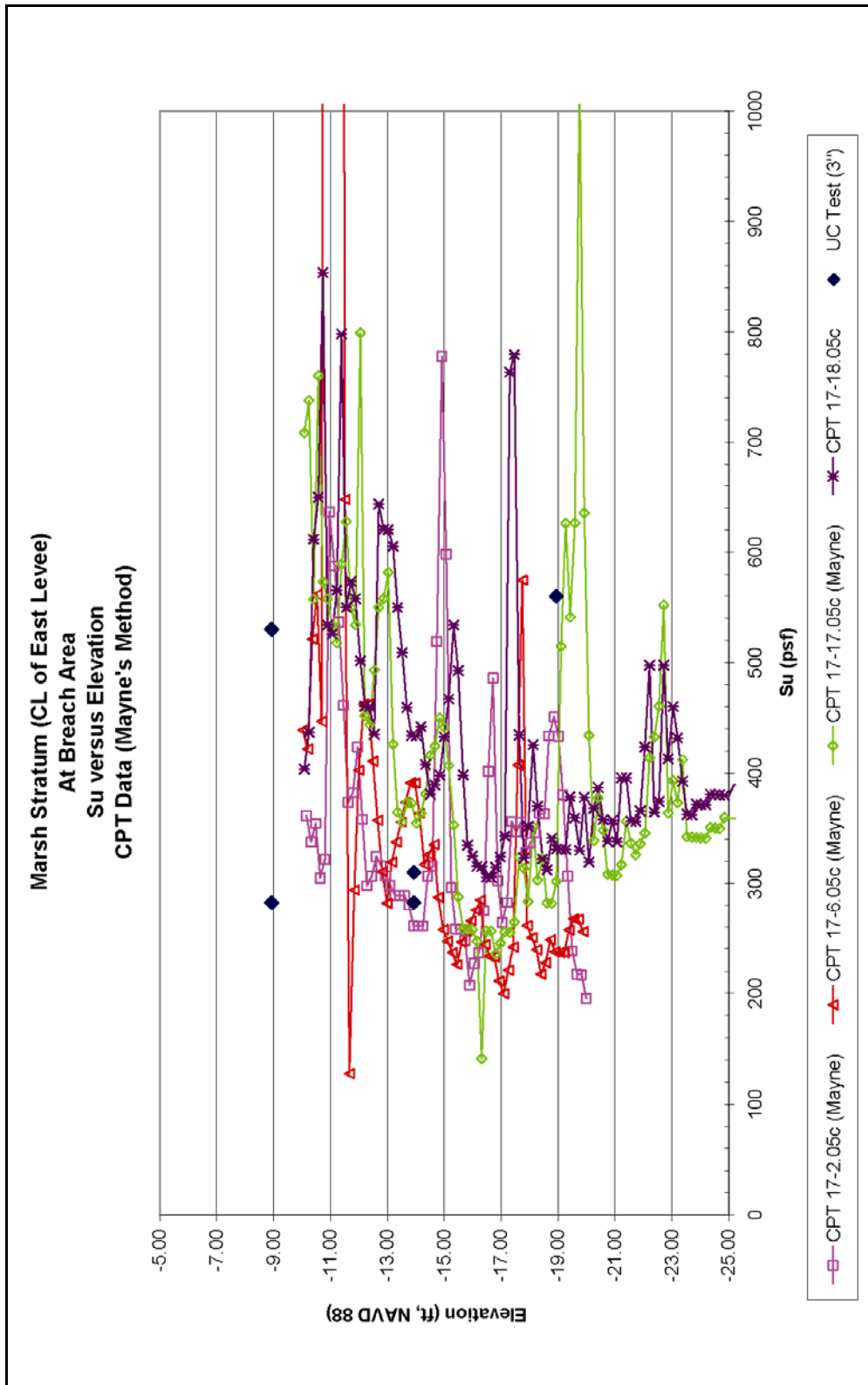


Figure K1-32. Marsh Stratum (CL of East Levee – At Breach Area), Su versus Elevation (CPT Data – Mayne's Method)

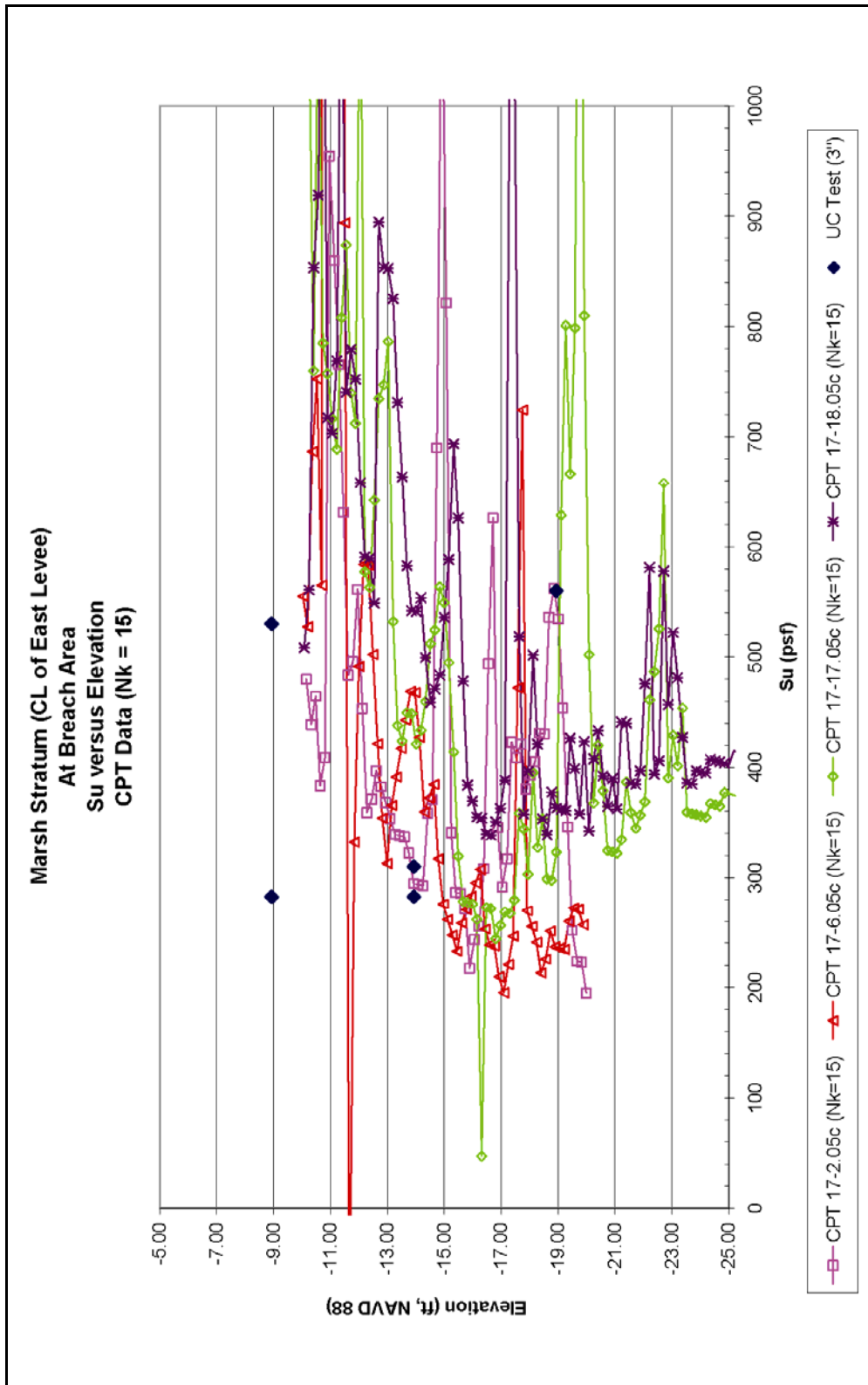


Figure K1-33. Marsh Stratum (CL of East Levee), Su versus Elevation (CPT Data – Nk=15)

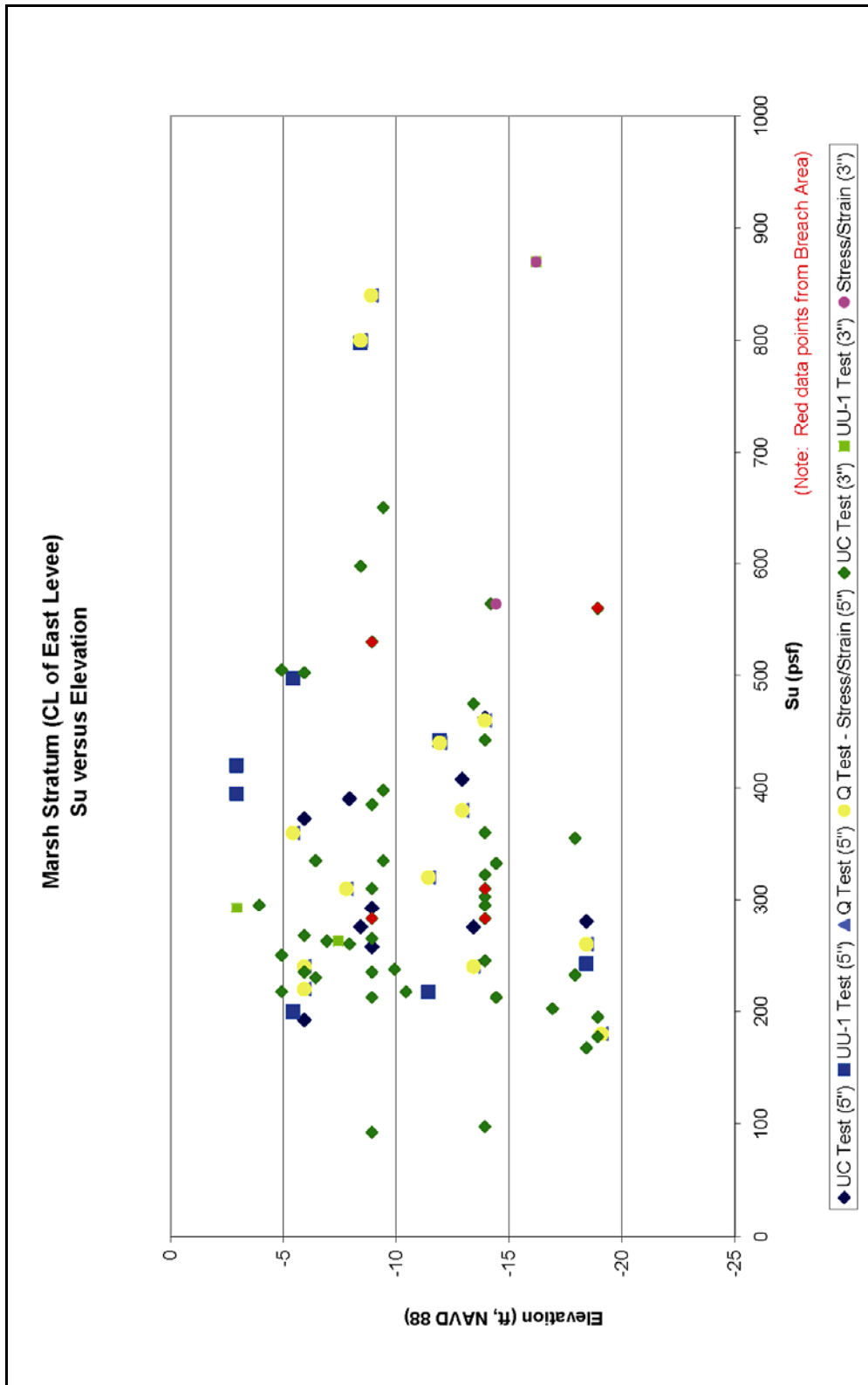


Figure K1-34. Marsh Stratum (CL of East Levee), Su versus Elevation

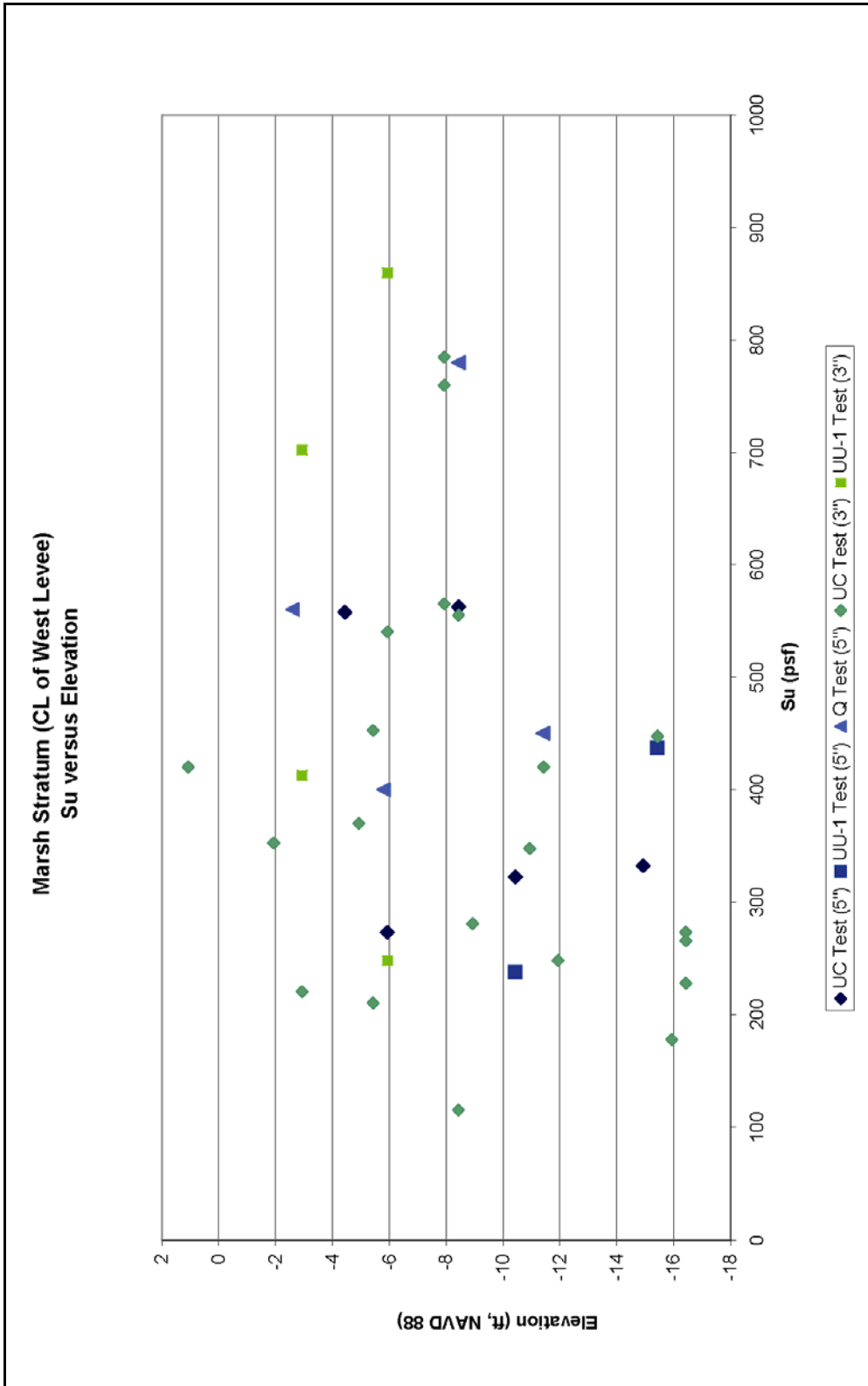


Figure K1-35. Marsh Stratum (CL of West Levee), Su versus Elevation

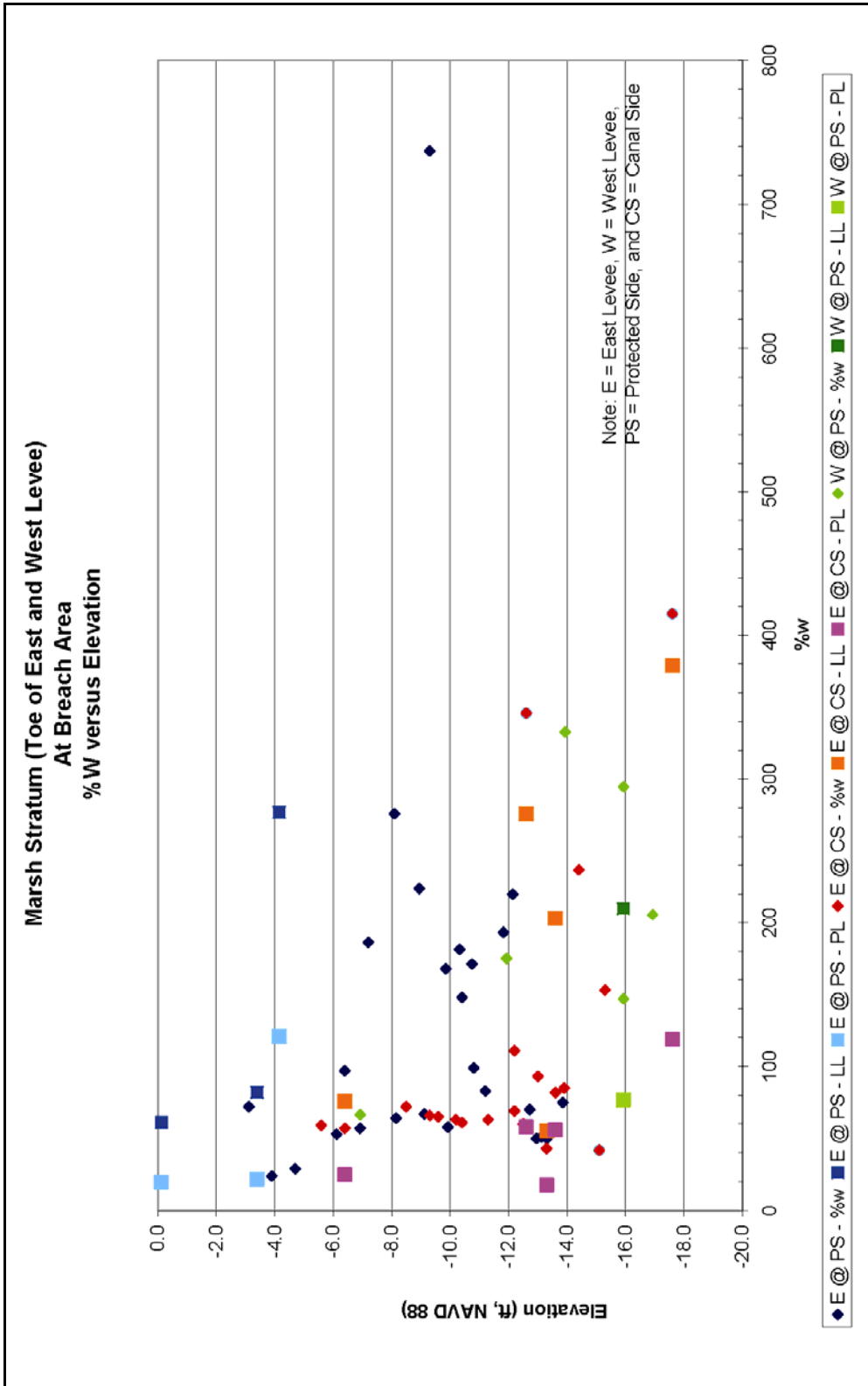
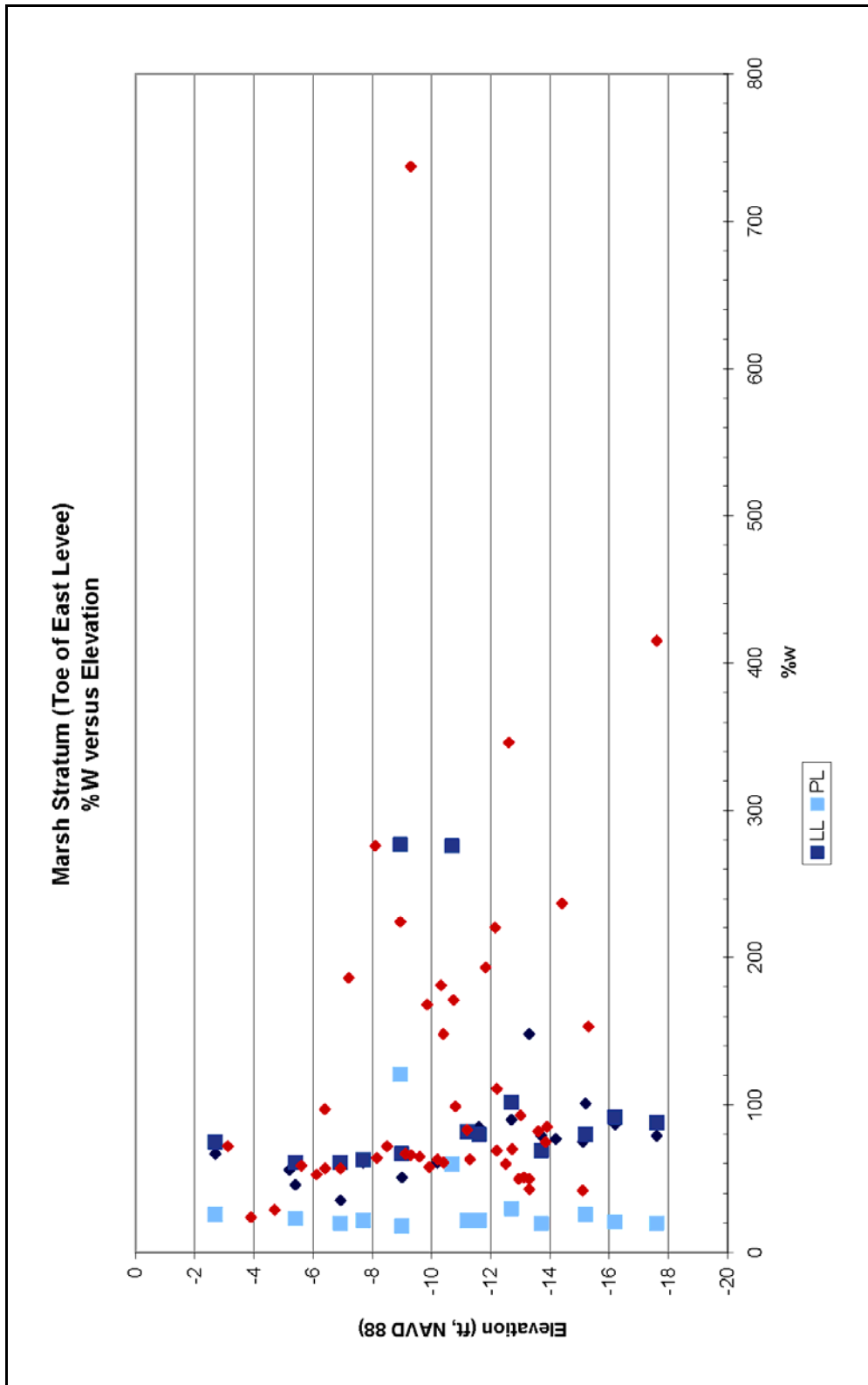


Figure K1-36. Marsh Stratum (Toe of East and West Levee – At Breach Area), %w versus Elevation



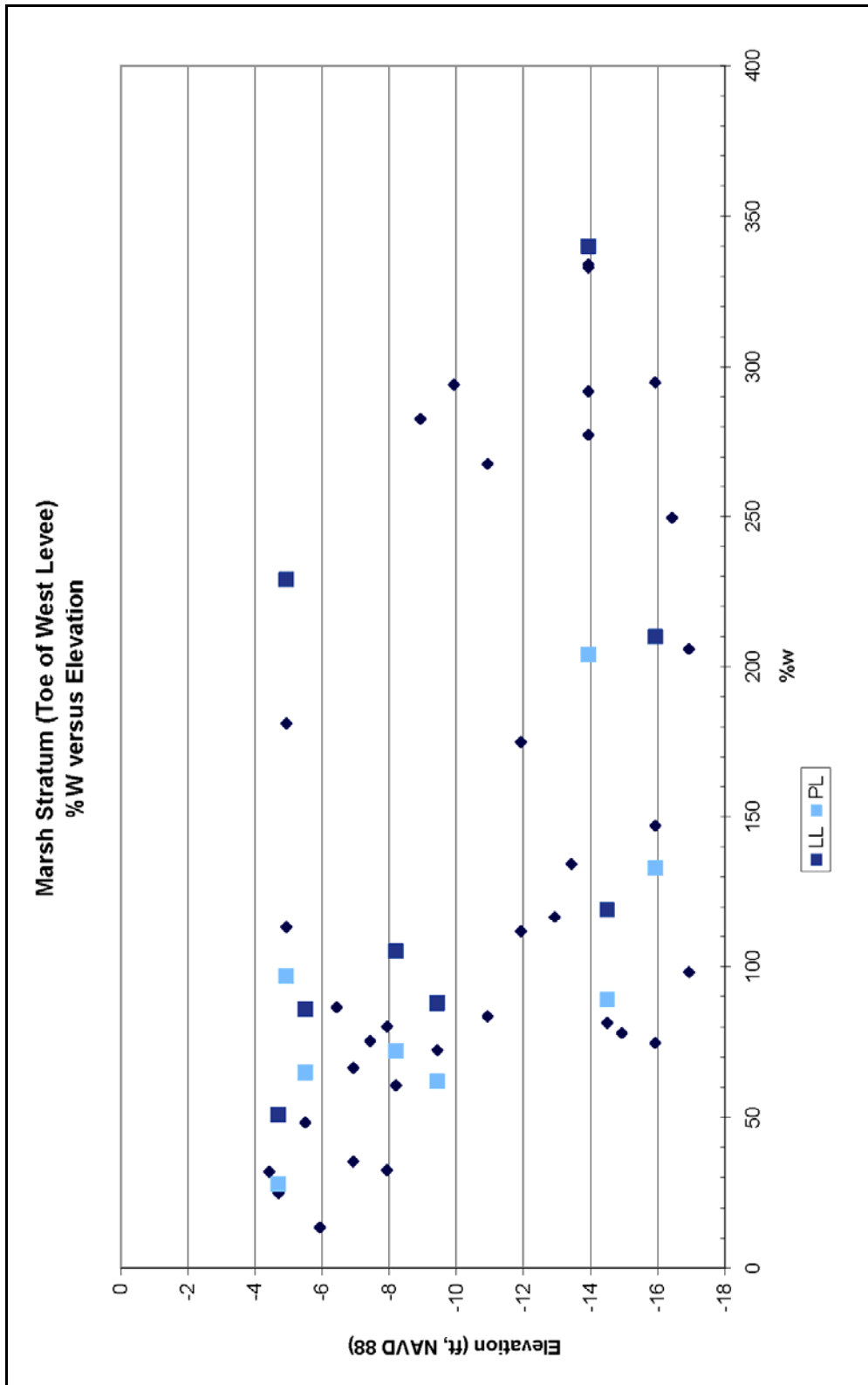


Figure K1-38. Marsh Stratum (Toe of West Levee), %w versus Elevation

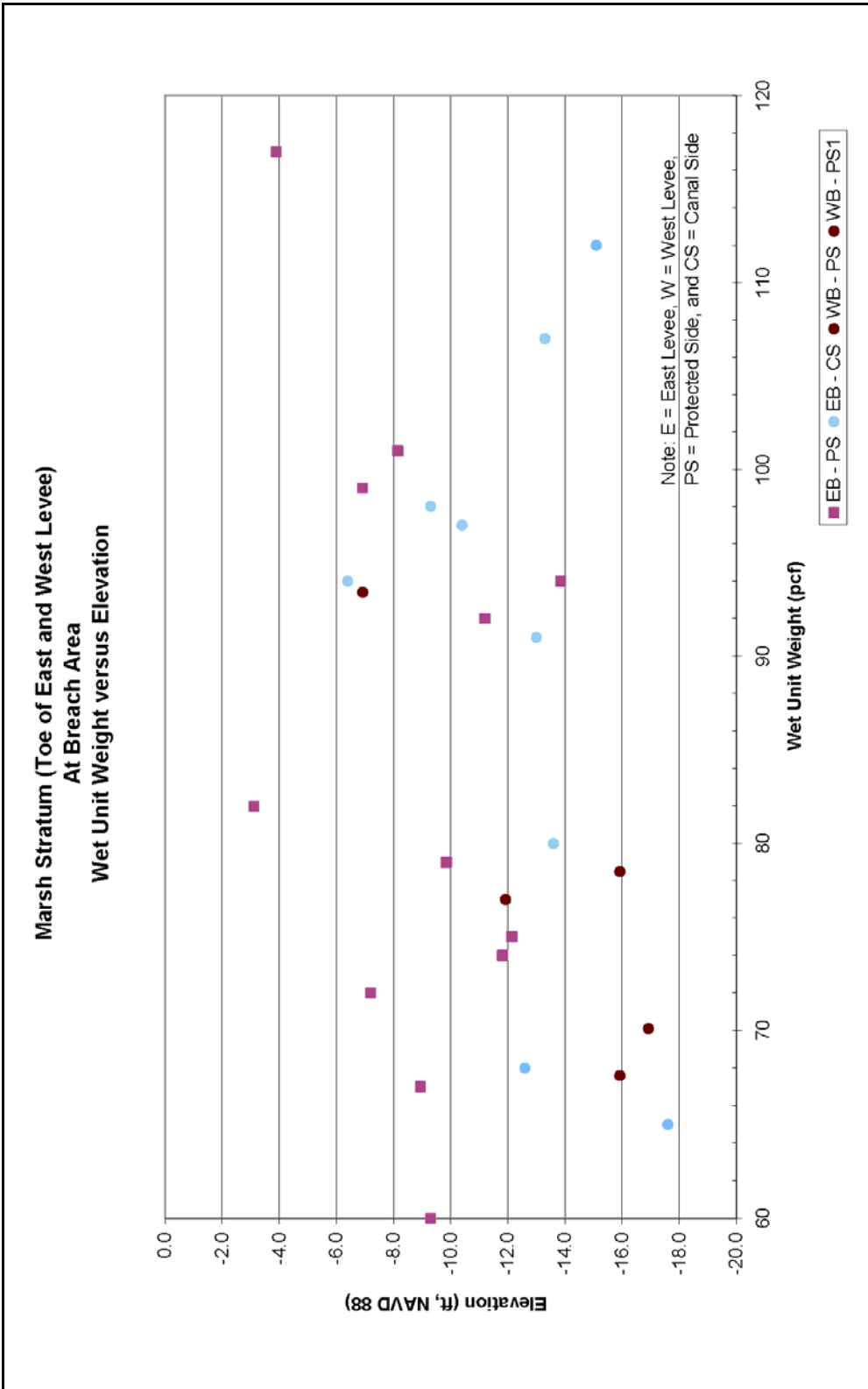


Figure K1-39. Marsh Stratum (Toe of East and West Levee – At Breach Area), Wet Unit Weight versus Elevation

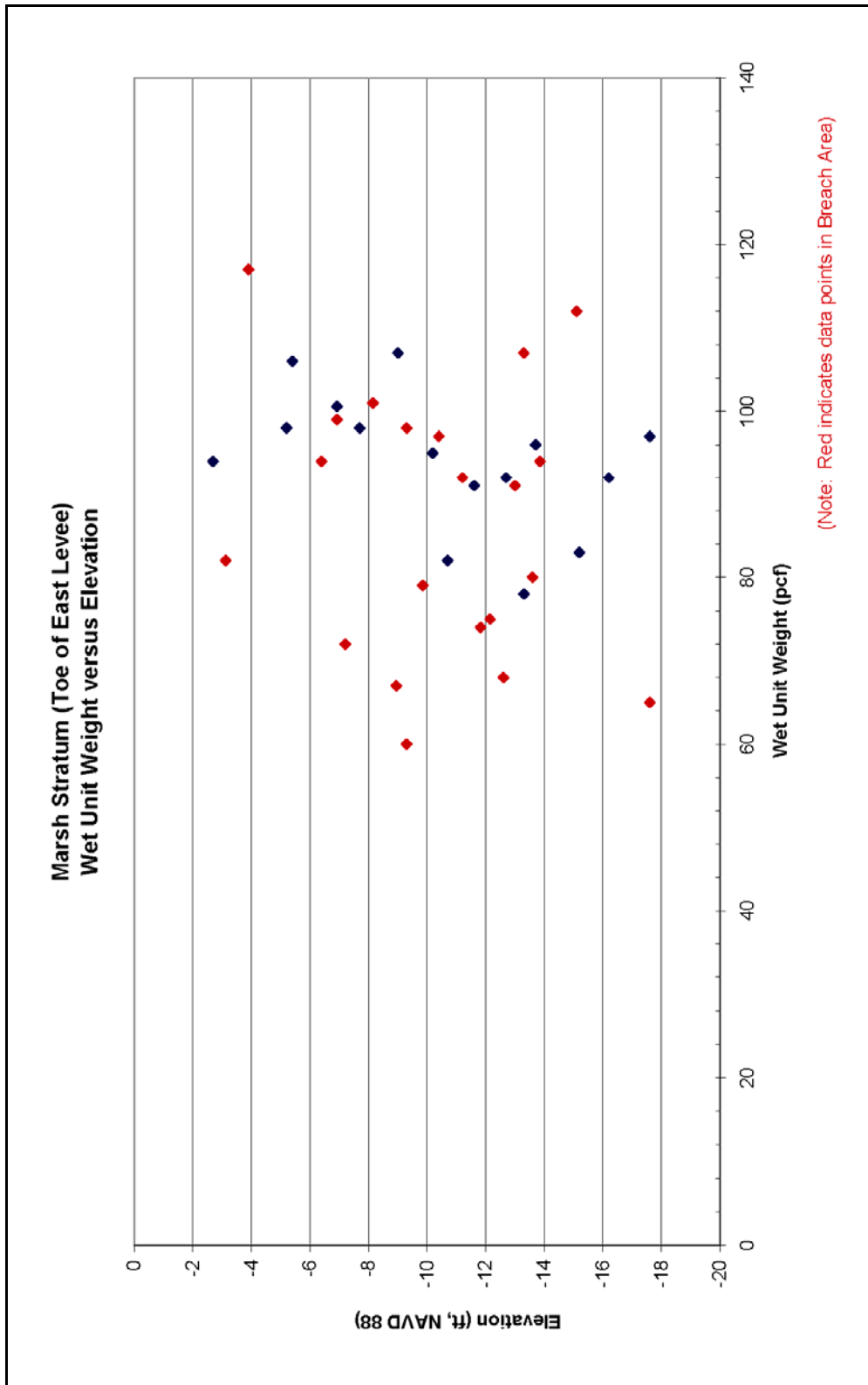


Figure K1-40. Marsh Stratum (Toe of East Levee), Wet Unit Weight versus Elevation

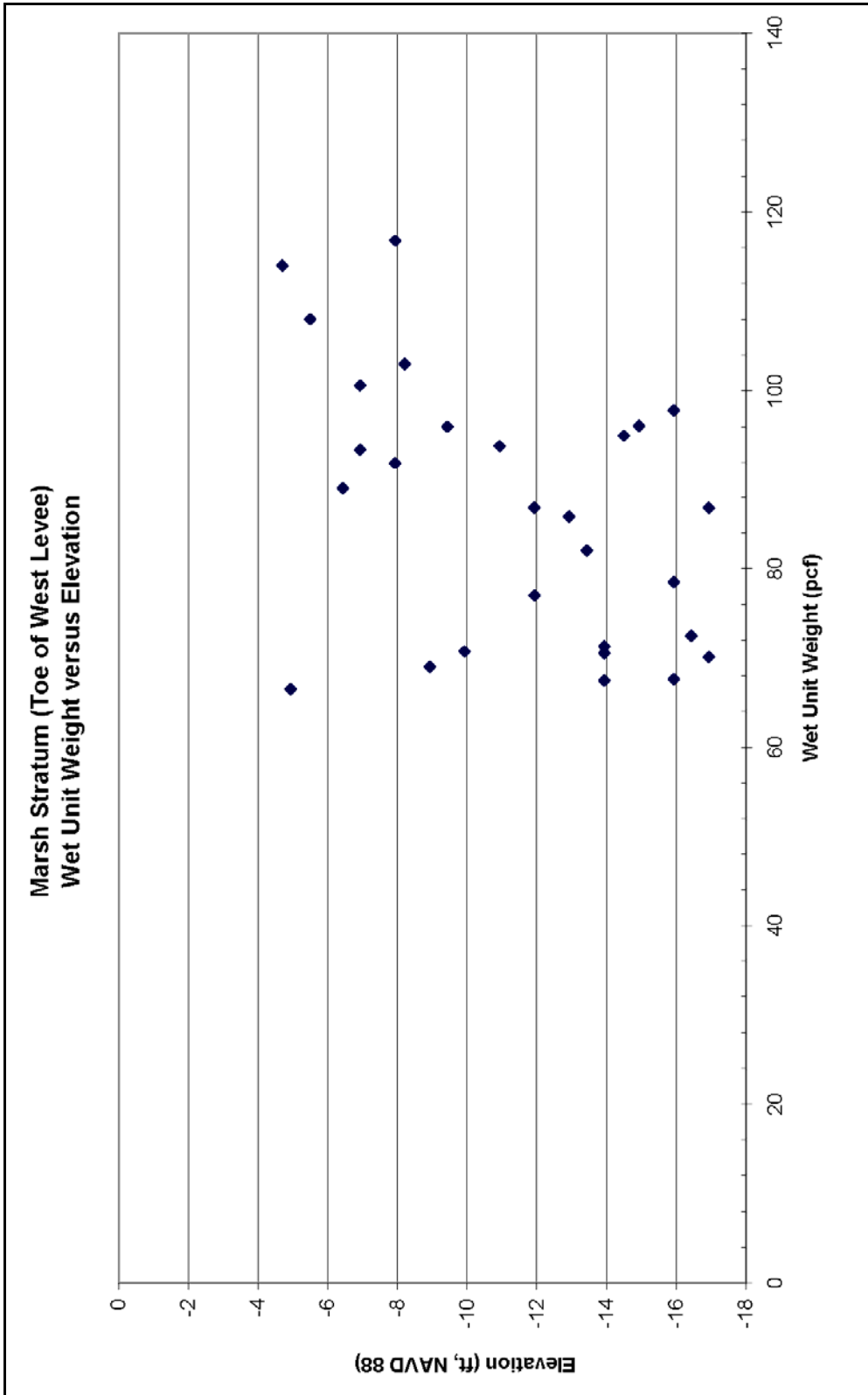


Figure K1-41. Marsh Stratum (Toe of West Levee), Wet Unit Weight versus Elevation

The undrained shear strength determined from the laboratory tests conducted on samples in the breach area is shown in Figure K1-42. Undrained shear strength data in the breach area plotted with undrained shear strength data for the entire east levee are shown in Figure K1-43. Undrained shear strength data for the entire west levee are shown in Figure K1-44.

Lacustrine Stratum

The data for the lacustrine stratum will be divided into two groups: data from under the levee embankment, and data from the toe of the levee.

Under the Levee Embankment

Data on the lacustrine stratum under the levee embankment consist of five borings shown in the 1990 GDM, and four cone penetrometer tests (CPT) taken on the east levee. Of the five GDM borings, four borings collected 3-in. (diameter) undisturbed samples, and one boring collected 5-in. (diameter) undisturbed samples. From the 3-in. samples, ten unconfined compression (UC) tests were performed. From the 5-in. samples, four UC tests were performed, and two one-point unconsolidated-undrained triaxial compression tests (UU-1), confined at existing overburden pressures, were performed. From these laboratory tests, moisture content and wet unit weights were determined. The moisture contents (%w) in the breach area are shown in Figure K1-45. The wet unit weight data in the breach area are shown in Figure K1-46.

Interpretation of the undrained shear strength from the CPTs using the bearing capacity equation ($N_k=15$) is plotted with laboratory test results in Figure K1-47. These interpretations were provided by Dr. Thomas Brandon (Virginia Tech).

At the Toe of Embankment

Data on the marsh stratum under the toe of the levee embankment consist of five borings taken in 2005 on the protected side, four borings taken in 2005 on the canal side, and three borings on the west levee toe shown in the 1990 GDM. Of the borings on the protected side of the east levee, four borings collected 5-in. (diameter) undisturbed samples, and one boring collected 3-in. (diameter) undisturbed samples. Of the borings on the canal side of the east levee, three borings collected 5-in. (diameter) undisturbed samples, and one boring collected 3-in. (diameter) undisturbed samples. Of the three GDM borings taken on the protected side of the west levee, two borings collected 3-in. (diameter) samples, and one boring collected 5-in. (diameter) undisturbed samples. From the 3-in. samples, 14 UC tests were performed, and five one-point unconsolidated-undrained triaxial compression tests (UU-1), confined at existing overburden pressure, were performed. From the 5-in. samples, 25 UC tests were performed, 19 unconsolidated-undrained triaxial compression tests (Q), and 7 one-point unconsolidated-undrained triaxial compression tests (UU-1), confined at existing overburden pressure, were performed. From these laboratory tests, moisture content and wet unit weights were determined. The moisture contents (%w) in the breach area are shown in Figure K1-44. The wet unit weight data in the breach area are shown in Figure K1-49.

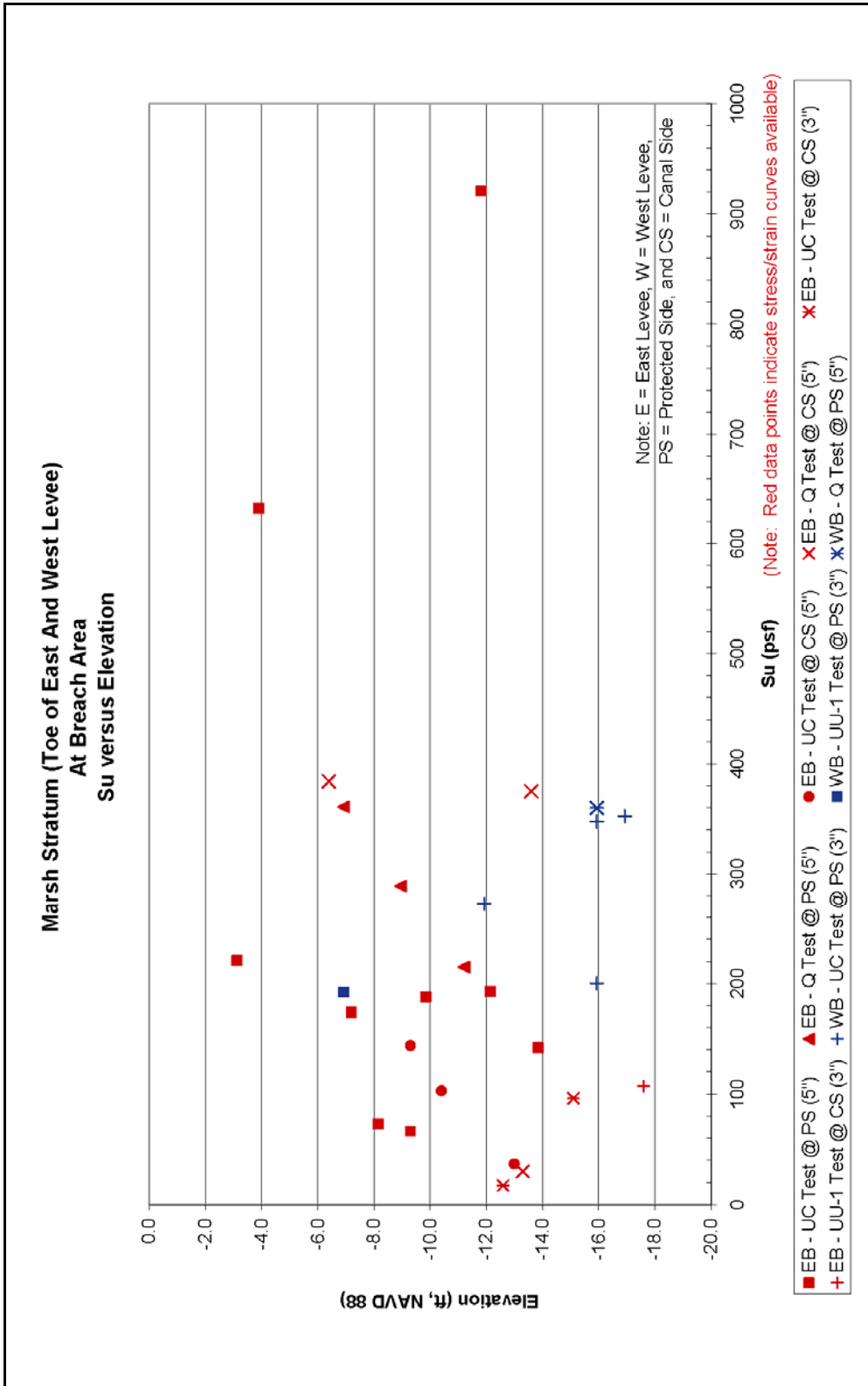


Figure K1-42. Marsh Stratum (Toe of East and West Levee – At Breach Area), Su versus Elevation

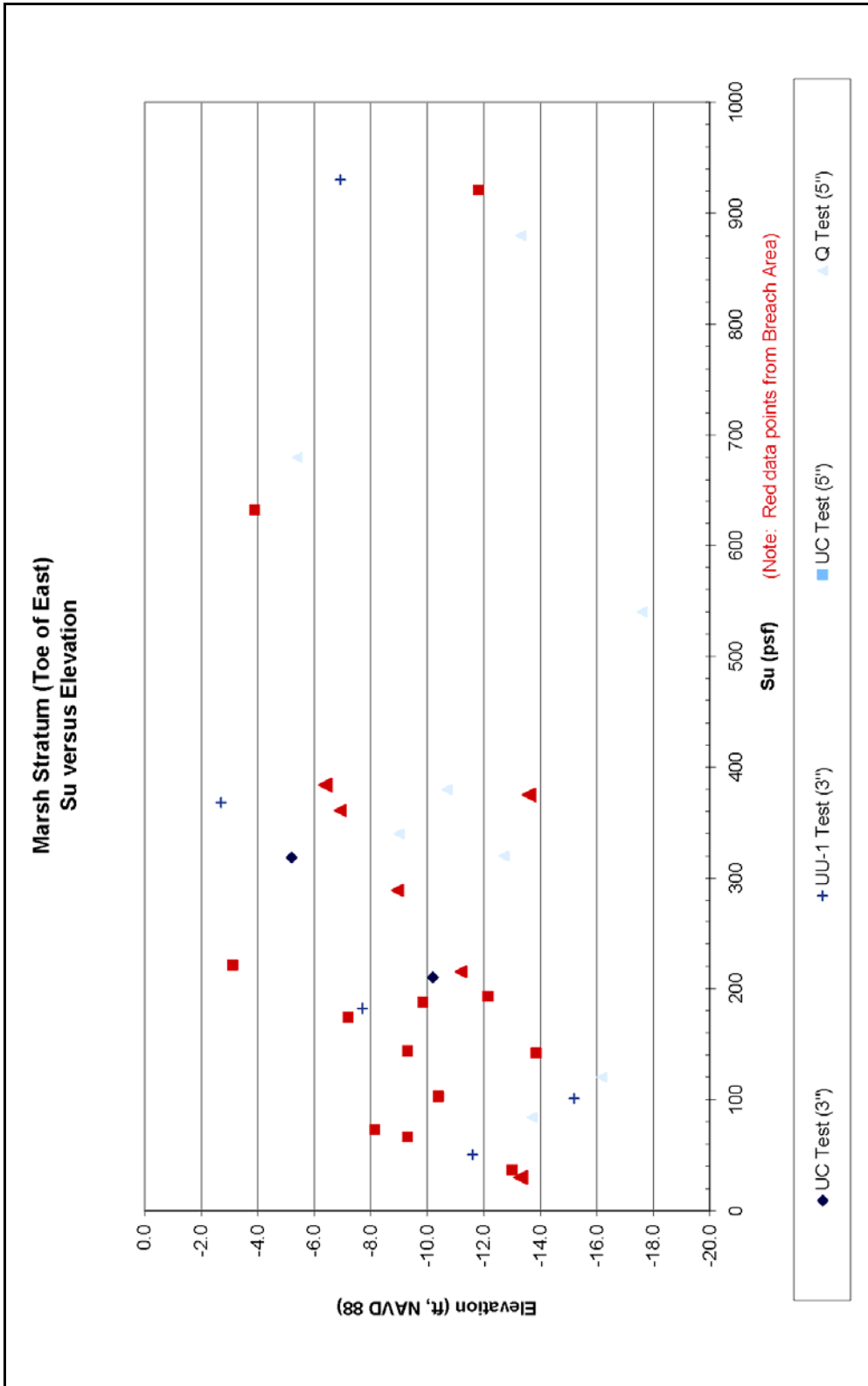


Figure K1-43. Marsh Stratum (Toe of East Levee), Su versus Elevation

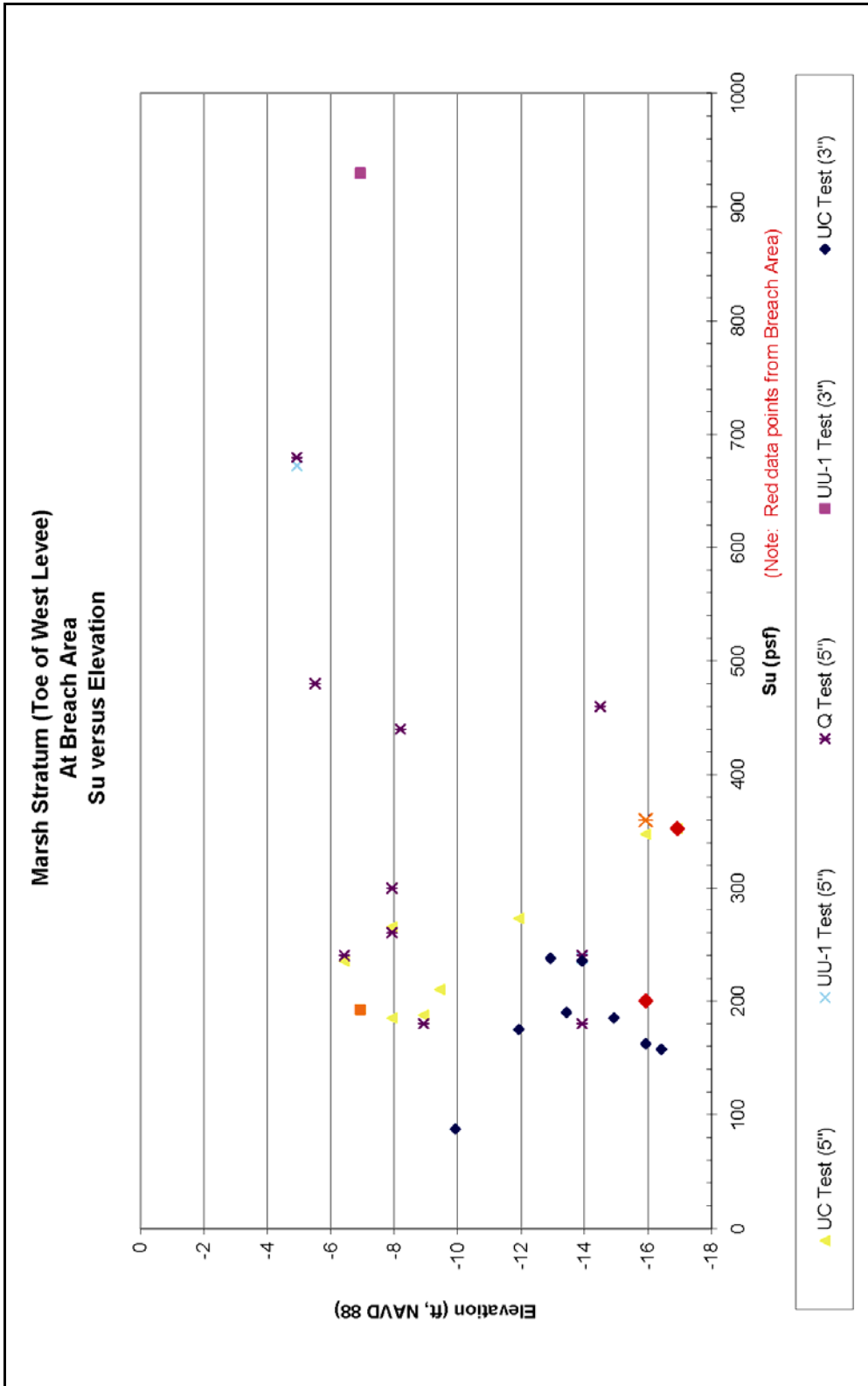


Figure K1-44. Marsh Stratum (Toe of West Levee), Su versus Elevation

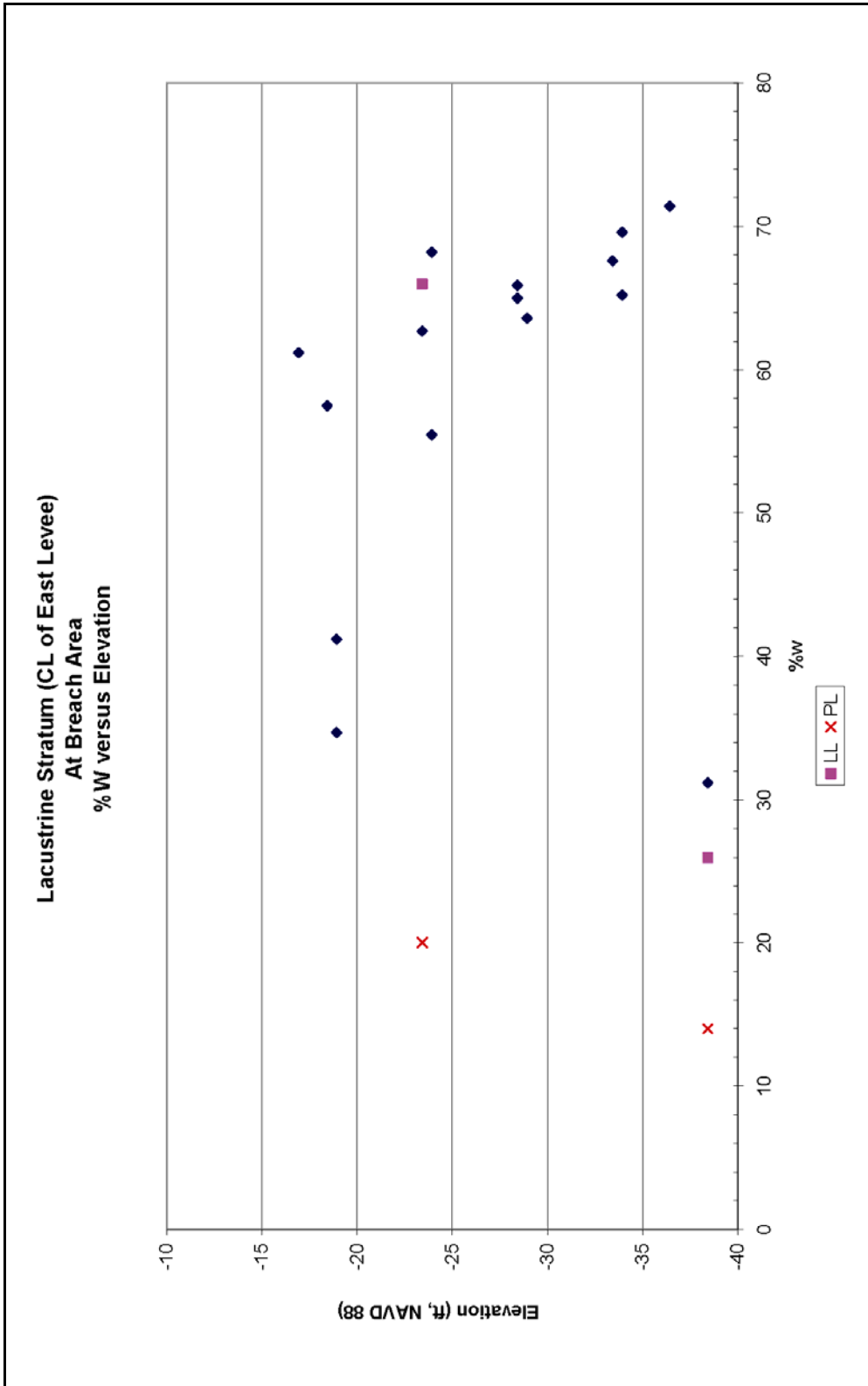


Figure K1-45. Lacustrine Stratum (CL of East Levee – At Breach Area), %w versus Elevation

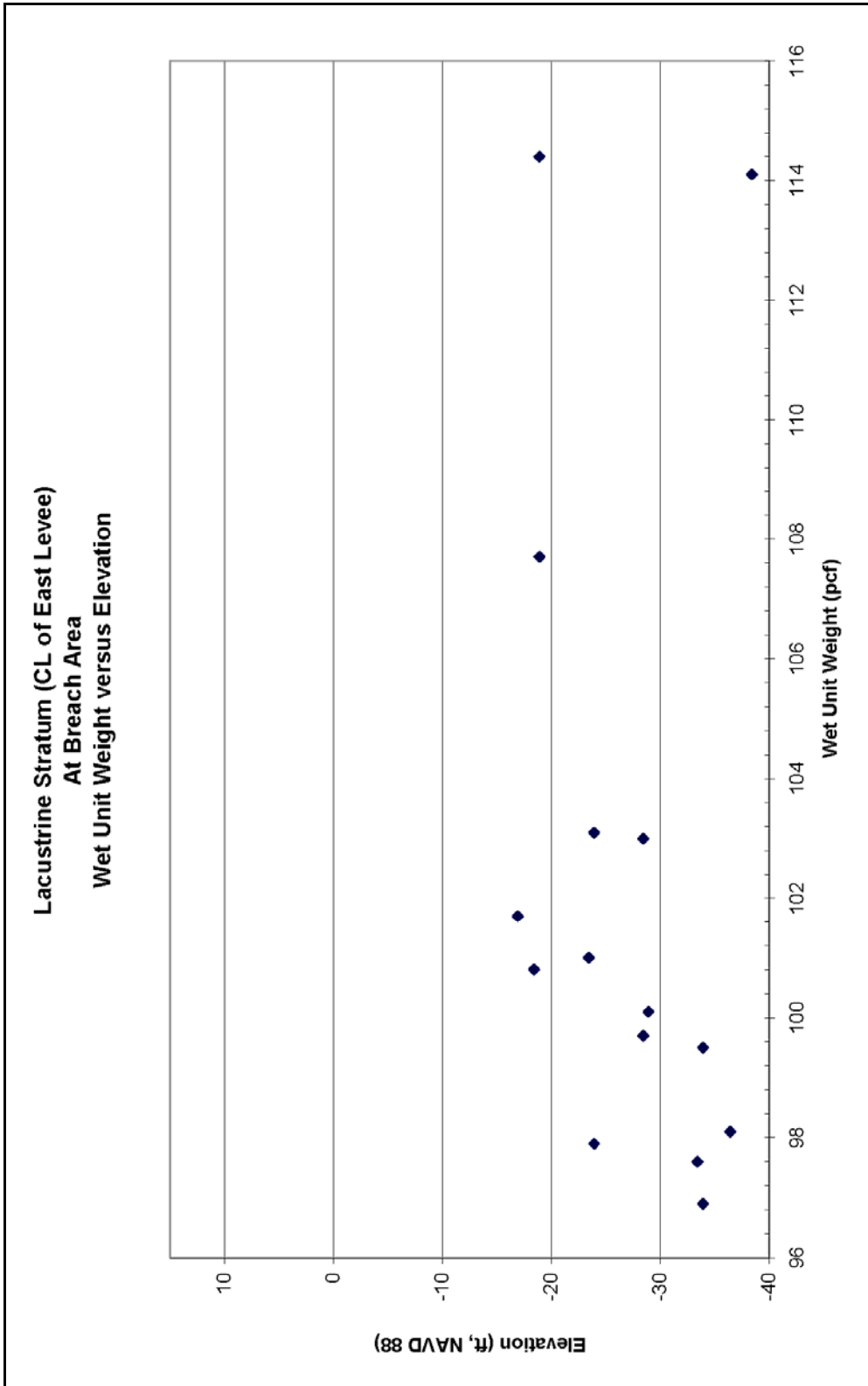


Figure K1-46. Lacustrine Stratum (CL of East Levee – At Breach Area), Wet Unit Weight versus Elevation

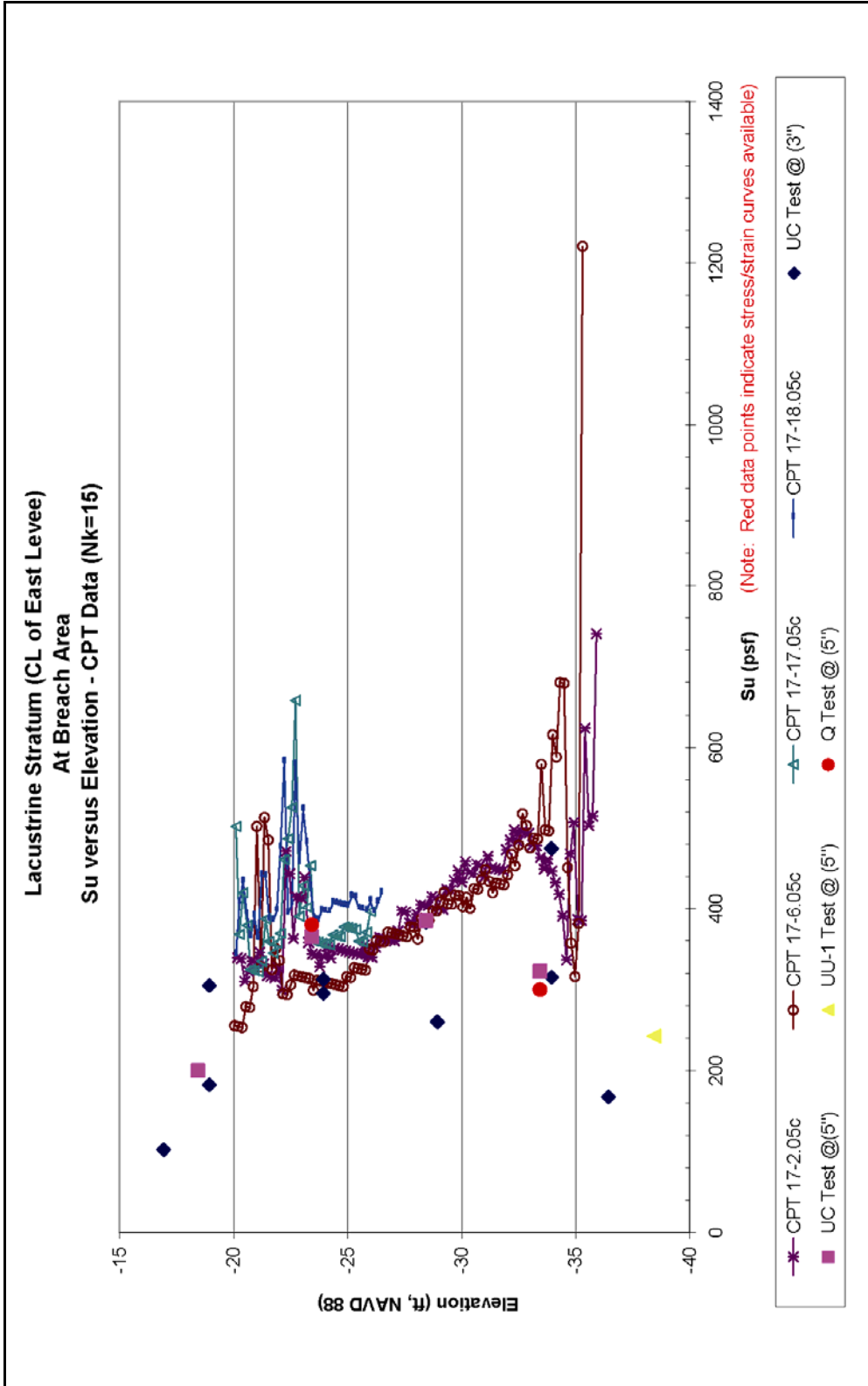


Figure K1-47. Lacustrine Stratum (CL of East Levee – At Breach Area), Su versus Elevation (CPT Data – Nk=15)

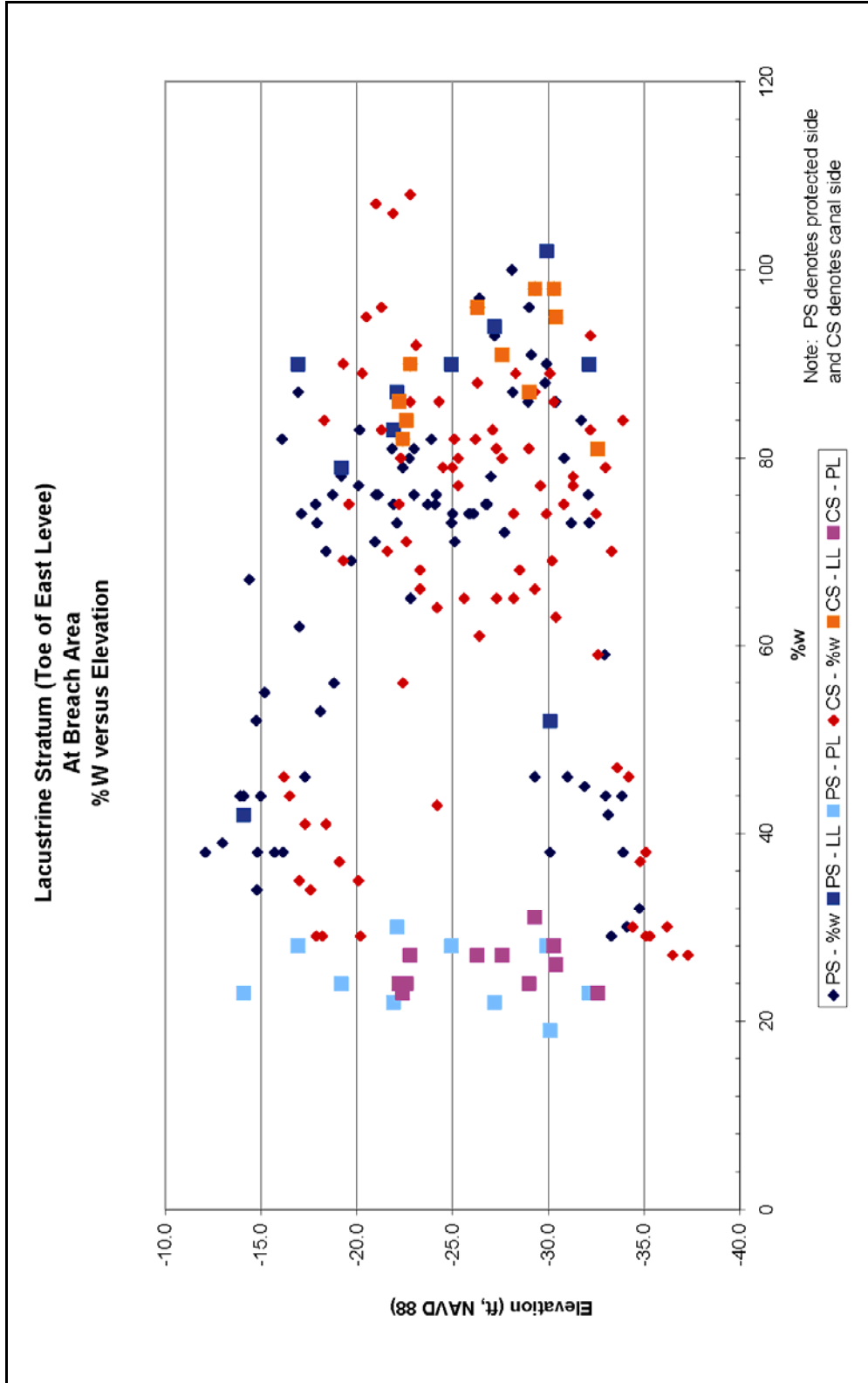


Figure K1-48. Lacustrine Stratum (Toe of East Levee – At Breach Area), %w versus Elevation

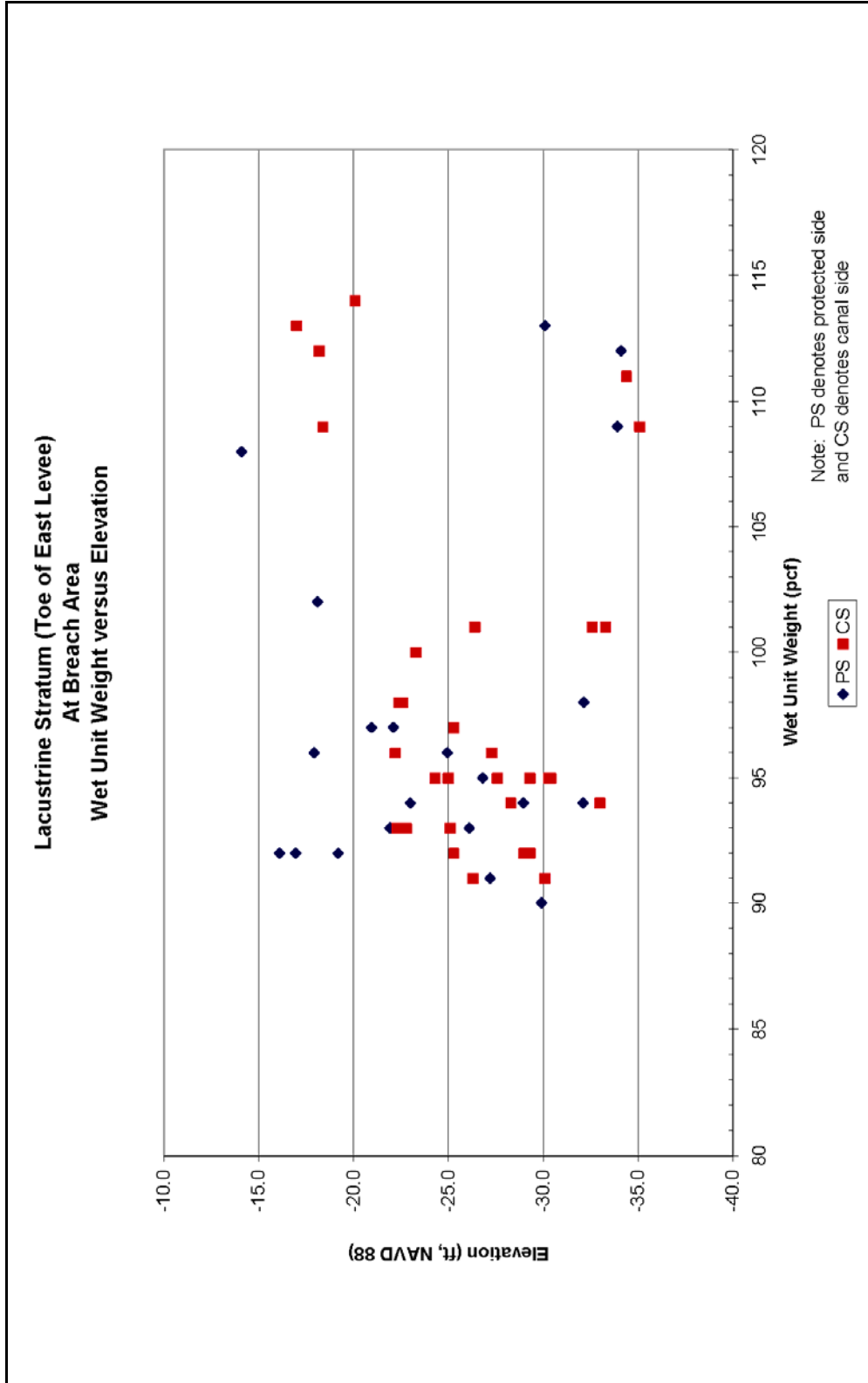


Figure K1-49. Lacustrine Stratum (Toe of East Levee – At Breach Area), Wet Unit Weight versus Elevation

The undrained shear strength determined from the laboratory tests conducted on samples in the breach area is shown in Figure K1-50. The Su/P ratio for the shear strengths samples is shown in Figure K1-51.

Beach Sand Stratum. Forty standard penetration tests (SPT) were conducted in the beach sand stratum in the breach area. The field (uncorrected) standard penetration number for the beach sand stratum is shown in Figure K1-48. Interpretation of the SPT number from the CPTs will be provided later. Dissipation tests with the CPT were conducted at this stratum at 17-2.05c and 17-6.05c. At 17-2.05c, the head in the sand was about 7.8 ft below the top of the hole or at elevation -3.68 (NAVD 88). At 17-6.05c, the head in the sand was about 6 ft below the top of the hole or at elevation -1.3 (NAVD 88).

Assessment of Shear Strength Data

The assessment of strength data described in the following sections had three objectives:

1. To develop a “shear strength model” for use in stability analyses and soil-structure interaction analyses of the I-walls at the 17th Street Canal, using all data available in February 2006. This strength model includes strengths for the levee fill, the strengths of the peat, the clay, and the sand in the foundation.
2. To compare this strength model to the strength model that was used for design of the I-walls in the area where the breach occurred.
3. To compare the strengths in the breach area with strengths in other sections of the 17th Street Canal I-wall.

Stratigraphy

The northern section of the 17th Street Canal where the breach occurred is shown in the longitudinal sections in Figures K1-7, K1-8, and K1-9, and by the cross sections for Station 8+30 (Figure K1-11), Station 10+00 (Figure K1-12), and Station 11+50 (Figure K1-13).

The levee fill is compacted CL or CH material, with an average Liquid Limit of about 45. The average moist unit weight of the fill is about 110 pcf.

Beneath the fill is a layer of peat or “marsh” 5 ft to 10 ft thick. The peat is composed of organic material from the cypress swamp that occupied the area, together with silt and clay deposited in the marsh. The average moist unit weight of the peat is about 80 pcf. Water contents of the peat are as high as 737%, the average water content is approximately 112%. The peat is fibrous at the top of the layer, and more amorphous near the bottom, indicating more advanced decomposition of the older organic materials at depth.

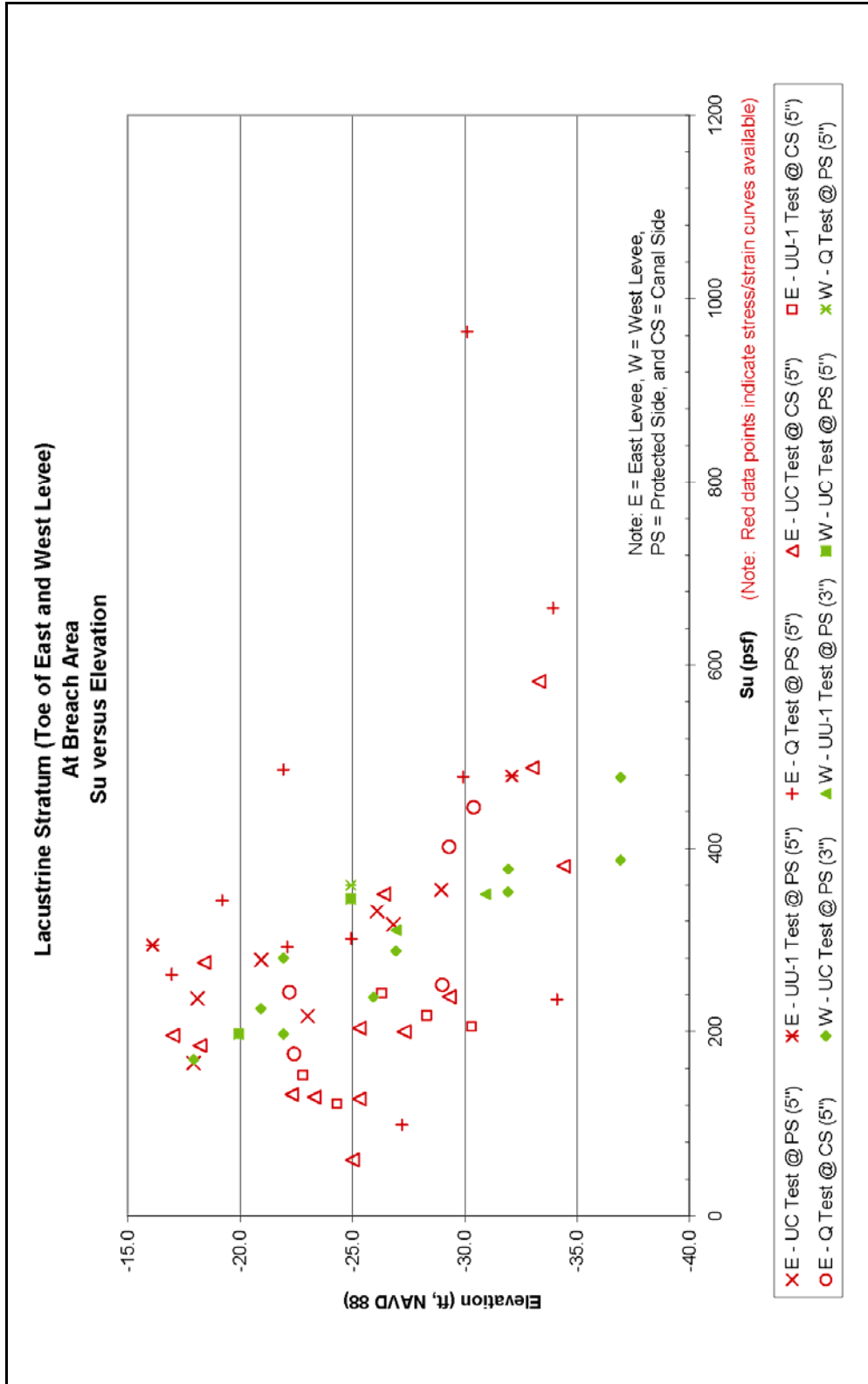


Figure K1-50. Lacustrine Stratum (Toe of East and West Levee – At Breach Area), Su versus Elevation

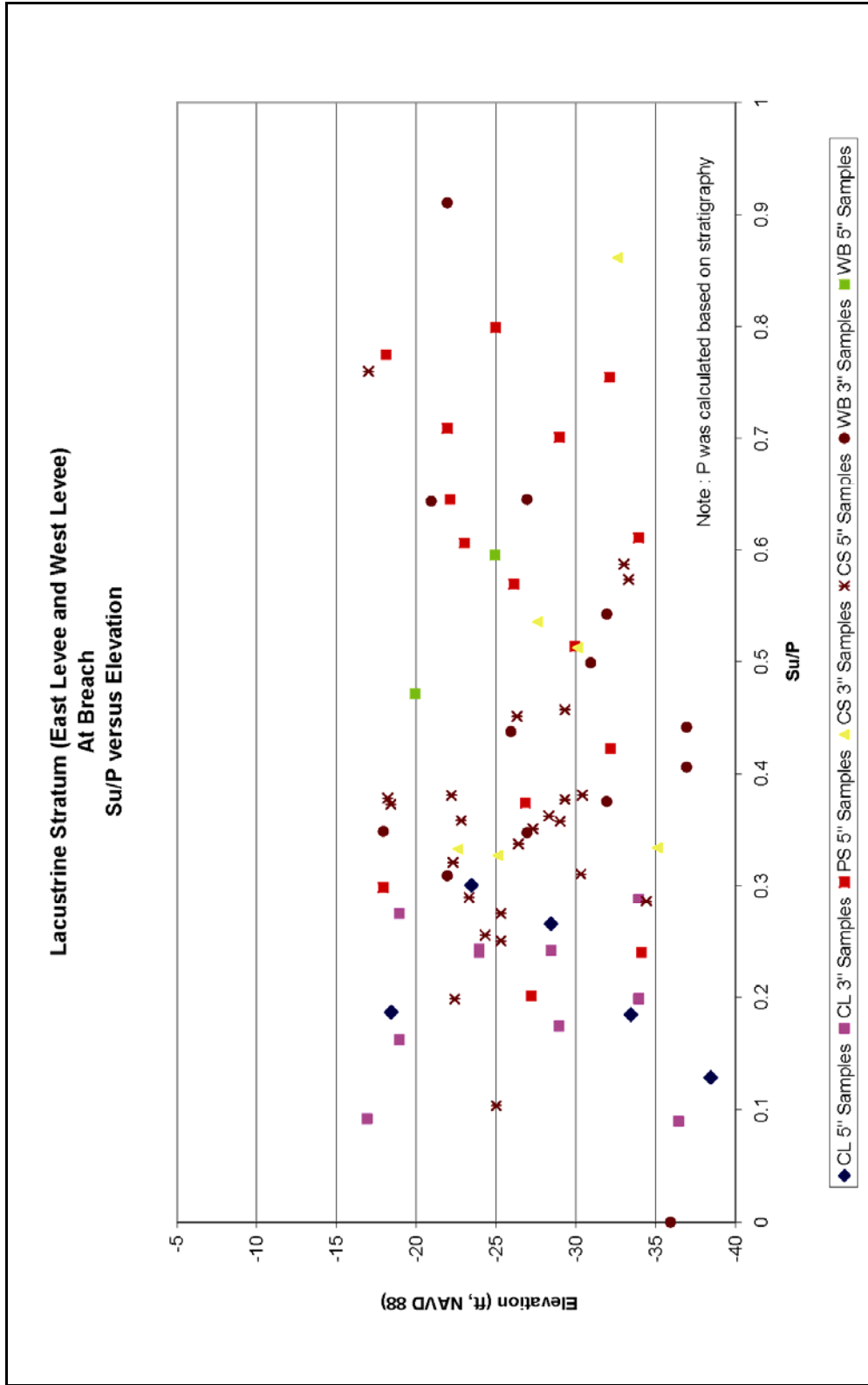


Figure K1-51. Lacustrine Stratum (East and West Levee), Su/P ratio versus Elevation

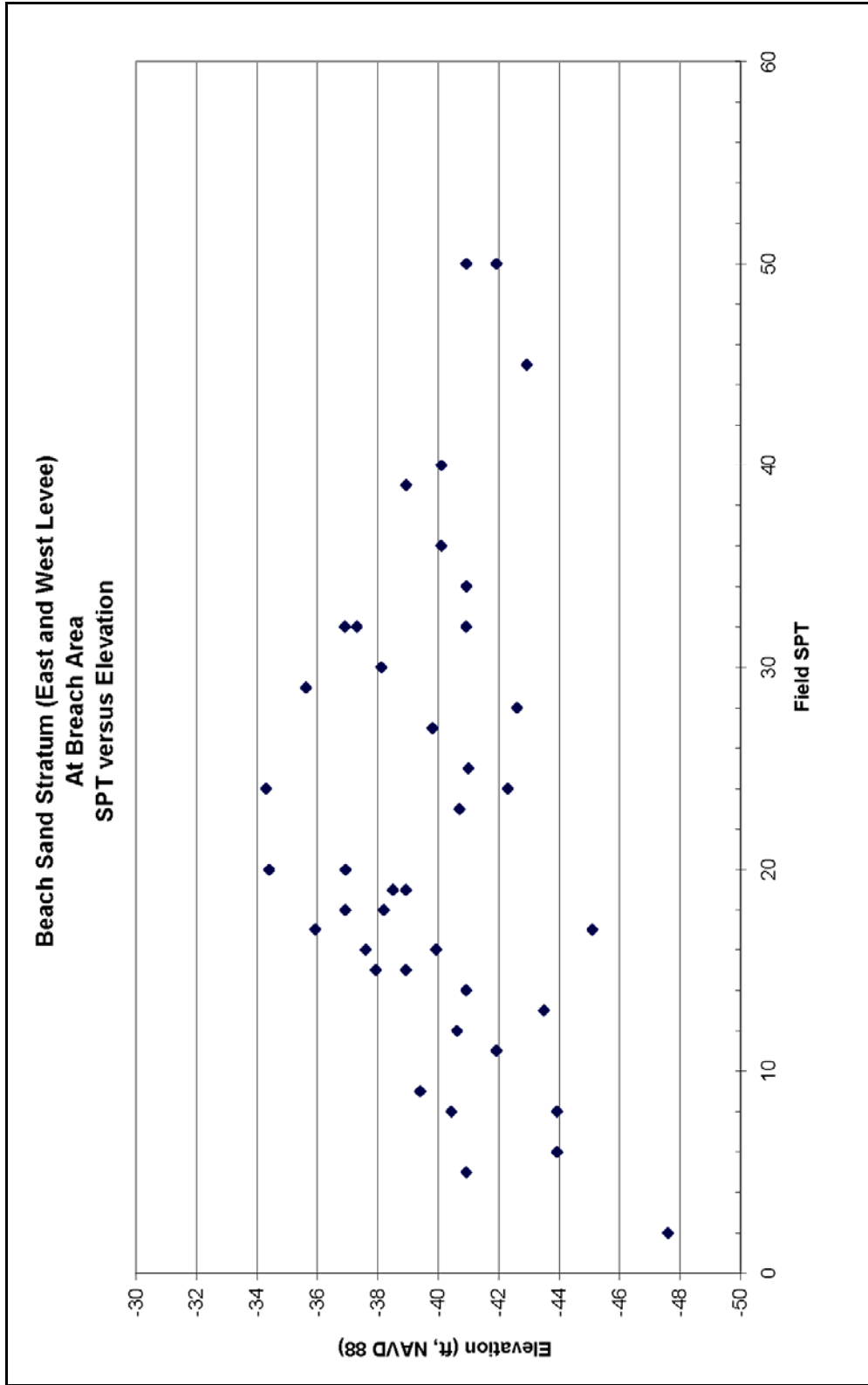


Figure K1-52. Beach Sand Stratum (East and West Levee – At Breach Area), Field SPT versus Elevation

Beneath the peat is a clay or “lacustrine” layer, with an average Liquid Limit of about 95%. The clay is normally consolidated throughout its depth, having been covered and kept wet by the overlying layer of peat. The average moist unit weight of the clay is about 109 pcf, and the average water content is approximately 65%.

Beneath the clay is a layer of Pine Island Beach sand, a silty sand with Standard Penetration blow counts ranging from 2 to 50. This layer is not involved in observed or calculated mechanisms of instability, and its strength is therefore of little importance in stability analyses, except as a more resistant layer beneath the clay.

Sources of information on shear strengths

A considerable number of borings were drilled in the breach area and in neighboring areas before the failure. Additional borings have been drilled, cone penetration tests have been performed, and test pits have been excavated since the failure.

Several hundred unconfined compression tests, UU tests performed using only one confining pressure rather than a range of confining pressures (called UU-1 tests), and conventional UU tests performed using a range of confining pressures have been conducted on the soils at the site. Tests were performed on specimens trimmed from three-inch and five-inch diameter samples. Statistical analyses have been performed on the data from these tests to compute minimum, maximum, and average values of strength, and standard deviations of strength for the levee fill, the peat, and the clay.

Four cone penetration tests with pore pressure measurements (CPTU tests) were performed near the area of the breach after the failure, which have proven to be very useful for evaluating the undrained strength of the clay, and for distinguishing the clay from the overlying peat and the underlying sand.

The evaluation described here focused on undrained shear strengths of the levee fill, the peat and the clay. Because the water loads that resulted in failure of the I-walls increased over a period of hours, there is little doubt that the levee fill and the clay beneath the peat were undrained during the event. Determining whether the peat should be modeled as drained or undrained will require laboratory consolidation tests to determine how quickly it drains when subjected to changes in load. Those tests are being performed at this time. The discussion below considers only undrained strength of the peat. If it is determined that the drained strength, or partially drained strength, is more appropriate for the peat, additional tests will be needed.

Shear strength of levee fill

Data is available from two borings in the breach area (Borings 62 and 64) and several more in the neighborhood of the breach. In all, about 125 strength

tests were performed on the fill materials. Much of the fill is below the static water table, and an $s_u = c$, $\phi_u = 0$ strength interpretation is therefore appropriate. Shear strengths measured in unconfined compression tests are lower than those measured in UU-1 or UU tests.

The measured shear strengths scatter very widely, from about 120 psf to more than 5,000 psf. With such widely scattered values, an average value may not be meaningful, and considerable judgment is needed to select a representative value. Placing greatest emphasis on data from UU tests on five-inch diameter samples, $s_u = 900$ psf appears to be a reasonable value to represent the levee fill. This strength can be compared to a value of 500 psf used in the design analyses.

Shear strength of peat

The peat (or marsh) deposit is stronger beneath the levee crest where it had been consolidated under the weight of the levee, and weaker at the toe of the levee and beyond, where it has not been compressed. The same types of tests were used to measure peat strengths as were used for fill strengths, and samples were performed on three-inch and five-inch diameter samples. Tests were also performed on two-inch diameter samples, but these were not included in the evaluation described here, because it was considered that such small samples would likely be too disturbed to be representative of field conditions.

The measured shear strengths scatter very widely, from about 50 psf to about 920 psf. Values of $s_u = 400$ psf beneath the levee crest, and $s_u = 300$ psf beneath the levee toe appear to be reasonably representative of the measured values. These strengths can be compared to a value of 280 psf used in the design analyses.

Shear strength of clay

The clay is normally consolidated, and its undrained shear strength increases with depth. Figure K1-53 shows variations of undrained shear strength with depth determined using Mayne's method (Mayne 2003)¹. Mayne's method uses the relationship among undrained strength, effective overburden pressure, and preconsolidation pressure that was proposed by Ladd (1991)², and has been found to give more reasonable values of undrained shear strength than use of constant values of the cone factors N_k or N_{kt} .

Whereas other methods of interpreting undrained shear strength from cone results are based on bearing capacity theory, Mayne's method considers tip resistance in relation to pore pressure and overburden pressure. For this reason it does not correspond to a single value of N_{kt} .

¹ Mayne, P. W. (2003). "Class 'A' Footing Response Prediction from Seismic Cone Tests," Proceedings, Deformation Characteristics of Geomaterials, Vol. 1, Lyon, France.

² Ladd, C. C. (1991) "Stability Evaluation During Staged Construction," Terzaghi Lecture, ASCE Journal of Geotechnical Engineering, 117 (4), 540-615.

With Mayne's method, the undrained shear strength is related to cone tip resistance by the equation

$$s_u = 0.091(\sigma'_v)^{0.2} (q_t - \sigma_v)^{0.8} \quad (1)$$

where s_u = undrained shear strength, σ'_v = effective vertical stress, q_t = total cone tip resistance adjusted for pore pressure effects, and σ_v = total vertical stress.

The undrained shear strength calculated with this method is assumed to be equal to that measured using Direct Simple Shear (DSS) tests. This strength is lower than that measured by conventional triaxial compression tests and greater than that measured by triaxial extension tests. Ladd (1991) suggests that this is a reasonable average value for design purposes.

For the soft and very soft clay along the 17th Street Canal, the values of undrained shear strength are very close to values calculated using $N_{kt} = 15$, a value often used for computing undrained strengths of soft clays from CPTU test results.

As shown in Figure K1-53, the variations of undrained strength with depth within the clay computed using Equation (1) are very nearly the same for all four CPTU tests. The straight line representing the average undrained shear strength in the clay has a slope of 11 psf per foot of depth. This rate of strength increase with depth compares to values of 8.4 psf per foot of depth to 13.5 psf per foot of depth determined using laboratory strength test results for samples from borings B-1, B-2, B-3, B-4, and B-6, which appeared to have the most consistent test results.

The rate of increase of strength with depth is directly related to the s_u/p' ratio for the clay, and its buoyant unit weight, as follows:

$$\frac{s_u}{p'} = \frac{\text{rate of increase of } s_u \text{ with depth}}{\text{rate of increase of } p' \text{ with depth}} = \frac{\Delta s_u / \Delta z}{\gamma_{\text{buoyant}}} \quad (2)$$

The value of γ_{buoyant} for the clay is $109 \text{ pcf} - 62.4 \text{ pcf} = 46.6 \text{ pcf}$. Thus the value of s_u/p' is:

$$\frac{s_u}{p'} = \frac{11 \text{ psf per ft}}{46.6 \text{ pcf}} = 0.24 \quad (3)$$

which is a reasonable value for this normally consolidated clay.

These values provide a good basis for establishing undrained strength profiles in the clay. The undrained strength at the top of the clay is equal to 0.24 times the effective overburden pressure at the top of the clay, and the undrained strength increases with depth in the clay at a rate of 11 psf per foot. With this model, the undrained shear strength of the clay varies with lateral position, being greatest beneath the levee crest where the effective overburden pressure is

greatest, and varying with depth, increasing at a rate of 11 psf per foot at all locations.

This model does not consider details of the stress distribution beneath the levee, which would result in “load spread” effects. These effects would result in rotation of principal stresses beneath the levee, and in components of stress due to the levee load decreasing with depth. Including these complex effects would complicate the model considerably. In our opinion, such refinement would make the model impractical, and is not justified. The model described in the previous paragraphs uses a simple stress distribution beneath the levee that satisfies vertical equilibrium, and it reflects the fact that the undrained strength is proportional to consolidation pressure, certainly the most important aspect of the strength of the clay.

The computer program SLIDE¹ uses two-dimensional interpolation to compute strengths that vary in both the horizontal and vertical direction, as is the case with the strength model described above. This feature provides a convenient means for representing the New Orleans levee clay strengths in stability analyses performed with SLIDE.

Shear strength of sand

Correlations with Cone Penetration tip resistance were used to estimate a value of $\phi' = 35$ degrees for the silty sand beneath the clay. As noted previously, the sand layer is not involved in observed or computed failure mechanisms, and the value of ϕ' assigned to it therefore has no influence on computed factors of safety.

Comparison with strengths used in design

The design analyses used undrained strengths for the levee fill, the peat, and the clay, and a drained friction angle to characterize the strength of the sand layer beneath the clay, as does the strength model described above. Thus the strengths are directly comparable.

The values of strength for the levee fill, the peat, and the sand that were used in the design analyses for the 17th Street Canal I-wall, Stations 552+70 to 635+00 (new Stations 0+00 to 82+30) are shown in Table K1-2. This interval includes the breach area, which extends approximately from new Station 7+50 to new Station 12+20.

¹ Available from Rocscience Inc., 31 Balsam Avenue, Toronto, Ontario, Canada M4E 3B5

The design strength values shown in Table K1-2 are taken from Plate 56 of the 17th Street Canal Geotechnical Design Memorandum (GDM)¹. Also shown in Table X are the values of strength from the strength model discussed above.

| Table K1-2 Comparison of strengths of levee fill, peat and sand used in design for Stations 552+70 to 635+00 with the strength model based on all data available in February 2006 | | |
|--|-----------------------------------|--|
| Material | Strength uses for design | Strength model based on all data available in February 2006 |
| Levee fill | $s_u = 500 \text{ psf}, \phi = 0$ | $s_u = 900 \text{ psf}, \phi = 0$ |
| Peat | $s_u = 280 \text{ psf}, \phi = 0$ | $s_u = 400 \text{ psf}, \phi = 0$ beneath levee crest $s_u = 300 \text{ psf}, \phi = 0$ beneath levee toe |
| Sand | $\phi' = 30 \text{ degrees}$ | $\phi' = 35 \text{ degrees}$ |

It can be seen that the strengths for the levee fill, the peat and the sand used in design are consistently lower than those estimated using all of the data available in February 2006.

The values of strength for the clay vary with depth and laterally, as discussed above. The values of undrained strength used in design are compared with those described above in Figures K1-54, K1-55, and K1-56. These figures show the strengths for the strength model discussed previously as dotted lines, superimposed on photocopies of the GDM figure. Minor variations in the strengths at Stations 8+30, 10+00 and 11+50 occur because the thicknesses of the levee fill and peat are slightly different in the three cross sections, and the effective stresses at the top of the clay are therefore slightly different.

In each of the three cases the rate of increase of strength with depth (11 psf per foot) are essentially the same in the strength model as for the design strengths. Beneath the levee crest, the design strengths are very close to those determined from the strength model. At the toe of the levee, however, the strengths used in design are considerably higher than the strengths from the strength model.

Comparison of strengths within the breach area with strengths elsewhere

Field observations and preliminary analyses show that the most important shear strength is the undrained strength of the clay. Critical slip surfaces intersect only small sections within the peat and the levee fill, and do not intersect the sand layer beneath the clay at all. Therefore the strengths of these materials have small influence on stability, and minor variations in these strengths from section to section would not control the location of the failure.

¹ Design Memorandum No. 20, General Design, Orleans Parish – Jefferson Parish, 17th Street Outfall Canal, U. S. Army Engineer District, New Orleans, March 1990.

For this reason, the comparison of strengths in the breach area with strengths elsewhere has been focused on the undrained strength of the clay.

Within the breach area, only two borings drilled before the failure (Borings 62 and 64) are available. The strengths measured on undisturbed specimens from these borings are listed in Table K1-3.

| Table K1-3 | | | |
|--|------------------|---|----------------|
| Undrained strengths of clay for specimens from the breach area. | | | |
| Boring 62 | | | |
| Depth | Test type | s_u | Average |
| 24 ft | UC | 305 psf | 280 psf |
| 34 ft | UC | 260 psf | |
| 42 ft | UU-1 | 178 psf (very loose clayey sand – ignore) | |
| Boring 64 | | | |
| Depth | Test type | s_u | Average |
| 22 ft | UC | 103 psf | 240 psf |
| 33.5 ft | UC | 383 psf | |
| 41.5 ft | UC | 168 psf (likely disturbed – ignore) | |

The strengths summarized in Table K1-3 can be compared with the strengths of specimens from borings to the north and south of the breach, which are summarized in Tables K1-4 and K1-5.

| Table K1-4 | | | |
|---|------------------|--|----------------|
| Undrained strengths of clay for specimens from borings north of the breach area. | | | |
| Boring 66 | | | |
| Depth | Test type | s_u | Average |
| 28.5 ft | UC | 235 psf | 317 psf |
| 38.5 ft | UC | 398 psf | |
| Boring 68 | | | |
| Depth | Test type | s_u | Average |
| 33 ft | UC | 340 psf | 353 psf |
| 33 ft | UU | 360 psf | |
| 39 ft | UU | 360 psf | |
| 42.5 ft | UU-1 | 250 psf (likely sand, not clay – ignore) | |
| 42.5 ft | UU | 240 psf (likely sand, not clay - ignore) | |

| Table K1-5 Undrained strengths of clay for specimens from borings south of the breach area. | | | |
|--|------------------|--------------------------------------|----------------|
| Boring 60 | | | |
| Depth | Test type | s_u | Average |
| 24 ft | UC | 200 psf | 326 psf |
| 29 ft | UC | 365 psf | |
| 29 ft | UU | 380 psf | |
| 34 ft | UC | 385 psf | |
| 39 ft | UC | 323 psf | |
| 39 UU | UU | 300 psf | |
| 44 ft | UU-1 | 243 psf (loose clayey sand – ignore) | |
| Boring 58 | | | |
| Depth | Test type | s_u | Average |
| 24 ft | UC | 183 psf | 324 psf |
| 29 ft | UC | 313 psf | |
| 39 ft | UC | 475 psf | |
| Boring 56 | | | |
| Depth | Test type | s_u | Average |
| 29 ft | UC | 295 psf | 305 psf |
| 39 ft | UC | 315 psf | |

The average strengths from Tables K1-3, K1-4, and K1-5 are compared in Table K1-6 and Figure K1-57.

| Table K1-6 Comparison of undrained strengths from breach area borings with strengths from borings north and south of the breach. | | |
|---|-------------------------------|------------------------------|
| Area | Range of s_u | Average s_u |
| Breach (Borings 62 and 64) | 240 psf to 280 psf | 260 psf |
| North of breach (Borings 66 and 68) | 317 psf to 353 psf | 335 psf |
| South of breach (Borings 56, 58 and 60) | 305 psf to 326 psf | 318 psf |

Although the data is sparse, it is fairly consistent, and it appears that the clay strengths in the areas north and south of the breach are higher than those in the breach. Based on the average values shown in Table X4 and Figure X4, the undrained strengths of the clay in the areas adjacent to the breach are 20% to 30% higher than those in the breach area. Strength differences of this magnitude are significant. They indicate that the reason the failure occurred where it did is very likely that the clay strengths in that area were lower than in adjacent areas to the north and south.

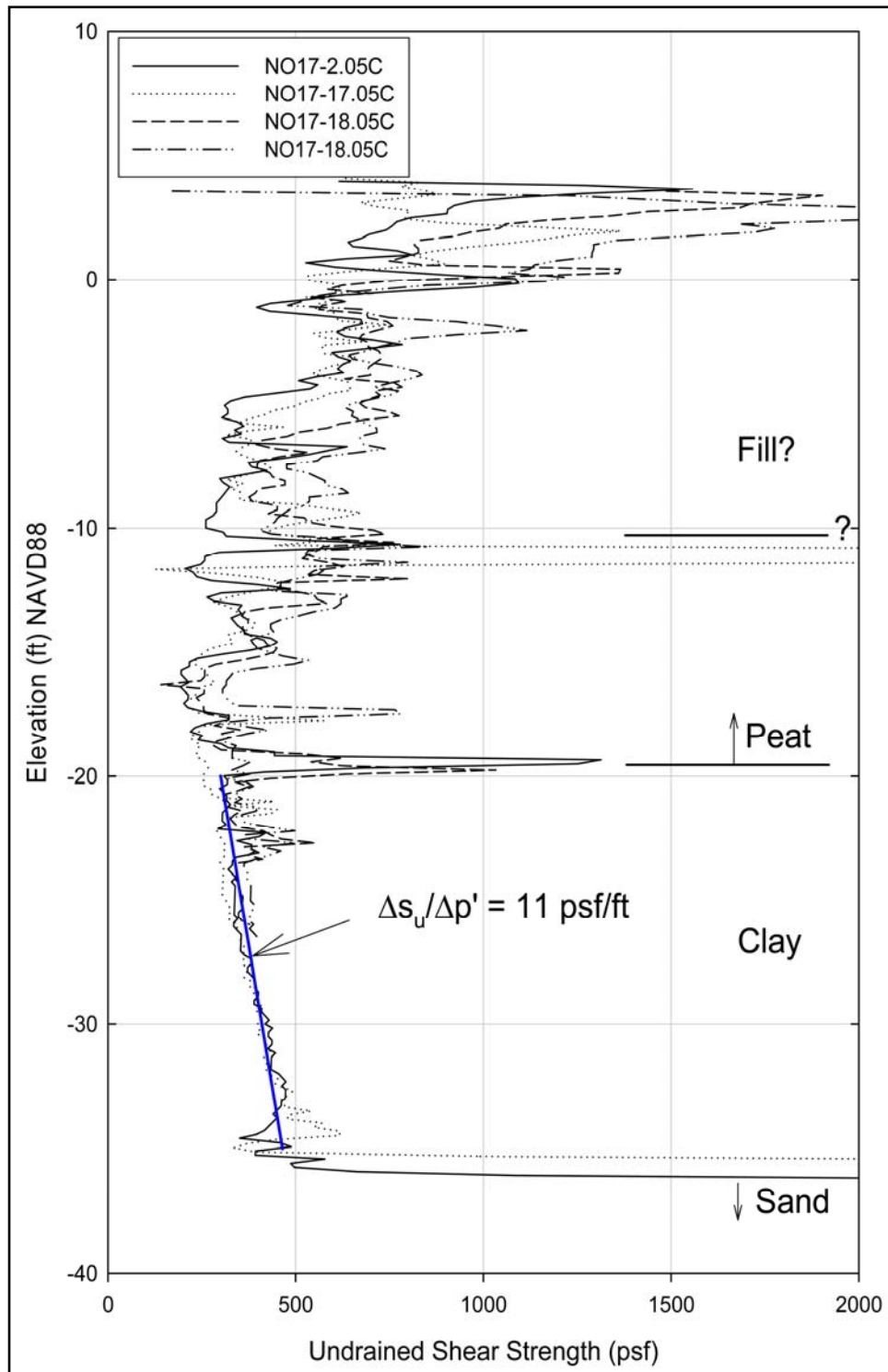


Figure K1-53. Undrained shear strength calculated from CPTU tests using Mayne's method.

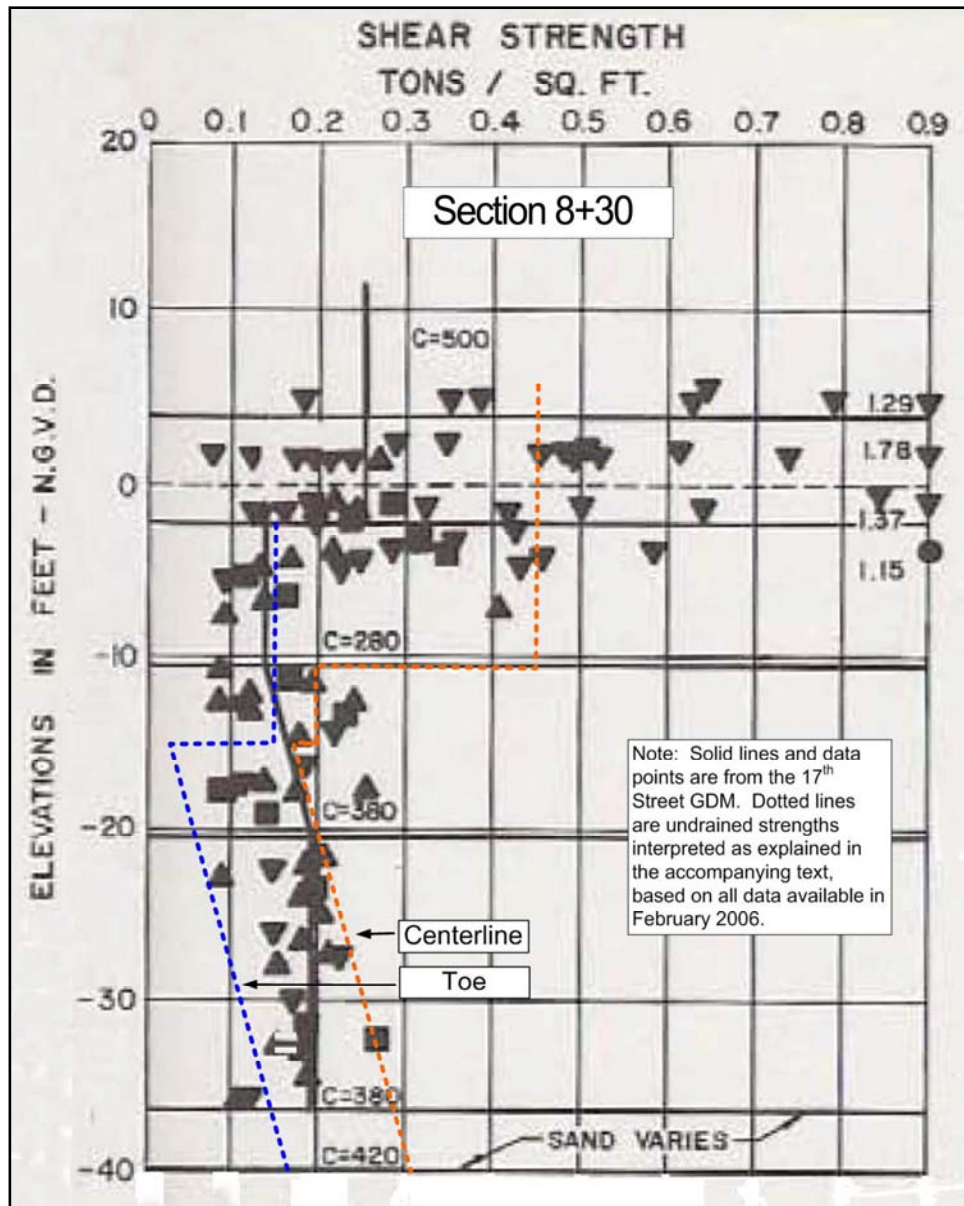


Figure K1-54. Comparison of undrained shear strength profiles used for 17th Street I-wall design with strength profiles interpreted from data available in February 2006, for Section 8+30.

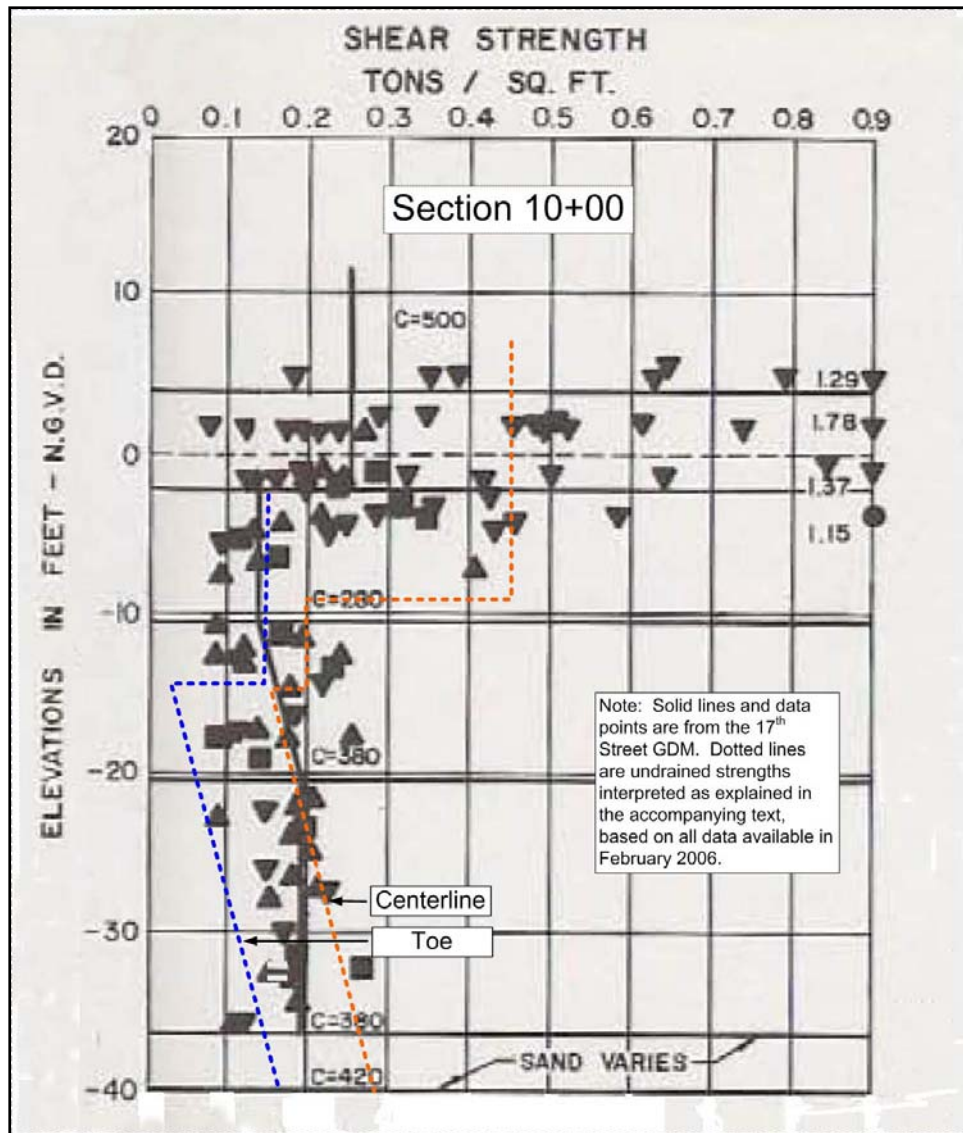


Figure K1-55. Comparison of undrained shear strength profiles used for 17th Street I-wall design with strength profiles interpreted from data available in February 2006, for Section 10+00.

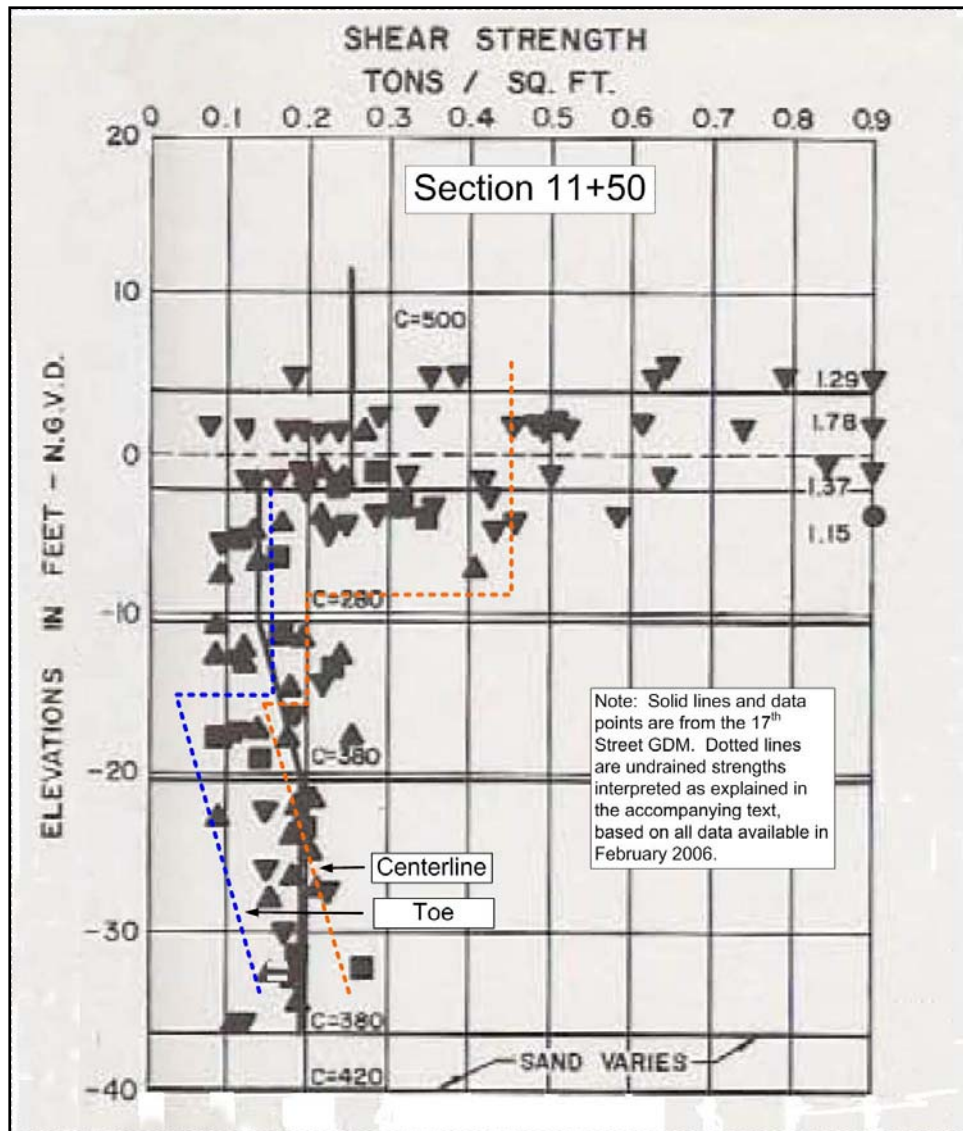


Figure K1-56. Comparison of undrained shear strength profiles used for 17th Street I-wall design with strength profiles interpreted from data available in February 2006, for Section 11+50.

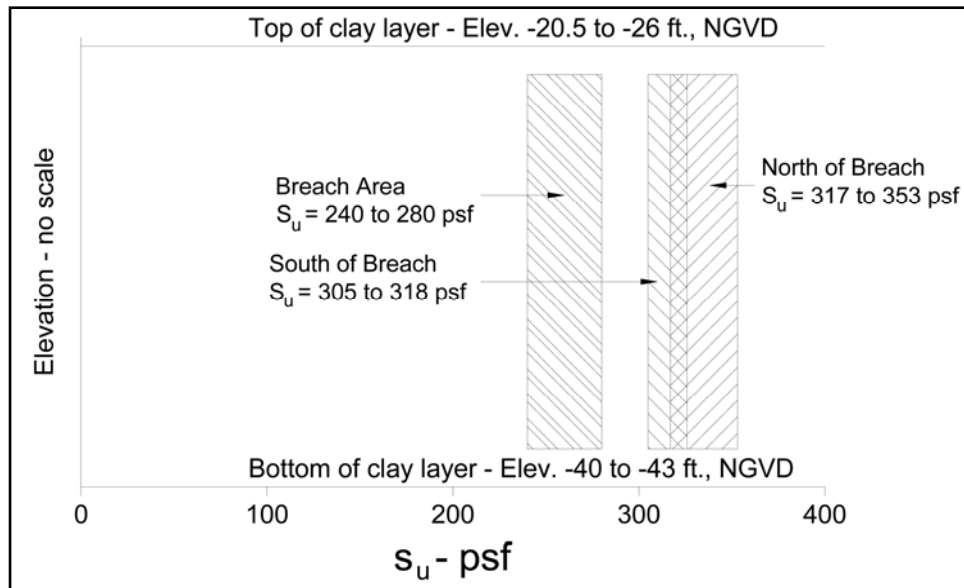


Figure K1-57. Comparison of undrained strengths from breach area borings with strengths from borings north and south of breach.

Appendix A: Description of New Orleans Area Geology, Environments of Deposition, and General Engineer Properties of these Environments

Extracted from

Dunbar, J. B., Torrey, V. H., III, Wakeley, L. D., 1999. "A Case History of Embankment Failure, Geological and Geotechnical Aspects of the Celotex Levee Failure, New Orleans, Louisiana," Technical Report GL-99-11, Engineer Research and Development Center, Waterways Experiment Station, Vicksburg, Mississippi

1 Introduction

The following summary describes the geology and the Holocene history of the New Orleans area, and the relationships between the associated environments of deposition and general engineering properties. This information has been extracted from a technical report on the geological and geotechnical aspects of the Celotex Levee failure, which occurred along the west bank of the Mississippi River in 1985 in the greater New Orleans area (Figure 1). Only the geology sections are presented in this Appendix. This information serves as background information for evaluation of the various canal failures during Hurricane Katrina.

The geologic portions of the Celotex Report were presented in Chapter 2 and Appendix A. Chapter 2 describes the geologic history and geology of the New Orleans area as determined from a review of the technical literature, an evaluation of numerous engineering borings, aerial photo interpretation, and preparation of several detailed cross-sections (Figures 2 through 5 of Chapter 2, see enclosed). Appendix A of this same report provides detailed descriptions and information about the engineering properties of the depositional environments that are present at the surface and in the subsurface. Chapter 2 and Appendix A are presented here in their original order of presentation because of their logical arrangement in the text. The descriptions of the environments are important when examining soil types and physical properties from the respective environments.

Additionally, various references are identified in the text and are presented at the end of this summary appendix. Many of the Corps of Engineer cited publications and maps for the New Orleans area are now presented at the ERDC website on the Geology of the Lower Mississippi Valley (see lmvmapping.erd.usace.army.mil)

A final note, the lacustrine environment is not identified in the summary description and is an important lithostratigraphic unit. This environment is unique to this area because of the protection afforded by the now buried Pine Island beach complex during the filling of the New Orleans area with subsequent sediment by the various Mississippi River distributary channels during the Middle to Late Holocene. The lacustrine environment has been mapped for the back or northern side of the beach ridge in various GDMs, while the front or seaward side has been mapped as being interdistributary. This distinction is primarily a matter of semantics, as opposed to any significant differences between lithology and/or engineering properties of these respective two environments. For purposes of this discussion and overall context, these two environments are nearly identical. The discussion of the interdistributary environment will be representative for the lacustrine environment identified throughout many of the GDMs.

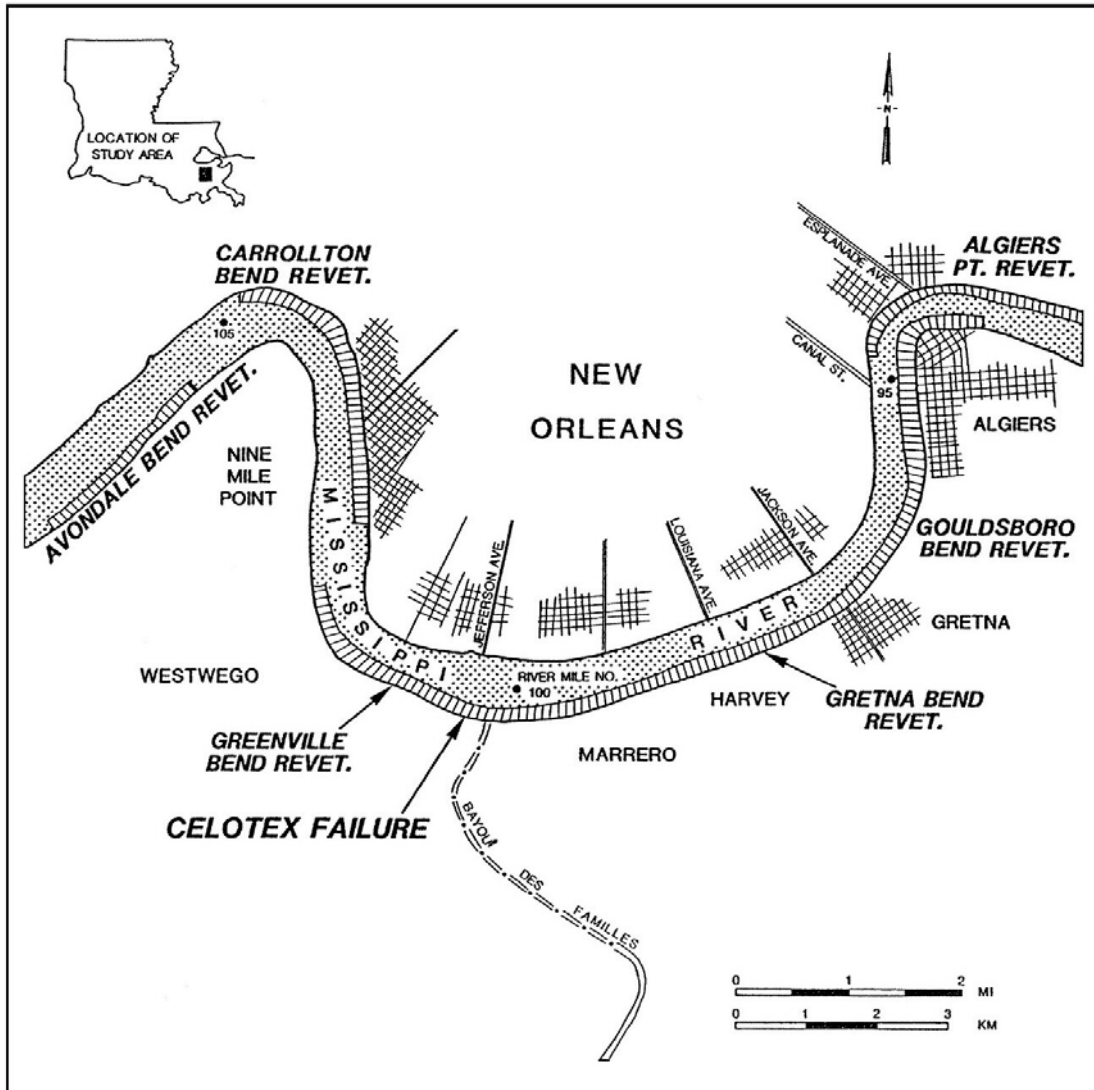


Figure 1. Map of study area showing location of the Celotex levee failure

2 Geology

Physiography

The study area is located in the southern portion of the lower Mississippi Valley and is a part of the Mississippi River's deltaic plain. Broad natural levees associated with the Mississippi River and Bayou des Familles, a prehistoric distributary channel, are the most prominent physiographic features in this area. Surface topography is generally of low relief with surface elevations ranging from approximately 25 ft (7.6 m) NGVD along the levee crests to sea level throughout much of the study area. Over a significant part of the New Orleans Metropolitan area the surface elevation is at or below sea level.

In the New Orleans area, the meander pattern of the Mississippi River is distinctive, making four nearly right angle turns which have changed very little during the past 100 years (Figure 1). The width of the Mississippi River within the study area (river mile 91.0 to 106.0 (146.45 to 170.59 km)) ranges from 1,750 to 2,700 ft (533 to 823 m). The river thalweg elevations through this reach range from -70 ft (-21 m) to about -190 ft (-58 m) NGVD. The top of the bank elevation through the study reach averages about 10 ft (3 m) NGVD. Channel bendways are characterized by deep "permanent" scour pools separated by shallower crossings. Revetment protection along the river corresponds to the deeper scour pools at Avondale, Carrollton, Greenville, Gretna, Gouldsboro, and Algiers (Figure 1).

Geologic Setting and History

The scope of this study permits a summary of the major events to explain the significance of the engineering geology in the study area. The general geologic chronology that has been defined for the Mississippi River's deltaic plain is based upon thousands of engineering borings drilled during the past 50 years, hundreds of radiometric age determinations of organic deltaic sediments, and numerous geologic studies conducted in this region (Fisk 1944; Kolb and Van Lopik 1958a and 1958b; Kolb 1962; Kolb, Smith, and Silva 1975; Autin et al. 1991; Frazier 1967; Saucier 1969 and 1974; May et al. 1984; Dunbar et al. 1994 and 1995; Smith, Dunbar, and Britsch 1986). Boring data identify a diverse surface and subsurface geology that is related to the different course shifts by the Mississippi River and associated deltaic advances during the Holocene (last 10,000 years).

To better understand the geology of the area, it is first necessary to briefly review the geologic history of coastal Louisiana since the late Pleistocene (17,000 to 10,000 years ago). Approximately 17,000 years ago, glaciers covered much of North America and sea level was approximately 300 ft (91 m) below the present level (Kolb, Smith, and Silva 1975). The Gulf shoreline was much farther seaward than at its present location.

The ancestral Mississippi River and its tributaries below Baton Rouge, LA, were entrenched into the underlying Pleistocene surface and had developed a broad drainage basin, approximately 25 miles (40 km) wide, which extended southeasterly beneath the present deltaic plain (Kolb and Van Lopik 1958a). Geologic mapping (Kolb and Van Lopik 1958a and 1958b; May et al. 1984) indicates that the axis of the valley entrenchment occurs in the vicinity of Houma, LA, approximately 45 miles (72 km) southwest of New Orleans.

The underlying Pleistocene surface represents deposits from a much older Mississippi River deltaic plain sequence and associated nearshore environments. These sediments were deposited during the previous interglacial cycle (Sangamon interglacial period), approximately 125,000 to 70,000 years ago. Fisk (1944) collectively called these Pleistocene sediments the Prairie Formation. Sediments of the Prairie Formation outcrop at the surface just north of Lake Pontchartrain.

Sea level began rising approximately 17,000 years ago because of glacial melting and reached its present level between 4,000 and 6,000 years before the present. Rising sea level corresponds to a period of valley-wide aggrading of the ancestral alluvial valley by the existing fluvial systems. Melting glaciers released large quantities of sediment to the Pleistocene drainage system and filled the entrenched valley with coarse sediments (sand and gravel). A dense network of shallow and swiftly flowing braided stream courses formed within the ancestral alluvial valley because of overloading by the massive influx of glacial outwash. Along the length and width of the Lower Mississippi Valley, basal substratum sands are present in the subsurface which represent the relic braided stream or outwash plain sediments from glacial melting (Fisk 1944; Kolb et al. 1968; Krinitzsky and Smith 1969; Saucier 1964 and 1967; Smith and Russ 1974). The change in deposition from a braided system to a meandering Mississippi River system occurred approximately 12,000 years before the present (Saucier 1969; and Krinitzsky and Smith 1969).

Advent of the modern sea level began creation of the modern deltaic plain and led to the present land surface. Present day coastal Louisiana is the product of numerous, but generally short lived, seaward prograding delta systems. These deltas are subsequently reworked by coastal transgressive processes and modified. Five major deltaic systems have been built seaward during the past 6,000 years as shown by Figure 2 (after Frazier 1967). Each delta system consists of several major distributary channels and numerous individual delta lobes (Figure 3). The relative ages of these delta systems are generally well established by radiocarbon dating techniques. Limits of the different delta systems and the chronology of the major distributary channels associated with each system are summarized in Figures 2 and 3 (after Frazier 1967).

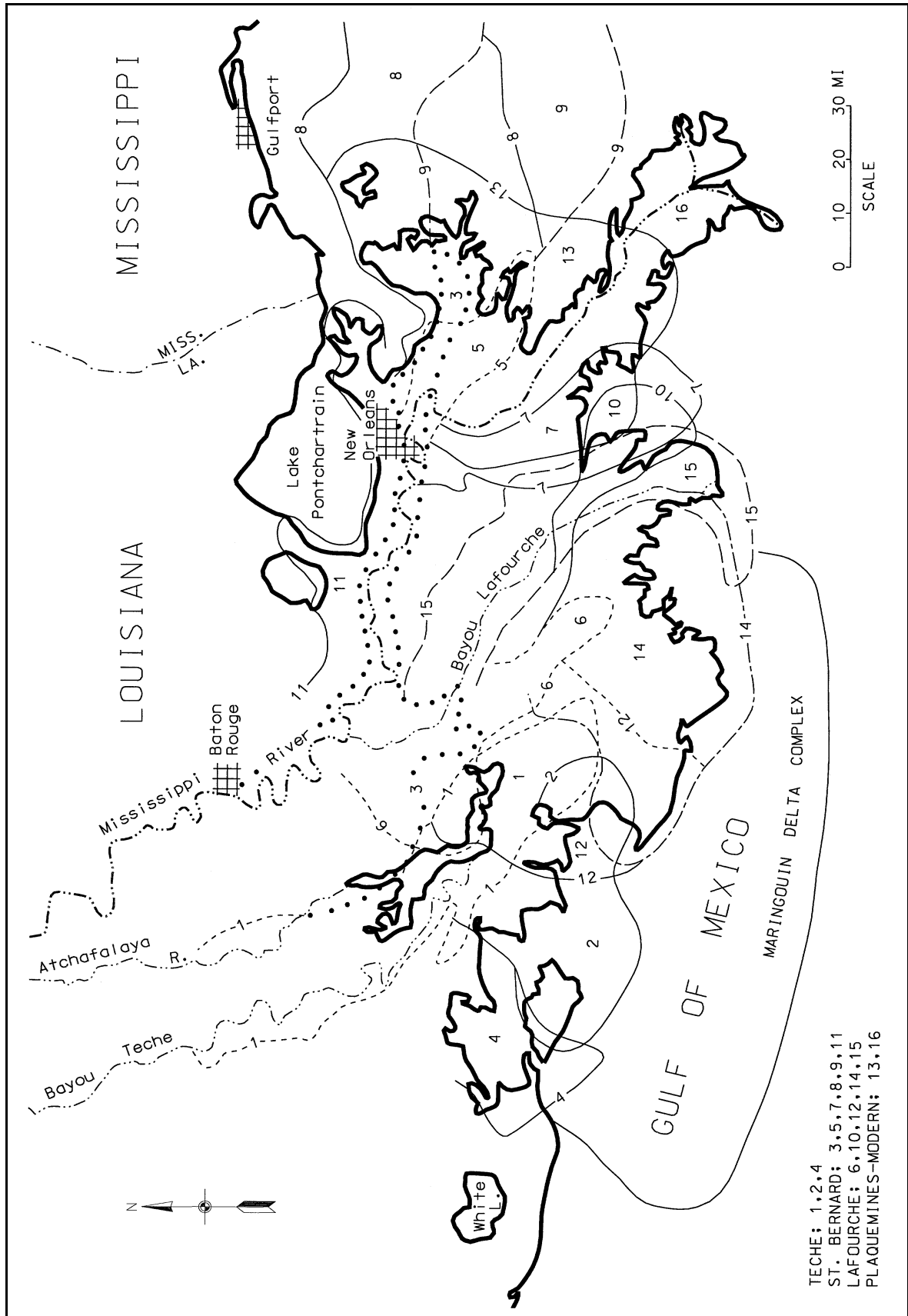


Figure 2. Holocene delta and distributary systems (after Frazier 1967)

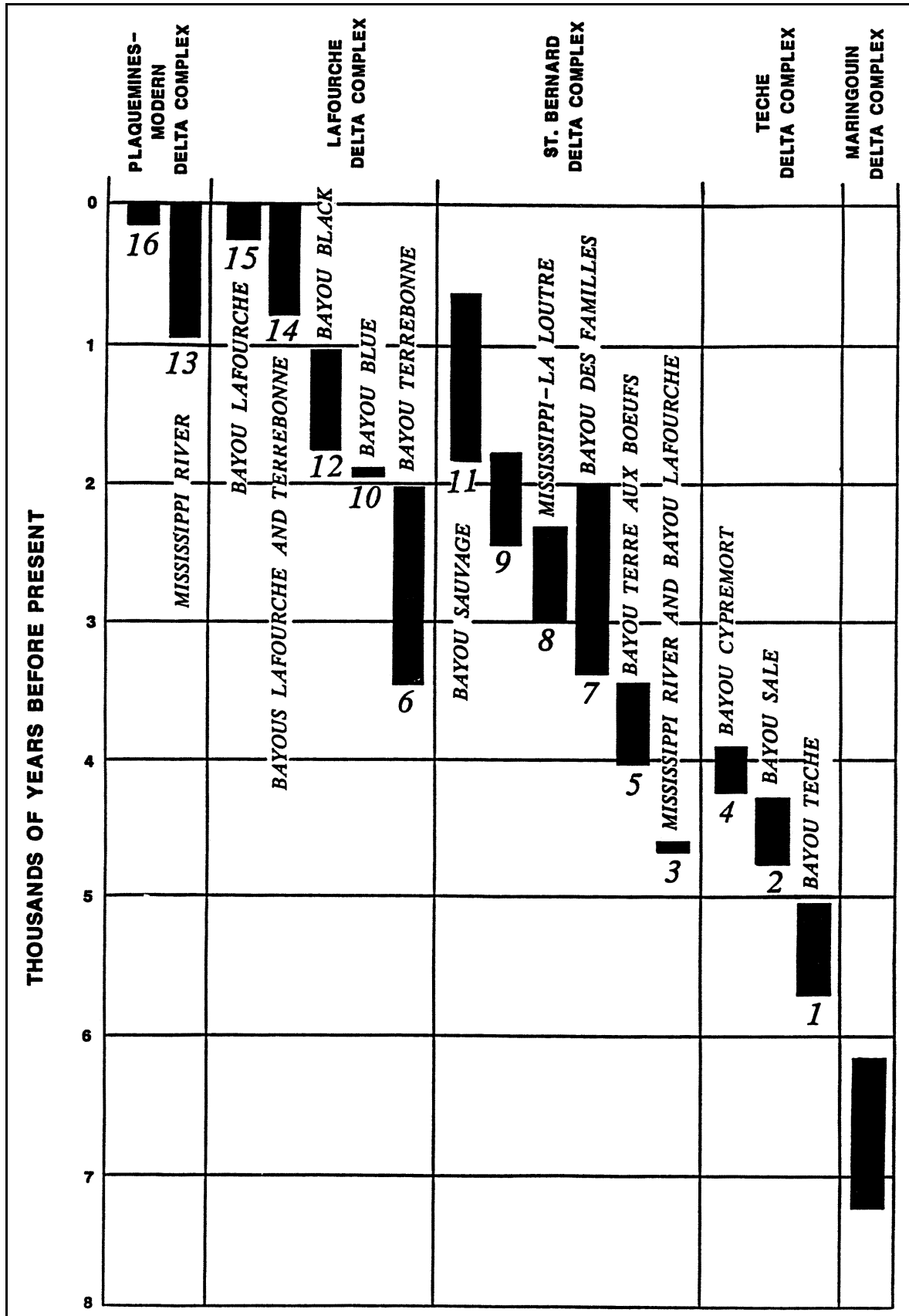


Figure 3. General chronology of Mississippi River delta and distributary systems (after Frazier 1967)

The first advance of a major delta system into the New Orleans area occurred with the St. Bernard system. The present course of the Mississippi River through the New Orleans area was established during the active St. Bernard delta. Partial Mississippi River flow continued to pass through the New Orleans reach following abandonment of the St. Bernard system for the Lafourche delta complex. During the active Lafourche system, the Mississippi River flowed southward at Donaldsonville, through Bayou Lafourche, and to the Gulf of Mexico. After abandonment of the Lafourche system approximately 500 years ago, nearly full Mississippi River flow returned to the present day course.

Geologic Structure

The study area is part of the seaward thickening wedge of Quaternary sediments which dip gently gulfward and fill the Gulf of Mexico geosyncline. Major structures within this sedimentary prism are piercement salt domes and growth faults. In the study area there are no buried salt domes. The vast majority of Louisiana's salt domes are located south and west of the New Orleans area (New Orleans Geological Society 1962 and 1983; and Halbouty 1967).

Faulting has been identified in the subsurface throughout the deltaic plain and in the Pleistocene deposits exposed at the surface north of Lake Pontchartrain (Wallace 1966; and Snead and McCulloh 1984). These faults are not tectonically active. Instead, they are related to sedimentary loading of the Gulf of Mexico basin. Faulting has been identified in the Pleistocene sediments beneath Lake Cataouatche (approximately 8 miles (12.8 km) southwest of New Orleans) and beneath Lake Pontchartrain (Wallace 1966; and Kolb, Smith, and Silva 1975). Fisk (1944) identified several normal faults in the buried Pleistocene sediments beneath New Orleans. He interpreted these faults based on the orientation of stream courses, lake shores, and the Mississippi River. The presence of these faults based solely on this type of evidence is speculative without more detailed stratigraphic evidence to support their existence. Non-tectonic geomorphic and stratigraphic processes can produce these types of linear features without faulting as the underlying mechanism. A detailed engineering study of Pleistocene sediments in the New Orleans area by Kolb, Smith, and Silva (1975) did not identify subsurface faults near the Celotex failure site or for the general New Orleans area. Their study identified only one fault in the New Orleans area (in Lake Pontchartrain) and was based on combined boring and geophysical (subbottom profiling) data.

No faults were identified during this investigation in the study area. Surface faults in Holocene sediments are difficult to detect, because unconsolidated sediments tend to warp rather than shear. Geologic mapping and boring data evaluated during the course of this study did not identify any surface or subsurface faulting in the study area.

Geology and Environments of Deposition

Surface geology

The first objective of this investigation was to map and define the surface and subsurface geology of the study area. Definition of the geology was accomplished by examination and interpretation of historic aerial photography, subsurface data (engineering borings and electrical logs), different hydrographic survey periods, historic maps, and by review of the available geologic literature (Autin et al. 1991; Eustis Engineering Company 1984; Frazier 1967; Kemp 1967; Kolb 1962; Kolb and Van Lopik 1958a and 1958b; Kolb, Smith, and Silva 1975; Kolb and Saucier 1982; Miller 1983; Saucier 1963; Self and Davis 1983). A map of the surface geology for the study area is presented in Figure 4.

Environments of deposition mapped at the surface in Figure 4 include natural levee, point bar, inland swamp, fresh marsh, and several abandoned distributary channels. A complete description of the different environments of deposition present in the study area is contained in Appendix A. Natural levee deposits identified on the geologic map in Figure 4 are shown with the underlying environment of deposition. The surface geology consists primarily of Mississippi River natural levee and point bar deposits, several abandoned distributary channels, and their associated fluvial and deltaic deposits.

Formation of the study area is directly related to the past and present courses of the Mississippi River and its abandoned distributary channels. Abandoned distributary channels within the study area are associated with two major distributary systems, Bayou des Familles-Barataria and Bayou Sauvage-Metarie Bayou (Figure 4). Bayou Des Familles-Barataria is a major St. Bernard distributary channel or Mississippi River course which extends due south from the Mississippi River at the Celotex failure site to Barataria, LA. This distributary system was active from approximately 2,000 to 3,400 years before the present (Frazier 1967).

The second major distributary course mapped in the study area is Bayou Sauvage-Metarie Bayou. According to Frazier (1967), this course was active from about 800 to 1,800 years before the present (Figure 3). However, Saucier (1963) and Kolb and Van Lopik (1958a) indicate that this system may have been active even earlier. Radiocarbon dates from organic sediments beneath the natural levees of Metarie Bayou range from 2,300 to 2,600 years before the present and indicate that a marsh surface was developed within this area. Metarie Bayou intersects the Mississippi River at Kenner and extends eastward, branching into two segments north of Algiers Point. The northern branch extends northeast toward Chef Menteur, Louisiana, as Bayou Sauvage. The southern branch, labeled Unknown Bayou by Saucier (1963), intersects the Mississippi River at Algiers Point (Figures 1 and 4), follows the Mississippi River between Algiers Point and Gretna, and then extends due southeast where it intersects the Mississippi River at 12 Mile Point.

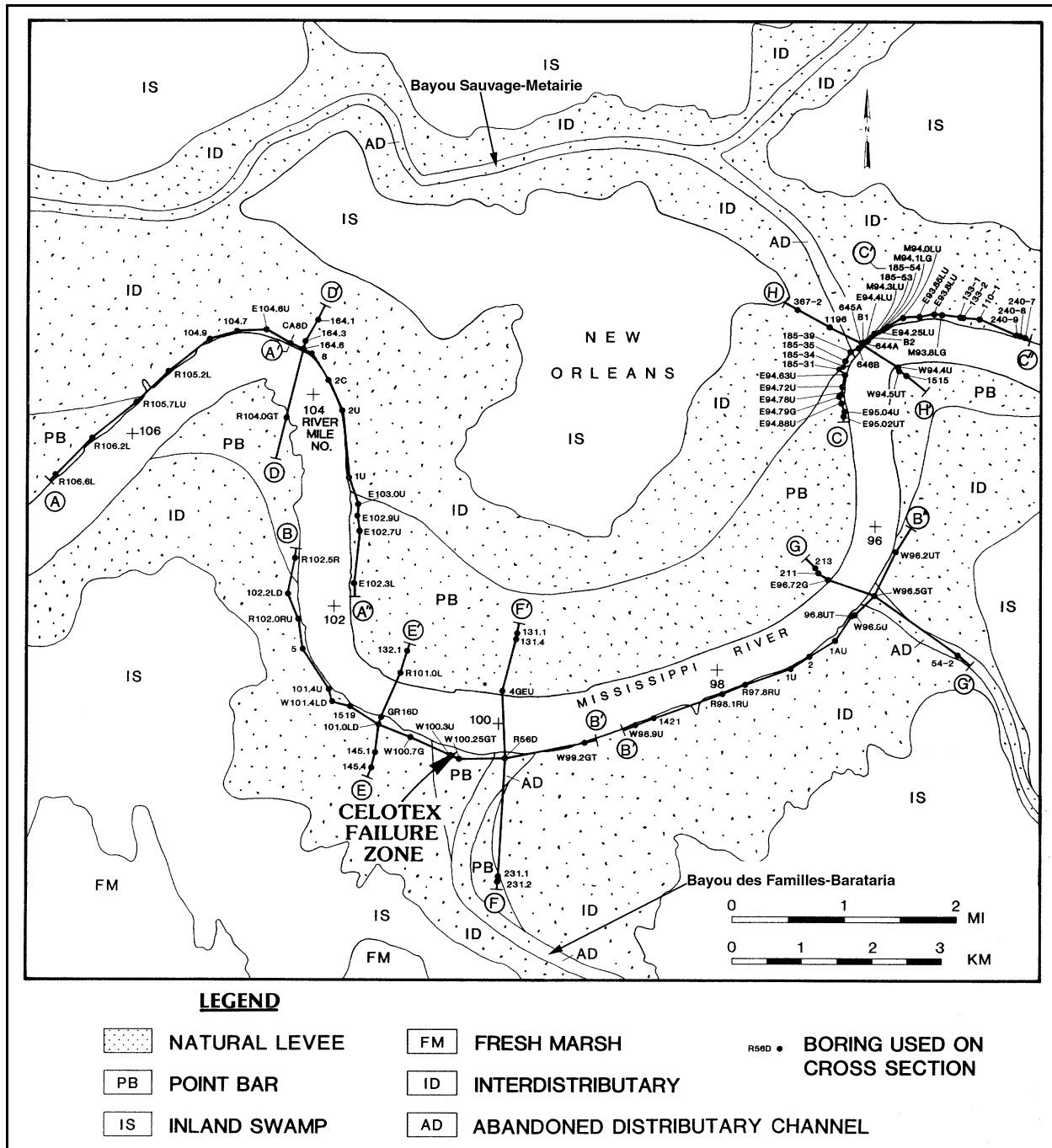


Figure 4. Geologic map of the study area showing boring and cross section locations

Subsurface geology

Eight geologic cross sections were constructed from borings collected and evaluated during this study. The locations of the cross sections are shown on the geologic map in Figure 4. Cross sections A through H are presented as Figures 5a through 5k, respectively. The longer cross sections are presented as

two separate sections or figures for illustration purposes. A legend of symbols and soil types identified on the sections is presented in Figure 51. Sections were constructed such that each revetment reach includes sections parallel and perpendicular to the river bank. Parallel sections were constructed for only the cutbank or concave side as this is the side for maximum erosion and potential bank instability. The majority of soil types shown on the geologic sections are classified according to the Unified Soil Classification System (USCS). Borings not using the USCS (e.g., borings from private engineering companies) are shown with their textural soil types identified. The geologic cross sections show the vertical and horizontal limits of the various environments of deposition adjacent to the river as well as the soil types that form these different environments. Depositional environments present in the subsurface include interdistributary, intradelta, and nearshore gulf. A general description of these environments is contained in Appendix A. For readers desiring further engineering soils data beyond what is presented in this report, a detailed summary of soil engineering properties for the various environments of deposition is presented by Kolb (1962) and Montgomery (1974).

Beneath the nearshore gulf sequence is the Pleistocene surface. The nearshore gulf sediments represent the deposits formed by the transgression of sea level onto the Pleistocene surface. These sediments were deposited under shallow-water conditions, before the advancement of the two major St. Bernard distributary systems into the study area. Establishment of the St. Bernard distributary systems into the study area produced the interdistributary sediments that were deposited into shallow-water, freshwater areas between the active distributary channels. Interdistributary sediments over time filled these shallow areas, and emergent vegetation in the form of fresh marsh began developing when interdistributary filling approached sea level. Closer to the active distributary systems, overbank deposition from the active distributary channels developed well drained natural levees and inland swamps.

A generalized contour map of the Pleistocene surface is presented in Figure 6 (Kolb, Smith, and Silva 1975). In general, the Pleistocene surface throughout the study area dips to the south and southwest at approximately 3 ft per mile (1 m per 1.6 km). Surface elevations on this surface are variable due to erosion by the preexisting Pleistocene drainage system and later Holocene scouring by past and present courses of the Mississippi River and its distributaries. Elevations of the Pleistocene surface range from -50 ft (-15 m) NGVD to greater than -150 ft (-46 m) NGVD in the bendways of the present Mississippi River channel.

Pleistocene deposits are characterized by a significant increase in stiffness and shear strength as compared to the overlying Holocene sediments. Pleistocene soils are fairly resistant to erosion from fluvial scouring. Where these soils occur in the riverbank, they represent a "hard point" which restrains the river's migration and deepening. Pleistocene deposits in the bed and bank of the river have had a significant influence on the river's ability to meander through the study area. There has been very little migration of the channel during the past 100 years as determined from comparison of old hydrographic surveys in Chapter 3 of this report.

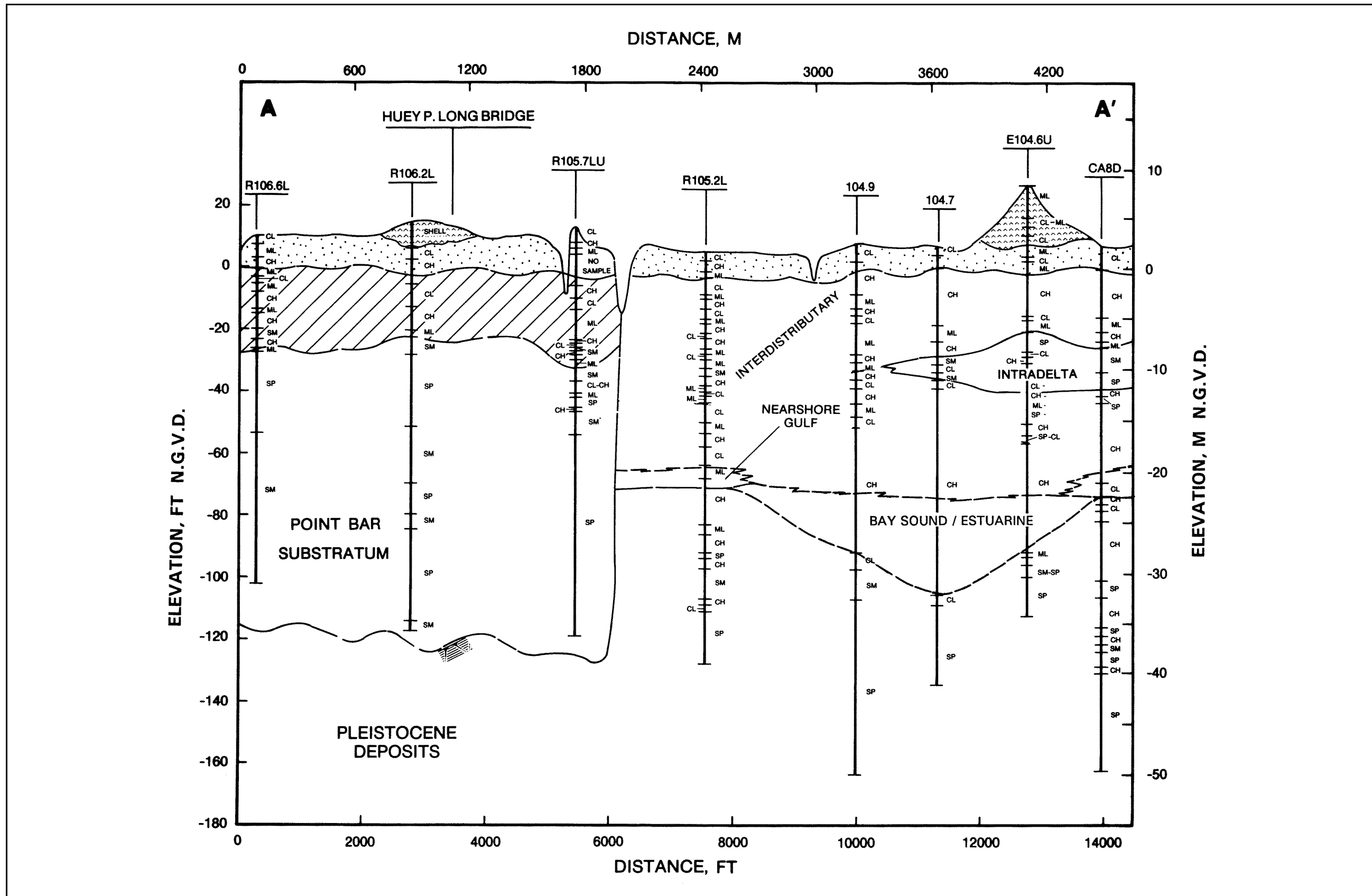


Figure 5a. Geologic cross section A-A' (see Figure 5l for symbol legend)

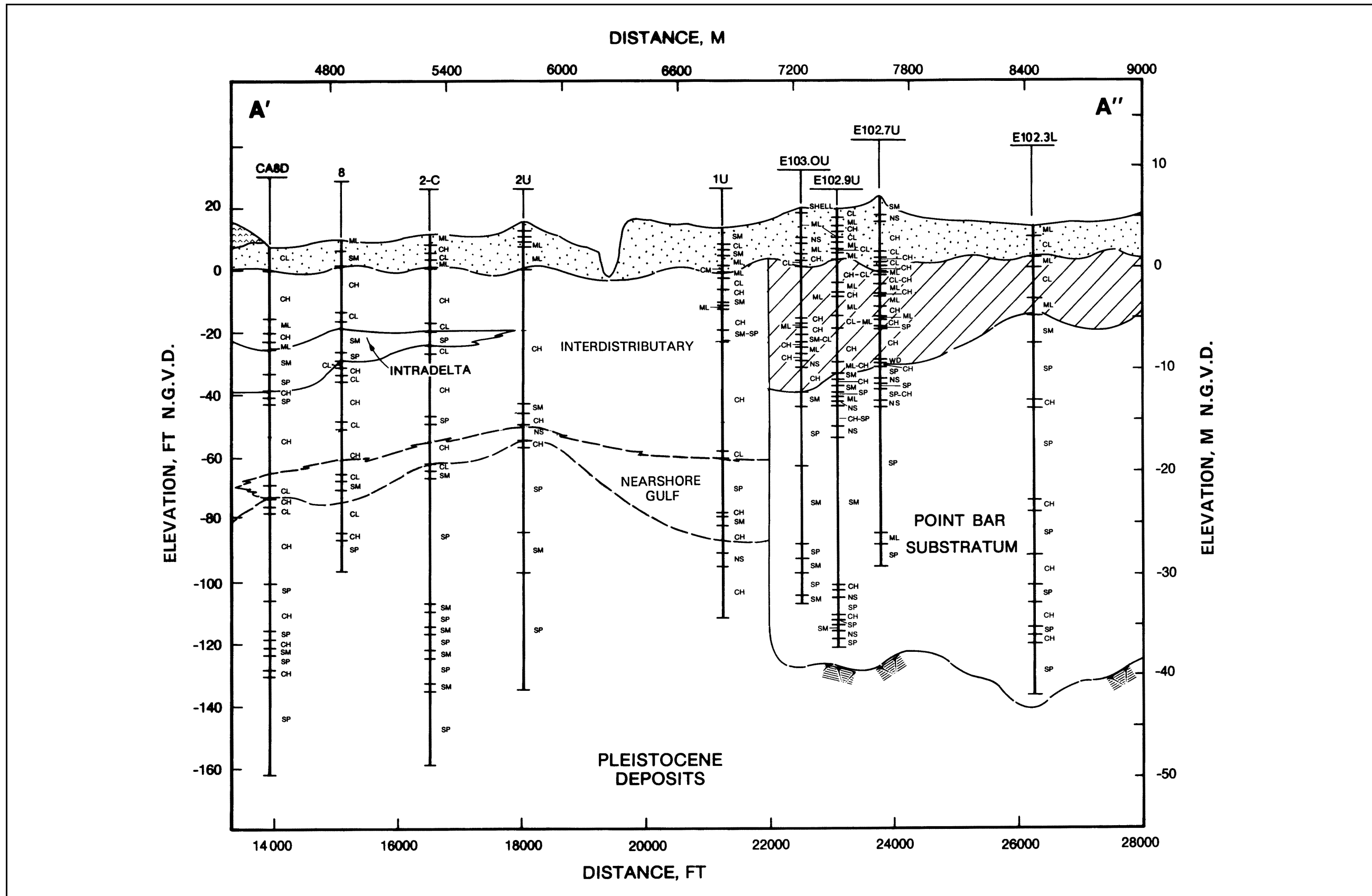


Figure 5b. Geologic cross section A'-A'' (see Figure 5l for symbol legend)

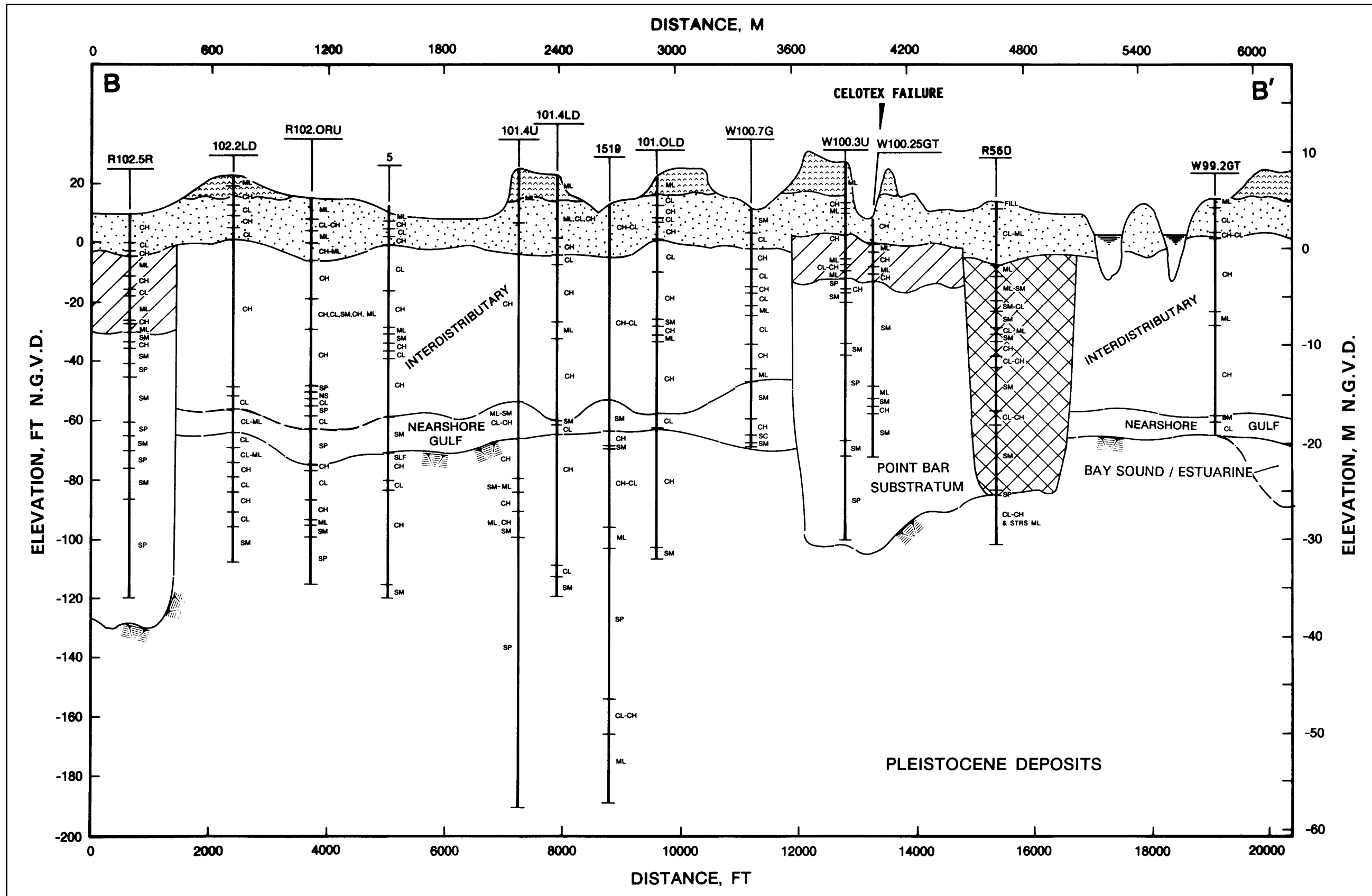


Figure 5c. Geologic cross section B-B' (see Figure 5l for symbol legend)

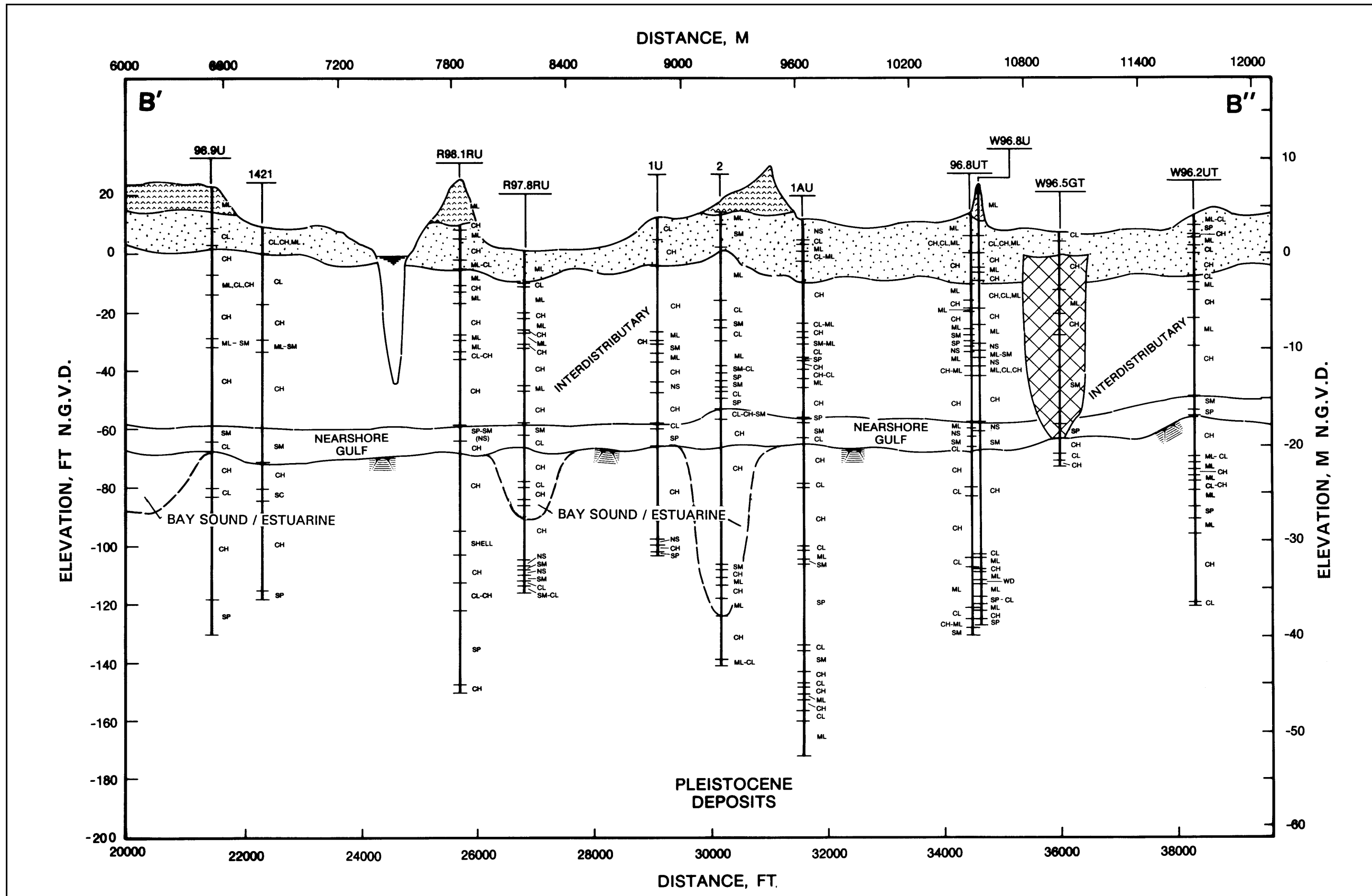


Figure 5d. Geologic cross section B'-B'' (see Figure 5l for symbol legend)

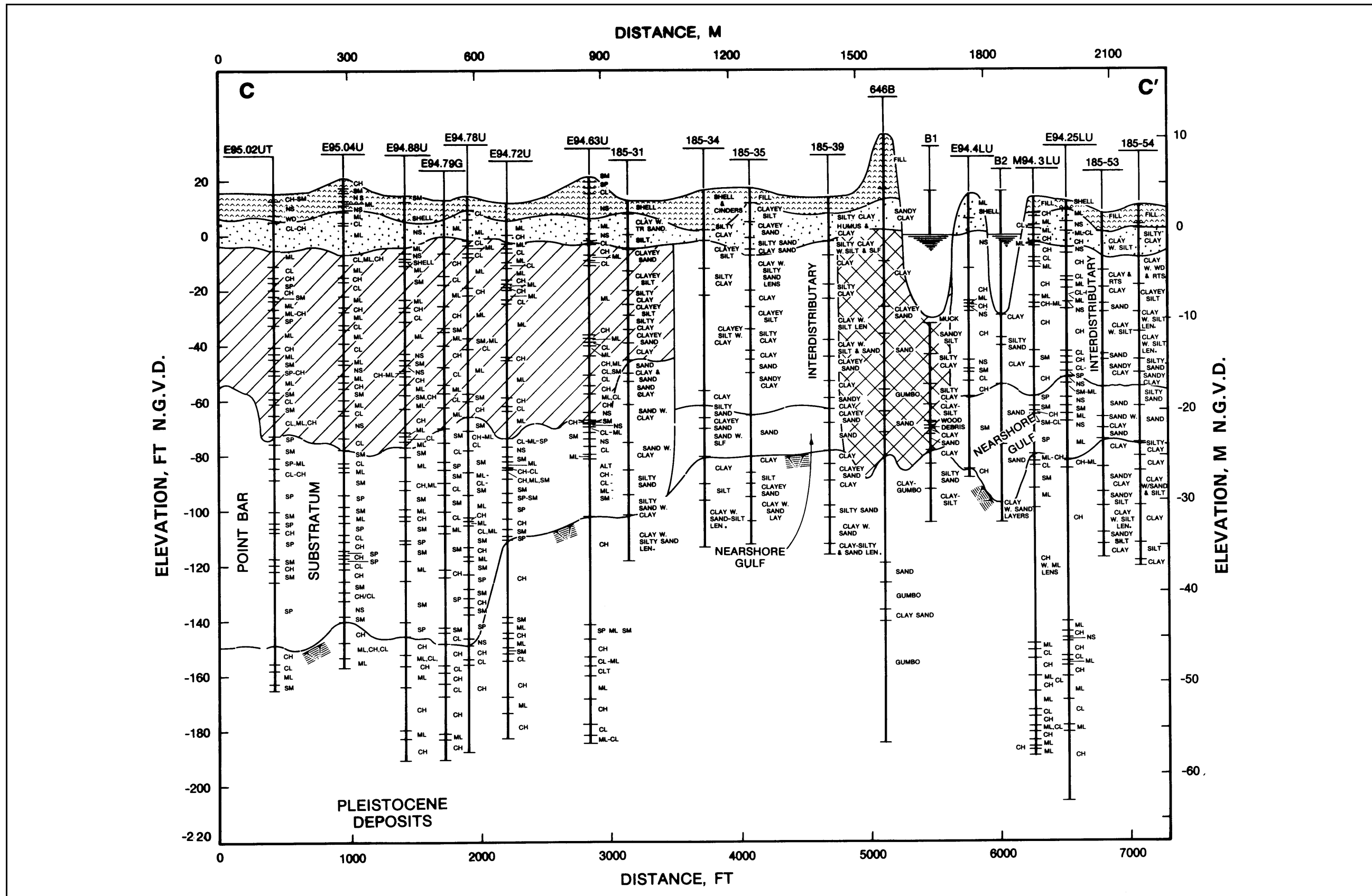


Figure 5e. Geologic cross section C-C' (see Figure 5l for symbol legend)

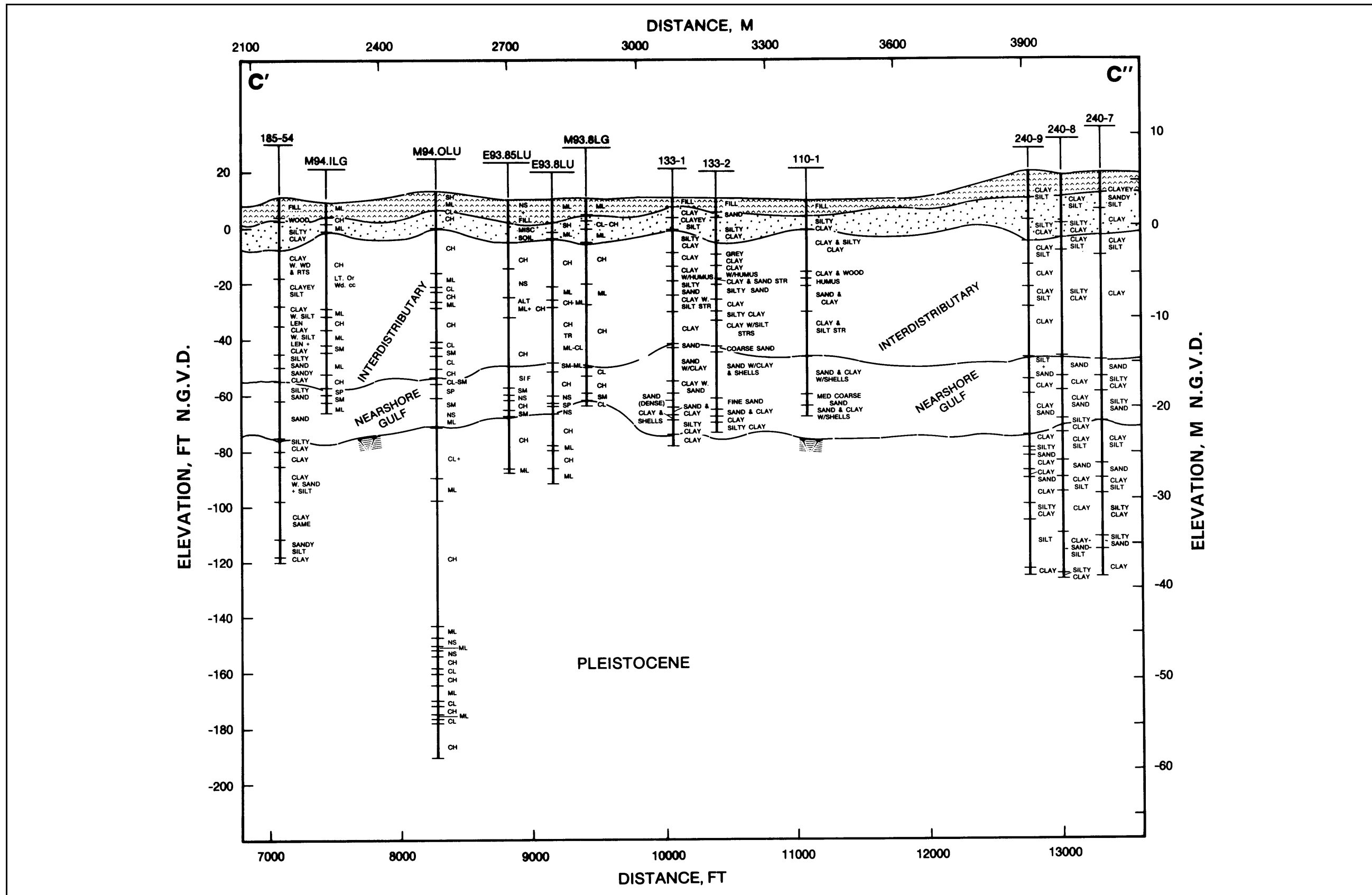


Figure 5f. Geologic cross section C'-C'' (see Figure 5l for symbol legend)

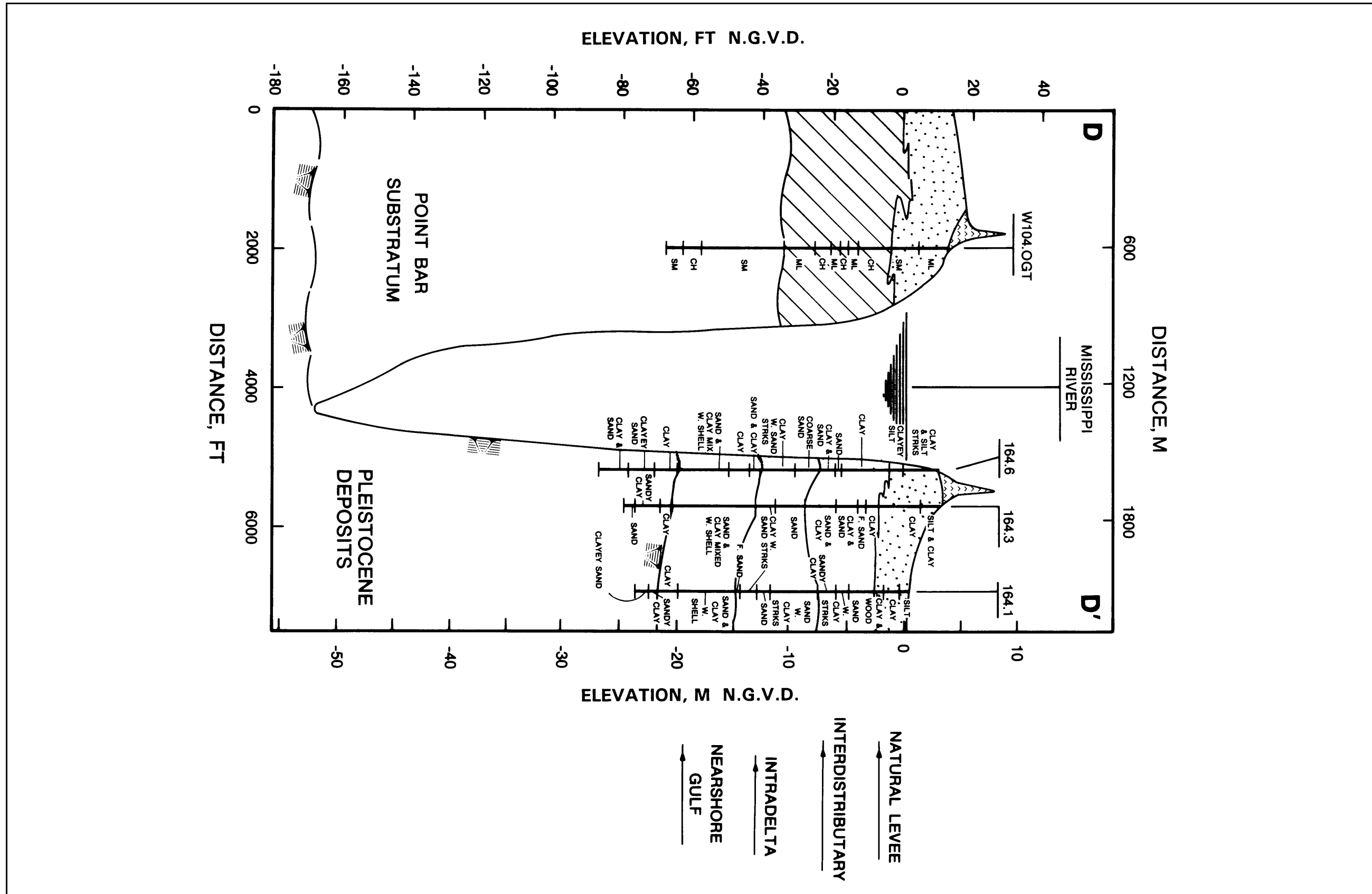


Figure 5g. Geologic cross section D-D' (see Figure 5l for symbol legend)

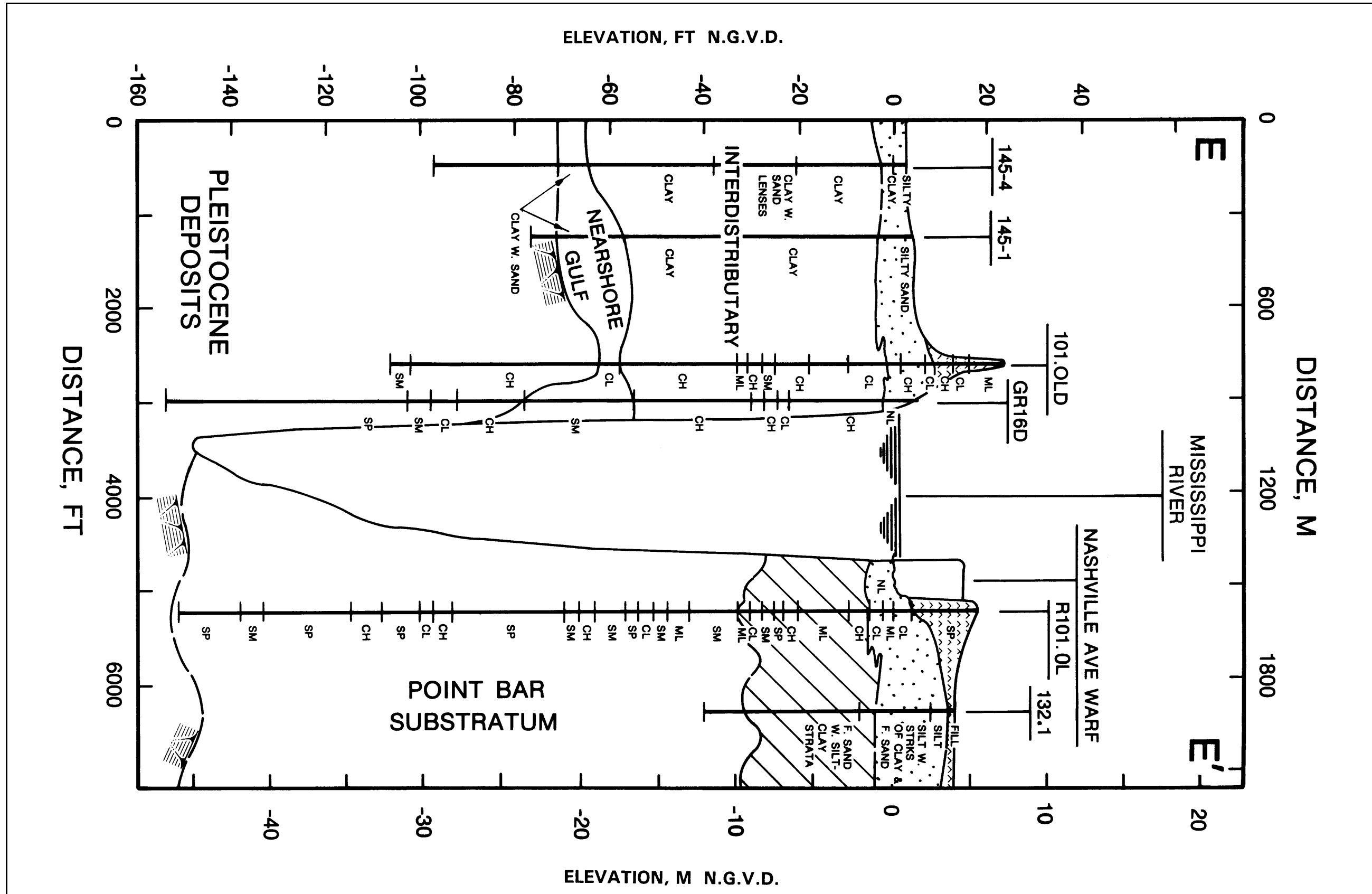


Figure 5h. Geologic cross section E-E' (see Figure 5l for symbol legend)

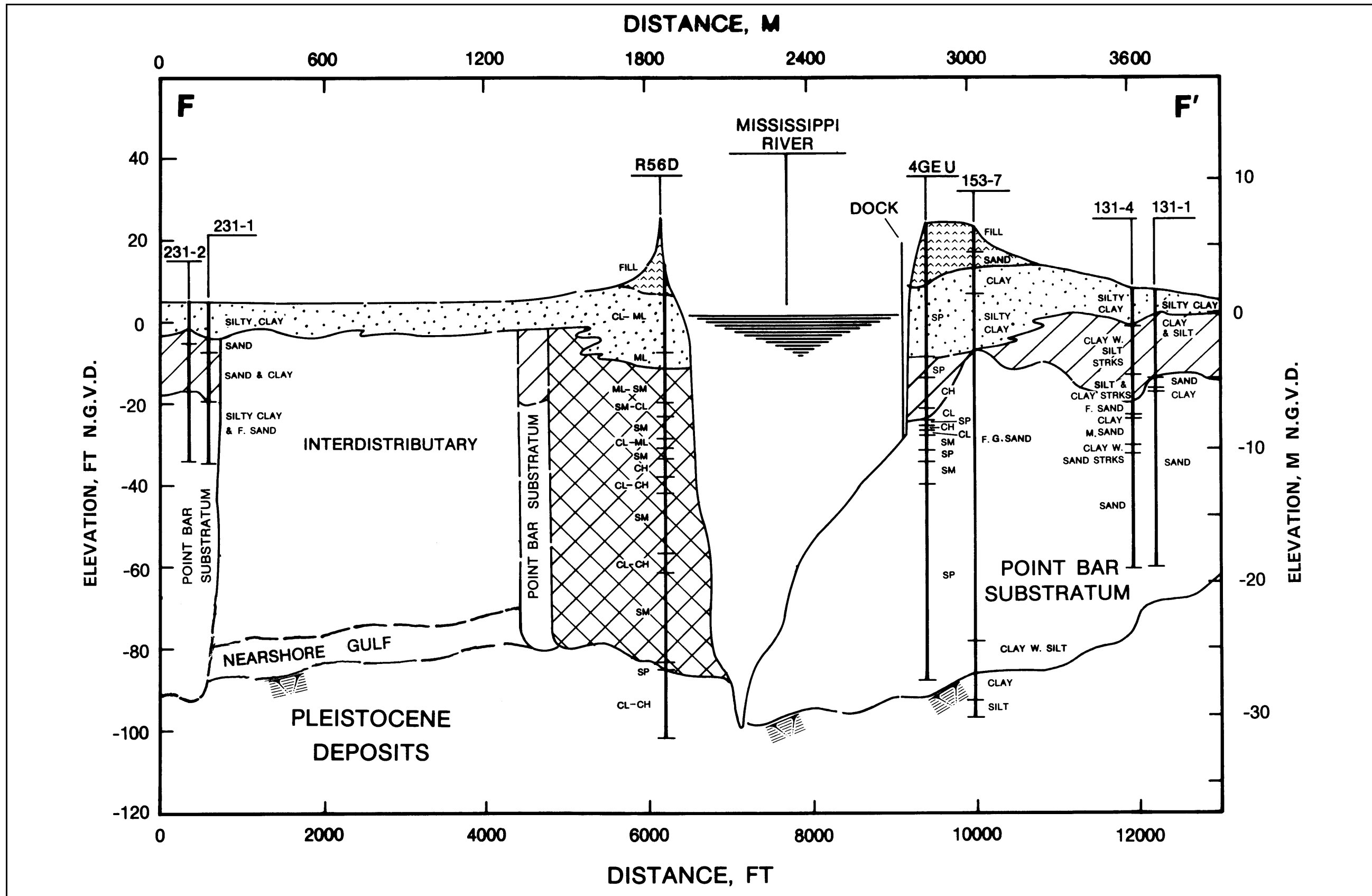


Figure 5i. Geologic cross section F-F' (see Figure 5l for symbol legend)

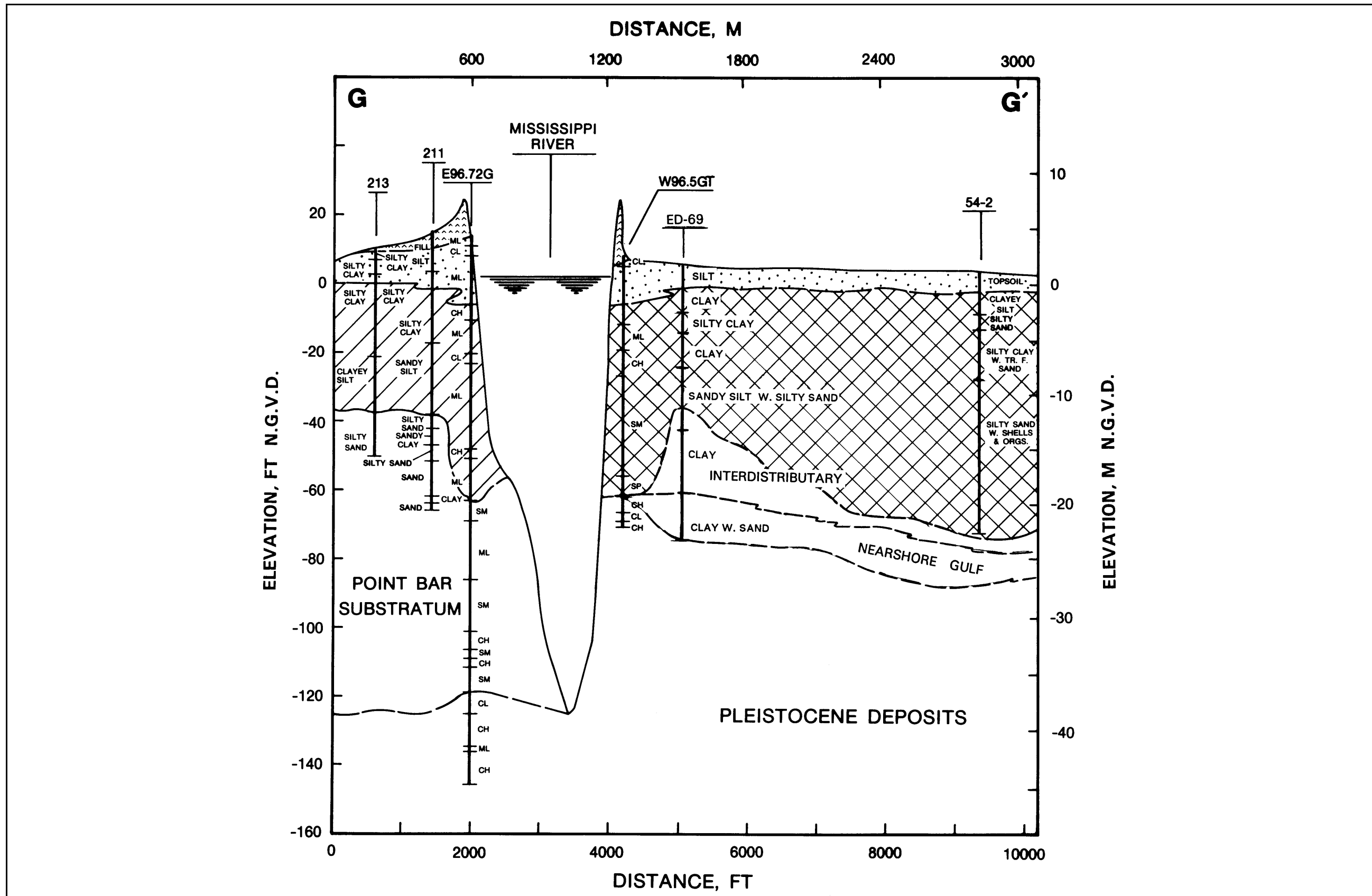


Figure 5j. Geologic cross section G-G' (see Figure 5i for symbol legend)

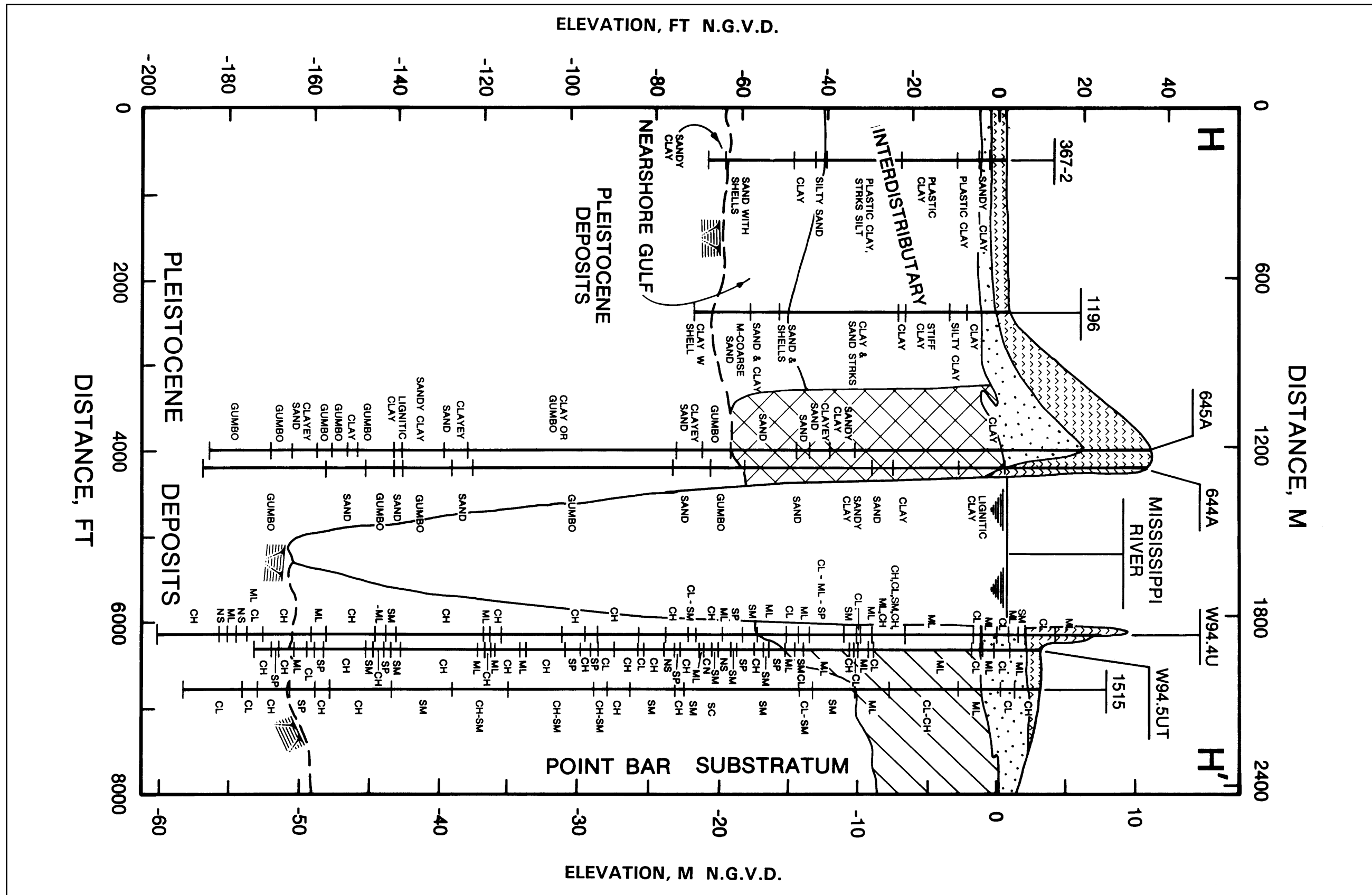
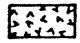
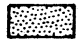
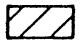
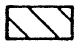



Figure 5k. Geologic cross section H-H' (see Figure 5l for symbol legend)


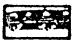
LEGEND

ENVIRONMENTS OF DEPOSITION

TOPSTRATUM DEPOSITS

-  LEVEE FILL
-  NATURAL LEVEE
-  POINTBAR
-  BACKSWAMP
-  ABANDONED COURSE

SUBSTRATUM DEPOSITS

-  UNDIFFERENTIATED SAND AND GRAVEL
-  UPPER FINE-GRAINED PLEISTOCENE SURFACE

SOIL TYPES (USCS)

- | | |
|-------------------------------------|-----------------------------------|
| CH — CLAY | SP — POORLY GRADED SAND |
| CL — SILTY CLAY, SANDY CLAY | SW — WELL-GRADED SAND |
| ML — SILT, SANDY SILT, CLAY SILT | GM — SILTY SAND-GRAVEL |
| SC — CLAYEY SAND | GW — WELL-GRADED SAND-GRAVEL |
| SM — SILTY SAND | GP — POORLY GRADED SAND-GRAVEL |

Figure 5l. Legend for the geologic sections of Figures 5a through 5k

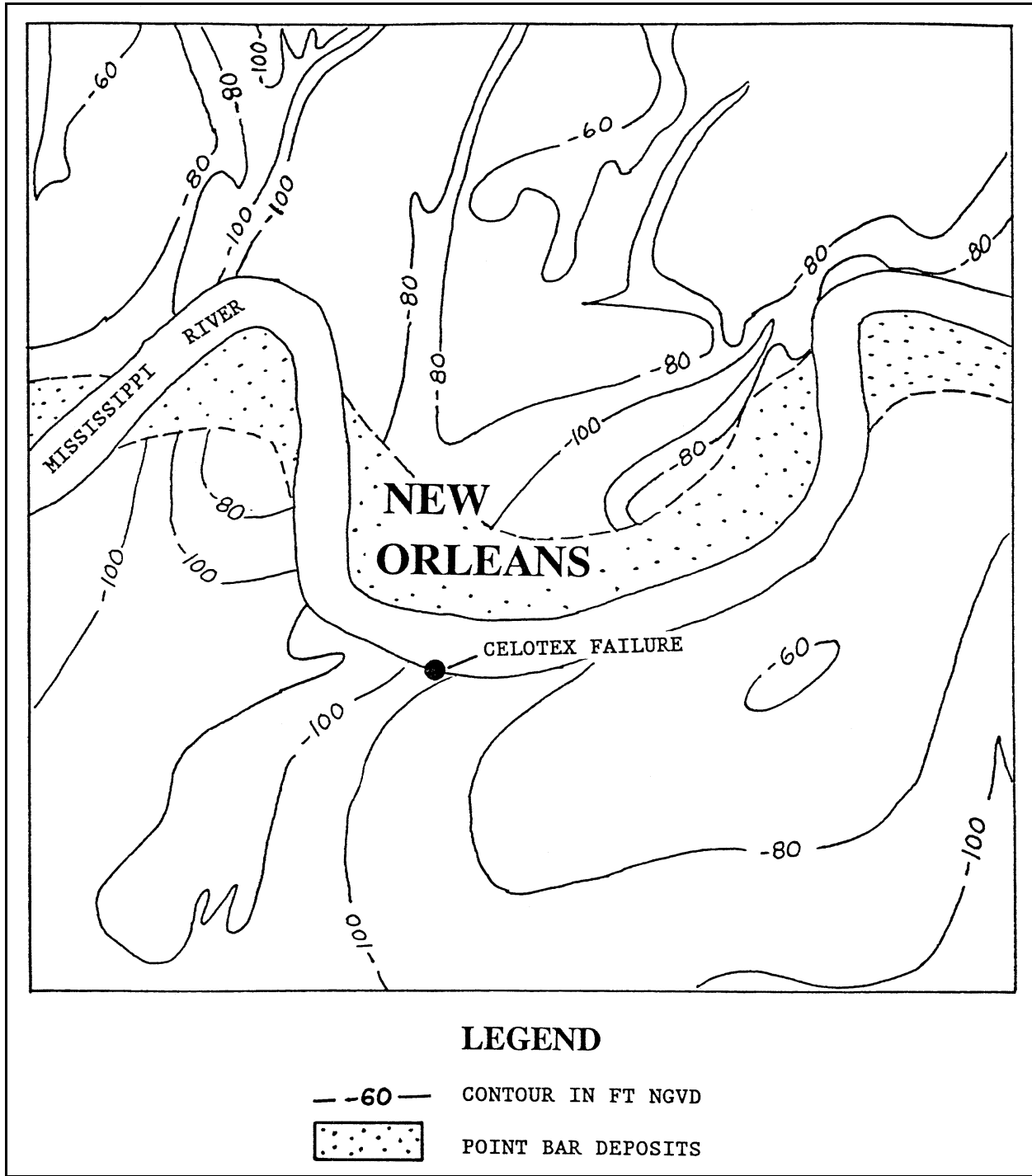


Figure 6. Generalized contour map of the Pleistocene surface (modified after Kolb, Smith, and Silva 1975)

Each of the different depositional environments present in the study area has distinct physical characteristics reflected by differences in soil types and associated engineering properties. Therefore, the geology of the study area will have a major influence on river scouring, lateral migration, and bank stability.

Geology of Selected Revetment Reaches

Celotex failure site and Greenville Bend revetment

This riverbank reach extends from river mile 98.3 to 102.0 (158.2 to 164.1 km) on the right descending bank. The subsurface geology of the Celotex failure site is shown by cross sections B-B' (Figure 5c) and F-F' (Figure 5i). The locations of these sections are shown in Figure 4. Areal photography and boring data identify a point bar sequence (Figure 4 and 5c) associated with Bayou des Familles (Figure 5i). This distributary channel was a major course of the Mississippi River during the active St. Bernard delta complex.

The exact intersection and lateral limits of Bayou des Familles at the Mississippi River are not well defined from areal photography because this area has been extensively developed by industrial and residential construction. The position and lateral extent of the Bayou des Familles channel at the Mississippi River was interpreted from available historic charts, maps, and boring data.

Soil types within the point bar-abandoned distributary sequence are primarily coarse-grained, consisting mainly of silty sands (SM) and well sorted or poorly graded sands (SP). The available boring data indicate that the point bar-abandoned distributary sequence extends approximately 100 ft (30.5 m) below the ground surface before encountering the oxidized and erosion-resistant Pleistocene surface.

The geology immediately upstream and downstream from the Bayou des Familles point bar sequence consists of interdistributary deposits underlain by a generally coarser nearshore gulf sequence (CL, ML, SM, and SC). Soil types are variable within these two depositional environments. Interdistributary sediments consist primarily of clay (CL and CH) with disseminated organics.

Carrollton Bend and Carrollton Bend revetment

This bank reach extends from about river mile 102.0 to 105.0 (164 to 169 km) and encompasses the Carrollton Bend revetment which is on the left descending bank. The subsurface geology of the Carrollton Bend reach is shown on cross sections A-A' (Figure 5a), A'-A'' (Figure 5b), and D-D' (Figure 5g) (see Figure 4 for section locations). The geology consists of natural levee, interdistributary, intradelta, and nearshore gulf sediments. Soil types are variable within the individual environments as shown by the cross sections. The Pleistocene surface ranges between elevations -50 to -75 ft (-15.2 to -22.9 m) NGVD. Where the Mississippi River has entrenched itself into the Pleistocene, the river has formed thick point bar sediments in excess of 120 ft (36.6 m) deep.

Gretna Bend and Gouldsboro revetments

This revetted bank lies between river miles 95.5 and 98.3 (153.6 and 158.2 km). The Gretna Bend and Gouldsboro revetments are contiguous from upstream to downstream, respectively, along the right descending bank. The

subsurface geology of the Gretna Bend and Gouldsboro Revetment reach is shown by cross sections B'-B'' (Figure 5d) and G-G' (Figure 5j) (see Figure 4 for section locations). The geologic sequence is similar to the two upstream revetment reaches already described. The Pleistocene surface ranges between elevations -55 to -70 ft (-16.8 to -21.3 m) NGVD and is overlain by nearshore gulf, interdistributary, and natural levee sediments.

As shown by the surface geology map in Figure 4, there is an abandoned distributary channel which intersects the Mississippi River and extends southeast at approximately river mile 96.5 (155.3 km). The existence of this former distributary channel is indicated by the presence of well-developed natural levees several miles southeast of the Mississippi River. The intersection of this distributary channel with the present Mississippi River is indicated by boring W96.5GT. At this location, a thick sand sequence was encountered in the subsurface.

Algiers Point revetment

This revetment reach lies between river mile 93.7 and 95.5 (150.8 and 153.7 km) on the right descending bank. The subsurface geology of Algiers Point is shown by cross sections C-C' (Figure 5e), C'-C'' (Figure 5f), and H-H' (Figure 5k). The permanent scour pool along Algiers Point is one of the deepest of the Mississippi River entrenchment below Baton Rouge. River thalweg elevations have historically been between -175 and -200 ft (-53.3 and -61 m) NGVD. At Algiers, along the point bar side of the river, fluvial scouring has created a 170-ft (51.8-m) thick point bar sequence (see cross section H-H' of Figure 5k). Soil types are variable within this thick sequence, but are primarily coarse-grained.

Along the concave or left bank of the river, the subsurface geology at Algiers Point consists of interdistributary sediments, separated by point bar deposits and an abandoned interdistributary channel (see Figure 4 and cross section C-C' of Figure 5e). These sediments are underlain by the Pleistocene surface. The lateral and vertical limits of the different depositional environments are shown by the surface geology map and the respective geologic cross sections. Soil types are highly variable as defined by the sections.

The abandoned distributary channel shown in Figure 4 is a former St. Bernard distributary which branches from the main Bayou Sauvage-Metarie Bayou course northwest of Algiers Point. The intersection of this distributary channel at the Mississippi River is defined by coarse-grained sediments in the subsurface in borings located within the former distributary channel (see sections C-C' of Figure 5e and H-H' of Figure 5k).

Appendix A

Environments of Deposition

General

This appendix provides a general description of the environments of deposition which produced the surface and subsurface geology encountered in the study reach. The distribution of surface deposits is shown by the geologic map in Figure 4 of the main text. Subsurface limits of the various depositional environments are shown by the cross sections in Figures 5a through 5k. A geologic legend is presented in Figure 5l that identifies symbols used in the geologic cross sections.

In addition to the general descriptions of the individual environments of deposition, this appendix also provides a very generalized indication of the engineering properties for each environment. Correlation of engineering properties and soil types to the different environments of deposition is based primarily on work by Kolb (1962)¹ and is summarized in Table A1. Additionally, Montgomery (1974) expanded upon Kolb's original work for several of the major depositional environments which form the bulk of the land area in the deltaic plain. Montgomery's work is summarized in Table A2 and provides further engineering data on the following selected environments of deposition: natural levee, point bar, backswamp, prodelta, intradelta, and interdistributary deposits.

In terms of their engineering significance, the biggest contrast occurs between the Pleistocene and Holocene age sediments as shown by the engineering data in Table A1. Pleistocene sediments have higher cohesive strengths, lower water contents, and are much denser than Holocene soils. Holocene deposits in contrast are less consolidated, have higher water contents, and are more variable in density.

The biggest contrast in Holocene soils occurs between the high- and low-energy depositional environments. High-energy environments are generally associated with maximum fluvial and/or wave activity and are mainly composed of coarse-grained sediments. These environments include point bar, substratum, abandoned course, abandoned distributary, beach, nearshore gulf, estuarine/bay

¹ References are listed following the main text.

sound, and intradelta deposits (Table A1). Low-energy environments are composed primarily of fine-grained sediments and include marsh, swamp, natural levee, prodelta, and interdistributary. Only the environments of deposition that are present in the study area are examined in the following section. The environments are presented and described by their order and distribution of occurrence. Deltaic environments not present in the study area but identified in Table A1 are described in further detail by Kolb (1962) or Kolb and Van Lopik (1958a,b) for readers desiring further information.

Surface Environments of Deposition

Natural levee

Natural levees are vertical accretion deposits formed when the river overtops its banks during flood stage and sediment suspended in the flood flow is deposited immediately adjacent to the channel. The resulting landform is a low, wedge-shaped ridge decreasing in thickness away from the channel. The limits of natural levee deposits in the study area are shown in Figure 4 of the main report. Natural levee deposits are mapped in Figure 4 with the underlying environment of deposition (i.e., interdistributary, point bar, or inland swamp). Natural levee deposits cover approximately 40 percent of the study area and involve the Mississippi River and abandoned distributary channels from the active St. Bernard delta complex (i.e., Bayou des Familles-Barataria, Metairie Bayou, Bayou Sauvage, and two unnamed bayous).

Natural levee widths in the study area vary from about 3/4 to approximately 2 miles wide along the Mississippi River, and between 1/4 and 1/2 mile wide along the abandoned St. Bernard distributary channels (Figure 4). Natural levees are thickest adjacent to the main channel, ranging from 10 to 20 ft in thickness (Figures 5a to 5k). Their thickness decreases away from the river, eventually merging with inland swamp deposits.

Natural levee deposits in the study area are composed primarily of clay and silt with minor sand lenses. Soils associated with natural levee deposits are identified in Figures 5a through 5k of the main report. These deposits are generally coarser-grained near the channel, composed of silt (ML) and silty clay (CL), and become finer-grained (i.e., CL and CH) further from the river. Color varies from reddish brown or brown near surface to grayish brown, and medium to dark gray with depth. Darker colored natural levee soils are due to the higher organic content. Organic content is generally low and is in the form of small roots and occasionally disseminated wood fragments. Larger wood fragments are uncommon as oxidation has reduced organic materials to a highly decomposed state. Frequently associated with natural levee deposits are small calcareous nodules, formed as a result of groundwater percolating through the permeable soils and precipitated from solution. Natural levee soils are well-drained, have low-water contents, and generally have a stiff to very stiff consistency (Tables A1 and A2).

| | DEPOSITIONAL TYPES | LITHOLOGY PER CENT | PREDOMINANT SOIL TEXTURES ⁽¹⁾ | NATURAL WATER CONTENT PER CENT DRY WEIGHT | UNIT WEIGHT LB/CU FT | SHEAR STRENGTH ⁽²⁾ | | REMARKS | |
|---------------------|------------------------|--------------------|--|---|----------------------|--|---|---|---|
| | | | | | | COHESIVE STRENGTH LB/SQ FT | ANGLE OF INTERNAL FRICTION IN DEGREES | | |
| RECENT ENVIRONMENTS | NATURAL LEVEES | | CH, CL, ML & SM | | | VALUES RANGE TO APPROXIMATELY 2500 CHARACTERISTIC RANGE 800-1200 | ML 20-35 | Disposed in narrow bands flanking the Mississippi River and its abandoned courses and distributaries. Consists of interfingering layers of fat and lean clays and sandy silt along the Mississippi River and its abandoned courses. Natural levee materials along abandoned distributaries usually much finer. Thickness varies from 25 ft near Baton Rouge to 0 at sea level. Thickness along distributaries usually on the order of 5 ft or less. | |
| | POINT BAR SANDY | | ML, SM & SP | | INSUFFICIENT DATA | INSUFFICIENT DATA | SP 25-35 | Usually found flanking the more prominent bends of the present and abandoned courses to a depth of more than 100 ft. Consists of a bedded topstratum 25 to 75 ft thick of silty sand, sandy silt, and sand coarsening with depth. The substratum consists of essentially clean sand. | |
| | POINT BAR SILTY | | CL & ML | | INSUFFICIENT DATA | ----- | ----- | ML 20-30 | An unusually fine-grained point-bar deposit consisting almost entirely of silt. Identified just upstream from Donaldsonville and at Laplace. |
| | PRODELTA CLAYS | | CH | | | | ----- | 0 | A homogeneous fat clay in offshore areas and at depth. Contains increasing amounts of lean clay disposed in thin layers near the mouths of active distributaries. Thickness normally varies with depth to Pleistocene. Thicknesses range between 50 and 600 ft. |
| | INTRADELTA | | CH, ML & SM | | INSUFFICIENT DATA | INSUFFICIENT DATA | INSUFFICIENT DATA | ----- | Relatively coarse sediments bottoming bays and sounds. Thickness ranges from 3 to 20 ft and averages 15 ft. Because of the reworking of bottom sediments by narrowing marine organisms soils have a mottled appearance due to the inclusion of lumps or pockets of coarse material in a fine matrix or fine material in a coarse matrix. |
| | INTERDISTRIBUTARY | | CH | | | | ----- | 0 | Forms clay wedges between major distributaries. Clay sequence interrupted by silty or sandy materials associated with myriad small distributaries. Minor amounts of silt and fine sands typically occur in very thin but distinct layers between clay strata giving deposit a "warved" appearance. Thickness similar to intradelta above. |
| | ABANDONED DISTRIBUTARY | | CH & CL | INSUFFICIENT DATA | INSUFFICIENT DATA | INSUFFICIENT DATA | INSUFFICIENT DATA | ----- | Forming belts of clayey sediments from a few feet to more than 1,000 ft in width and from less than 10 to more than 50 ft in depth. A wedge of coarser material is normally found at the upstream end, this wedge of material may range from fine sand for the larger distributaries to silty clays for the smaller. |
| | ABANDONED COURSE | | CH & SP | INSUFFICIENT DATA | INSUFFICIENT DATA | INSUFFICIENT DATA | INSUFFICIENT DATA | ----- | Forming belts of fairly coarse sediment in abandoned Mississippi River courses. Average width 2,500 ft. Depth may be 75 to 150 ft. Lower portion of course filled with sandy material which thickens in an upstream direction. Upper portion filled with silts and clays. |
| | SWAMP | | CH | | | INSUFFICIENT DATA | INSUFFICIENT DATA | ----- | Tree-covered organic deposits flanking the inner borders of the marsh and subject to fresh-water inundation; also mangrove-choked areas found landward of the barrier beaches and fringing the mainland. Deposits average 3 to 10 ft thick. |
| | MARSH | | PT | VALUES RANGE TO APPROXIMATELY 800 | INSUFFICIENT DATA | VERY LOW | ----- | ----- | Forms 90 per cent of the land surface in the deltaic plain. Ranges from watery organic ooze to fairly firm organic silts and clays. Maximum thicknesses (30 ft or more) normally associated with areas of greatest subsidence. Average thickness 10 ft. |
| | SAND BEACH | | SP | SATURATED | INSUFFICIENT DATA | 0 | 30-35 | Border the open gulf except in areas of active deltaic advance. May be a mile or more in width and more than 10 miles in length. Beach sand may pile as high as 30 ft above gulf level and subside to depths of 30 ft below gulf level. Buried sand beaches reach a thickness of 35 ft in New Orleans area. | |
| | BAY-SOUND | | ML & SM | | | | 15-30 | Relatively coarse portion of subaqueous delta. Intricately interfingering deposits. Disposed in broad wedges about abandoned courses and major distributaries. Thickness of intradelta associated with present Mississippi on order of 200 ft. Thickness of intradelta associated with abandoned courses much less, averaging between 25 to 100 ft. | |
| | NEARSHORE GULF | | SP | SATURATED | INSUFFICIENT DATA | 0 | 25-35 | Found at the borders of the open ocean seaward of the sand or barrier beaches. Thickness appears to increase with distance from shore - maximum thickness believed to be on order of 25 ft. Discontinuous blanket of this material occurs directly above Pleistocene. | |
| | ESTUARINE | | SP | SATURATED | INSUFFICIENT DATA | 0 | 30-40 | Sandy facies correlative with nearshore gulf deposits but filling minor valleys entrenched into underlying Pleistocene surface. | |
| | BACKSWAMP | | CH & CL | | | VALUES RANGE TO APPROXIMATELY 1745 CHARACTERISTIC RANGE 450-1450 | 0 | Thick clays overlying substratum sands upstream from College Point. Occasional lenses of shell are found indicating interfingering fluvial-marine deposits. | |
| SUBSTRATUM | | SP | SATURATED | INSUFFICIENT DATA | 0 | 30-40 | Massive sand and gravel deposits filling entrenched valley and grading laterally into nearshore gulf deposits. Material becomes coarser with depth. Maximum thickness on the order of 300 ft in deepest portion of entrenched valley. | | |
| PRE-RECENT | PLEISTOCENE | | CH & CL | | | VALUES RANGE TO APPROXIMATELY 3500 CHARACTERISTIC RANGE 900-1700 | 0 | Ancient former deltaic plain of Mississippi River. Consists of environments of deposition and associated lithologies similar to those found in recent deltaic plain. Depth to this ancient, eroded surface increases in a southerly and westerly direction in southeastern Louisiana. | |

LEGEND

GRAVEL (>2.0 MM)
 SAND (2.0-0.05 MM)
 SILT (0.05-0.005 MM)
 CLAY (<0.005 MM)
 ORGANIC MATERIAL
 SHELL
 TYPICAL RANGE OF VALUES INDICATED BY LENGTH OF BAR. BAR WIDTH INDICATES RELATIVE DISTRIBUTION OF VALUES.

(1) SYMBOLS BASED ON UNIFIED SOIL CLASSIFICATION SYSTEM.
(2) SHEARING STRENGTHS OF CLAYS BASED ON UNCONFINED COMPRESSION TESTS.

Table A1. Engineering Properties of Depositional Environments from the Mississippi River Deltaic Plain (from Kolb 1962)

Table A2. Engineering properties of selected depositional environments from the Mississippi River deltaic plain (from Montgomery, 1974)

| Deposit | Grain Size and Organic Content | Natural Water Content % | Liquid Limit % | Plasticity Index % | Liquidity Index | Dry Density pcf | Specific Gravity | Void Ratio e | s _v P _v Ratio | Shear Strength | |
|-----------------------|--------------------------------|-------------------------|----------------|--------------------|------------------|-----------------|------------------|------------------|-------------------------------------|------------------------|------------------------|
| | | | | | | | | | | Q _c T/sq ft | c _r T/sq ft |
| Natural levee | | 18-83 (45) | 29-129 (66) | 2-90 (42) | 0.14-1.18 (0.54) | 50-92 (76) | 2.62-2.74 (2.69) | 0.82-6.16 (1.46) | -- | 0.08-0.68 (0.20) | 8-22 (13) |
| Point bar (silty) | | 26-79 (44) | 31-87 (54) | 7-63 (33) | 0.22-1.60 (0.74) | 54-98 (78) | 2.65-2.77 (2.69) | 0.70-2.12 (1.12) | 0.14-0.37 (0.27) | 0.11-1.24 (0.20) | 2-22 (13) |
| Backswamp (organic) | Insufficient data | 42-367 (127) | 58-397 (152) | 43-218 (106) | 0.16-1.41 (0.70) | 16-73 (43) | 2.10-2.74 (2.46) | 1.36-6.73 (3.11) | -- | 0.03-0.27 (0.14) | 7-20 (13) |
| Backswamp (inorganic) | | 31-98 (59) | 27-148 (83) | 19-86 (56) | 0.03-1.26 (0.55) | 48-91 (65) | 2.52-2.75 (2.66) | 0.85-2.57 (1.62) | 0.07-0.76 (0.26) | 0.1-0.72 (0.13) | 4-27 (12) |
| Prodelta | | 31-70 (53) | 39-100 (79) | 16-72 (51) | 0.12-1.08 (0.51) | 49-90 (72) | 2.67-2.80 (2.72) | 0.84-2.06 (1.32) | 0.11-0.39 (0.22) | 0.18-0.85 (0.20) | 2-22 (13) |
| Intradelta | | 24-132 (58) | 25-212 (77) | 5-164 (52) | 0.39-1.52 (0.69) | 33-98 (67) | 2.57-2.76 (2.70) | 0.64-2.84 (1.57) | 0.07-0.65 (0.23) | 0.01-0.50 (0.20) | 2-22 (13) |
| Inter-distributary | | 24-113 (57) | 38-179 (82) | 19-162 (59) | 0.13-1.03 (0.61) | 45-94 (66) | 1.59-2.74 (2.64) | 1.01-2.59 (1.58) | 0.22-0.85 (0.37) | 0.01-0.50 (0.20) | 2-22 (13) |

LEGEND

Clay (0.005 mm)

Silt (0.05-0.005 mm)

Sand (2.0-0.05 mm)

Organic material

Notes: (1) Numbers in parentheses are average values.
 (2) Insufficient consolidated-undrained and drained shear strength data were available for the natural levee, point bar, prodelta, intradelta, and interdistributary deposits. The data shown represent all five deposits.
 (3) Insufficient data were available to clearly establish the amount of organic matter typically occurring in each deposit.
 (4) Shear strengths are given in cohesion (c), tons per square foot and angle of internal friction (φ) in degrees.
 Q denotes unconsolidated-undrained triaxial compression tests.
 R denotes consolidated-undrained triaxial compression tests.
 S denotes consolidated drained direct shear tests.

(5) Grain-size characteristics based on references 2 and 10.

Inland swamp

Before describing characteristics of inland swamps and their distribution in the study area, a clarification of terminology is in order. Usage of the term inland swamp is restricted to the deltaic plain, whereas the term backswamp is restricted to the Mississippi River alluvial valley. Mapping by May et al. (1984) adopted the usage of the term inland swamp and defined the upvalley margin of this environment. Inland swamps are not bounded by valley margins or older meander belt ridges as in the alluvial valley. Instead, inland swamps in the deltaic plain are areas of high ground and woody vegetation formed because of the high sediment rates from advancing distributary channels.

Kolb (1962) recognized that the term backswamp was inappropriate for the deltaic plain and had reservations about using this term to describe swamp sediments below Donaldsonville, LA. May et al. (1984) have placed the boundary between backswamp and inland swamp near the vicinity of Houma, LA. The boundary separating the two swamp types occurs at the junction of Bayou Teche and Bayou LaFourche, two former Mississippi River courses. Consequently, the summary descriptions and engineering properties in Tables A1 and A2 for backswamp are more appropriate to inland swamp as the samples were derived primarily from inland swamp sediments. The primary distinction here is in process and the ultimate nature of the sediments derived by these processes. In theory, inland swamp sediments are considered to be much finer-grained than backswamp sediments since they are transported by smaller-scale distributary channels to locations on the deltaic plain that are well removed from the main channel. As shown by Figure 3 in the main report, primary Mississippi River flow was not confined to a single main channel during the period of active Holocene delta building but rather was shared by several smaller major distributary courses.

Inland swamps are vertical accretion deposits that receive sediment during times of high-water flow, when the natural levees are crested and suspended sediment in the flood waters is deposited in areas well removed from the main distributary channel. Inland swamp environments are low, often poorly drained, tree-covered areas flanking the main distributary channel. Inland swamps are low areas that are settling basins for flood flow and sediment, and represent one of the final stages in land building by the passing delta front. Sediment supply is sufficient to elevate the land surface to above sea level and allow woody vegetation to develop and become stable.

Inland swamps are the dominant surface environment in the study area and comprise approximately 50 percent of the Holocene deposits depicted in Figure 4. The surface of the inland swamp environment begins at about the 0 ft NGVD elevation. These deposits are approximately 10 to 15 ft thick with the base of this sequence grading into marsh and interdistributary sediments between -10 to -15 ft NGVD (Dunbar et al. 1994).

Inland swamps are composed of uniform, very fine-grained soils, primarily silty clay (CL) and clay (CH). Sand (SM and SP) and silt (ML) may be present but is considered a minor constituent of the total depositional sequence (Table A1 and A2, and Figures 5a through 5k of the main report). These deposits typically contain moderate to high organic contents in the form of

decayed roots, leaves, and wood. Disseminated pyrite is a common but a very minor constituent of these soils and is commonly found in more poorly drained areas which promotes reducing conditions. Inland swamp soils may become well drained during times of low water and undergo short periods of oxidation, lending a mottled appearance to the soil. Inland swamp soils are gray, dark gray, or occasionally black. Inland swamp soils have generally high-water contents, between 30 and 90 percent, as shown by Tables A1 and A2 (backswamp environment).

Point bar

Point bar deposits are lateral accretion deposits formed as a river migrates across its flood plain. River channels migrate across their floodplain by eroding the outside or concave bank and depositing a sandbar on the inside or convex bank. With time the convex bar grows in size and the point bar is developed. Associated with the point bar are a series of arcuate ridges and swales. The ridges are formed by lateral channel movement and represent relic lateral bars separated by low lying swales. The swales are locations for fine-grained sediments to accumulate. Point bar deposits are as thick as the total depth of the river that formed them. These deposits become coarser-grained with increasing depth. Maximum grain size is associated with the river's bedload (coarse sand and fine gravel) while the fine-grained soils occur near the surface. The basal or coarse-grained portion of the point bar sequence is deposited by lateral accretion while the fine-grained or upper portion of the point bar sequence is deposited by vertical accretion.

Point bar deposits in the study area are considered to be young, generally less than 3,500 years old. They began forming along Bayou des Familles-Barataria when the St. Bernard delta system was active but didn't fully develop along the main river until the present Mississippi River course began forming less than 1,000 years before the present.

Soil types in a point bar sequence grade upward from coarse-grained sands and fine gravels near the base to clays near the surface. These deposits are variable, but in the study area are generally composed of at least 50 percent poorly graded fine sand (Figures 5a through 5h and Tables A1 and A2). Point bar deposits are separated into two distinct units, a predominantly fine-grained upper sequence or point bar top stratum, and a coarse-grained lower sequence or point bar substratum. Soil types associated with each unit are identified in the geologic sections in Figures 5a through 5f of the main report.

Abandoned course

An abandoned course as the name implies is a relic fluvial course that is abandoned in favor of a more hydraulically efficient course. An abandoned course contains a minimum of two meander loops and forms when the river's flow path is diverted to a new position on the river's floodplain. This event usually is a gradual process that begins by a break or a crevasse in the river's natural levee during flood stage. The crevasse forms a temporary channel that may, over time, develop into a more permanent channel. Eventually, the new

channel diverts the majority of flow and the old channel progressively fills. Final abandonment begins as coarse sediment fills the abandoned channel segment immediately downstream from the point of diversion. Complete filling of the abandoned course is a slow process that occurs by overbank deposition. The complete filling process may take several hundreds or even thousands of years to complete.

The Bayou des Familles-Barataria abandoned course is a prominent physiographic feature that extends due south from the Mississippi River at approximately river mile 100 (Figures 1 and 4 of the report). The abandoned course extends well beyond the limits of the study area and continues south to Barataria Bay (May et al. 1984, Dunbar et al. 1994). It contains broadly developed natural levees which are easily identified on aerial photography and topographic maps. Well developed natural levees and a meandering plan form distinguish the abandoned course from its short lived predecessor, the crevasse channel.

Boring information from the greater New Orleans area indicates channel fill from the Bayou des Familles abandoned course consists primarily of thick sand deposits capped by a thin layer of silt and clay. Detailed boring information from the abandoned course at its confluence with the Mississippi River is presented in Figures 5c and 5i of the main report. Engineering properties of abandoned course sediments are not sufficiently categorized in Table A1 due to lack of boring data. However, these sediments are considered to be similar in composition to sandy point bar deposits for which data are present.

Abandoned distributary channel

Distributary channels are channels that diverge from the trunk channel dispersing or “distributing” flow away from the main course. By definition, distributary channels do not return flow to the main channel on a delta plain (Bates and Jackson 1987). Distributary channels originate initially as crevasse channels during high flow periods when the main channel is unable to accommodate the larger discharge. If the flood is of sufficient duration, a permanent distributary channel is soon established through the crevasse. Abandonment of a distributary channel or distributary network occurs either as a major course shift upstream or the distributary becomes over extended and loses its gradient advantage in favor of a much shorter distributary channel. Complete abandonment usually occurs because of an improved gradient advantage by the new distributary.

Distributary channel abandonment closely parallels the abandonment of a course. During abandonment, the base of the channel is filled with poorly sorted sands, silts, and organic debris. As the channel continues to fill, the flow velocities are decreased, and the channel is filled by clay, organic ooze, and peats. Abandoned distributaries in the study area are approximately their original width, but only a fraction of their original depth due to infilling. Abandoned distributary channels in the study area are Metairie Bayou, Bayou Sauvage, and two unnamed distributaries that intersect the Mississippi River on the east and west banks (Figure 4). These distributary channels have all been partially or completely filled with sediments.

Often the distal ends of abandoned distributaries have been buried due to subsidence, destroyed by coastal erosion, or closer to the trunk channel, buried by later natural levee deposits (Figure 4). Metarie Bayou in the northern portion of the study area has been buried by later Mississippi River natural levee deposits and altered by the historic activities of man north of the river. Natural levees are ideal for urban development since these areas are topographically higher than the surrounding area.

Abandoned distributaries are recognized on aerial photographs by their natural levees and the urban development associated with these levees. In the subsurface, distributary sediments are recognized by soil types (Table A1) and sedimentary structures characteristic of channel fill deposits. Engineering properties of abandoned distributary sediments are not sufficiently categorized in Table A1 due to lack of boring data. Upper channel fill consists of parallel and wavy laminated silts and silty clays, interbedded with highly burrowed clays with high-water contents. Distorted bedding, slump structures, organic layers, and minor shell material are also common in abandoned distributary deposits.

Freshwater marsh

In the southwestern portion of the study area there is an area of freshwater marsh, a nearly flat expanse where grasses and sedges are the only vegetation. Organic sedimentation plays an important role in the formation of marsh deposits. Peats, organic oozes (mucks), and humus are formed as the marsh plants die and are buried. Decay is largely due to anaerobic bacteria in stagnant water. Vegetative growth and sedimentation maintain the surface elevation at a fairly constant level, and the marsh deposits thicken as a result of subsidence over time. When marsh growth fails to keep pace with subsidence, the marsh surface is eventually inundated by water.

Peats are the most common form of marsh strata remains, and they consist of black fibrous masses of decomposed plants. Detrital organic particles, carried in by marsh drainage, and vegetative tissues form the mucks. Mucks are watery oozes that can support little or no weight. Sedimentation occurs in the marsh when floodwater overtops the natural levees, depositing clays and silts onto the marsh surface. Sediments are also transported to the marsh during lunar tides, wind tides, and hurricane tides when sediment laden marine waters inundate the marsh surface.

Marsh sediments are found in the subsurface as peats (Figures 5b through 5k) and represent a time during the Holocene where the land surface was at sea level and supporting marsh vegetation. Often marsh deposits grade vertically upward in a prograding delta system into inland swamp, followed by natural levee deposits. The reverse sequence is also true (i.e., marsh, natural levee, inland swamp, marsh). Engineering properties of marsh sediments are identified in Table A1.

Subsurface Environments of Deposition

Interdistributary

Interdistributary deposits are sediments deposited in low areas between active distributary channels, usually under brackish water conditions. Sediment laden waters overtop the natural levees of distributary channels during flood stage and deposit the coarsest sediment (silt) near the channel. The finer sediment (silty clay and clay) is transported away from the active distributary channel and settles out of suspension as interdistributary deposits. In this manner, considerable thicknesses of clay are deposited as the distributary builds seaward. Interdistributary clays often grade downward into prodelta clays and upward into the highly organic clays of swamp and marsh deposits.

Interdistributary deposits are found throughout the study area in the subsurface (Figure 5b through 5k of the main report). These deposits range in thickness from 30 to 60 ft and start between 0 to -10 ft NGVD as shown by the cross sections in Figures 5b through 5k. Interdistributary deposits consist of saturated gray clays which are highly bioturbated and contain some silt laminae. Shell fragments and minor amounts of organic debris are also commonly distributed throughout the interdistributary sequence as shown by Tables A1 and A2.

Buried beach

Interdistributary sediments associated with Metairie Bayou, an abandoned St. Bernard distributary in the northern edge of the study area, overlie and grade laterally with buried beach deposits. Buried beach deposits are part of the Pine Island Beach trend, an early Holocene beach trend associated with active sedimentation from the Pearl River (Saucier 1963). Approximately 5,000 years ago, when sea level was slightly lower than the present, longshore drift created a southwest to northeast trending offshore spit or barrier beach complex in the New Orleans area. Sediments forming the spit were derived from sandy fluvial sediments transported by the Pearl River. This spit originated at the river's mouth and extended southwest to the vicinity of New Orleans. This buried beach complex forms the southern shore of Lake Pontchartrain and acted as a natural barrier for filling of Lake Pontchartrain by advancing distributary channels during the active St. Bernard stage of delta growth.

Metairie Bayou (Figure 4) follows the seaward edge of the Pine Island Beach trend and was blocked from entering the main body of Lake Pontchartrain by the higher topography of the relic beach. Instead, Metairie Bayou follows the relic beach trend northeast toward the coastal mainland as the Bayou Sauvage distributary channel. Coastal drainage into Lake Pontchartrain from the Pleistocene uplands breached the beach ridge and formed "The Rigolets," a pass into Lake Pontchartrain at the eastern edge of the deltaic plain (Figure A1 from Saucier 1963).

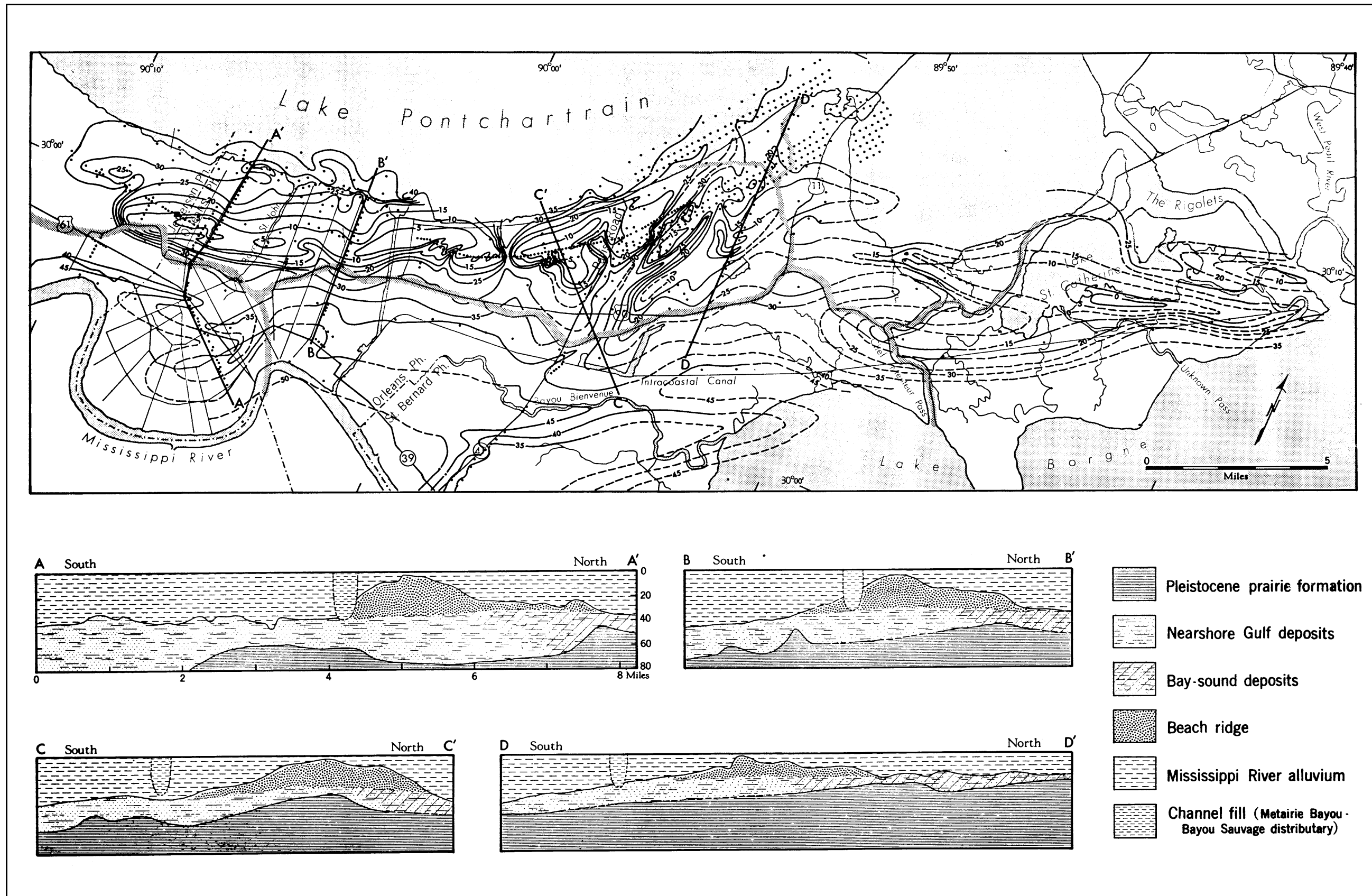


Figure A1. Topography of the buried Pine Island beach trend (Saucier 1963)

The beach trend grades laterally into intradelta and abandoned distributary deposits (Figure A1). Boring data identifies the buried beach deposits as consisting of uniform, fine to medium grained, quartz sand, ranging in color from gray to tan, and white upon exposure at the surface (Saucier 1963). Beach sand is generally well sorted and contains shell fragments.

Intradelta

Intradelta deposits form at the mouth of distributary channels and consist of coarse-grained or sandy sediments. At the mouth of a distributary, the water velocity decreases upon entering open water, depositing coarse-grained sediments from suspension as distributary mouth bars. The coarse sediments are deposited on the bar crest or as fans along the sides of the bars. As the distributary is built seaward, it may cut through or split around the bar. The process is then repeated in each of the smaller, branching distributary channels. These deposits interfinger and merge with interdistributary clays.

Intradelta deposits are identified in the subsurface in borings near the Mississippi River (Figures 5a, 5b, 5e, and 5g). They consist primarily of clean sands and silty sands with some silts. Intradelta deposits are thickest nearer the distributary channels or channel source areas. Engineering properties of intradelta sediments are summarized in Tables A1 and A2.

Nearshore gulf

Nearshore gulf deposits are generally coarse-grained sediments formed by the transgression and interaction of the rising Holocene sea level with the drowned Pleistocene surface. Nearshore gulf deposits represent sediments eroded, transported, and deposited at the land/sea level interface, often at maximum wave energy and under storm conditions. These deposits generally consist of coarse-grained sediments and are primarily characterized by sand and shell hash. Available engineering data is presented in Table A1. The subsurface distribution of this depositional environment is shown by the cross sections in Figures 5a through 5k of the main report. Generally, this environment directly overlies the Pleistocene surface throughout the deltaic plain region.

Estuarine and bay sound

Both of these environments are marine and are a minor environment in the subsurface (see Figures 5a through 5l). Both of these environments directly overlie the Pleistocene surface. These two environments were formed early during the Holocene, or perhaps even Late Pleistocene, when sea level advanced onto the Pleistocene surface. As sea level advanced, it drowned the existing Pleistocene drainage network and created small estuaries and bays.

An estuary is a river valley where fresh water comes into contact with sea water (Bates and Jackson 1987). A bay sound is a partly enclosed brackish water body which is sheltered from direct access to the Gulf and is dominated by both fluvial and marine processes. Since the bay sound is partly restricted from

the Gulf, the depositional energy and associated geomorphic processes are less severe than those associated with the nearshore gulf environment. Sediments deposited within an estuary or bay sound environment have a much greater range in grain size than sediments deposited within the nearshore gulf environment (Table A1). Silt and clay are usually more common within the estuarine and the bay sound environment than the nearshore gulf environment as shown by Table A1.

Substratum

Substratum or “braided stream/outwash plain” deposits related to glacial melting and sea level rise are not present in the study area. Substratum deposits as identified in this report are coarse-grained sediments associated with the point bar environment. The term substratum as used in this report and on the cross sections in Figures 5a through 5k is used in conjunction with and is a modifier of the point bar environment. Point bar substratum deposits are typically the lateral accretion or coarse-grained component of the point bar sequence. The upper boundary occurs at the base of the fine-grained or vertical accretion component of the point bar sequence and is defined by the first nearly continuous silty sand (SM) contact.

Pleistocene

Pleistocene deposits are present only in the subsurface and are correlative to the Prairie Formation. The Prairie Formation is the youngest of Fisk’s (1944) four major interglacial fluvial and deltaic sequences and was deposited during Sangamonian time, approximately 70,000 to 125,000 years ago. The Prairie Formation is similar in origin to the Holocene age deposits which overlie the Prairie. They were both envisioned by Fisk (1944) as fining upward from a coarse-grained substratum to a fine-grained top stratum. Both are products of rising sea level and deposition following continental glaciation. However, detailed analysis of glacial chronology from the midwest, combined with detailed geologic mapping from the Lower Mississippi Valley in recent years, indicates that the four-cycle model of Pleistocene glaciation and the accompanying interglacial deposition are an oversimplification (Autin et al. 1991). Recent studies indicate that the geology of the Prairie Formation in the study area is highly complex (Cullinan 1969; Kolb, Smith, and Silva 1975; Saucier 1977; Dunbar et al. 1994).

Lithologic and stratigraphic data on the Prairie Formation are based on surface exposures north of Lake Pontchartrain in St. Tammy, St. Helena, Tangipahoa, and Washington Parishes, Louisiana, and foundation engineering borings from the greater New Orleans metropolitan area. Pleistocene age soils outcropping on the north shore of Lake Pontchartrain were mapped by Cullinan (1969) as being typically light gray, light brown, or yellowish orange in color and composed of muddy, fine sandstones or fine to very fine sandy siltstones. Beneath the Holocene sediments in the New Orleans area, numerous engineering borings drilled into the Pleistocene surface identify the Prairie as being composed primarily of clay and silty clay and having the following characteristics (Kolb and VanLopik 1958a,b, Kolb 1962): (a) oxidized tan, yellow, or

greenish gray color, (b) a marked decrease in water content, (c) distinctive stiffening in soil consistency and a general increase in shear strength, and (d) the presence of concretions. Pleistocene age soils forming the subsurface in the New Orleans area are usually easily distinguished from Holocene age soils by their sharp contrast in engineering properties, lithology, and stratigraphy. Soil color, water content, and shear strength are the most diagnostic criteria distinguishing Pleistocene from Holocene soils (Table A1).

Between the fine-grained Pleistocene sediments beneath the New Orleans area and the more coarse-grained sediments that outcrop at the surface north of Lake Pontchartrain, there is a transition which may be due to variations within environments of deposition or stratigraphy during the Late Pleistocene. The New Orleans area Pleistocene soils may have formed under several depositional settings, including inland swamp, interdistributary, bay sound, and/or estuarine environments, while the coarser-grained soils north of Lake Pontchartrain are perhaps related to mainland beach and terrestrial fluvial environments draining the Pleistocene uplands. The Prairie surface is a highly complex stratigraphic sequence that consists of multiple depositional facies which formed over a period of several tens of thousands of years, followed by thousands of years of subaerial oxidation and erosion during maximum glacial episodes and lowered sea levels, and then later burial by Holocene sediments.

The Pleistocene surface dips gently to the south and southwest at about 3 to 5 ft per mile (Figure 6 of the main report). Elevations on the Pleistocene surface range from approximately -60 ft NGVD in the northern portions of the study area to more than -100 ft NGVD south of the Mississippi River. The base of the Prairie Formation beneath the Celotex failure site occurs somewhere between elevation -500 and -600 ft NGVD (Cullinan 1969).

References

- Autin, W. J., Burns, S. F., Miller, B. J., Saucier, R. T., and Snead, J. I. (1991). "Chapter 18: Quaternary geology of the Lower Mississippi Valley." Vol K-2, *The Geology of North America*. The Geological Society of North America, Boulder, CO, 547-581.
- Bates, R. L., and Jackson, J. A. (1987). *Glossary of Geology*, 3rd ed., American Geological Institute, Alexandria, VA.
- Clough, G. W. (1966). "Ground water level in silty and sandy Mississippi River upper banks," Mississippi River Commission, Corps of Engineers, Vicksburg, MS. (Mr. F. J. Weaver, Lower Mississippi Valley Division, was a principal assistant in this study).
- Cullinan, T. A. (1969). "Contributions to the geology of Washington and St. Tammy Parishes, Louisiana," U.S. Army Engineer District, New Orleans, LA.
- Dunbar, J. B., Blaes, M. Dueitt, S., and Stroud, K. (1994). "Geological investigation of the Mississippi River deltaic plain, Report 2 of a Series," Technical Report GL-84-15, U.S. Army Engineer Waterways Experiment Station, Vicksburg, MS.
- Dunbar, J. B., Blaes, M., Dneitt, S., and May, J. (1995). "Geological investigation of the Mississippi River deltaic plain, Report 3 of a Series," Technical Report GL-84-15, U.S. Army Engineer Waterways Experiment Station, Vicksburg, MS.
- Dunbar, J. B., and Torrey, V. H. (1991). "Geologic, geomorphological and geotechnical aspects of the Marchand Levee failure, Marchand, Louisiana," Miscellaneous Paper GL-91-17, U.S. Army Engineer Waterways Experiment Station, Vicksburg, MS.
- Eustis Engineering Company. (1984). "Geotechnical investigation: Soil stratification and foundation conditions for residential development," Report for City of New Orleans, Sewerage and Water Board of New Orleans, New Orleans, LA.
- Fisk, H. N. (1944). "Geological investigation of the alluvial valley of the Lower Mississippi River," U.S. Army Corps Engineers, Mississippi River Commission, Vicksburg, MS.

- Frazier, D. E. (1967). "Recent deltaic deposits of the Mississippi River: Their development and chronology." *Gulf Coast Association of Geological Societies. Transactions 17th annual meeting*. San Antonio, TX.
- Halbouty, M. T. (1967). *Salt Domes, Gulf Region, United States and Mexico*. Gulf Publishing Company, Houston, TX.
- Hvorslev, M. J. (1956). "A review of the soils studies," Potamology Investigations Report No. 12-5, U.S. Army Engineer Waterways Experiment Station, Vicksburg, MS.
- Kemp, E. B. (1967). "Geologic setting of New Orleans." *Guidebook New Orleans, LA and vicinity field trip*. The Geological Society of America and Associated Societies, Annual meetings.
- Kolb, C. R. (1962). "Distribution of soils bordering the Mississippi River from Donaldsonville to Head of Passes," Technical Report No. 3-601, U.S. Army Engineer Waterways Experiment Station, Vicksburg, MS.
- Kolb, C. R., and Saucier, R. T. (1982). "Engineering geology of New Orleans," *Geological Society of America, Reviews in Engineering Geology* 5, 75-93.
- Kolb, C. R., Smith, F. L., and Silva, R. C. (1975). "Pleistocene sediments of the New Orleans-Lake Pontchartrain area," Technical Report S-75-6, U.S. Army Engineer Waterways Experiment Station, Vicksburg, MS.
- Kolb, C. R., Steinriede, W. B., Krinitzsky, E. L., Saucier, R. T., Mabrey, P. R., Smith, F. L., and Fleetwood, A. R. (1968). "Geological investigation of the Yazoo Basin, Lower Mississippi Valley," Technical Report 3-480, U.S. Army Engineer Waterways Experiment Station, Vicksburg, MS.
- Kolb, C. R., and VanLopik, J. R. (1958a). "Geology of the Mississippi River Deltaic Plain," Technical Report No. 3-483, Vol 1 and 2, U.S. Army Engineer Waterways Experiment Station, Vicksburg, MS.
- _____. (1958b). "Geological investigation of the Mississippi River-Gulf Outlet Channel," Miscellaneous Paper No. 3-259, U.S. Army Engineer Waterways Experiment Station, Vicksburg, MS.
- Krinitzsky, E. L. (1965). "Geological influences on bank erosion along meanders of the Lower Mississippi River," Potamology Investigations, Report 12-15, U.S. Army Engineer Waterways Experiment Station, Vicksburg, MS.
- Krinitzsky, E. L., and Smith, F. L. (1969). "Geology of backswamp deposits in the Atchafalaya Basin, Louisiana," Technical Report S-69-8, U.S. Army Engineer Waterways Experiment Station, Vicksburg, MS.
- Krinitzsky, E. L., Turnbull, W. J., and Weaver, F. J. (1966). "Bank erosion in cohesive soils of the Lower Mississippi Valley," Vol 92, No. SM1, *Journal of Soil Mechanics and Foundations Division, Proceedings American Society of Civil Engineers*, 121-136.

- May, J. R., Britsch, L. D., Dunbar, J. B., Rodriguez, J. P., and Wlonsinski, L. B. (1984). "Geological investigation of the Mississippi River Deltaic Plain," Technical Report GL-84-15, U.S. Army Engineer Waterways Experiment Station, Vicksburg, MS.
- Miller, W. (1983). "Stratigraphy of newly exposed quaternary sediments, Eastern Orleans Parish, Louisiana," *Tulane Studies in Geology and Paleontology* 17(3, 4), 85-104.
- Montgomery, R. L. (1974). "Correlation of engineering properties of cohesive soils bordering the Mississippi River from Donaldsonville to Head of Passes, LA," Miscellaneous Paper S-74-20, U.S. Army Engineer Waterways Experiment Station, Vicksburg, MS.
- New Orleans Geological Society. (1962). "Salt domes of South Louisiana," Vol 1 and 2, J. C. Stipe and J. P. Spillers, ed., New Orleans, LA.
- _____. (1983). "Salt domes of South Louisiana," Vol 3, S. J. Waguespack, ed., New Orleans, LA.
- Padfield, C. J. (1978). "The stability of riverbanks and flood embankments," Final Technical Report, U.S. Army European Research Office, London, England.
- Saucier, R. T. (1963). "Recent geomorphic history of the Pontchartrain Basin, Louisiana," Technical Report 16, Part A, United States Gulf Coastal Studies, Coastal Studies Institute, Contribution No. 63-2, Louisiana State University, Baton Rouge, LA.
- _____. (1964). "Geological investigation of the St. Francis Basin," Technical Report 3-659, U.S. Army Engineer Waterways Experiment Station, Vicksburg, MS.
- _____. (1967). "Geological investigation of the Boeuf - Tensas Basin Lower Mississippi Valley," Technical Report 3-757, U.S. Army Engineer Waterways Experiment Station, Vicksburg, MS.
- _____. (1969). "Geological investigation of the Mississippi River area, Artonish to Donaldsonville, Louisiana," Technical Report S-69-4, U.S. Army Engineer Waterways Experiment Station, Vicksburg, MS.
- Saucier, R. T. (1974). "Quaternary geology of the Lower Mississippi Valley," Arkansas Archeological Survey, Research Series No. 6, Fayetteville, AR.
- _____. (1977). "The Northern Gulf Coast during the Farmdalian Substage: A search for evidence," Technical Report S-69-4, U.S. Army Engineer Waterways Experiment Station, Vicksburg, MS.
- Saucier, R. T., and Kolb, C. R. (1967). "Alluvial geology of the Yazoo Basin, Lower Mississippi Valley," 1:250,000 map, U.S. Army Engineer Waterways Experiment Station, Vicksburg, MS.

- Self, R. P., and Davis, D. W. (1983). "Geology of the New Orleans area," *The Compass of Sigma Gamma Epsilon* 60(2), 29-38.
- Smith, F. L., and Russ, D. P. (1974). "Geological investigation of the Lower Red River-Atchafalaya Basin area," Technical Report S-74-5, U.S. Army Engineer Waterways Experiment Station, Vicksburg, MS.
- Smith, L. M., Dunbar, J. B., and Britsch, L. D. (1986). "Geomorphological investigation of the Atchafalaya Basin, Area West, Atchafalaya Delta, and Terrebonne Marsh, Vol 1 and 2," Technical Report GL-86-3, U.S. Army Engineer Waterways Experiment Station, Vicksburg, MS.
- Snead, J. I., and McCulloh, R. P. (1984). "Geologic map of Louisiana, scale 1:500,000, Baton Rouge, LA."
- Torrey, V. H., III. (1988). "Retrogressive failures in sand deposits of the Mississippi River, Report 2, Empirical evidence in support of the hypothesized failure mechanism and development of the levee safety flow slide monitoring system," Technical Report GL-88-9, U.S. Army Engineer Waterways Experiment Station, Vicksburg, MS.
- Torrey, V. H., III, Dunbar, J. B., and Peterson, R. W. (1988). "Retrogressive failures in sand deposits of the Mississippi River, Report 1, Field investigations, laboratory studies and analysis of the hypothesized failure mechanism," Technical Report GL-88-9, U.S. Army Engineer Waterways Experiment Station, Vicksburg, MS.
- Torrey, V. H., III, and Weaver, F. J. (1984). "Flow failures in Mississippi riverbanks." *Proceedings IV International Symposium on Landslides*. Vol 2, Toronto, Canada, 355-360.
- Turnbull, W. J., Krinitzky, E. L., and Weaver, F. J. (1966). "Bank erosion in soils of the Lower Mississippi Valley." *Proceedings of the American Society of Civil Engineers, Journal of the Soil Mechanics and Foundation Division*, 92(SM1), 121-136.
- U.S. Army Corps of Engineers. (1909). "Survey of the Mississippi River, Chart Nos. 69 and 70," Mississippi River Commission, Vicksburg, MS.
- U.S. Army Corps of Engineers. (1921). "Survey of the Mississippi River, Chart Nos. 69 and 70," Mississippi River Commission, Vicksburg, MS.
- _____. (1950). "Piezometer observations at Reid Bedford Bend and indicated seepage forces," Potamology Investigations Report No. 5-4, Vicksburg, MS.
- U.S. Army Corps of Engineers. (1975). "Master index, upper and lower Mississippi River surveys for period 1879-80 to 1928 and some historic maps prior to this period," Vol 2, Mississippi River Commission, Vicksburg, MS.
- U.S. Army Engineer District, New Orleans. (1938). "Maps of the Mississippi River, Angola, La., to the Head of Passes," New Orleans, LA.

U.S. Army Engineer District, New Orleans. (1952). "Mississippi River hydrographic survey, 1949-1952, Angola, La., to Head of Passes and South and Southwest Passes and Pass A Loutre," New Orleans, LA.

_____. (1965). "Mississippi River hydrographic survey, 1961-1963, Black Hawk, La., to Head of Passes and South and Southwest Passes and Pass A Loutre," New Orleans, LA.

_____. (1976). "Mississippi River hydrographic survey, 1973-1975, Black Hawk, La., to Head of Passes and South and Southwest Passes and Pass A Loutre," New Orleans, LA.

_____. (1984). "Mississippi River levees, Item M-181.1 to 180.2-L, Marchand Levee setback, final report," New Orleans, LA (internal report, unpublished).

_____. (1986). "Mississippi River levees, Item M-100.4-R, Celotex Levee and Batture restoration, final report," New Orleans, LA (internal report, unpublished).

_____. (1988). "Mississippi River hydrographic survey, 1983-1985, Black Hawk, La., to Head of Passes and South and Southwest Passes and Pass A Loutre," New Orleans, LA (internal report, unpublished).

Wallace, W. E. (1966). "Fault and salt map of South Louisiana," *Gulf Coast Association of Geological Societies*, Vol 16.

K2 – Limit Equilibrium (Slope Stability) Analysis of 17th Street Canal

Limit equilibrium analyses is used to examine stability of the levees and I-wall section of the floodwall, and to examine possible mechanisms of failure at each breach site. The results of these analyses are interpreted in terms of factors of safety and probabilities of failure. This interim report will examine the factors of safety for the 17th Street Canal levee and I-wall section based on the IPET shear strength model described in the Data Report – 17th Street Canal in this Appendix K.

Objectives

The analyses of stability described in the following sections were performed to answer these questions:

- (1) What are the factors of safety for the 17th Street Canal I-wall based on the IPET shear strength model, and how do the factors of safety vary with water level in the canal?
- (2) How are these factors of safety affected by assuming that a crack forms between the canal side of the wall and the levee fill, as the water level rises on the canal side of the wall?
- (3) What water level is needed for a factor of safety equal to 1.0, and how does this differ for Stations 8+30, 10+00, and 11+50?
- (4) How do factors of safety calculated using the New Orleans District Method of Planes compare to factors of safety calculated using Spencer's Method?
- (5) How do factors of safety calculated for design compare with those calculated using the IPET shear strength model and Spencer's Method?
- (6) How do factors of safety calculated for the breach area compare to factors of safety calculated for adjacent reaches of the I-wall, north and south of the breach area?

- (7) What are the probabilities of failure in the breach and adjacent areas?

Conditions Analyzed

Fifteen slope stability analyses (Cases 1 through 15 in Table K4-1) were performed for cross sections at Stations 8+30, 10+00, and 11+50 which are shown in Figures K1-11, K1-12, and K1-13 of the data report. The shear strength profiles for these analyses are shown in Figures K1-54, K1-55, and K1-56 of the shear strength evaluation report. These strengths are identified as “IPET” in Table K2-1.

Five slope stability analyses (Cases 16 through 20 in Table K2-1) were performed using the cross section and strength profile used in the 17th Street Canal design memorandum¹. These are identified as “GDM 20” in Table K2-1.

Average values of moist unit weight were used in the analyses: $\gamma_{\text{sat}} = 109$ pcf for the levee fill, $\gamma_{\text{sat}} = 80$ pcf for the peat, and $\gamma_{\text{sat}} = 109$ pcf for the clay beneath the peat, based on values measured in laboratory tests on undisturbed samples.

The critical slip surfaces found in the analyses did not extend down to the sand beneath the clay, and the sand strength and unit weight therefore did not influence the results of the analyses.

The analyses were performed for undrained conditions in the levee fill, the peat, and the clay beneath the peat. Based on available information, it appears that the permeabilities of all three of these materials were low enough so that dissipation of excess pore pressures during the rise of the water level in the canal would have been negligible, and would have had at most a minor influence on stability.

Analyses were performed for two conditions regarding contact between the I-wall and the adjacent soil on the canal side of the wall. These are indicated by “yes” or “no” in the column labeled “Crack” in Table K2-1.

- For the “no crack” analyses, it was assumed that the soil on the canal side of the wall was in intimate contact with the wall. Water pressures were applied to the surface of the levee fill, and to the I-wall where it projected above the crown of the levee, but were not applied to the face of the wall below the crown of the levee.
- For the “crack” analyses, it was assumed that the I-wall was separated from the levee fill on the canal side of the wall as the water level in the canal rose and caused the wall to deflect away from the canal. Full hydrostatic water pressures were applied to the I-wall, from the water level in the canal to the bottom of the wall.

¹ General Design Memorandum #20 – 17th Street Outfall Canal – Volume 1 (GDM20).

**Table K2-1
Results of Slope Stability Analyses for Stations 8+30, 10+00, and 11+50 of the 17th Street Canal Floodwall.**

| Case | Section | Slip Surface | Method | Strength Model | Crack | Water Elev. Ft. NGVD | F |
|------|---------|--------------|-----------|----------------|-------|----------------------|------|
| 1 | 8+30 | Crit. Circle | Spencer's | IPET | no | 8.5 | 1.75 |
| 2 | 8+30 | Crit. Circle | Spencer's | IPET | yes | 8.5 | 1.32 |
| 3 | 8+30 | Crit. Circle | Spencer's | IPET | no | 11.5 | 1.41 |
| 4 | 8+30 | Crit. Circle | Spencer's | IPET | yes | 11.5 | 1.04 |
| 5 | 8+30 | Crit. Circle | Spencer's | IPET | yes | 12.1 | 1.00 |
| 6 | 10+00 | Crit. Circle | Spencer's | IPET | no | 8.5 | 1.57 |
| 7 | 10+00 | Crit. Circle | Spencer's | IPET | yes | 8.5 | 1.21 |
| 8 | 10+00 | Crit. Circle | Spencer's | IPET | no | 11.5 | 1.28 |
| 9 | 10+00 | Crit. Circle | Spencer's | IPET | yes | 11.5 | 0.99 |
| 10 | 10+00 | Crit. Circle | Spencer's | IPET | yes | 11.3 | 1.00 |
| 11 | 11+50 | Crit. Circle | Spencer's | IPET | no | 8.5 | 1.60 |
| 12 | 11+50 | Crit. Circle | Spencer's | IPET | yes | 8.5 | 1.21 |
| 13 | 11+50 | Crit. Circle | Spencer's | IPET | no | 11.5 | 1.29 |
| 14 | 11+50 | Crit. Circle | Spencer's | IPET | yes | 11.5 | 1.03 |
| 15 | 11+50 | Crit. Circle | Spencer's | IPET | yes | 11.7 | 1.00 |
| 16 | GDM 20 | Crit. Circle | Spencer's | GDM 20 | no | 8.5 | 1.77 |
| 17 | GDM 20 | Crit. Circle | Spencer's | GDM 20 | yes | 8.5 | 1.60 |
| 18 | GDM 20 | Crit. Circle | Spencer's | GDM 20 | no | 11.5 | 1.45 |
| 19 | GDM 20 | Crit. Circle | Spencer's | GDM 20 | yes | 11.5 | 1.24 |
| 20 | GDM 20 | Crit. Circle | Spencer's | GDM 20 | yes | 13.6 | 1.00 |

Analyses were performed for the following canal water levels:

- Elevation 8.5 ft NGVD¹, the approximated water level at the time of failure. As of March 1, 2006 it is estimated that the water level in the 17th Street Canal at the time I-wall began to fail was 7.5 ft to 9.5 ft.
- Elevation 11.5 ft, the water level used as the principal design loading condition.
- The elevations that resulted in computed factors of safety equal to 1.0 at 8+30, 10+00, and 11+50. These were different elevations for the three stations.
- Elevation 13.6 ft, the elevation that resulted in a computed factor of safety equal to 1.0 for the GDM20 cross section and strength. This was analyzed only for the GDM20 cross section and strength model used in design.

¹ All elevations here are referred to NGVD datum. Elevations will be adjusted to NAVD88 when the required information becomes available.

The analyses described here were performed using the computer program SLIDE¹. Critical circular slip surfaces were located for each case, using the search routines available in SLIDE. The analyses were performed using Spencer's method², which satisfies all conditions of equilibrium. Methods that satisfy all conditions of equilibrium have been shown to result in values of factor of safety that are not influenced appreciably by the details of the assumptions they involve³.

In all, 20 cases were analyzed. The conditions analyzed and results of these analyses are summarized in Table K2-1. The critical circles for these cases are shown in Figures K2-1 through K2-15, and K2-17 through K2-21.

Effect of Canal Water Level

The higher the water level in the canal, the lower was the calculated factor of safety, all other things being equal. This can be seen for the no crack condition by comparing Cases 1 and 3, for Station 8+30. Raising the canal water level from elevation 8.5 ft to elevation 11.5 ft results in a decrease in the computed factor of safety of 0.34, from 1.75 to 1.41. For Station 10+00, raising the water level from elevation 8.5 to 11.5 results in a decrease in factor of safety of 0.29 (Cases 6 and 8). For Station 11+50, the reduction is 0.31 (Cases 11 and 13).

Raising the water level also reduces the factor of safety for the cracked condition, as can be seen by comparing Cases 2 and 4, Cases 7 and 9, and Cases 12 and 14. The reduction in the value of F for these cases varies from 0.18 to 0.28.

Effect of a Crack on the Canal Side of the Wall

Assuming that a crack formed on the canal side of the wall, and that hydrostatic water pressure acted through the full depth of the crack, causes a very significant reduction in the value of the calculated factor of safety.

For Station 8+30, with the canal water level at elevation 8.5 ft, the calculated factor of safety for the cracked condition is 1.32, as compared to 1.75 for the uncracked condition. With the water level at 11.5 ft, introducing a crack reduces the factor of safety from 1.41 to 1.04.

For Station 10+00, with the canal water level at elevation 8.5 ft, the calculated factor of safety for the cracked condition is 1.21, as compared to 1.57 for the uncracked condition. With the water level at 11.5 ft, introducing a crack reduces the factor of safety from 1.28 to 0.99.

¹ Available from Rocscience Inc., 31 Balsam Avenue, Toronto, Ontario, Canada M4E 3B5

² Spencer, E. (1967) "A Method of Analysis of the Stability of Embankments Assuming Parallel Inter-Slice Forces," *Geotechnique*, Institution of Civil Engineers, Great Britain, Vol. 17, No. 1, March, pp. 11-26.

³ Duncan, J. Michael, and Wright, Stephen G. (2005), *Soil Strength and Slope Stability*, John Wiley and Sons, New York, 293 pp.

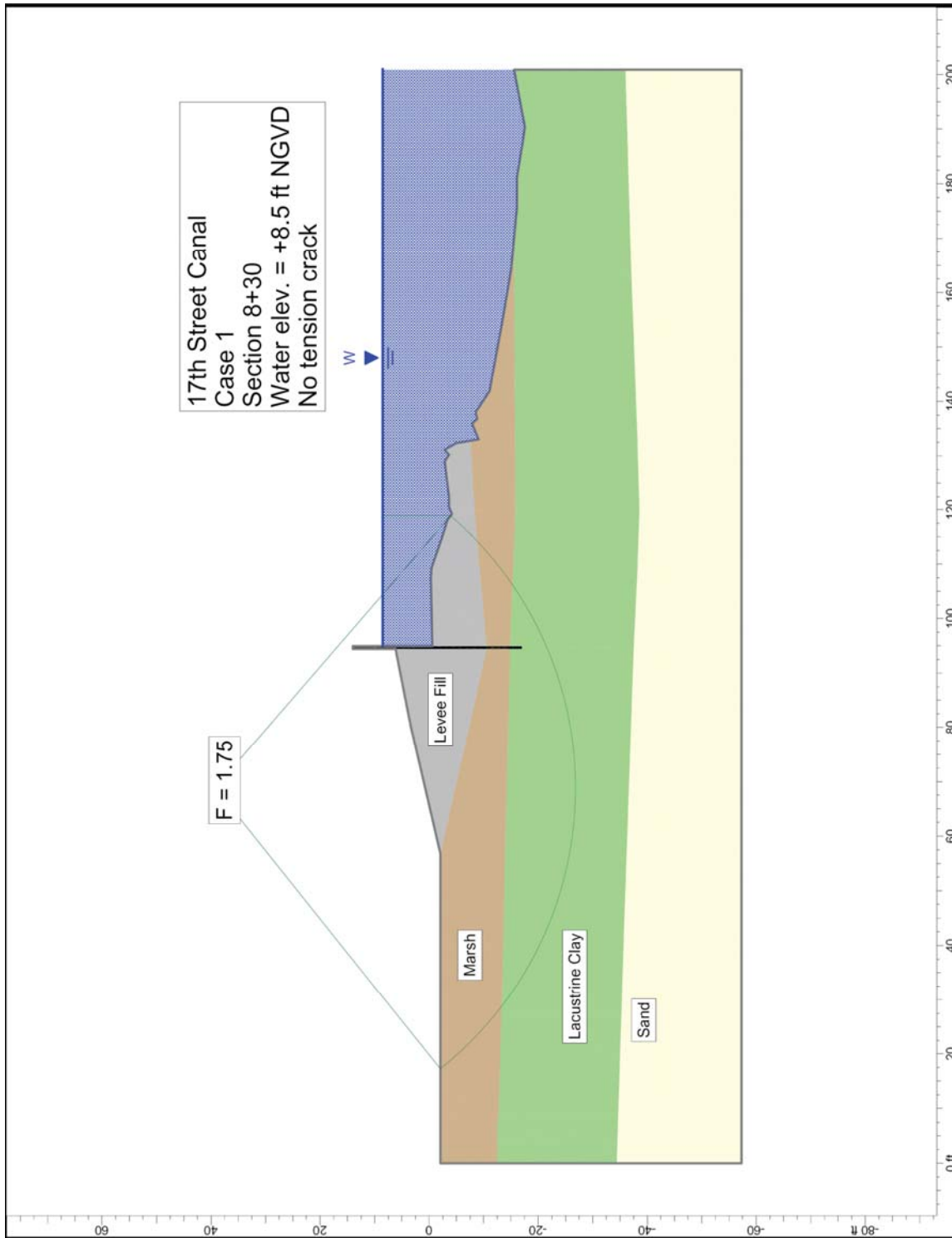


Figure K2-1. Critical circle for 17th Street Canal Station 8+30 – water elevation 8.5 ft, no tension crack.

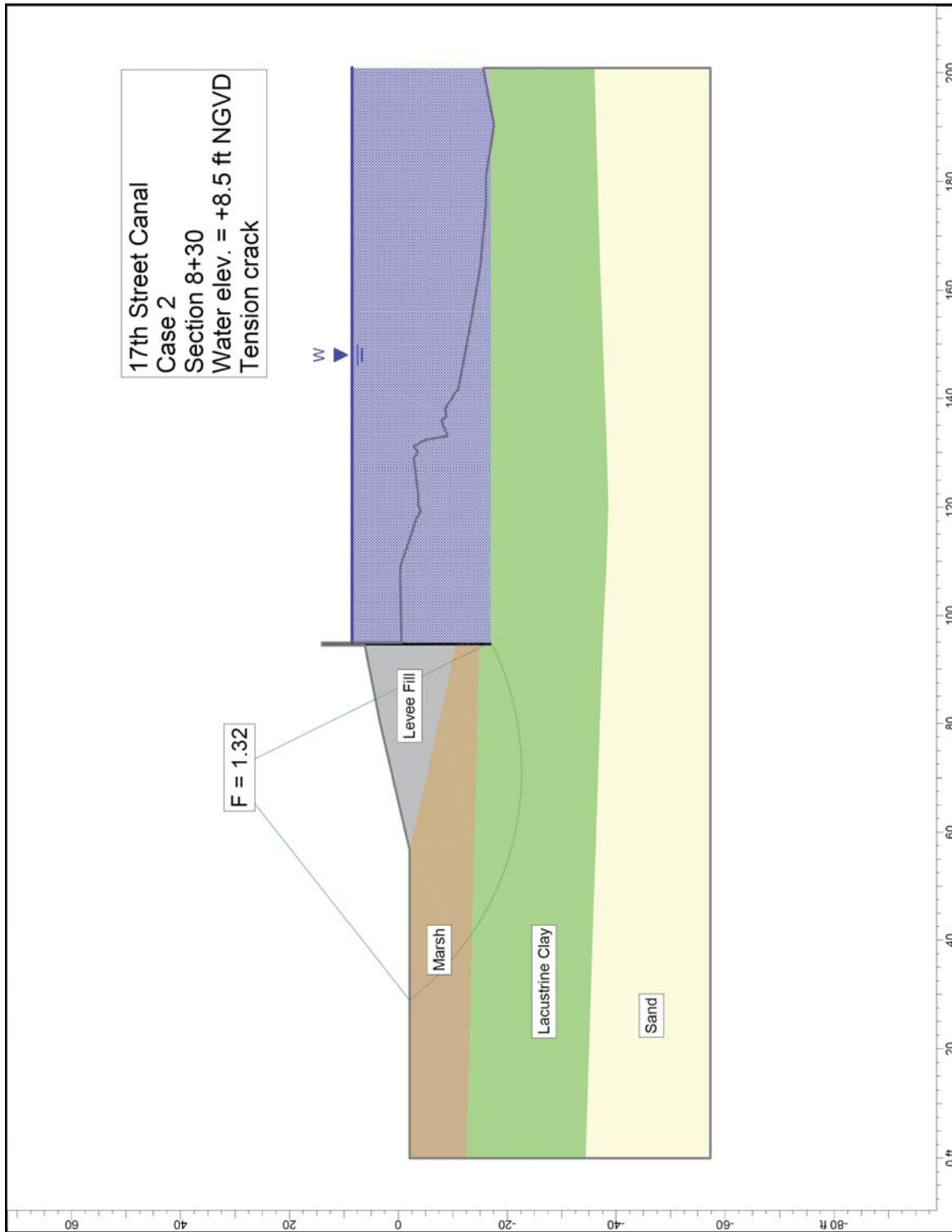


Figure K2-2. Critical circle for 17th Street Canal Station 8+30 – water elevation 8.5 ft, tension crack.

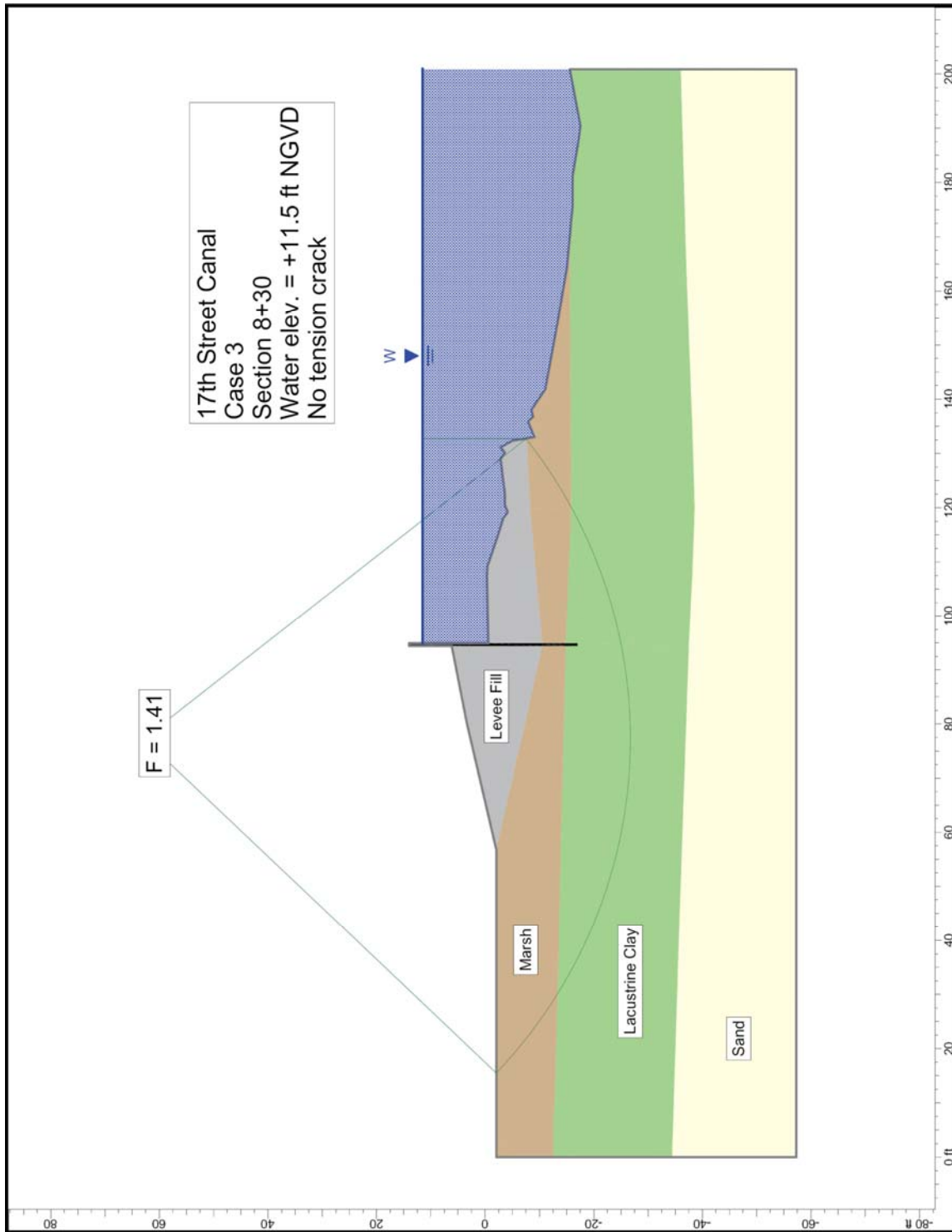


Figure K2-3. Critical circle for 17th Street Canal Station 8+30 – water elevation 11.5 ft, no tension crack.

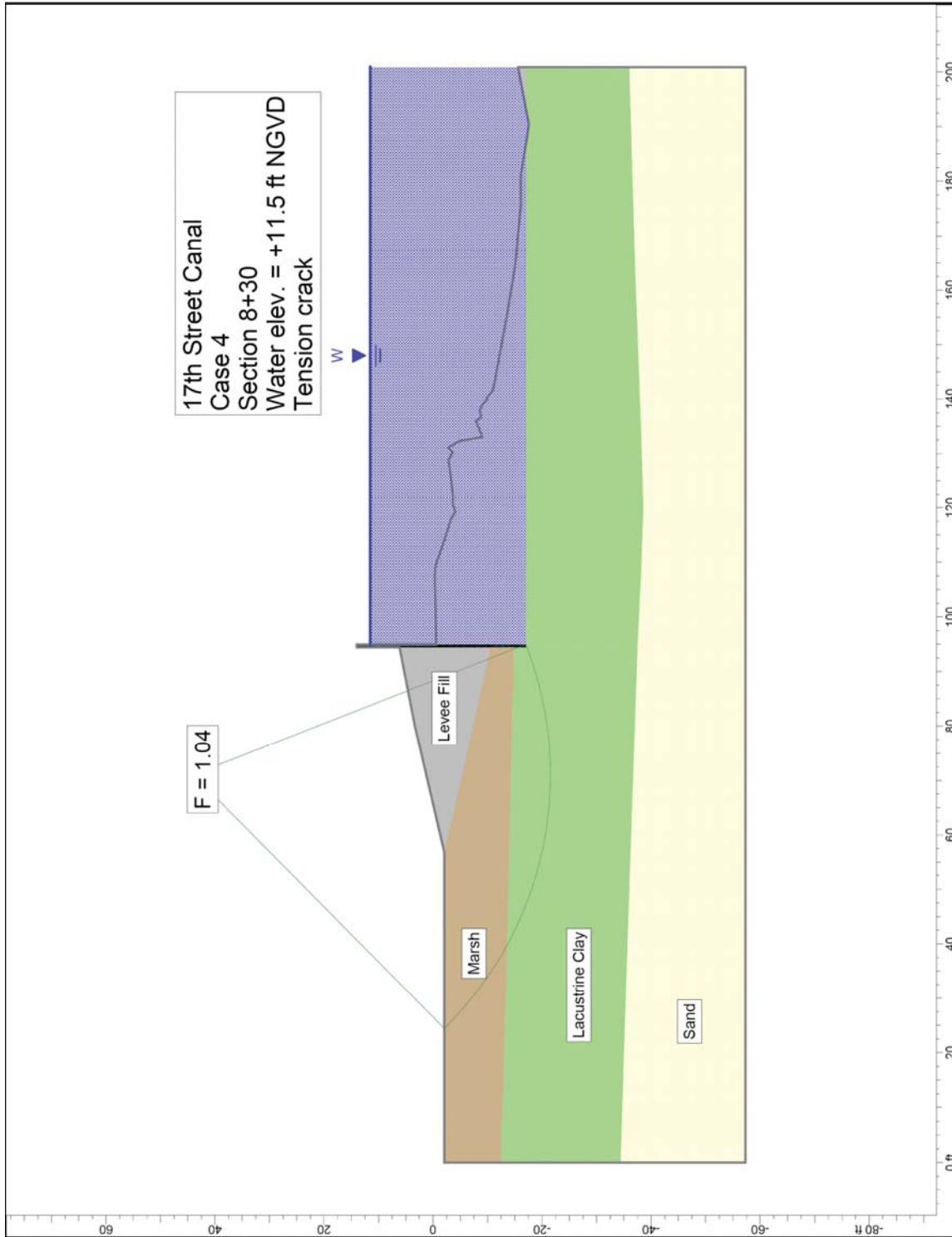


Figure K2-4. Critical circle for 17th Street Canal Station 8+30 – water elevation 11.5 ft, tension crack.

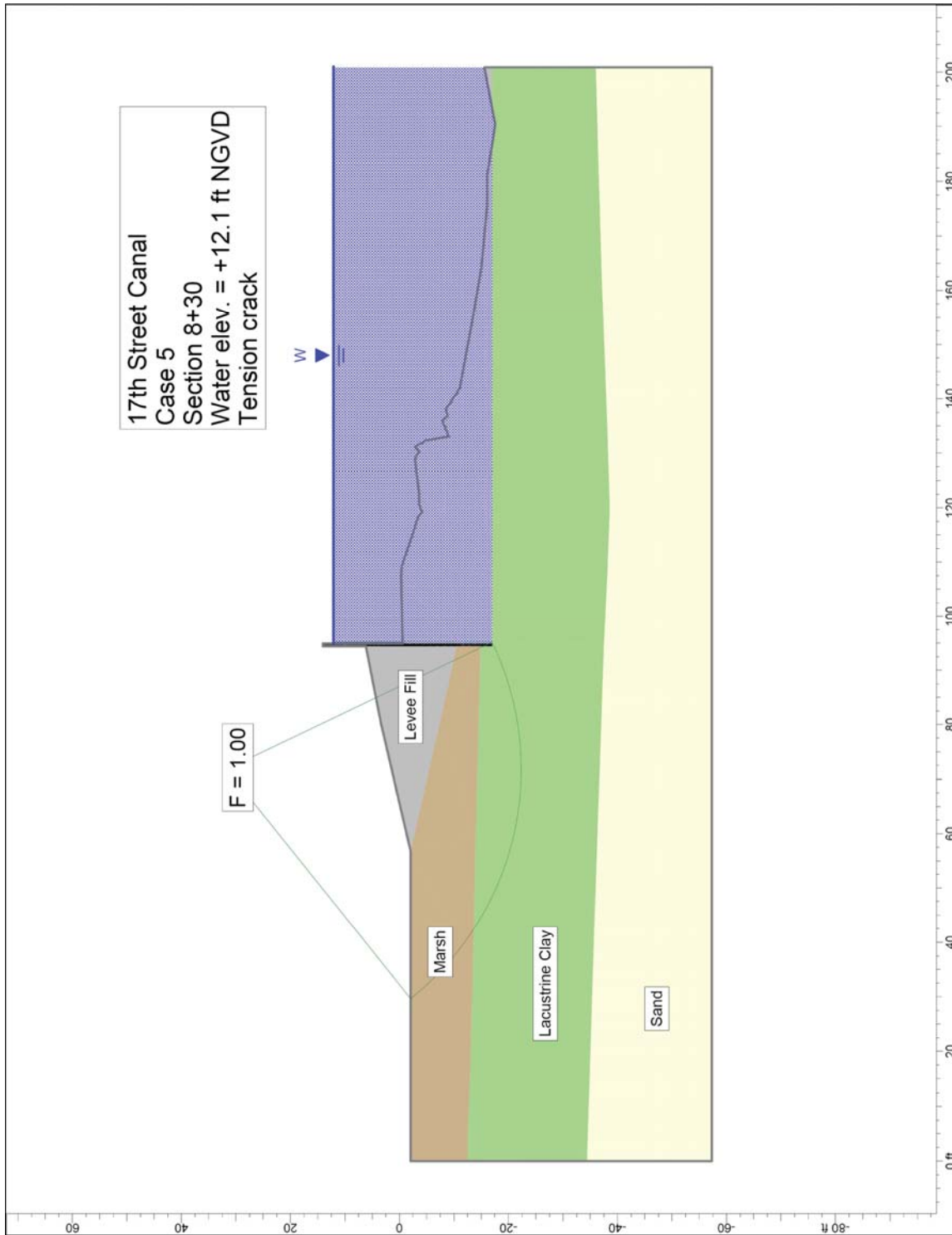


Figure K2-5. Critical circle for 17th Street Canal Station 8+30 – water elevation 5.9 ft, tension crack.

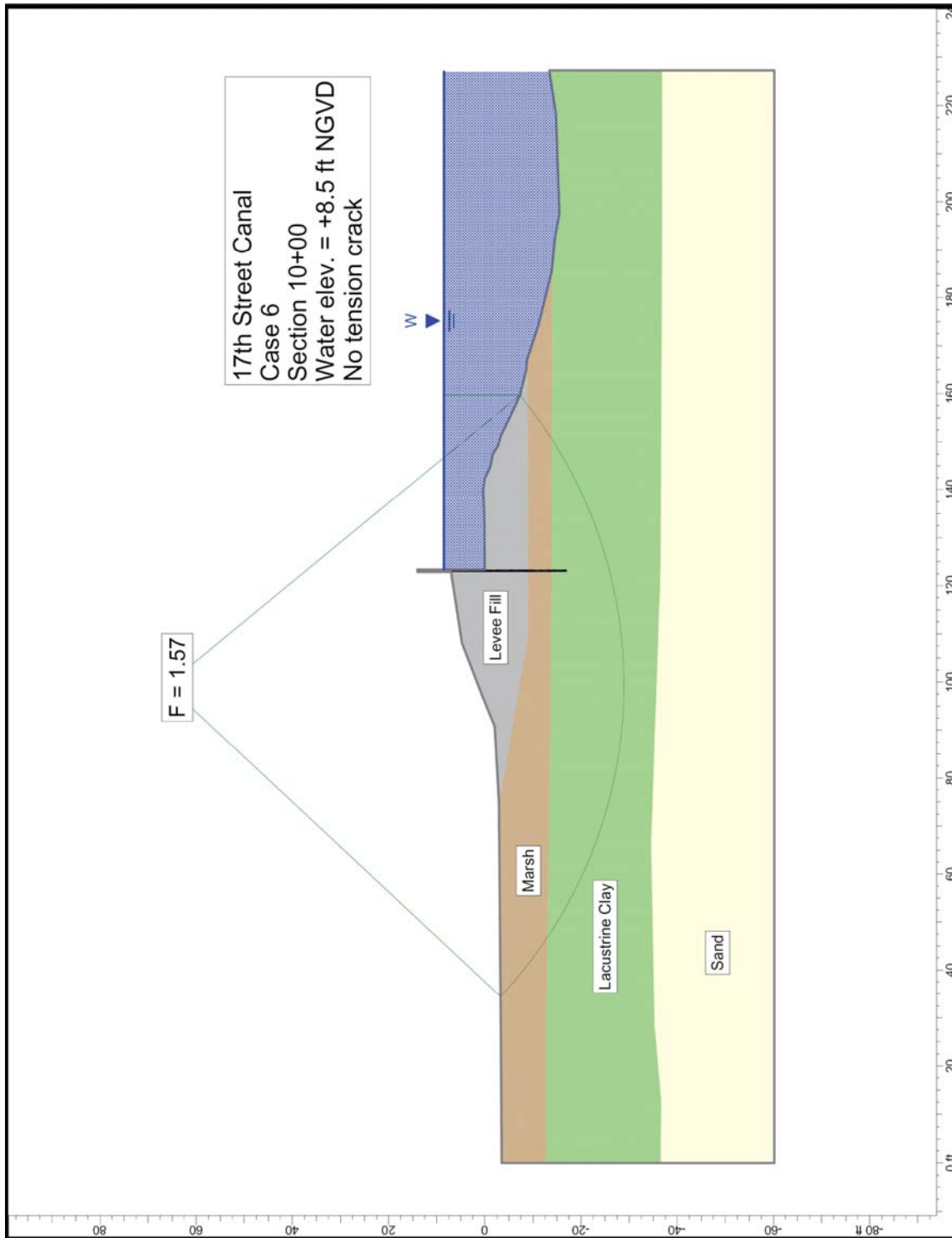


Figure K2-6. Critical circle for 17th Street Canal Station 10+00 – water elevation 8.5 ft, no tension crack.

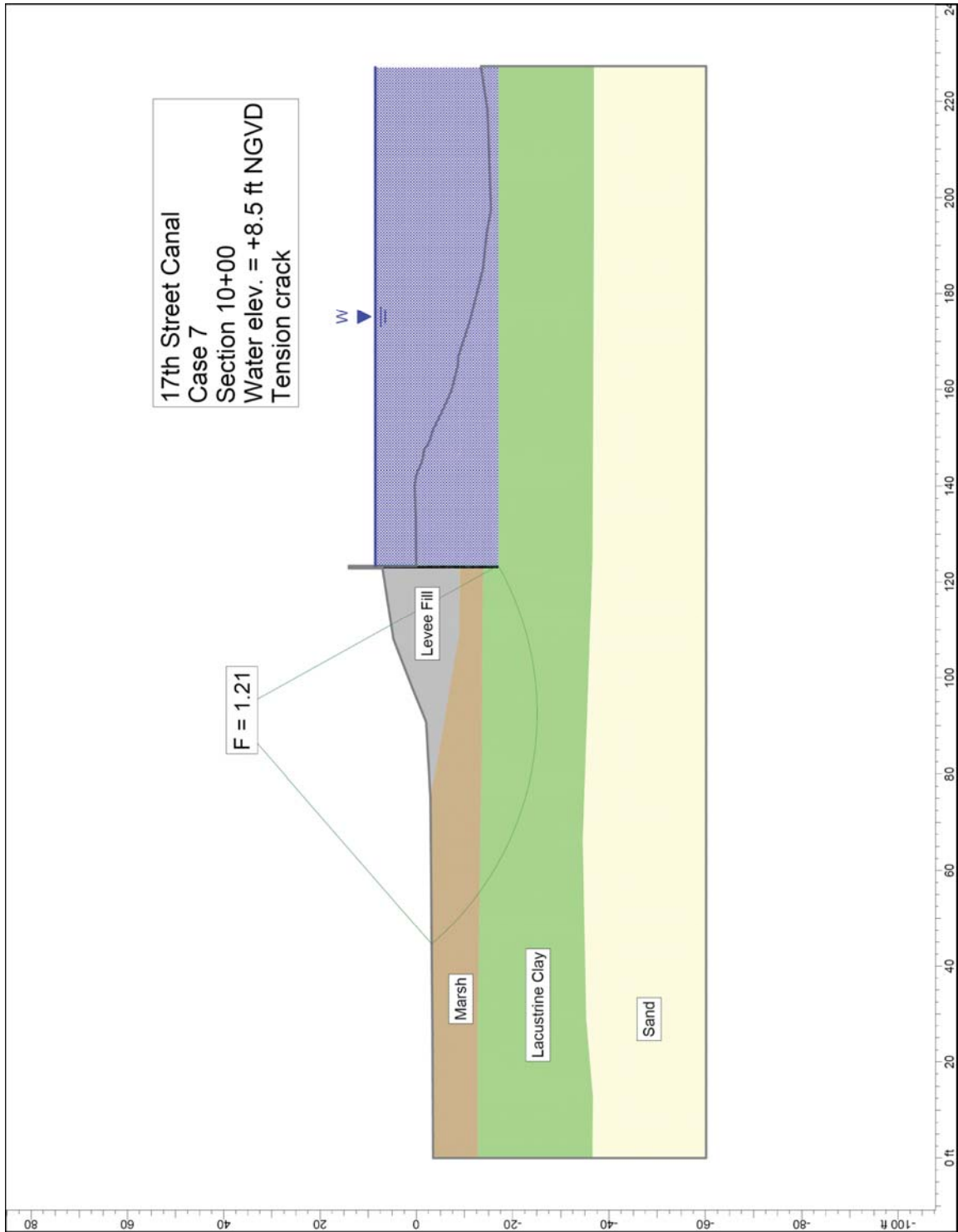


Figure K2-7. Critical circle for 17th Street Canal Station 10+00 – water elevation 8.5 ft, tension crack.

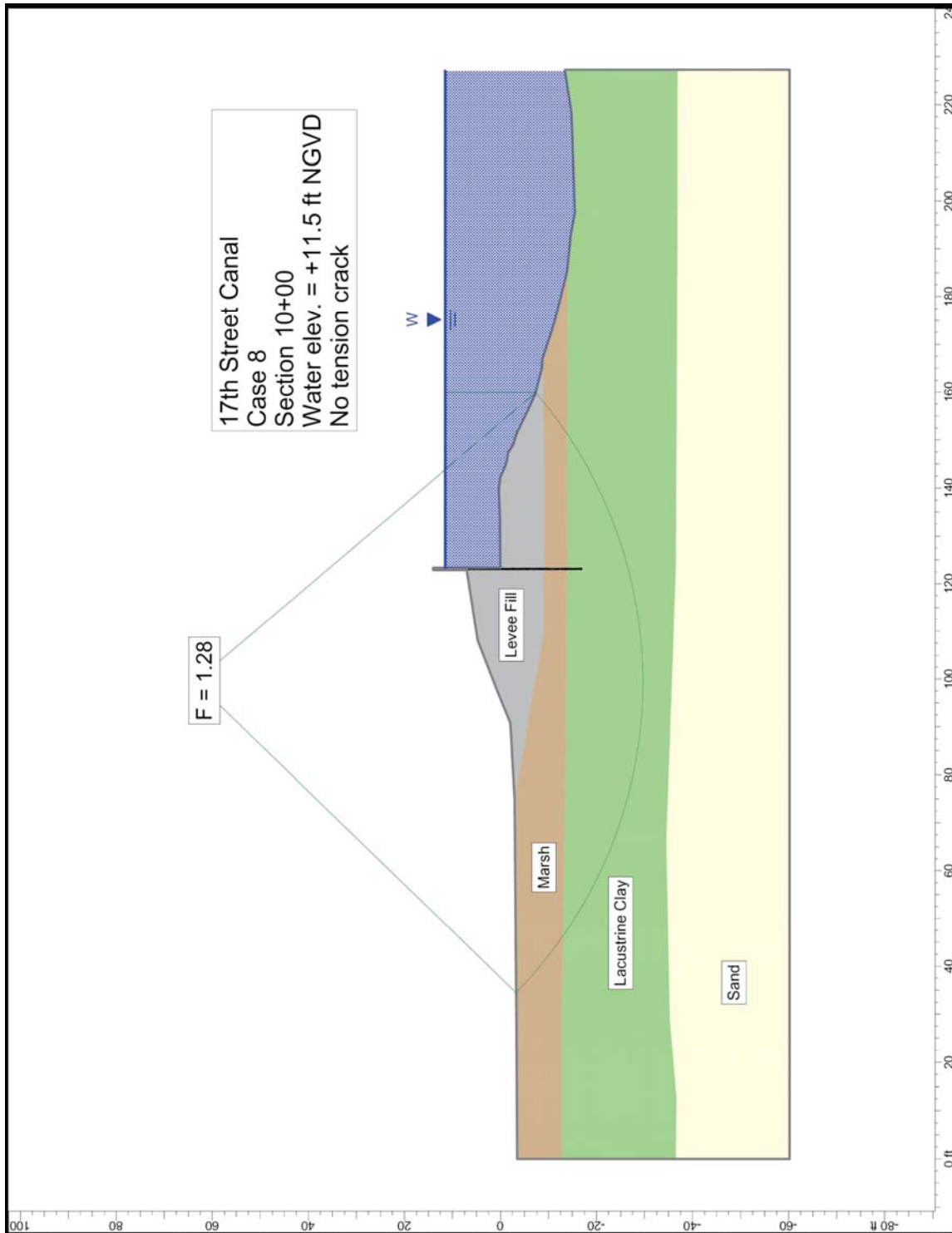


Figure K2-8. Critical circle for 17th Street Canal Station 10+00 – water elevation 11.5 ft, no tension crack.

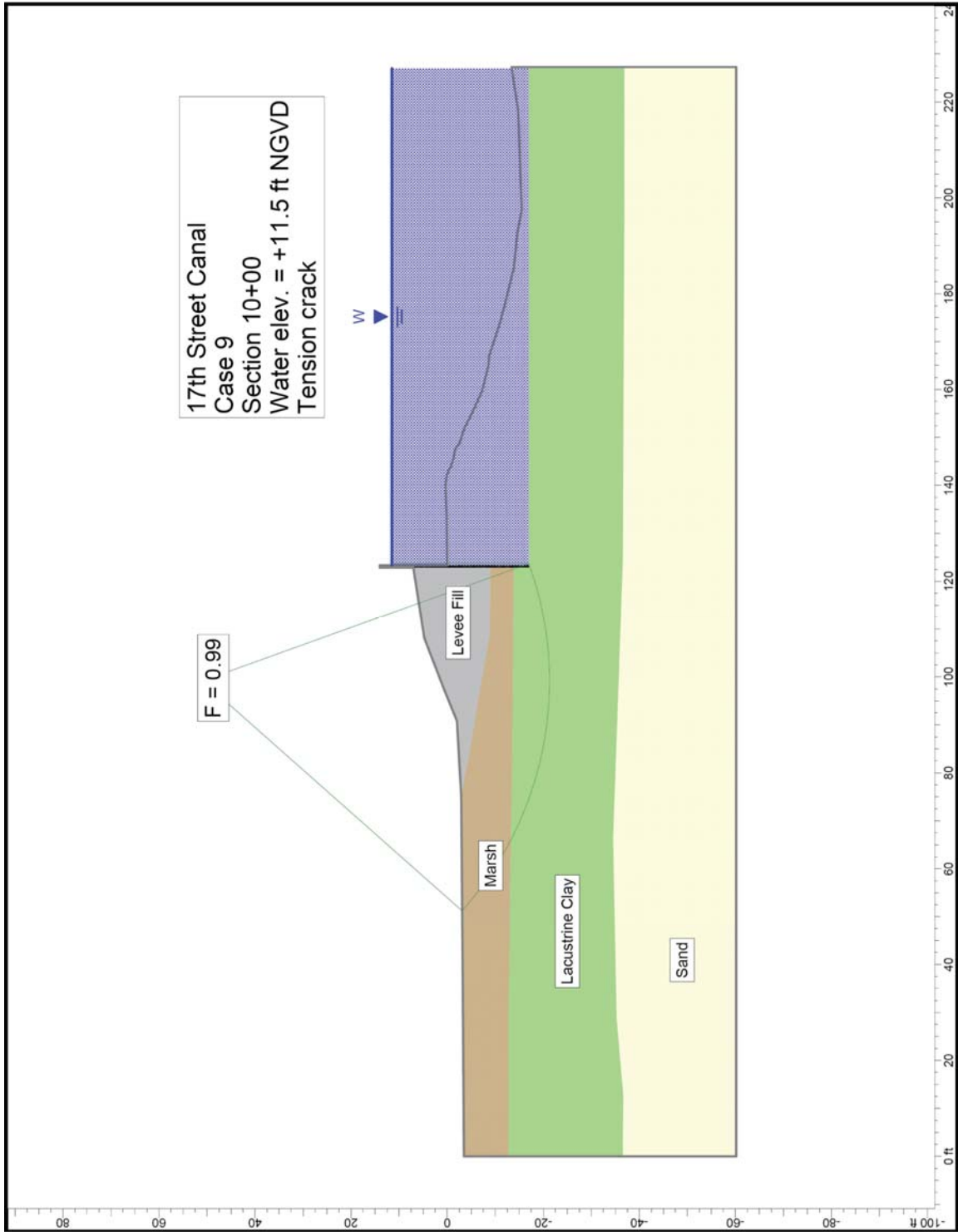


Figure K2-9. Critical circle for 17th Street Canal Station 10+00 – water elevation 11.5 ft, tension crack.

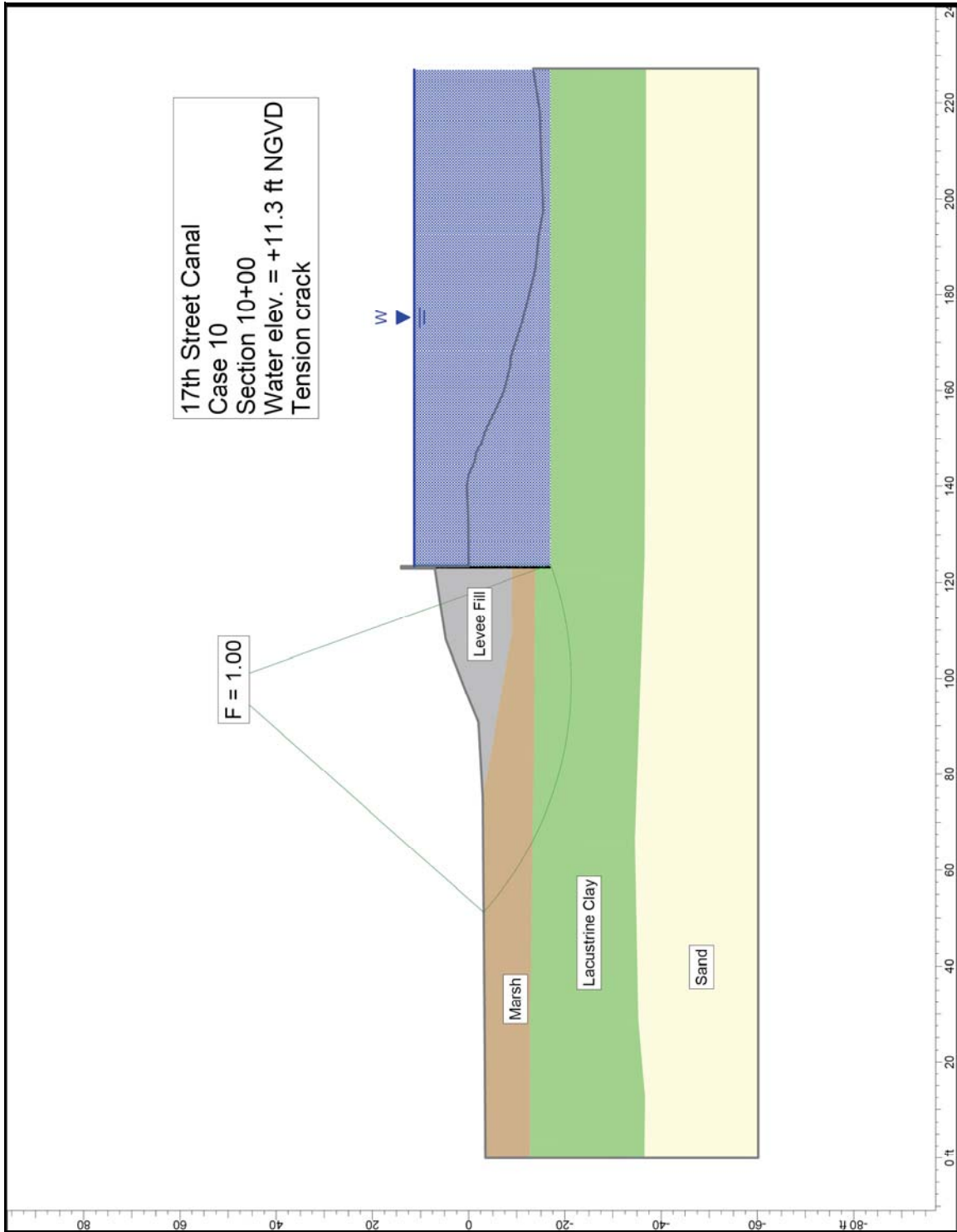


Figure K2-10. Critical circle for 17th Street Canal Station 10+00 – water elevation 11.3 ft, tension crack.

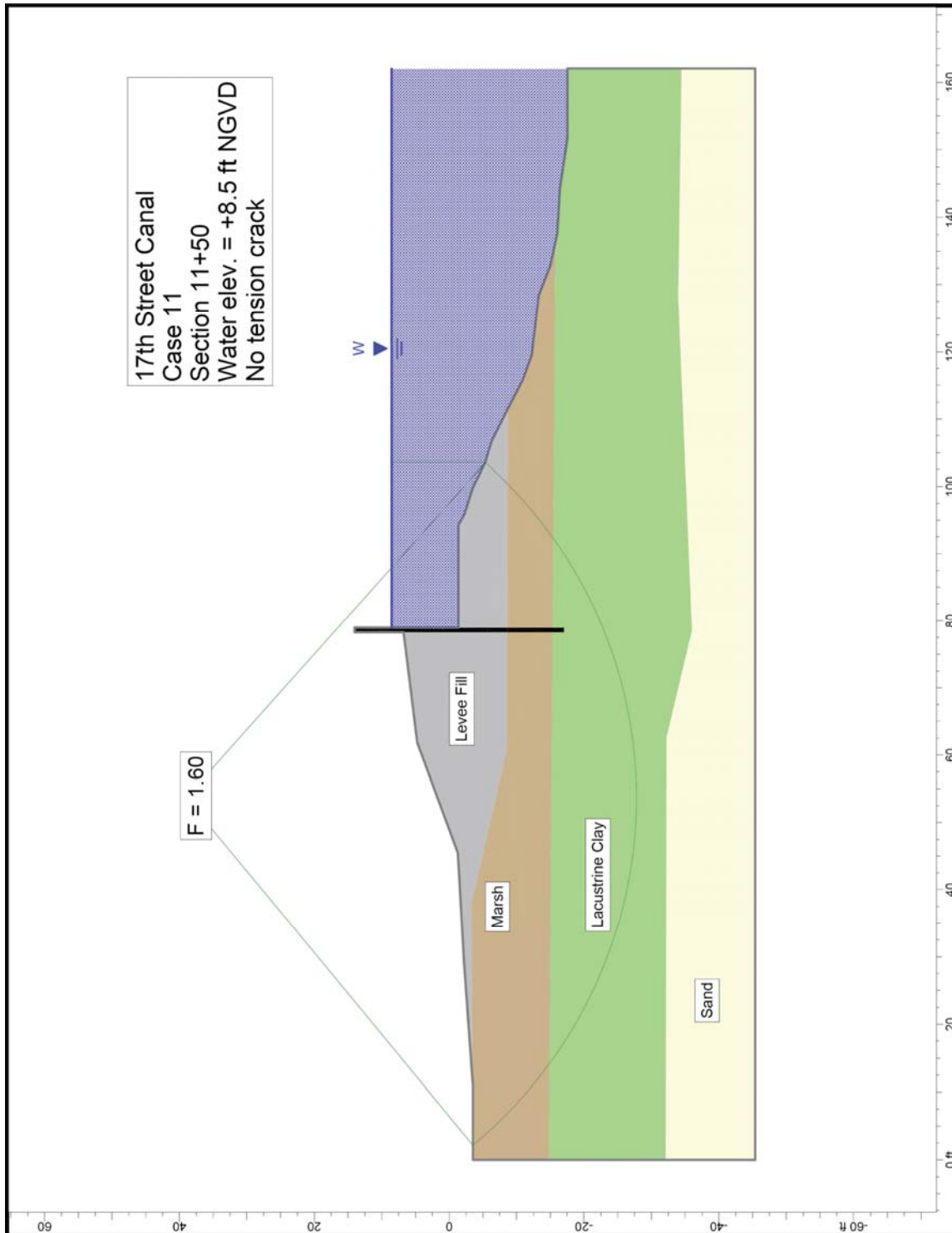


Figure K2-11. Critical circle for 17th Street Canal Station 11+50 – water elevation 8.5 ft, no tension crack.

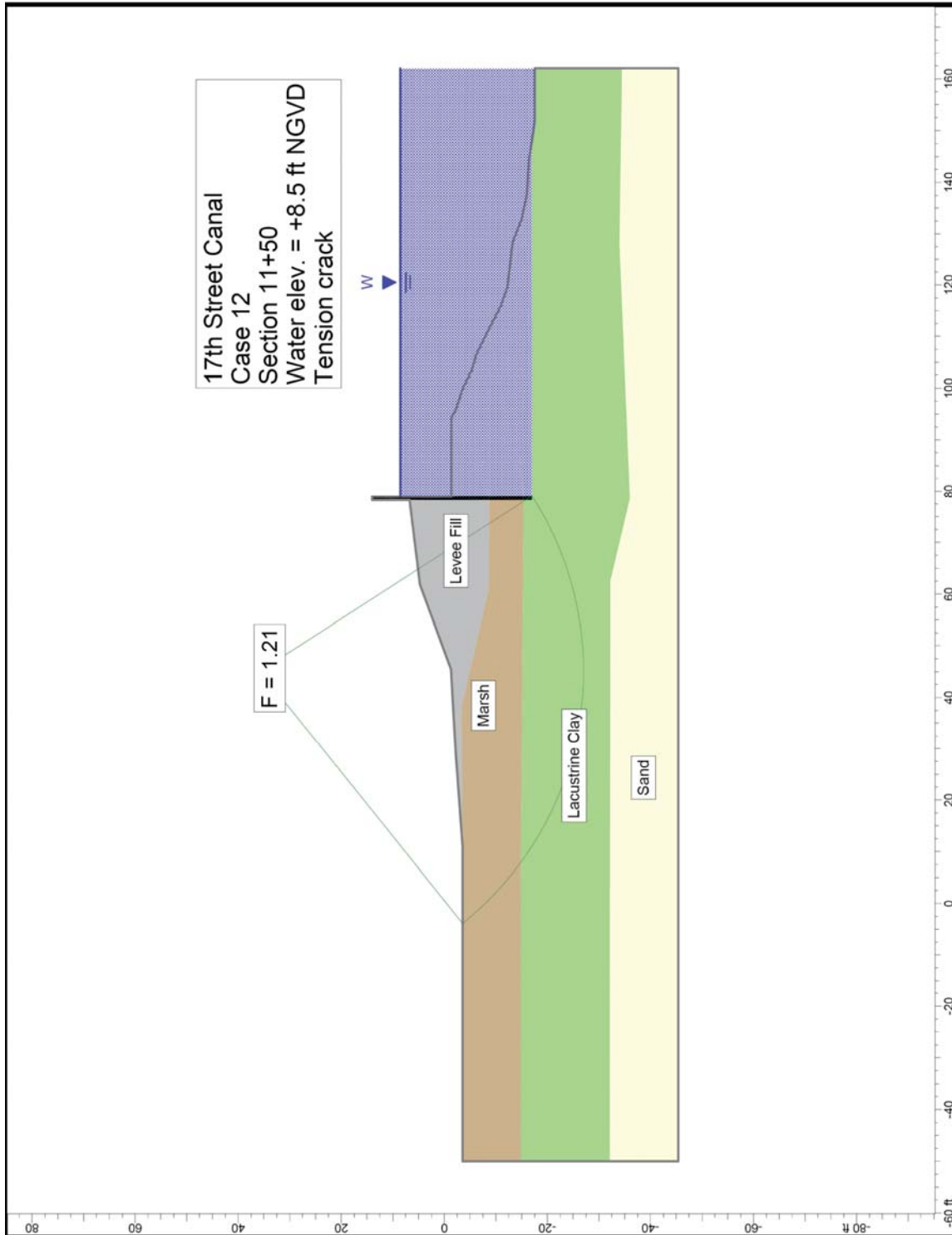


Figure K2-12. Critical circle for 17th Street Canal Station 11+50 – water elevation 8.5 ft, tension crack.

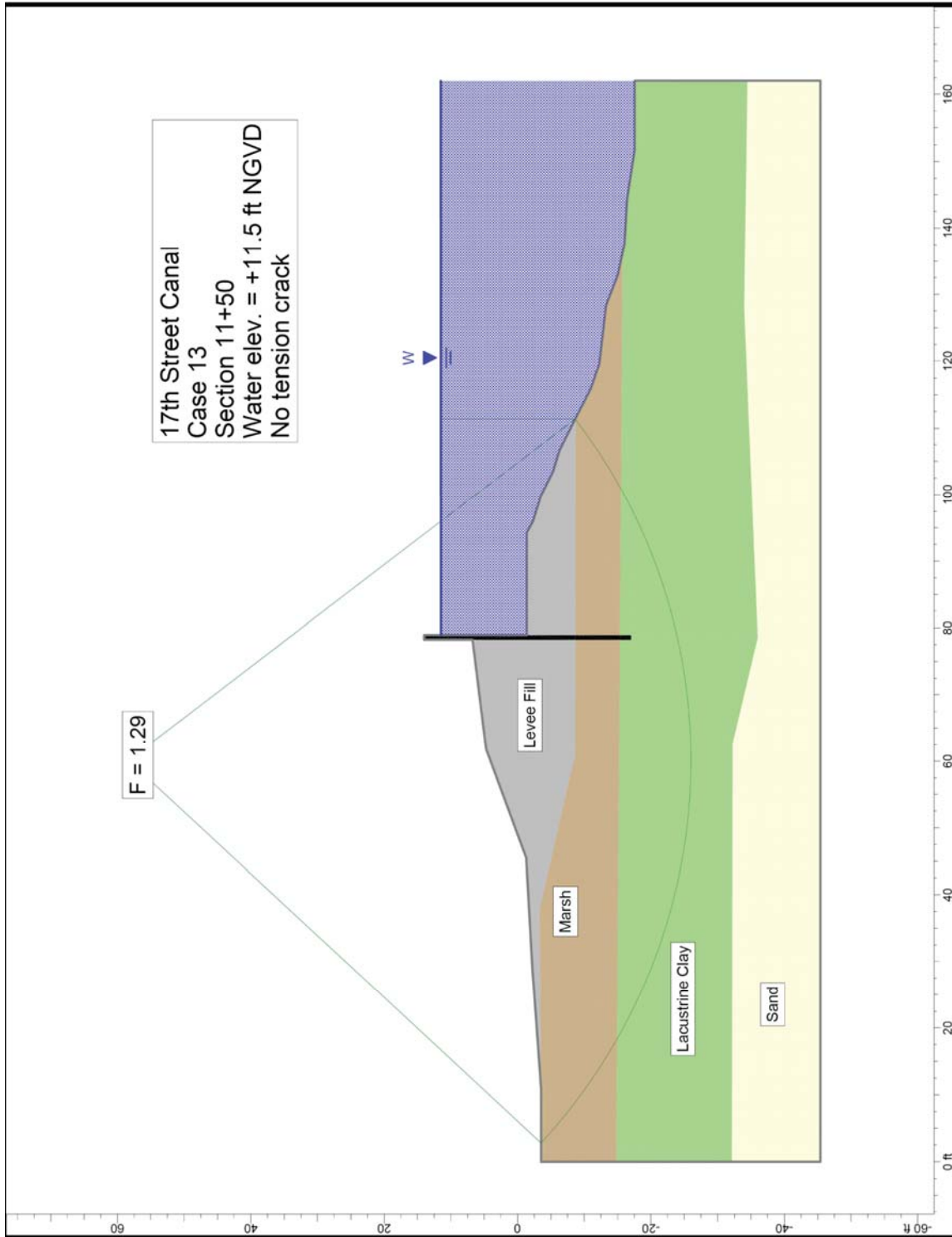


Figure K2-13. Critical circle for 17th Street Canal Station 11+50 – water elevation 11.5 ft, no tension crack.

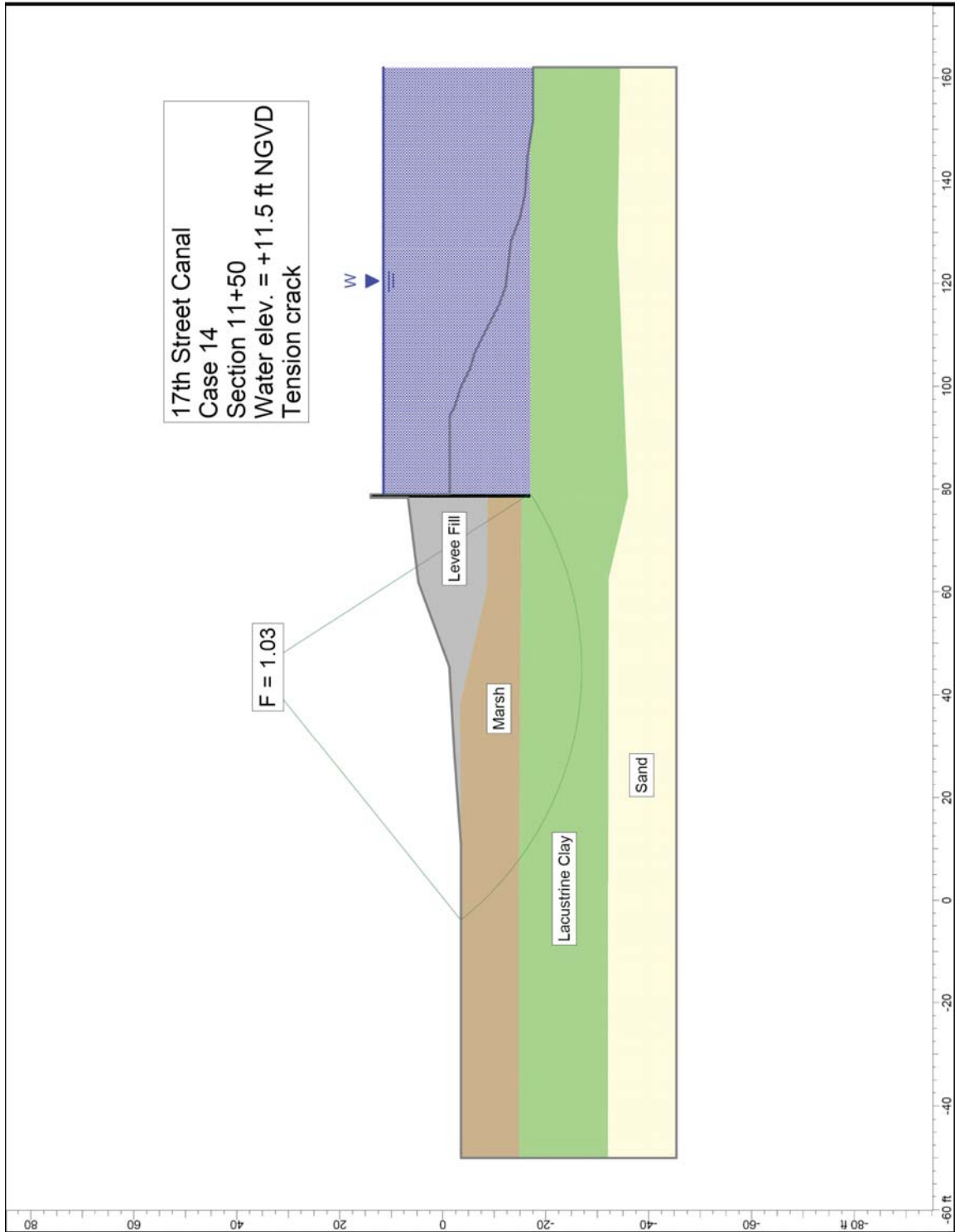


Figure K2-14. Critical circle for 17th Street Canal Station 11+50 – water elevation 11.5 ft, tension crack.

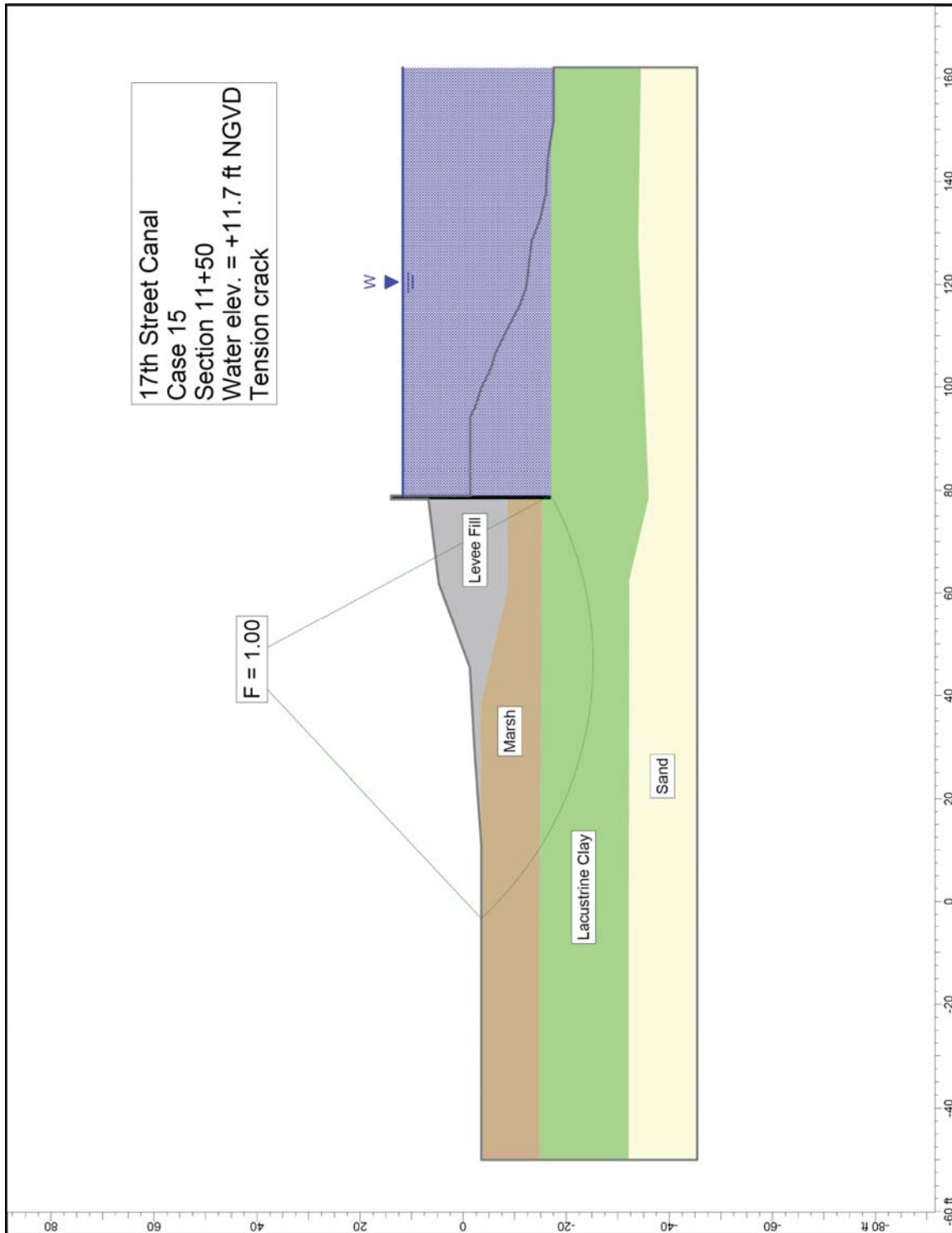


Figure K2-15. Critical circle for 17th Street Canal Station 11+50 – water elevation 11.7 ft, tension crack.

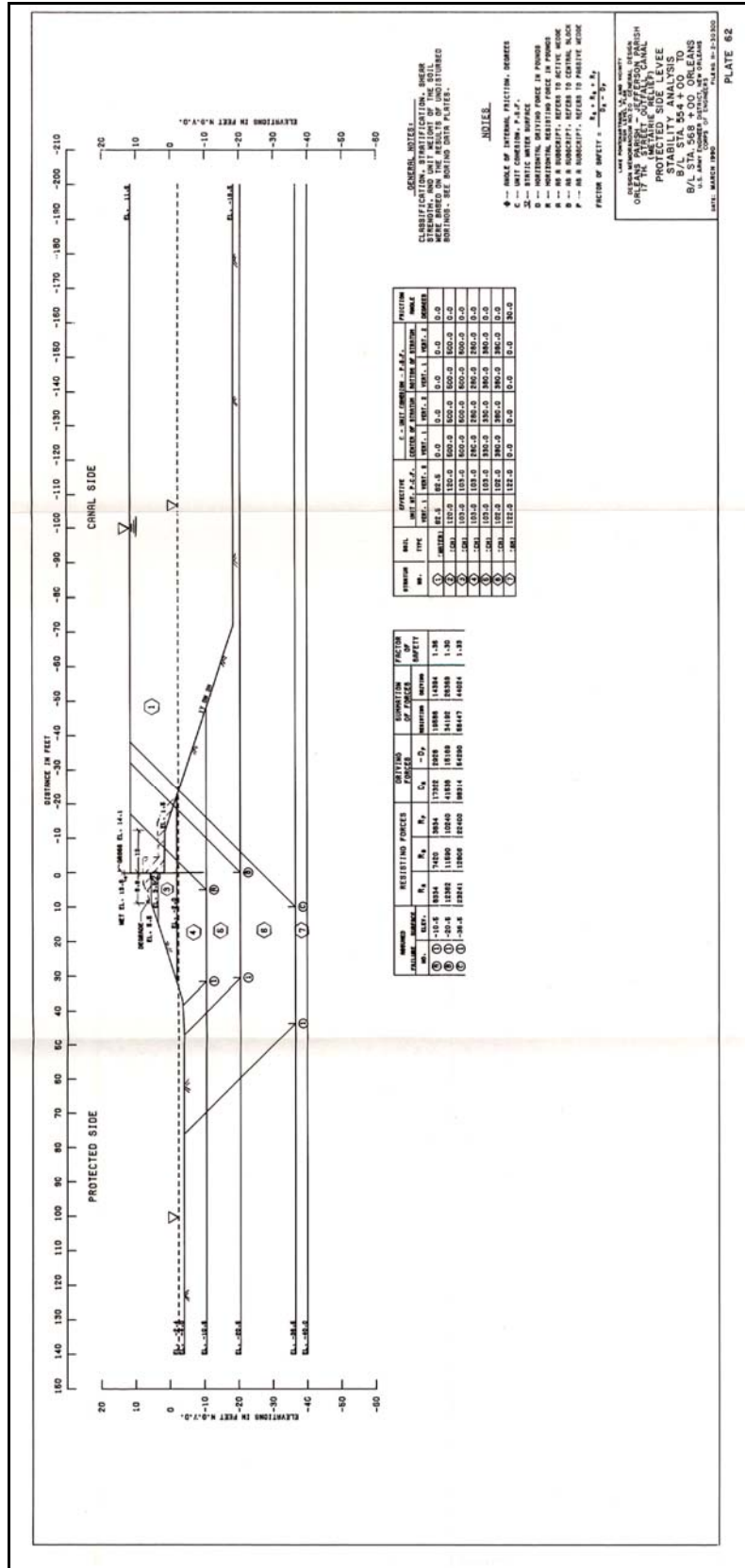


Figure K2-16. Design cross section, from GDM 20, Plate 62.

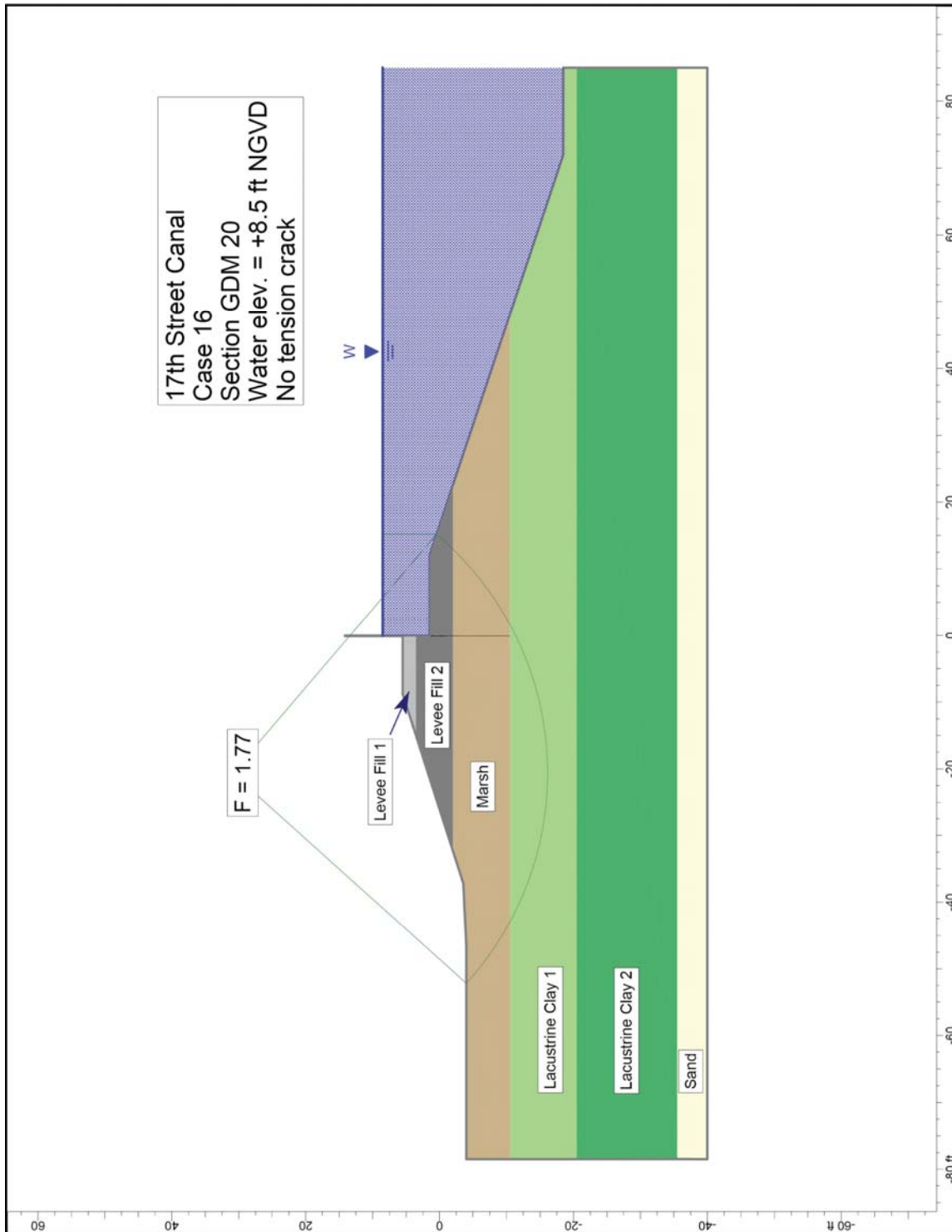


Figure K2-17. Critical circle for 17th Street Canal Design cross section – water elevation 8.5 ft, no tension crack.

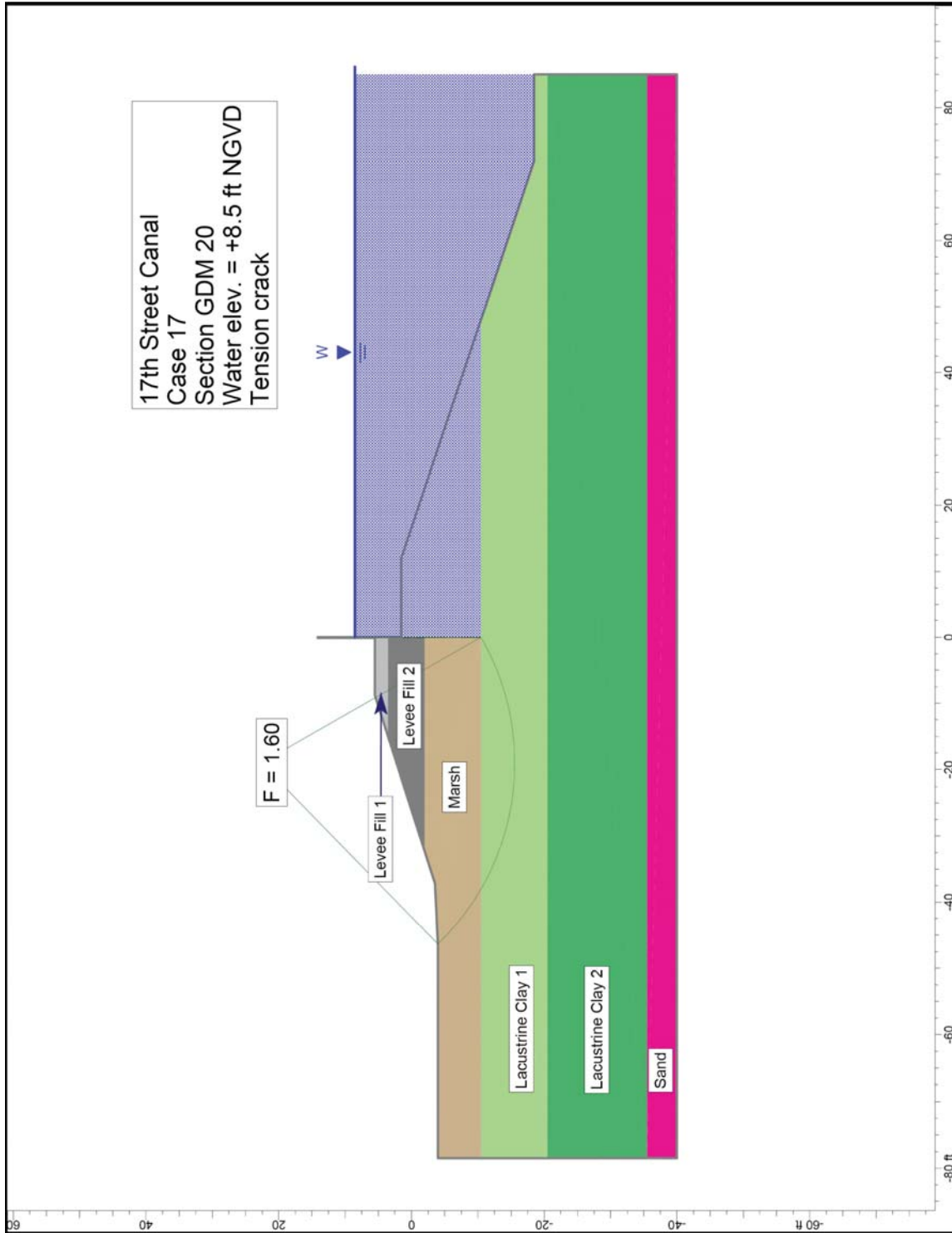


Figure K2-18. Critical circle for 17th Street Canal Design cross section – water elevation 8.5 ft, tension crack.

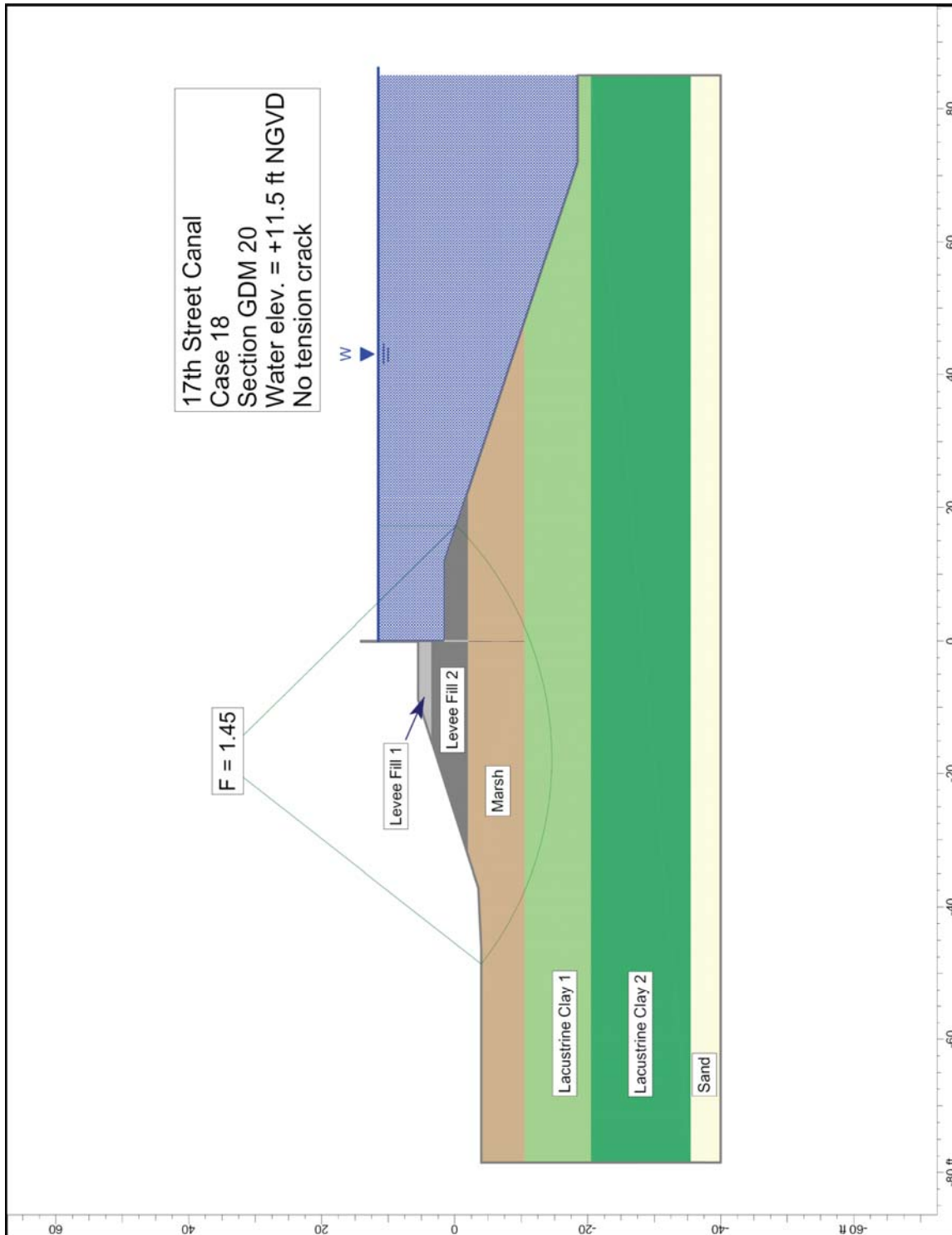


Figure K2-19. Critical circle for 17th Street Canal Design cross section – water elevation 11.5 ft, no tension crack.

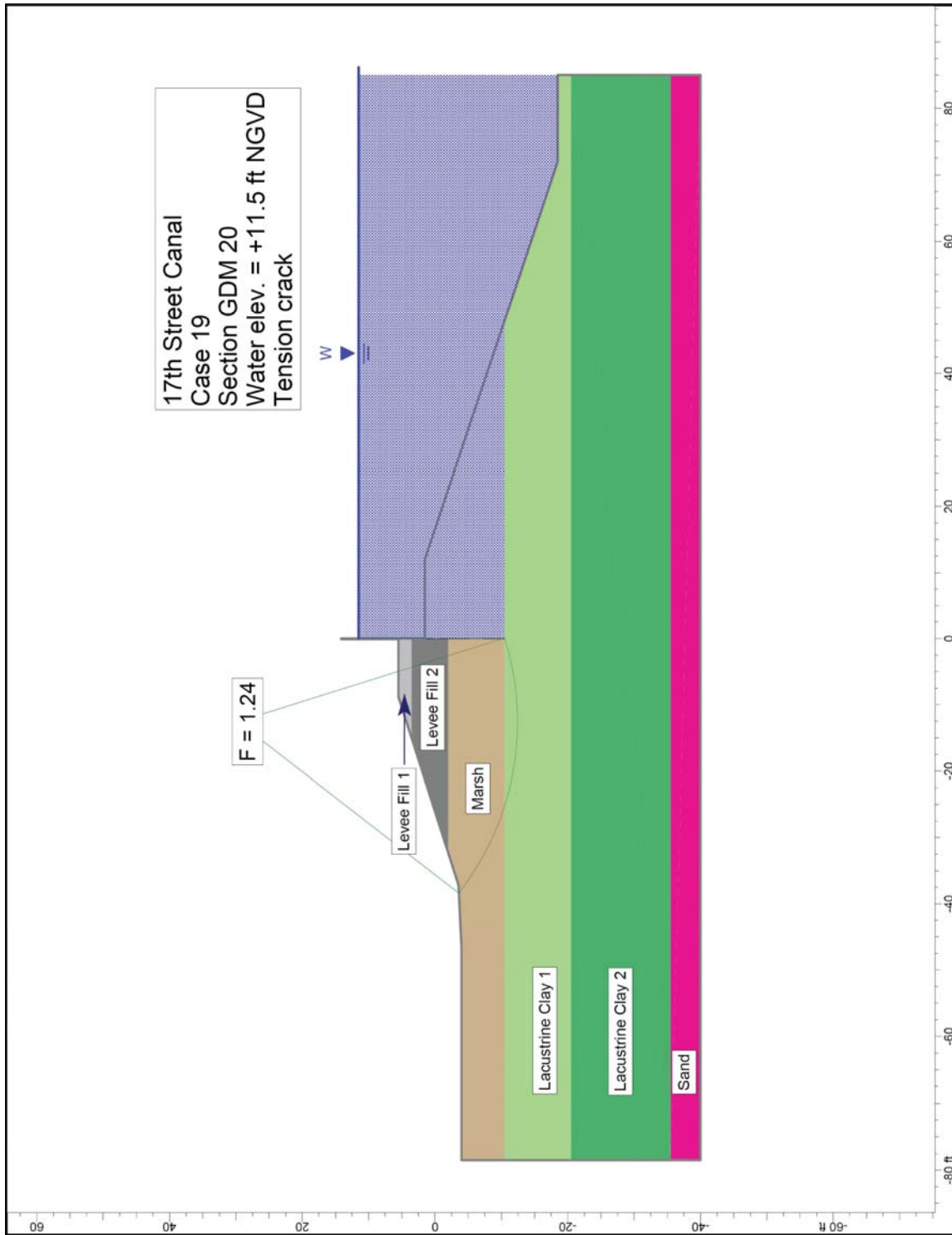


Figure K2-20. Critical circle for 17th Street Canal Design cross section – water elevation 11.5 ft, tension crack.

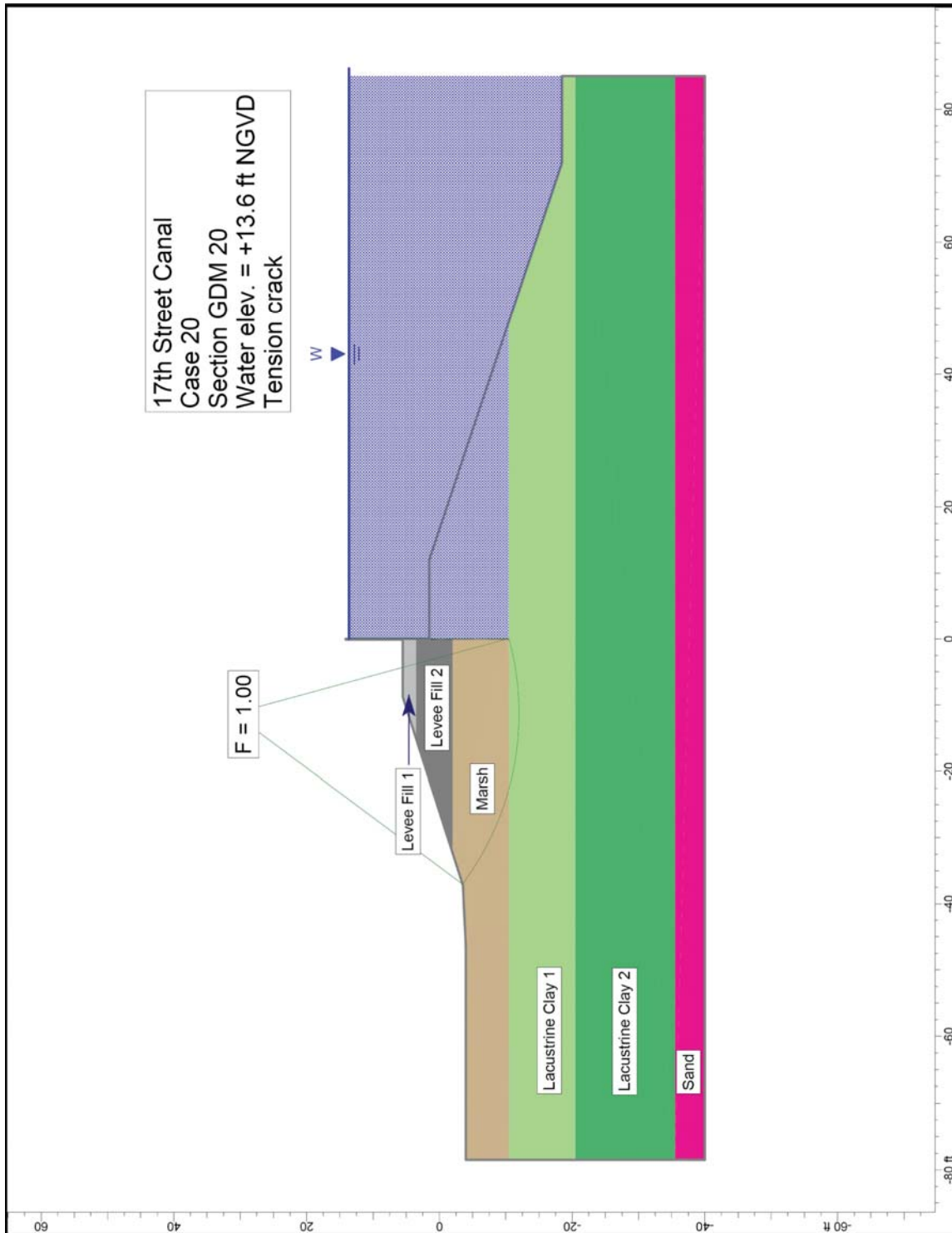


Figure K2-21. Critical circle for 17th Street Canal Design cross section – water elevation 13.6 ft, tension crack.

For Station 11+50, with the canal water level at elevation 8.5 ft, the calculated factor of safety for the cracked condition is 1.21, as compared to 1.60 for the uncracked condition. With the water level at 11.5 ft, introducing a crack reduces the factor of safety from 1.29 to 1.03.

The soil-structure interaction analyses and centrifuge tests yet to be performed may be capable of showing the relationship between water level and the likelihood of development of a crack on the canal side of the wall. These further studies may also show whether the crack extends to the bottom of the wall as assumed here, or only part way. The “no crack” and “full crack” conditions considered here represent the extremes that are possible.

It seems likely that the failure was progressive, with a gradual reduction in factor of safety as the water rose, followed by a more sudden reduction in factor of safety when the crack formed and water filled it. This appears to be a key factor in the mechanism of failure.

For the canal water level at elevation 8.5 ft, the calculated factor of safety is lowest at Station 10+00. This is approximately the same location where an eyewitness report indicates the failure began. The eyewitness report said that failure began at Station 11+00. Subsequently, failure spread to other locations in the breach area.

A sequence of events consistent with the eyewitness report and the calculated results is this:

- As the canal water level rose, a crack did not form until the water reached an average elevation (not accounting for wave effects) of 7.5 ft to 9.5 ft, and the factor of safety before the crack formed was above 1.0.
- When the average water level reached elevation 7.5 ft to 9.5 ft, and the static water pressure force was increased by wave effects, a crack formed between the I-wall and the levee fill on the canal side of the wall, resulting in a reduction in the factor of safety, and the wall began to fail at the location where the factor of safety was lowest.

Static Water Level for Factor of Safety Equal to 1.0

The canal water level was varied to determine the static water level at which the calculated factor of safety would be equal to 1.0, with a crack. Calculated water levels for factors of safety equal to 1.0 for the cracked condition vary from 11.3 ft to 12.1 ft NGVD, as compared with a water level of 7.5 ft to 9.5 ft when failure began based on an eyewitness report. It appears that wave effects might raise the effective water level by 1 to 2 feet, to as much as 11.5 ft. This would reduce the difference between calculated and observed water levels to cause failure to one to two feet. This may indicate that the IPET shear strengths are a little higher than the actual shear strengths.

The difference between calculated and observed water levels causing failure could also be due to the fact that, so far, the stability analyses have only considered circular slip surfaces. Further analyses will be performed using noncircular slip surfaces. While the critical noncircular slip surfaces are assured to have lower factors of safety than the critical circular slip surfaces, it remains to be seen whether the difference is significant or not. Even without this refinement of the analyses, it can be concluded that the IPET strength model is a reasonable representation of the actual conditions in the 17th Street Canal breach area, and that the stability analysis mechanism described here is consistent with the field observations.

Comparison of Spencer’s Method with the Method of Planes

Cases 16 through 20 of Table K2-1 used the design cross section and the shear strengths used in design. The cross section is shown in Figure K2-16, which is taken from Plate 62 of GDM20. The shear strengths are shown in Figures K1-54, K1-55, and K1-56 of the shear strength evaluation report (the design strength profile is the same in all three figures). This cross section and these shear strengths were used as the basis for design of the wall from Wall Stations 554+00 to 568+00, which includes the area where the breach occurred.

The factor of safety computed using the Method of Planes for these conditions was 1.30, with the canal water level at 11.5 ft, and no crack on the canal side of the wall. The factor of safety for this same condition computed using Spencer’s Method (Case 18 in Table K2-1) was 1.45. This shows that the Method of Planes is a conservative method of slope stability analysis.¹

Comparison of Design Analyses With Analyses Performed Using the IPET Strength Model and Spencer’s Method

The design analyses were based on these conditions:

- (1) The analyses were performed for the cross section shown in Figure K2-16.
- (2) The design strength profile shown in Figures K1-54, K1-55, and K1-56 of the shear strength evaluation report were used in the analyses. The same strengths were used under the embankment crest, under the slope, and beyond the toe of the levee.

¹ The Method of Planes is a force equilibrium method. Such methods do not satisfy moment equilibrium, and they require assumptions concerning the orientations of side forces on slices. Depending on the assumed orientations, force equilibrium methods can result in factors of safety that are either higher or lower than factors of safety calculated using methods like Spencer’s Method, which satisfy all conditions of equilibrium.

- (3) The Method of Planes was used to calculate the factor of safety.
- (4) The wall was assumed to be in contact with the levee fill soil on the canal side (the no crack condition).
- (5) The water elevation was assumed to be at 11.5 ft NGVD.

As noted previously, for these conditions a factor of safety equal to 1.30 was calculated using the Method of Planes. Five variations on these conditions were analyzed using Spencer's Method. These are shown in Table K2-1 as Cases 16 through 20.

With the water level at 11.5 NGVD, and a crack between the wall and the soil on the canal side, the factor of safety calculated using Spencer's Method is 1.24. The water level required to reduce the factor of safety to 1.0 is 13.6 ft NGVD.

It appears that the most important difference between the conditions used as the basis for design and the conditions defined in this report is related to the strengths of the peat and clay soils beneath the levee. The design strengths and the IPET strengths are very nearly the same beneath the crest of the levee. However, beneath the levee slopes, and beyond the toe of the levee, the design strengths were higher than the IPET strengths.

Comparison of Factors of Safety in the Breach Area with those in Areas to the North and the South

In order to examine the effect on stability of the higher strengths in the sections north and south of the breach that were discussed in previous sections of this report, stability analyses were performed using shear strengths for the clay and the peat that were 20 percent higher than those estimated for the breach area. This 20 percent higher strength was based on the data available for the area south of the breach. North of the breach a greater difference in clay strength (about 30 percent) was indicated by the available strength data.

The analyses with higher strengths were performed for Station 10+00, with a crack at the canal side of the wall, full hydrostatic water pressure in the crack, and canal water levels at elevations 8.5 ft and 11.5 ft. The results of these analyses are shown in Table K2-2, together with the comparable results from Table K2-1.

For the canal water level at elevation 8.5 ft, a 20 percent increase in clay strength results in a 15 percent increase in factor of safety. A 20 percent increase in peat strength results in 4 percent increase in factor of safety. For the canal water level at elevation 11.5 ft, a 20 percent increase in clay strength results in a 13 percent increase in factor of safety. A 20 percent increase in peat strength results in 5 percent increase in factor of safety.

| Case | Section | Slip Surface | Method | Strength Model | Crack | Water Elev. Ft. NGVD | F |
|------|---------|--------------|-----------|----------------|-------|----------------------|------|
| 7 | 10+00 | Crit. Circle | Spencer's | IPET | yes | 8.5 | 1.21 |
| 7A | 10+00 | Crit. Circle | Spencer's | clay + 20% | yes | 8.5 | 1.40 |
| 7B | 10+00 | Crit. Circle | Spencer's | clay - 20% | yes | 8.5 | 1.02 |
| 7C | 10+00 | Crit. Circle | Spencer's | peat + 20% | yes | 8.5 | 1.26 |
| 7D | 10+00 | Crit. Circle | Spencer's | peat - 20% | yes | 8.5 | 1.16 |
| 9 | 10+00 | Crit. Circle | Spencer's | IPET | yes | 11.5 | 0.99 |
| 9A | 10+00 | Crit. Circle | Spencer's | clay + 20% | yes | 11.5 | 1.12 |
| 9B | 10+00 | Crit. Circle | Spencer's | clay - 20% | yes | 11.5 | 0.84 |
| 9C | 10+00 | Crit. Circle | Spencer's | peat + 20% | yes | 11.5 | 1.04 |
| 9D | 10+00 | Crit. Circle | Spencer's | peat - 20% | yes | 11.5 | 0.93 |

The factors of safety shown in Table K2-2 for increased clay and peat strengths are consistent with the fact that failure did not occur in these areas.

Probabilities of Failure

Probabilities of failure have been estimated using an approximate technique based on the Taylor Series method. The coefficient of variation of the average clay strength and the average peat strength were estimated to be 20 percent. The data available is sparse, and the scatter in measured values is influenced significantly by sample quality as well as variations in properties from one location to another. The estimate values of COV = 20 percent is thus largely based on judgment. Even so, it is valuable to examine what probabilities of failure would be associated with this level of uncertainty concerning shear strengths.

The Taylor Series numerical method^{1,5} was used to estimate the standard deviation (σ_F) and the coefficient of variation of the factor of safety (COV_F), using these formulas:

¹Wolff, T. F. (1994). "Evaluating the reliability of existing levees." Report, Research Project: Reliability of Existing Levees, prepared for U.S. Army Engineer Waterways Experiment Station Geotechnical Laboratory, Vicksburg, Miss.

$$\sigma_F = \sqrt{\left(\frac{\Delta F_{\text{clay strength}}}{2}\right)^2 + \left(\frac{\Delta F_{\text{peat strength}}}{2}\right)^2} \quad (1)$$

$$\text{COV}_F = \frac{\sigma_F}{F_{\text{MLV}}} \quad (2)$$

where $\Delta F_{\text{clay strength}}$ = difference between the values of the factor of safety calculated with the clay strength increased by one standard deviation and decreased by one standard deviation from its most likely value. $\Delta F_{\text{peat strength}}$ is determined in the same way. F_{MLV} is the “most likely value” of factor of safety, computed using the IPET shear strengths.

Using the factors of safety listed in Table K2-2 for water level = 8.5 ft, $\Delta F_{\text{clay strength}} = 1.40 - 1.02 = 0.38$, and $\Delta F_{\text{peat strength}} = 1.26 - 1.16 = 0.10$. Substituting these values in Eq (1) leads to $\sigma_F = 0.39$. With $F_{\text{MLV}} = 1.21$, the value of COV_F calculated using Eq (2) = $0.39/1.21 = 0.32$.

For water level = 11.5 ft, $\Delta F_{\text{clay strength}} = 1.12 - 0.84 = 0.28$, and $\Delta F_{\text{peat strength}} = 1.04 - 0.93 = 0.11$. Substituting these values in Eq (1) leads to $\sigma_F = 0.30$. With $F_{\text{MLV}} = 0.99$, the value of COV_F calculated using Eq (2) = $0.30/0.99 = 0.30$.

With both F_{MLV} and COV_F known, the probability of failure (p_f) can be determined using Table K2-3. For water level = 8.5 ft ($F_{\text{MLV}} = 1.21$, $\text{COV}_F = 0.32$), the probability of failure is about 30 percent. For water level = 11.5 ft ($F_{\text{MLV}} = 0.99$, $\text{COV}_F = 0.30$), the probability of failure is out of range of the values in Table K4-3, and exceeds 50 percent.

For areas north and south of the breach, where strengths and most likely values of factor of safety are higher, the probabilities of failure are lower. For water level = 8.5 ft ($F_{\text{MLV}} \approx 1.45$ and $\text{COV}_F \approx 30$ percent), the probability of failure would be between 10 percent and 15 percent. For water level = 11.5 ft ($F_{\text{MLV}} \approx 1.15$ and $\text{COV}_F \approx 30$ percent), the probability of failure would be between 30 percent and 40 percent.

Summary

The results of the analyses described in the preceding sections are reasonably consistent with the performance of the I-wall in the breach area. Calculated water levels for factors of safety equal to 1.0 for the cracked condition vary from 11.3 ft to 12.1 ft NGVD, as compared with a water level of 7.5 ft to 9.5 ft at the time failure began based on an eyewitness report. It appears that wave effects might raise the effective water level by 1 to 2 feet, to as much as 11.5 ft. This would reduce the difference between calculated and observed water levels to cause failure to one to two feet. This may indicate that the IPET shear strengths are a little higher than the actual shear strengths.

| Table K2-3 Probabilities of Failure Based on Lognormal Distribution of F⁴ | | | | | | | | | |
|---|---|------------|------------|------------|------------|------------|------------|------------|------------|
| F_{MLV} | COV_F = Coefficient of Variation of Factor of Safety | | | | | | | | |
| | 10% | 12% | 14% | 16% | 20% | 25% | 30% | 40% | 50% |
| 1.05 | 33.02% | 36.38% | 38.95% | 41.01% | 44.14% | 47.01% | 49.23% | 52.63% | 55.29% |
| 1.10 | 18.26% | 23.05% | 26.95% | 30.15% | 35.11% | 39.59% | 42.94% | 47.82% | 51.37% |
| 1.15 | 8.83% | 13.37% | 17.53% | 21.20% | 27.20% | 32.83% | 37.10% | 43.24% | 47.62% |
| 1.20 | 3.77% | 7.15% | 10.77% | 14.29% | 20.57% | 26.85% | 31.76% | 38.95% | 44.05% |
| 1.25 | 1.44% | 3.54% | 6.28% | 9.27% | 15.20% | 21.68% | 26.98% | 34.95% | 40.66% |
| 1.30 | 0.49% | 1.64% | 3.49% | 5.81% | 11.01% | 17.30% | 22.75% | 31.26% | 37.48% |
| 1.35 | 0.15% | 0.71% | 1.86% | 3.53% | 7.83% | 13.66% | 19.06% | 27.88% | 34.49% |
| 1.40 | 0.04% | 0.29% | 0.95% | 2.08% | 5.48% | 10.69% | 15.88% | 24.80% | 31.70% |
| 1.50 | 0.00% | 0.04% | 0.23% | 0.67% | 2.57% | 6.38% | 10.85% | 19.49% | 26.69% |
| 1.60 | 0.00% | 0.01% | 0.05% | 0.20% | 1.15% | 3.71% | 7.29% | 15.21% | 22.40% |
| 1.70 | 0.00% | 0.00% | 0.01% | 0.06% | 0.49% | 2.11% | 4.84% | 11.81% | 18.75% |
| 1.80 | 0.00% | 0.00% | 0.00% | 0.01% | 0.21% | 1.18% | 3.18% | 9.13% | 15.67% |
| 1.90 | 0.00% | 0.00% | 0.00% | 0.00% | 0.08% | 0.65% | 2.07% | 7.03% | 13.08% |
| 2.00 | 0.00% | 0.00% | 0.00% | 0.00% | 0.03% | 0.36% | 1.34% | 5.41% | 10.91% |
| 2.20 | 0.00% | 0.00% | 0.00% | 0.00% | 0.01% | 0.10% | 0.56% | 3.19% | 7.59% |
| 2.40 | 0.00% | 0.00% | 0.00% | 0.00% | 0.00% | 0.03% | 0.23% | 1.88% | 5.29% |
| 2.60 | 0.00% | 0.00% | 0.00% | 0.00% | 0.00% | 0.01% | 0.09% | 1.11% | 3.70% |
| 2.80 | 0.00% | 0.00% | 0.00% | 0.00% | 0.00% | 0.00% | 0.04% | 0.66% | 2.60% |
| 3.00 | 0.00% | 0.00% | 0.00% | 0.00% | 0.00% | 0.00% | 0.02% | 0.39% | 1.83% |

F_{MLV} = factor of safety computed using most likely values of parameters

The difference between calculated and observed water levels causing failure could also be due to the fact that, so far, the stability analyses have only considered circular slip surfaces. Further analyses will be performed using noncircular slip surfaces. While the critical noncircular slip surfaces are assured to have lower factors of safety than the critical circular slip surfaces, it remains to be seen whether the difference is significant or not. Even without this refinement of the analyses, it can be concluded that the IPET strength model is a reasonable representation of the actual conditions in the 17th Street Canal breach area, and that the stability analysis mechanism described here is consistent with the field observations.

The calculated factors of safety are about 25 percent lower when it is assumed that a crack develops between the wall and the levee fill on the canal side of the wall. The results calculated assuming that a crack formed, and that full hydrostatic water pressure acted in the crack, are consistent with field observations, indicating that it is highly likely that a crack did form in the areas where the wall failed. It seems likely that when a crack formed and the portion of the wall below the levee crest was loaded by water pressures, the factor of safety would have dropped quickly by about 25 percent. Soil structure

interaction analyses and centrifuge model tests will likely provide further understanding of crack formation and its relation to wall stability.

The New Orleans District Method of Planes is a conservative method of slope stability analysis. All other things being equal, the factor of safety calculated using the Method of Planes was about 10 percent lower than the factor of safety calculated using Spencer's method, which satisfies all conditions of equilibrium.

The factors of safety calculated in the design analyses were higher than the factors of safety calculated for the conditions that are believed to best represent the actual shear strengths, geometrical conditions, and loading at the time of failure. The principal differences between the design analyses and the conditions described in this report relate to (1) the assumption that a crack formed between the wall and the levee soil on the canal side of the wall, and (2) the fact that the design analyses used the same strength for the clay and the peat beneath the levee slopes, and for the area beyond the levee toe, as for the zone beneath the crest of the levee. The IPET strength model has lower strengths beneath the levee slopes and beyond the toe.

Factors of safety for areas adjacent to the breach, where clay strengths are higher, were about 15 percent higher than those calculated for the breach area. These differences in calculated factor of safety are not large, and it thus appears that the margin of safety was small in areas that did not fail. It is possible that areas adjacent to the breach remained stable primarily because cracks did not form in those areas, and the wall was therefore less severely loaded.

Estimates of probability of failure for a water level of 8.5 ft NGVD are about 30 percent in the breach area, and 10 percent to 15 percent in the areas north and south of the breach. For a water level of 11.5 ft, the estimated probability of failure is about 50 percent in the breach area and 30 percent to 40 percent north and south of the breach. If stability analyses considering noncircular slip surfaces result in appreciably lower factors of safety, the corresponding probabilities of failure will be higher.

K3 – Physical Modeling

Drainage Canals – Physical Centrifuge Modeling

Scale modeling using large geotechnical centrifuges at RPI and at ERDC has commenced with trial models of London Avenue and 17th Street canal levees and floodwalls based on the available site characterization and performance analyses. The conceptual design of the scale models and development of the experimental procedures has been based on established international practice, drawing upon the combined expertise and experience of the centrifuge modeling groups at ERDC, RPI, GeoDelft and Steedman & Associates. The experiment plan has been developed in close collaboration with numerical work being performed as part of the Levee Analysis, to ensure that the models can meet their primary objective of providing qualitative insight and independent validation of the numerical analyses. Bulk samples of peat from the field have been taken for direct use in the models. A kaolin clay and fine sand has been used to replicate the clay and sand layers in the field. In common with standard geotechnical centrifuge model practice, the models are designed to be geometrically similar, reduced scale models with all significant engineering parameters (dimensions, permeability, density, strength and stiffness) correctly reproduced. Custom built chambers have been constructed to contain the models with windows to facilitate video imagery of the onset of failure in the levee and foundations. The first trial models have been completed. The results are encouraging, showing that failure mechanisms consistent with the field observations can be realistically reproduced. Instrumental data from the model tests, particularly of the development of pore water pressure in the soil layers beneath the levee, are being examined and compared with numerical analyses. A full series of model tests will be carried out during March and April, using both centrifuge facilities as appropriate.

Simulation of Field Conditions

The design of the scale models has benefited from the extensive data collection and analysis in the field and from the site investigation and characterization activity under the levee performance analysis task. Collaboration with all members of the levee performance analysis group and subsequent exchange of cross-sections, long sections and soil properties have ensured that for each of the drainage canal sections investigated, the scale model design has proceeded with the best available information.

As the scale models are subject to a steady high acceleration field during a centrifuge ‘flight’, they are constructed within a strongbox that must be designed to resist the full field pressure from the free water (in the canal), ground water and soil acting on the side walls and base. For these experiments, new strongboxes have been designed and built specifically to accommodate the particular geometry and depths of the levees and their foundations. Based on the field observations and the Dutch experience of levee failures, it was considered important to include a substantial length of ground behind levees within the model to ensure that any failure mechanism had the freedom to extend ‘landward’ if it desired. Several boxes have been constructed to facilitate the model making process and provide duplication. The boxes were constructed from aluminum alloy plate, with a stiff, plexiglass window on one side for viewing. A schematic diagram of the model chamber is shown in Figure K3-1 showing the transparent window and water reservoir below the floor of the strongbox. The long walls of the strongbox are restrained from bowing outwards by their fixings along the end and base of the chamber, and by a frame bolted across the top prior to flight (not shown in the figure for clarity).

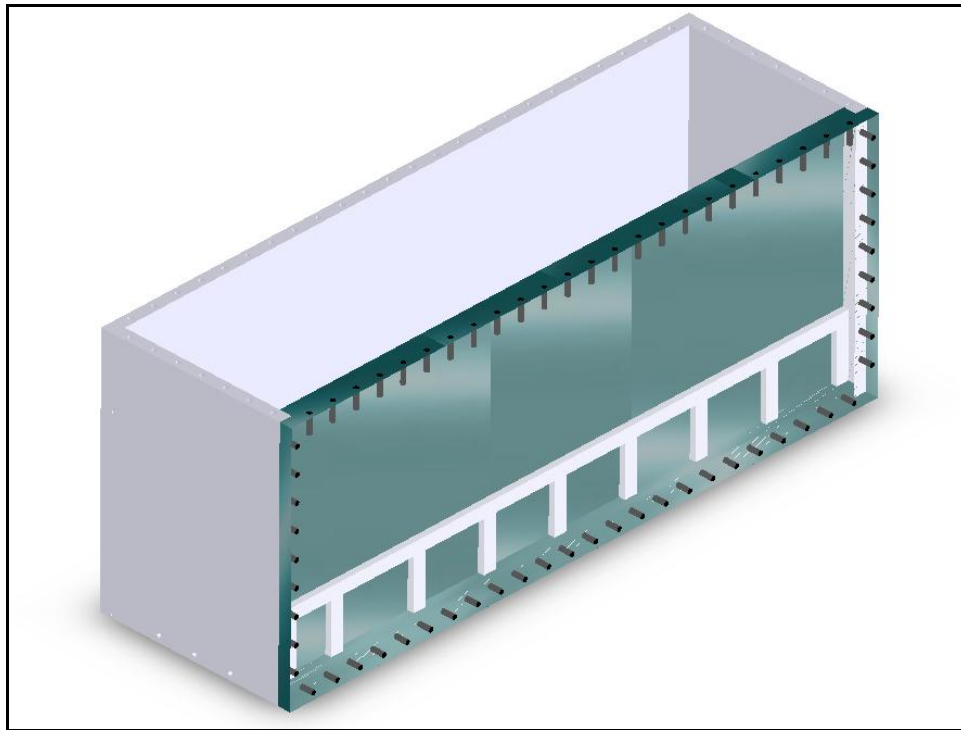


Figure K3-1. Diagram of the model chamber with top bracing omitted

Simulation of field conditions requires that all relevant mechanical properties of the engineered structures and natural ground conditions are accurately reproduced in the model. In the case of the structures, the significant elements are the levee itself and the sheet pile wall with concrete capping beam.

For the sheet pile wall, it is straightforward to scale the bending stiffness of the wall. Expressed simply, any deflection or bending of the wall under pressure from the water or soil should be geometrically the same in the scale model and in

the field. If the sheet pile wall in the field was to bend so that the top deflected one twentieth of its overall height, for example, it would be expected that the scale model wall would also deflect one twentieth of its height. From this requirement, it is easily deduced that for a 1/N scale model subject to a steady acceleration field of N times earth's gravity, the bending stiffness of the wall should be reduced by N^3 per unit length. A steel sheet pile wall such as the PMA-22 section with a moment of inertia of 22.4 in⁴ will then be correctly scaled by a steel plate 0.129" thick at 50g. Alternatively, the steel sheet pile section could be correctly represented at 50g by a solid aluminum alloy plate, with thickness of 0.18". The unit weight of the steel sheet pile wall and its plastic moment capacity are not relevant to the study, as there is no evidence that dynamic movement of the wall or plastic hinges in the wall (none of the sheet piles recovered from any of the levee failures show any sign of local plastic bending) contributed to the observed performance. Similarly, in the early stages of failure, no evidence has yet been put forward that water flow through the clutches of the sheet piles, separation of the clutches or fracture of the concrete capping beam contributed to the failure. It is therefore concluded that the sheet pile wall may be realistically represented by a metal plate (steel or aluminum alloy) with the correct bending stiffness.

Natural soils and constructed fill in the field have an inherent variability which is impossible to reproduce at a microscopic scale whether in analytical, numerical or physical models of performance, for design or for assessment. It is standard practice, therefore, to use site investigation techniques to measure soil properties and then to deduce an equivalent profile of strength and permeability that is appropriate to the situation under consideration. Using the currently available soil data, representative pre-Katrina cross-sections for the drainage canal levees, including undrained soil strength profiles and stratigraphy have been developed. These profiles have been adopted for the physical scale models also and, with the exception of the peat layer, reconstituted laboratory soils are being used for the clay and sand layers. Laboratory soils provide the same characteristics as field soils in terms of strength and compressibility, but may be handled more easily and reliably. The use of reconstituted, remoulded soils as equivalent field soils is well established and common practice.

The levees were constructed over many decades from compacted clay. Analysis has provided values for the strength of the levee to be used in the numerical models, and the same strength was therefore adopted for the physical scale models. For the first trial models, the strength of the clay in the levees was selected to be 500 psf, being the strength used for design. Later models will adopt a strength value of 900 psf, based on the assessment of site investigation data available at February 2006.

The foundations of the levee comprise layers of peat, clay and sand. Each of the three drainage canal breach sites have a different profile and each have been or will be modeled accordingly. The natural clay beneath the peat is normally consolidated throughout its depth, with an average unit weight of 109 pcf and average water content of approximately 65 percent. The properties of the natural clay have been adopted from analysis of design documents and field data, and reconstituted kaolin clay selected to represent the material in the scale model.

Kaolin clay is coarse grained clay used extensively in centrifuge model studies to represent natural clays. The beach sand stratum that underlies the lacustrine clay and/or peat stratum is fine medium dense sand, with typical strength and permeability characteristics. For the purposes of the scale model tests, the important parameters to model are the density and the permeability, which is controlled by the fine fraction in the soil. A fine laboratory sand (Nevada Sand with $D_{10} = 0.08\text{mm}$) has been used to reproduce this stratum. Full details of these materials may be found in Appendix K3-1.

The characteristics of the peat or marsh stratum have been assessed and determined to be comprised of two groups: the peat stratum under the levee embankment, and the peat stratum at the toe of the levee. Undisturbed samples taken from borings have provided laboratory samples from which compression tests, moisture content and unit weights have been determined. Close examination of the peat shows that it is relatively free of fibers and is similar in character to organic clay. In these circumstances, the appropriate course of action is to use the field material, cut from block samples and reconsolidated in the centrifuge to its original condition.

To create conditions in the scale model which are as realistic as possible, careful consideration must be taken in the construction of the model specimen. Two workshops have been held to review the experimental methods and model design, at GeoDelft and at RPI. The workshops addressed equipment, instrumentation, material and procedures for standardizing the model tests.

The generic model configuration is shown below, for London North. The sand layer was placed in the chamber first by raining it slowly from a hopper. The rate of pouring and height are calibrated to ensure that the appropriate density is achieved. Miniature instruments were positioned in the sand layer during the pouring process, as were markers in the sand against the window, to form a grid. The wall is placed into position, held by a temporary brace. Once the sand layer is completed, the chamber is evacuated, flushed with carbon dioxide and then the sand is saturated by slowly introducing de-aired water. The vacuum is released.

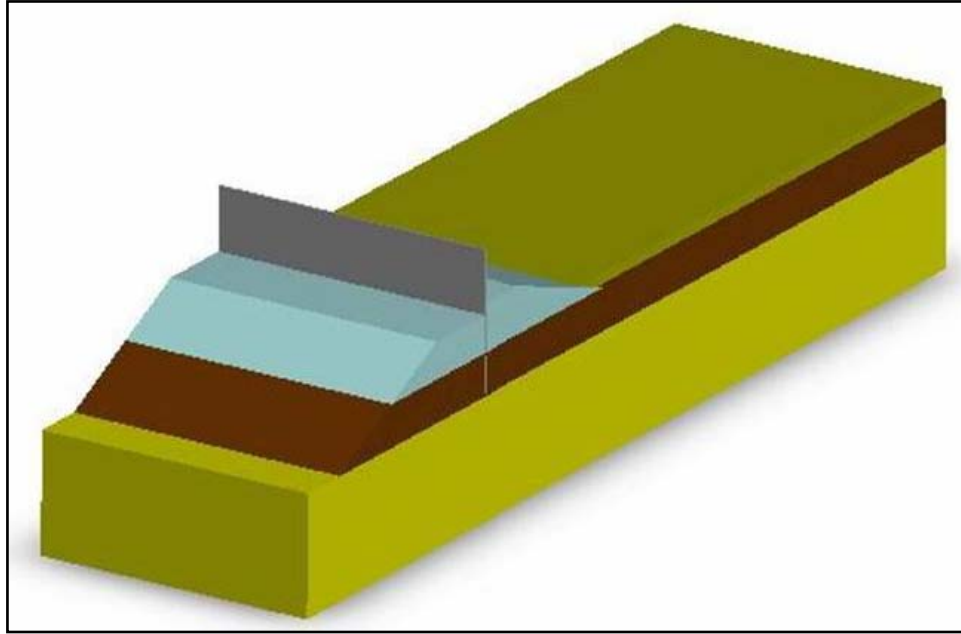


Figure K3-2. Schematic diagram of the model geometry (London Avenue North)

The peat layer, cut from the blocks of natural soil is placed on the sand bed on either side of the wall. A surcharge of gravel equivalent to the weight of the final levee and of similar profile is placed on the peat layer (temporarily protected by a geotextile membrane) and the specimen accelerated on the centrifuge until the weight of the gravel has consolidated the peat layer. This process will create a depression under the gravel mimicking the additional consolidation of the peat by the levee over time and satisfying the observation of varying strength in the peat layer under the levee and under the toe.

The levee is formed by consolidating a block of clay in two pieces, representing the flood side and protected side of the sheet pile wall. The blocks of clay for the levee were formed by consolidating the reconstituted kaolin clay to the required strength upside down in a wooden mould. The moulds have the form of the levee profile. The blocks were then trimmed to their final shape, the gravel (and protective membrane) removed and the two sections of the clay embankment placed in position against the wall. The temporary brace can now be removed and the specimen again accelerated on the centrifuge, water introduced and a steady flow regime established below the levee. Finally, the water level is brought up to the flood level and the performance of the levee observed.

For the physical model of 17th Street canal, the main elements are similar, except that the peat layer overlies a layer of clay, representing the lacustrine clay stratum in the field. To form this layer in the model, the reconstituted kaolin clay is placed at high water content and consolidated using the centrifuge before placing of the peat layer above. The advantage of the centrifuge consolidation process is that this will correctly reproduce the process of normal consolidation as in the field, resulting in a profile of strength of the clay increasing with depth that can be matched to the field profile. The process takes many hours before the clay layer is fully consolidated and is monitored by measuring the decay of the

excess pore water pressure in the clay over time. Determining the strength of the clay after placement in the model is achieved by calculation and laboratory testing based on correlations between density and moisture content versus resultant strength. Reconstituted kaolin clay has been used in centrifuge model tests since the 1960s and there is long experience of the accurate prediction of strength following mixing and consolidation.

The workshops also discussed the optimum acceleration level (expressed in multiples of earth's gravity, g) at which the experiments should be conducted. This 'g' level dictates the linear scale in geotechnical centrifuge scale modeling, such that for example the reduction in depth in the model is precisely compensated by the increase in self weight of the layers above, resulting in identical stresses in the model as in the prototype. The model tests will be carried out at 50g, sufficiently high to provide a model of sufficient size to replicate the field structure with negligible boundary effects from the model container and sufficiently low to provide reasonable detail in the layering and soil profile.

Miniature instrumentation is used both inside and outside the model container to capture information on the performance of the specimen during the model test. For these experiments, the main instrumentation will be pore pressure transducers, displacement transducers and video and still photography of the model and sheet pile wall. Consideration has also been given to the hydraulic arrangements for the control of water supply, and the optimum orientation of the model box on the centrifuge platform to minimize any errors associated with the radial acceleration field in the centrifuge.

The generic description of the model test process above is intended to provide a general overview of the experimental procedure. A more detailed discussion of centrifuge modeling, sources of error and limitations is provided in Appendix K3-1, together with additional information on the materials, equipment and typical data from the initial model tests carried out at RPI to confirm the proposed methodology.

Design of Trial Models for Drainage Canals

Prior to initiation of any physical modeling efforts, two workshops were held to discuss in detail the model design and test procedure based on the team's prior experience of physical modeling of levee structures and experience of model testing with very soft clays. These workshops were held in December 2005 and January 2006 at GeoDelft in the Netherlands and at RPI, NY. Both institutes operate internationally recognized centrifuge research facilities and are important centers of expertise. Both meetings reviewed the current information available on the pre and post-hurricane conditions of the levee systems (17th Street, London Avenue, and Industrial Canal). The design of the models requires consideration of possible failure mechanisms and the workshops therefore discussed a wide range of alternative mechanisms, based on post-failure observations and prior experience in the Netherlands of similar levee designs, including flow of water around the pile generating uplift pressures in the downstream material, and movement of the wall due to the relatively weak clay of the levee. The

workshops then discussed and agreed on the design of the trial models, selection of materials and test procedures, as described in detail below. The trial models were intended to test alternative model arrangements and methods of construction prior to the final models. In January at the second workshop, detailed planning of the test program and experimental methods (model preparation, boundary conditions, instrumentation, data acquisition and reporting) were reviewed and agreed in detail to ensure that a standard approach was adopted at ERDC and RPI during the model testing.

London Avenue Canal levee model

Cross sections of the levees on London Avenue drainage canal (London North failure and London Mirabeau failure) with the currently known soil layering and properties were reviewed. The London Avenue breach sites consist of, in general, a clay levee founded on a foundation of peat and fine sand, as shown in Figure K3-2 above. For the purposes of the trial models, the sheet pile wall was modeled using an aluminum plate, the sand using a Nevada Sand at 60 percent Relative Density, the levee using a reconstituted kaolin clay and the peat layer using the natural peat, cut from block samples from the field. Following the modeling principles discussed above, the design cross section through the 1/50 scale trial model is shown in Figure K3-3 below.

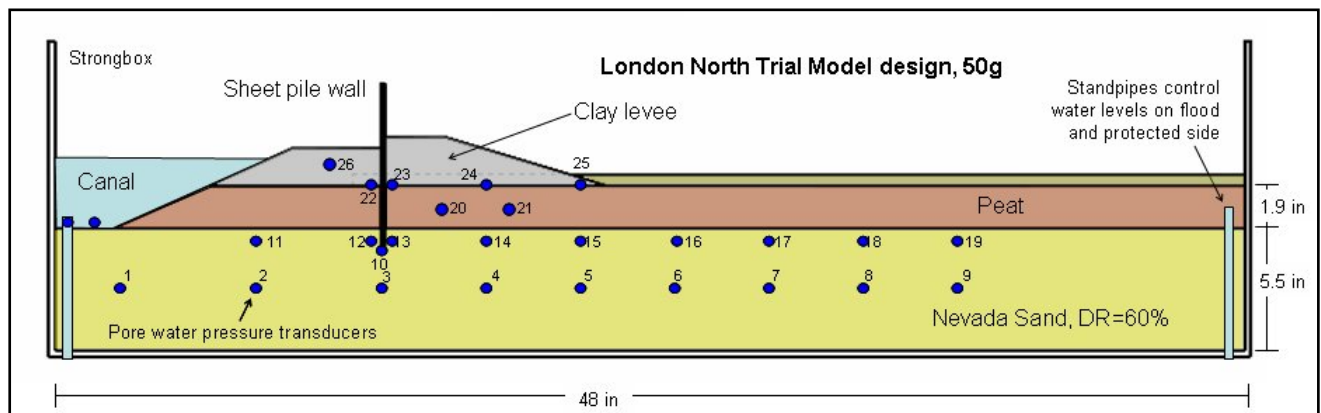


Figure K3-3. Diagram of London North Trial Model Design (model units)

The clay levee in the trial model had strength after consolidation of 500 psf (based on the original design values). For kaolin clay, this is equivalent to a saturated density of around 110 pcf. Future models will use an increased strength of 900 pcf (kaolin saturated density of 113 pcf), based on the latest assessment of all information. The geometry of the clay levee was based on information available from design documents, as-built documents, LIDAR surveys, and field reconnaissance. The peat layer will be formed from the natural peat samples taken from the field. The sheet pile wall will be modeled using a solid steel plate of thickness 0.125", such that the bending stiffness of the wall is a correct representation of the sheet pile wall in the field (based on the PMA-22 section), as discussed above.

Pore pressure transducers are located along the mid depth of the sand stratum and near the top of the sand, below the peat. As the canal fills with water, the

excess pore pressure in these transducers will rise, with the greatest rise occurring closest to the canal. If the wall rotates and a crack opens down the front of the wall, then transducers under the centerline of the levee will also experience a full head of water pressure.

17th Street Canal levee model

As with the London Avenue breaches, the 17th Street breach site was reviewed. The cross section here consists broadly of a clay levee on a foundation of peat and lacustrine clay. Following the procedures discussed above, the selection of materials for the trial model comprised speswhite kaolin clay for the levee and lacustrine clay stratum, and natural peat for the peat layer. The sheet pile wall was modeled using an aluminum plate. A cross section through the trial model is shown in Figure K3-4 below.

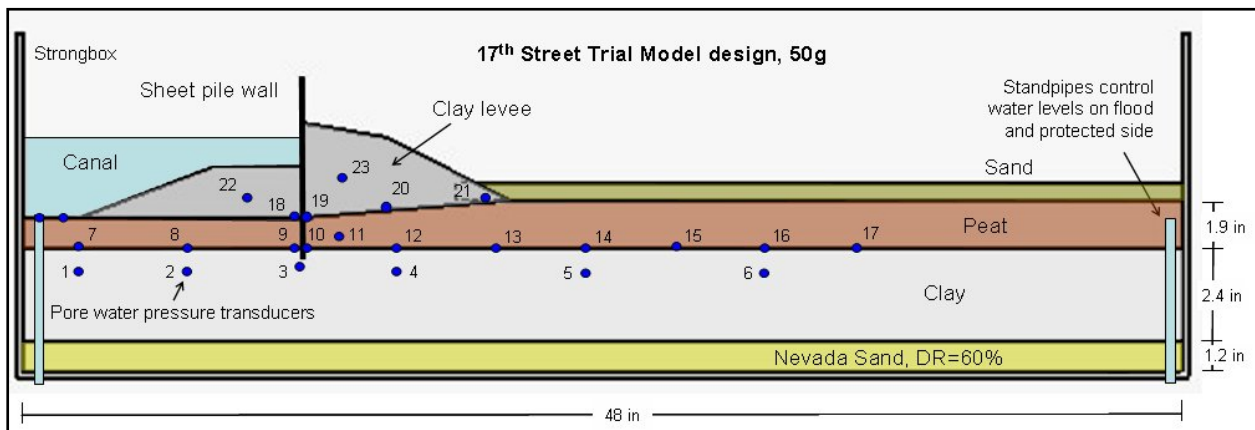


Figure K3-4. Diagram of 17th Street Trial Model Design (model units)

The clay levee in the trial model had strength after consolidation of 500 psf (based on the original design values). For kaolin clay, this is equivalent to a saturated density of around 110 pcf. Future models will use an increased strength of 900 pcf (kaolin saturated density of 113 pcf), based on the latest assessment of all information. The geometry of the clay levee was based on information as described above for the London North section. The peat layer will be formed from the natural peat samples taken from the field. As with the London North Model design, the steel sheet pile wall will be modeled for the 17th Street model using a solid steel plate of thickness 0.125", such that the bending stiffness of the wall is a correct representation of the sheet pile wall in the field (based on the PMA-22 section), as discussed above.

The underlying clay layer has strength after consolidation increasing from 280 psf to 390 psf at the base (an increase of 11 psf per foot depth). Constructed using reconstituted kaolin clay, the saturated density of the clay will again be around 110 pcf.

Pore pressure transducers are located on the interface between the peat and the clay stratum and within the clay layer and the clay levee. Once steady state conditions are established at the start of the model, the precise rate of rise of the

flood in the canal is immaterial as the performance of the foundation and levee will be undrained.

Interim Results

The results from the trial models have been encouraging. The model making process has been tested through the construction of the two trial models, one of which involved a sand bed beneath the peat and one of which involved a clay layer. Techniques for placing the sand and peat and for consolidating the clay have proved satisfactory and resulted in a layered model with densities and strengths close to the target density/strength profile based on the current available information. The approach, developed during the workshops, towards the sequence and method of construction of the levee and sheet pile wall has also proved successful. The hydraulic system to control water levels in the ground and the canal has permitted steady state conditions to be developed prior to the flood stage, and then for the water in the canal to be raised progressively until large scale movements of the levee and flood wall were initiated, as may be seen after the trial model test in Figure K3-5 for London Avenue North. Data from the miniature transducers buried in the soil beneath the levee have provided valuable information on the change in water levels (water pressure) as the canal floods. In the London North example below, Figure K3-6, the trend of increasing water level is seen in the sand layer beneath the levee as the water level in the canal rises. As expected, the rise is proportionately less further away (landward) from the canal. In this trial model the wall was seen to lean over as the water rose and there is an increase in the rate of rise of water level in the sand as this occurs. The rate increases as the wall starts to lean over landward.



Figure K3-5. Rotation of the sheet pile wall in the London Avenue Trial Model

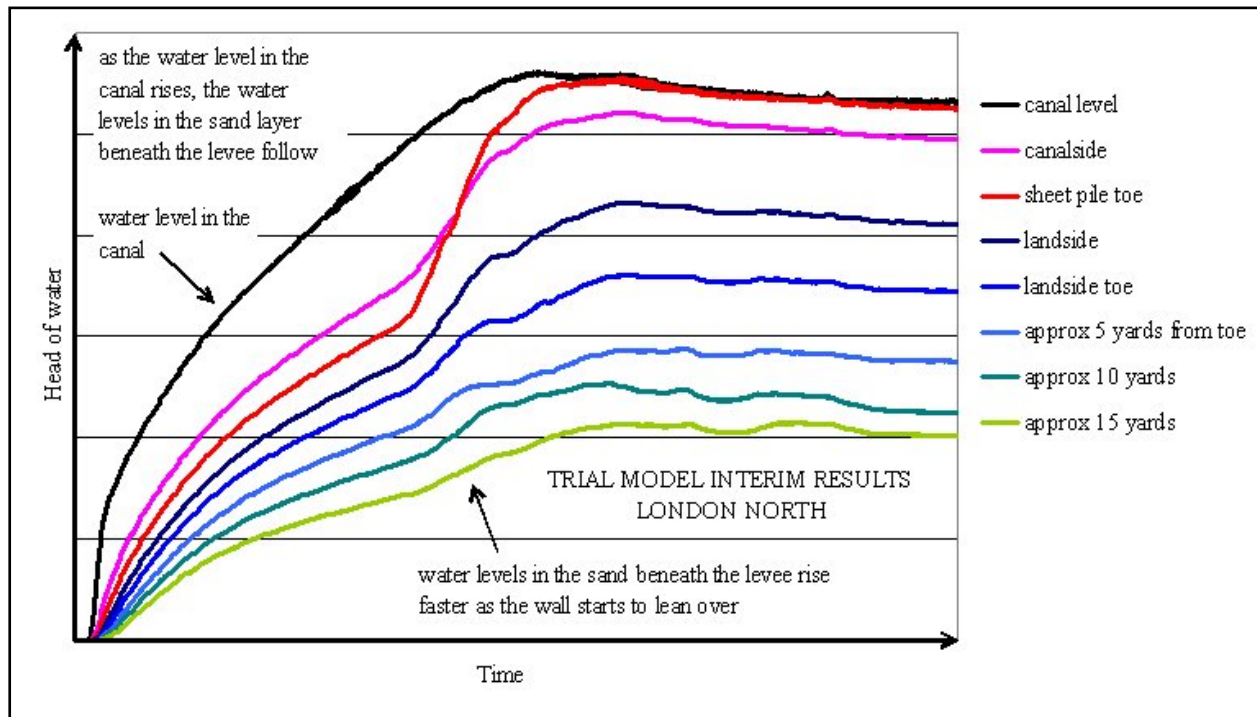


Figure K3-6. Rising water pressures in the sand in the London Avenue Trial Model

The second trial model, of 17th Street, has also provided good results, confirming the model process and design. Figure K3-7 shows the movement of the levee landward after the model test was completed and the water had been drained from the canal side (left).



Figure K3-7. Sliding movement of the levee landward (to the right) observed at the completion of the 17th Street trial model test

In this case, as the water rose in the canal the wall again started to lean over, which resulted in a sliding failure in the clay layer immediately below the peat. Data from both the trial models are being assessed in detail prior to the initiation of the main model test phase, planned to commence at ERDC in March.

Planned Work

The intention of the physical modeling work is to contribute to and support the overall analysis of the levee performance system. Particular strengths of the physical modeling are in exploring failure mechanisms and providing key information and insights to the numerical modeling work. The efforts that have been completed thus far and reported in this 60 percent report have already provided valuable information to the numerical modelers and clearly demonstrated the possibility of modeling realistic failure mechanisms. It should be noted that the geometry of the levee sections and material properties used in the physical modeling were those as understood from available information at the time of the modeling work. Future efforts for the physical modeling work will be as described following.

- Further refinement of the levee geometries, material properties, sheet pile characteristics and other relevant factors will be performed such that the final models will represent as accurately as possible the actual field levees.
- Continued improvements in the testing procedures and data collection procedures will be performed to insure that the quantity and quality of collected data are the highest quality.
- Perform a thorough analysis of the data collected from the London North and 17th Street models. The intention of this analysis will be to understand the failure mechanisms and improve all future models.
- Hold a meeting of the physical modeling team (ERDC, Steedman & Associates, RPI, GeoDelft) to review all data collected thus far and analysis performed to give careful consideration to future models.
- Complete duplicate physical models for each of the failures at London North, London Mirabeau, and 17th Street.
- Provide detailed data of pore pressure and displacement measurements to numerical modeling team for use in that analysis.
- Perform any additional physical models that are deemed necessary by the full team responsible for the levee performance analysis work.

Appendix K3-1

Levee Performance Analysis, Physical Modeling

Background and scaling principles

It is well known that the behavior of most geomechanical materials, such as soil and rock, is very dependent on stress level. In conventional small scale model tests, performed in the earth's gravitational field, it is not always possible to maintain similarity with prototype situations, and to ensure that stress levels in areas of interest reach field values. A geotechnical centrifuge can subject small models to centripetal accelerations that are many times the earth's gravitational acceleration. By selecting a suitable acceleration level the unit weight of the model being tested can be increased by the same proportion by which the model dimensions have been reduced. Thus stresses at geometrically similar points in the model and prototype will be the same. Three assumptions must be satisfied to provide a realistic representation in the model of the field performance. These are firstly, that the model is a correctly scaled version of the prototype, secondly that the $1/N$ scaled model when subjected to an ideal gravity field behaves like the prototype at $1g$; and thirdly that the centrifuge produces this ideal gravitational field. These assumptions are briefly examined below.

To satisfy this first assumption, that the model is an exactly scaled version of the prototype, requires that the scaling relationships between the model and prototype are met. These scaling relationships can be derived from either analysis of the relevant variables, or from consideration of the governing equation which describes the phenomenon being modeled. The establishment of correct scaling relationships is crucial if the prototype response is to be correctly modeled and any given specific problem may have a unique set of scaling relationships that may be derived by either of the two methods outlined above. Some of the more common relationships are given below in Table K3-1.

| Table K3-1 Useful Scaling Relationships for Centrifuge Models Subject to a Steady Acceleration Field Equivalent to Ng (N times earth's gravity, g) | |
|--|-----------------------|
| Parameter | Scaling factor |
| Acceleration | N |
| Seepage velocity (laminar) | N |
| Length | $1/N$ |
| Mass | $1/N^3$ |
| Stress | 1 |
| Strain | 1 |
| Force | $1/N^2$ |
| Time (diffusion events) | $1/N^2$ |
| Time (inertial events) | $1/N$ |

To illustrate how the scaling relations may be used to advantage in the centrifuge, consider the time scale of $1/N^2$ for diffusion processes. Consolidation occurs very slowly in the field, but as a laminar flow process, will occur N^2 times

faster in a reduced scale centrifuge model. For a model $1/N$ times the prototype dimensions, and if both model and prototype materials have the same properties, then the excess pore pressure dissipation will occur N^2 times faster in the model than in the corresponding prototype. This permits the re-consolidation of soil samples in the centrifuge to take place in a matter of hours, when in the field or at full scale this process would take years.

The second assumption that the $1/N$ scale model under an ideal Ng gravity field will perform exactly as in the field at full scale will be satisfied if the material properties of the model and prototype are the same. Consequently, the use of in-situ materials is often preferred, but in many cases is not necessary provided that the mechanical properties of the material can be effectively reproduced in an alternative. Thus it is common practice to use laboratory sand or reconstituted kaolin clay to substitute for block samples from the field, particularly when plastic deformation and remolding of the soil under high stress ratios will dominate the expected outcome.

The third assumption, that the centrifuge can supply an ideal Ng gravity field, cannot be completely satisfied. This condition would require that the acceleration at any point throughout the model would not change in magnitude or direction. However, since the acceleration at a point in the model is directly proportional to the radius of that point from the centre of rotation, there must be a variation in imposed acceleration from the surface to the base of the model. This variation in acceleration level also leads to a non-linear stress gradient through the model. From consideration of the stress gradient, it is found that the error is minimized by designing the model based on a gravity scale equivalent to the steady acceleration field calculated at a depth one third the depth below the model surface. The error in any event is negligible provided that the depth of the model is small relative to the radius of the model surface.

There will also be a variation in the acceleration field along flat horizontal surfaces of the model due to the radial nature of the acceleration field, which generates a small component parallel to the model's surface. The effect of this radial divergence of the acceleration field is easily imagined by considering the concave profile (aligned along a line of constant radius) that will be adopted by any free surface water in the model chamber. Again, by ensuring that the orientation of the model chamber on the platform is such that the long dimension is parallel to the axis of rotation, then any effect caused by the radial divergence of the acceleration field can be easily minimized. The most common issue to be addressed in this respect is the design of standpipes and calculations of the depth of free water at different locations on the model.

Finally, as in any rotating reference frame, there is a potential for the movement of particles to be distorted relative to the reference frame of the model chamber depending on the velocity of the particle and the direction of travel relative to the centrifuge platform. This error is caused by Coriolis accelerations and is particularly significant for fast moving particles, such as ejecta. For slow moving particles the effect is not noticeable.

Centrifuge facilities at ERDC and RPI

The centrifuge facility at ERDC is an Acutronic Model 680-1 balanced beam centrifuge used primarily for modeling geotechnical engineering field problems and also for studying other gravity related engineering phenomena in the fields of environmental, structures, blast, cold regions, hydraulics and coastal engineering. The centrifuge has a large capacity (1200 g-ton) and is capable of carrying a payload (such as a soil model) of 2 tons to 350g or 8 tons to 143g mounted on a swinging platform. The platform radius is 6.5 m and platform area is 1.3 m by 1.3 m. The centrifuge center has been operational since 1996.

The centrifuge facility at RPI is an Acutronic Model 665 balanced beam geotechnical centrifuge. This is a medium sized (150 g-ton) machine which has been in operation at RPI since August 1989. The machine has a radius of 3 m and for these purposes can carry a payload of up to 0.8 tons. The radius of the models is around 2.8m and hence the depth of the model is less than 1/10 of the radius of the centrifuge. A maximum acceleration level of 200g (265 rpm) can be achieved from rest in approximately 10 minutes. Details of the centrifuge specification and testing facility can be found at <http://www.nees.rpi.edu>.

Model chamber

The centrifuge model tests were performed in a rectangular strong box of internal dimensions 48 inches long x 13 inches wide x 14 inches deep. The intent of the long, narrow chamber is to create a plane strain model, which is appropriate to studying a two dimensional ‘slice’ through the levee running from the canal landward. In contrast with laboratory element tests typical field tests, the centrifuge can reproduce the performance of a very large area (and depth) of ground. At a steady acceleration of 50g, the design of the model chamber reproduces an area in the field some 54 feet wide by 200 feet long, or 10,800 square feet (1/4 acre). The mass of equivalent soil in the field contained within the model exceeds 40 million pounds. One long side of the strong box comprises a 2 inch thick Perspex window (48 inches long x 14 inches high) through which deformations of the plane model can be observed while the model is in flight.

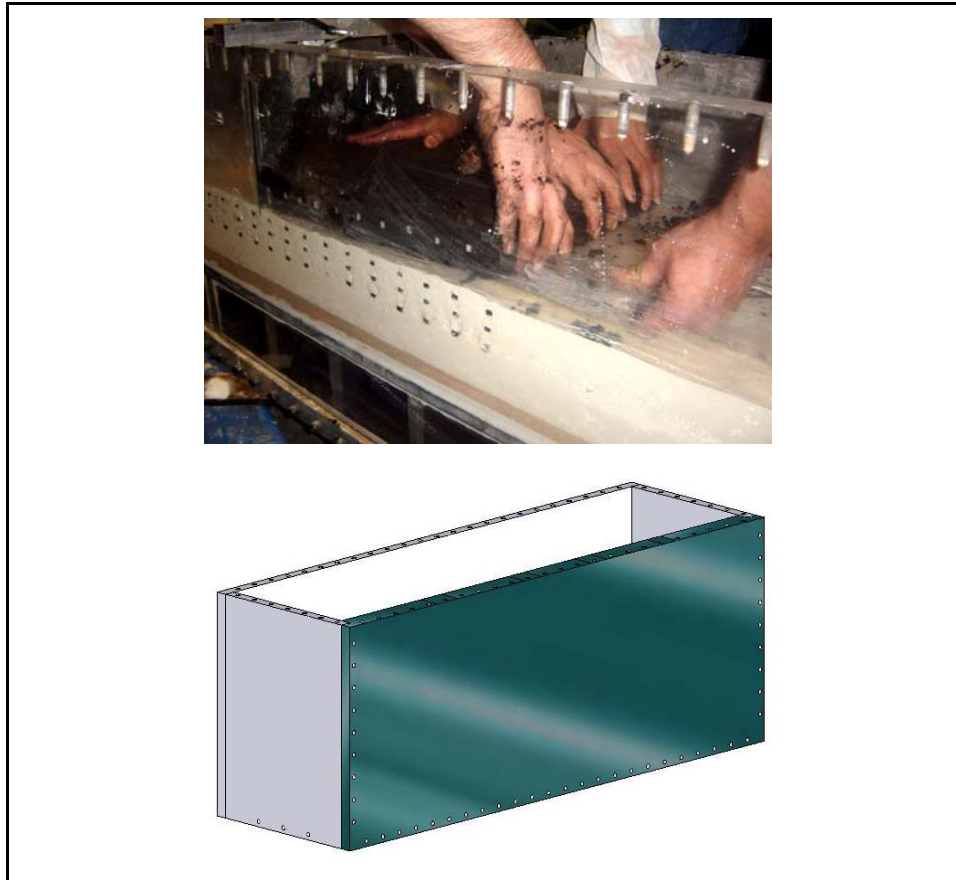


Figure K3-8. View of model chamber with perspex window

Instrumentation

Pore pressure transducers

Pore water pressures will be measured at various locations with the models by miniature pore pressure transducers manufactured by Druck Ltd. These transducers (PDCR81) are 6.35 mm in diameter and 11.3 mm in length. The transducer consists of a thin circular diaphragm machined from a silicon crystal and clamped to a supporting ring. Strain gauge circuits integrated into the back of the silicon diaphragm enable resistivity changes in the crystal to be correlated with applied pressures on the crystal diaphragm. A de-aired porous stone is fitted to protect the diaphragm and to ensure that pore pressures and not total stresses are measured. The wires from the strain gauge circuits are carried via a plastic sleeve out of the model, and this plastic sleeve also acts as an air passage to provide an atmospheric pressure behind the silicon diaphragm. Some versions of this miniature device are sealed and do not require to be vented.

The transducers are calibrated over their full working range and produce a linear response over the range of pressures experienced in the tests. Errors in pore pressure measurement due to temperature effects and flow of water into and

out of the porous stones have been discussed in the literature and can be considered to have no significant effect for the centrifuge model tests reported here.

Displacement transducers

The vertical displacements at various locations of the model will be measured using LVDTs (Linear Variable Differential Transformers). The LVDTs are manufactured by Schaevitz Engineering (Models MHR-500 and MHR-1000).

These LVDTs consist of a stationary coil assembly and a movable core. The coil assembly houses a primary and two secondary windings. The core is a steel rod of high magnetic permeability, smaller in diameter than the internal bore of the coil assembly; this contact free configuration eliminates measurement errors due to friction. When an AC excitation voltage is applied to the primary winding, a voltage is induced in each secondary winding through the magnetic core. The position of the core determines how strongly the excitation signal couples to each secondary winding. When the core is in the center, no signal is created. As the core travels to the left or to the right of center, an output voltage proportional to the displacement is created. The nominal linear ranges of the LVDTs to be used in this study are ± 12.7 mm and ± 25.4 mm.

Non-contact laser transducers will also be used to monitor the movement of the sheet pile walls and potentially to monitor the settlement of the downstream side of the levee. The laser transducers are manufactured by Keyence (Model LB70), and have the advantage (compared to LVDTs) that displacements can be accurately monitored without physical contact being maintained during movement (for example of the sheet pile wall).

Model Materials: Sand and Clay

Sand

The sand being used in this study is a standard laboratory sand known as Nevada sand, purchased from Gordon Sand Company of Compton, California. This sand has been used extensively by researchers to study a wide range of geotechnical problems. The sand is well characterized; as part of a major multi-laboratory investigation in the early 1990s, EARTH Technology Corporation carried out general laboratory tests on the sand which included sieve analyses, specific gravity tests, maximum and minimum density tests, and constant-head permeability tests (Arulmoli et al. 1992). The specific gravity of Nevada sand was determined to be 2.67 and the maximum and minimum dry densities were estimated as 17.33 kN/m^3 and 13.87 kN/m^3 respectively. The corresponding minimum and maximum void ratios were $e_{\min} = 0.511$ and $e_{\max} = 0.887$. Tables K3-2 and K3-3 summarize the results from the EARTH Technology laboratory tests and Figure K3-9 shows a typical grain size distribution for Nevada sand. Constant-head permeability tests were performed using reconstituted samples (Arulmoli et al. 1992). The permeability corresponding to a relative density of $D_r = 40$ percent, was $k = 6.6 \times 10^{-5} \text{ m/sec}$. The hydraulic conductivity versus

relative density is plotted in Figure K3-10, and Table K3-4 summarizes these results.

| Table K3-2 General test results for Nevada sand (Arulmoli et al. 1992) | |
|---|-------------------------|
| D ₁₀ | 0.08 mm |
| D ₅₀ | 0.15 mm |
| Specific gravity, G _s | 2.67 |
| Max. void ratio, e _{max} | 0.887 |
| Min. void ratio, e _{min} | 0.511 |
| Max. dry density | 17.33 kN/m ³ |
| Min. dry density | 13.87 kN/m ³ |

| Table K3-3 Sieve analysis for Nevada sand (Arulmoli et al. 1992) | | | | | | |
|---|-----|------|------|------|------|-------|
| Sieve number | 10 | 20 | 40 | 60 | 100 | 200 |
| Sieve size (mm) | 2 | 0.84 | 0.42 | 0.25 | 0.15 | 0.075 |
| Percent passing through sieve | 100 | 100 | 99.7 | 97.3 | 49.1 | 7.7 |

| Table K3-4 Constant-Head Permeability Tests Results for Nevada sand (Arulmoli et al. 1992) | | | | |
|---|----------------------------------|------------|----------------------|------------------------|
| Test No. | Dry density (kN/m ³) | Void ratio | Relative density (%) | Permeability (m/sec) |
| 1 | 16.95 | 0.55 | 91 | 2.3 x 10 ⁻⁵ |
| 2 | 15.08 | 0.742 | 40.2 | 6.6 x 10 ⁻⁵ |
| 3 | 15.76 | 0.667 | 60.1 | 5.6 x 10 ⁻⁵ |

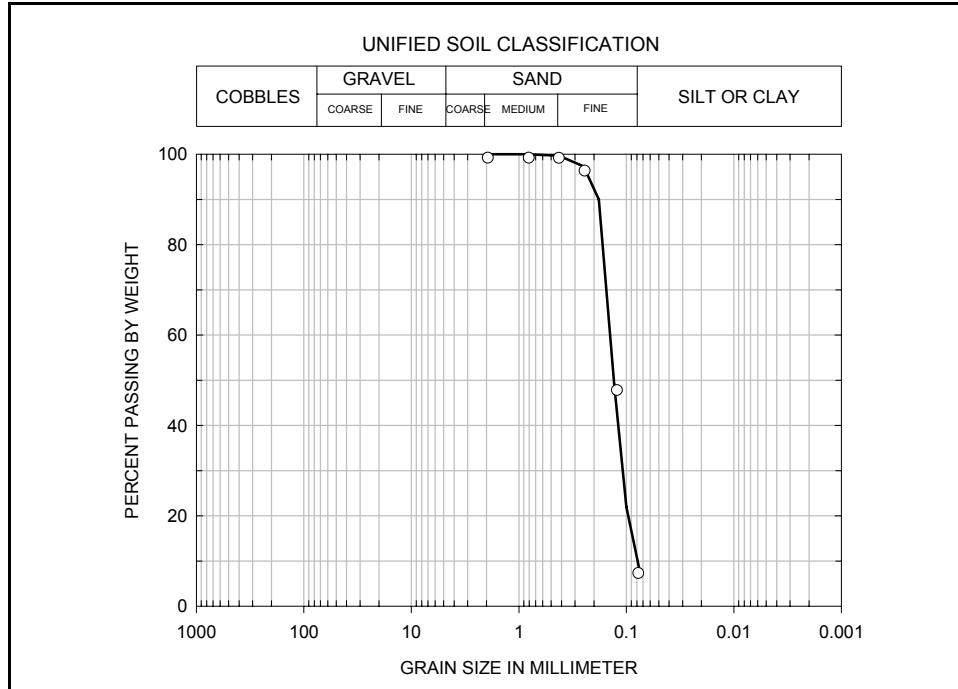


Figure K3-9. Grain size distribution for Nevada sand (after Arulmoli et al. 1992)

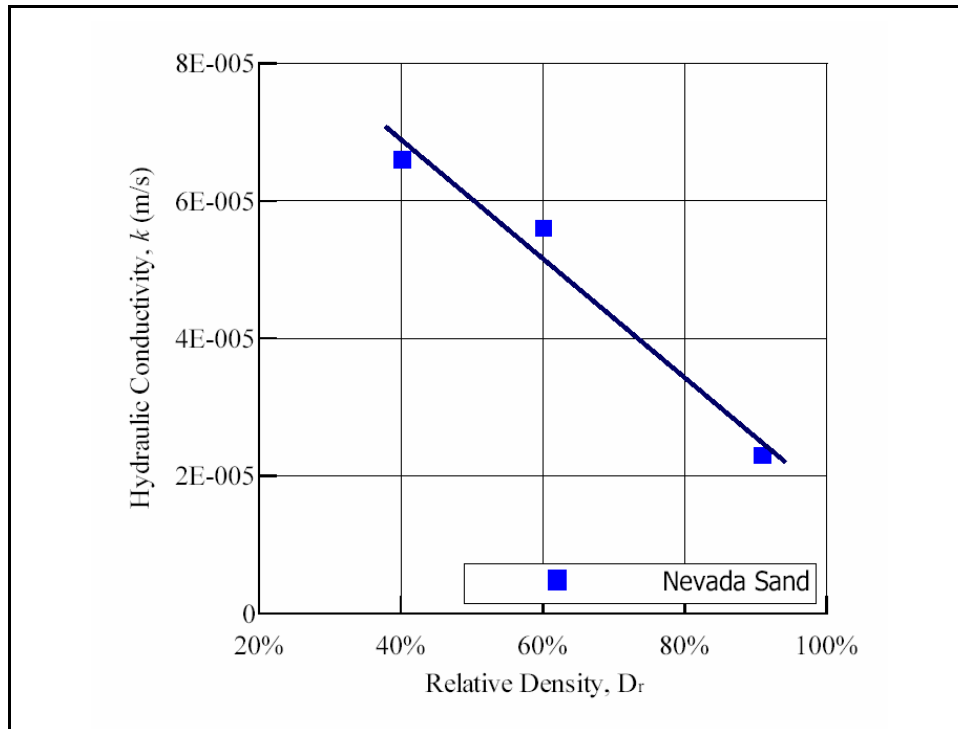


Figure K3-10. Hydraulic conductivity versus relative density for Nevada sand (after Arulmoli et al. 1992)

Dry Nevada sand is pluviated through air into the centrifuge container in a number of sub-layers (typically six). Each sub-layer may also be compacted by dropping an aluminum block to achieve the desired relative density. The dry pluviation and compaction procedure is calibrated in advance of the experiment to ensure that the target Relative Density of the sand can be reliably achieved (typically 60 percent RD). In the trial model, three layers of colored sand were also placed at intermediate depths to reveal mechanisms of piping or large scale movement.

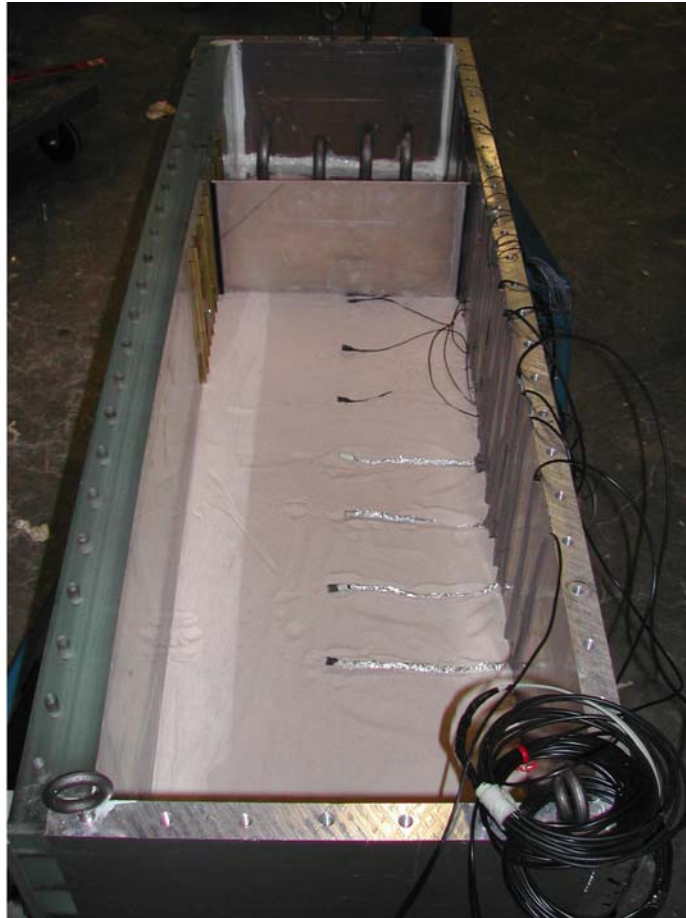


Figure K3-11. Positioning of pore pressure transducers in the sand layer

A number of pore pressure transducers were positioned installed at a height of 7 cm and 12 cm above the base of the Nevada sand. Once the thickness of the Nevada sand layer has reached exactly 14 cm and the whole layer is compacted to the target density, the sand will be saturated. The saturation process requires flushing with carbon dioxide prior to introduction of de-aired, de-ionized water under vacuum onto the surface of the sand until the whole layer is saturated. This saturation process may take as much as 24 hours. These procedures for saturating sand specimens in large centrifuge chambers have been developed over many years and are standard practice. Independent testing by use of p wave measurements in similar specimens has shown that the method achieves complete saturation.

Clay

The material selected to model the soft normally consolidated ‘laucustrine’ clay stratum was a speswhite kaolin clay (ASP 600) supplied by Engelhard Corporation, New Jersey. The main geotechnical properties of the kaolin are presented below in Table K3-5. Kaolin is a coarse grained clay which has the advantage of further accelerating consolidation of samples. It is widely used in geotechnical laboratory investigations and its properties and performance have been thoroughly researched and are widely documented.

| Table K3-5 Geotechnical Properties of Speswhite Kaolin | |
|---|------|
| Specific gravity g/cm^3 | 2.58 |
| Liquid limit (percent) | 58 |
| Plastic limit (percent) | 27 |
| Plasticity index (percent) | 31 |

Preparation of speswhite kaolin to a predetermined profile of consolidation is achieved by exploiting the relationship between Specific Volume, V and mean effective stress, p' for normal consolidation. Figure K3-12 illustrates the typical log-linear relationship found between specific volume and mean stress from which the consolidation characteristics of the clay can be deduced. The slope of the consolidation curve is commonly known as λ in $V - \ln p'$ space. The Specific Volume is defined as the total volume of void and solid assuming a unit volume of solid.

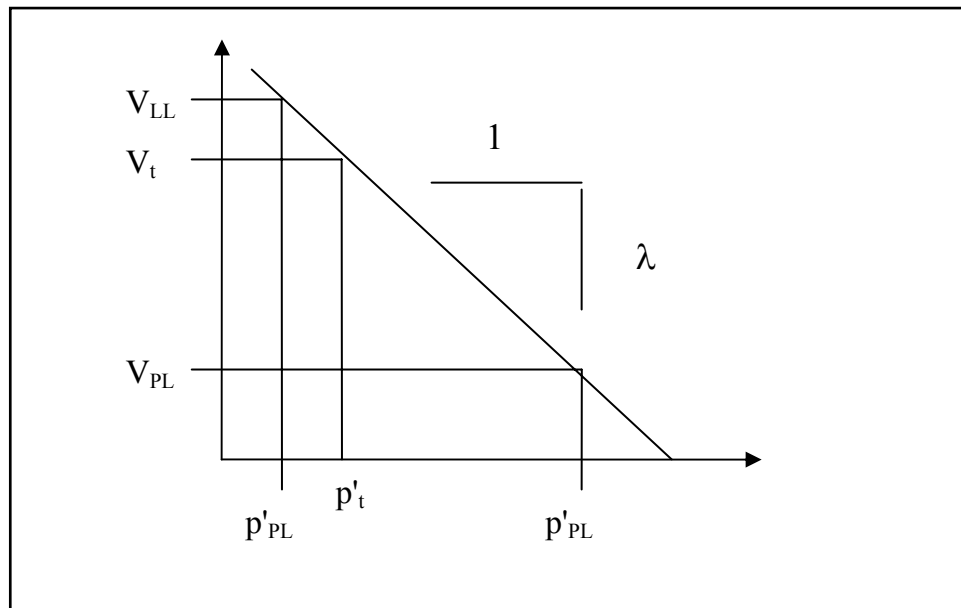


Figure K3-12. Log-linear relationship between Specific Volume and mean effective confining stress, p' for normally consolidated clay

By knowing the Specific Volume at the liquid limit (LL) and at the plastic limit (PL) of the clay, and the relationship between the strength of the normally consolidated clay and the moisture content (related to Specific Volume) between

these two limits (a factor of 100) then an estimate of the overburden load can be made to achieve any desired strength in the clay, following mixing from slurry. By this means, the clay levee can be constructed to a defined normally consolidated strength, which may then be tested by measurement of water content.

Once the target moisture content has been determined, the clay layer is pre-consolidated to its target strength profile from slurry placed in the centrifuge strong box or in the case of the levee block, by placing the slurry in a mold. Dry powdered kaolin clay is mixed with de-aired water to slurry at around 100 percent moisture content. The slurry was then carefully placed by hand into the strongbox to a depth of 13 cm or into the mold. An overburden load (sand) is placed over the slurry by first placing a layer of geotextile fabric on the slurry surface and then pluviating a sand surcharge (of calculated weight) to a depth of 10 cm. The sand was then saturated and the model chamber placed on the centrifuge, to use its own self weight to provide a gradient of effective stress through the specimen. The advantage of this process is the precise control of the gradient of stress in the clay layer, which is similar to the geological process that takes place over millennia as clay layers are laid down in the natural ground. The disadvantage is the time that the process may take, which can last many hours. The centrifuge is slowly accelerated at slew rate of 0.25 g/min to 10g, 20g, 30g, 40g and 50 g, being held at each g-level for approximately 30 minutes while consolidation of the clay is monitored through records of the vertical settlement and excess pore pressure dissipation. The target strength profile for the clay layer in the 17th Street trial model was 280 – 380 psf (13 – 18kPa). Once the consolidation process is completed, the centrifuge is stopped and the rest of the model assembled.

K4 – Concrete I-Wall and Sheet Piling Material Recovery, Sampling and Testing: 17th Street Canal Levee Breach

Introduction

On Monday and Tuesday, 12-13 December 2005, samples of the concrete I-wall and sheet piling were taken at or adjacent to the 17th Street Canal levee breach. The objectives of this exercise were a:) to verify conformance of material properties of the I-wall concrete and reinforcing steel, and the sheet piling with their respective specifications; b:) to verify the as driven length of the of the sheet piling and c:) potentially validate the Parallel Seismic testing that was performed in an attempt to determine, in situ, the sheet piling tip elevation

The 17th Street Canal breach is located on the east side of the canal just south of Hammond Highway. Figure K4-1 shows the breach shortly after Hurricane Katrina. The material samples were obtained from the (relatively) undisturbed I-wall sections at the north and south end of the breach. Concrete and rebar samples were obtained on Monday, 12 December and sheet piling were extracted on Tuesday, 13 December 2005.

The I-wall is comprised of a series of concrete wall panels separated by expansion joints and is founded on sheet piling driven through the levee. A typical cross section is shown in Fig. K4-2.

Material Sample Recovery

The material samples recovered from the site included two four foot square by 12 inch thick wall panel samples, two nominally six inch diameter cylindrical cores, one each from the wall panel samples, six samples of reinforcing steel from the wall panels and 14 sheet piles. All samples were marked and tagged and placed into a controlled and documented chain of custody.



Figure K4-1. 17th Street canal breach

The I-wall panels immediately north and south of the breach were designated H22 and H38, respectively. A four foot by four foot section was sawcut from the top of the north end of the I-wall section H38 and from the top of the south end of I-wall section H22. The contractor first drilled a six inch diameter core from the designated four foot square sample at the north end of wall panel H38.. The core drill and saw are shown mounted to the wall at panel H38 at the south end of the breach in Fig K4-3. Figure K4-4 shows the core being removed from panel H38. It was marked and tagged MH38C1C01 as shown in Fig. K4-5.

Prior to drilling, the cores were considered as potential compressive strength test specimens. However the core contained rebar and was not a valid test specimen. The resulting holes were used to for rigging to support and remove the four foot by four foot wall samples as shown in Figs. K4-6 and K4-7.

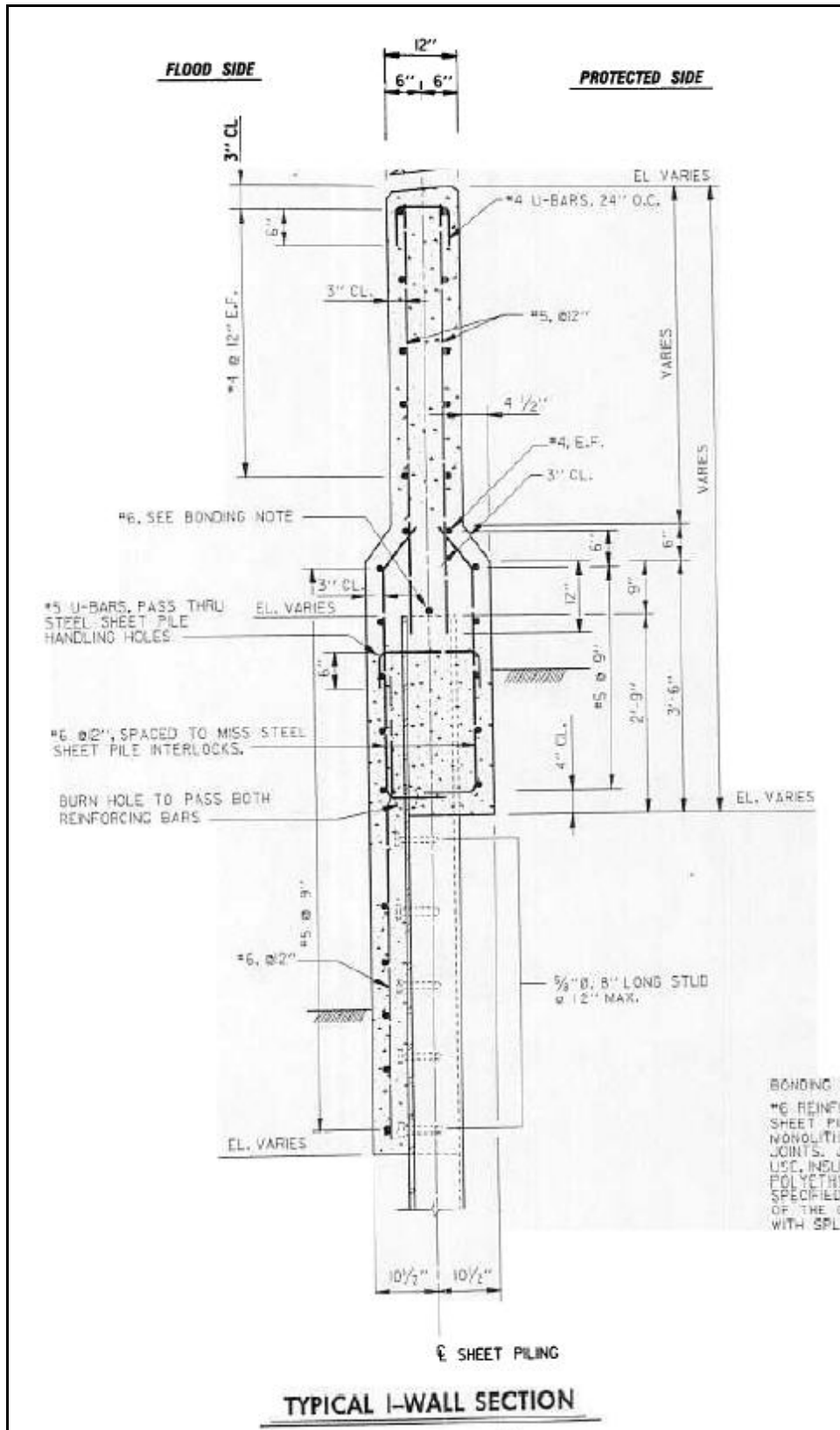


Figure K4-2. Typical I-wall section



Figure K4-3. Core drill and saw mounted to wall panel H38



Figure K4-4. core being removed from panel H38



Figure K4-5. Core from wall panel H38



Figure K4-6. Sawing of sample from wall panel H38



Figure K4-7. Removal of sample from wall panel H38

A similar procedure was used to obtain a four foot square sample from the south end of wall panel H22 at the north end of the breach as shown in Figs. K4-8 and K4-9. The concrete core was marked and tagged MH22C1C01 as shown in Fig. K4-10. This core also contained rebar and was not suitable for

testing. The wall panel sample was marked and tagged MH22C1 as shown in Fig. K4-11.



Figure K4-8. Core drill and saw mounted at panel H22



Figure K4-9. Sample being removed from wall panel H22



Figure K4-10. Cylindrical core from wall panel H22



Figure K4-11. Wall sample MH22C1

Rebar samples were then removed from the remaining sections of wall panels H38 and H22. A hoe ram was used for controlled demolition of wall panels in order to expose the rebar samples as shown in Fig. K4-12. Some of the demolition of the concrete around the rebar samples was done with a small hand

held jack hammer as shown in Fig. K4-13. A portable electric bandsaw was used to cut the rebar samples as shown in Fig K4-14.



Figure K4-12. Demolition of concrete for rebar sampling at panel H22



Figure K4-13. Demolition of concrete around rebar sample at panel H38



Figure K4-14. A portable electric bandsaw is used to cut rebar samples

At wall panel H38 a two foot long sample of the following rebar were obtained: 1) A #4 horizontal bar from the east face of the wall approximately 29 inches down from the top of the wall. The north end of the sample terminated at the vertical sawcut for the wall sample MH38C1. 2) A #5 vertical approximately 76 inches from the north end of panel H38. 3) A #6 vertical from the west face of the lower section of the wall. This #6 bar was approximately 8 inches from the north end of panel H38. (This sample has the orange paint shown in Fig. K4-15.) These rebar samples were marked and tagged MH38R1, MH38R2 and MH38R3, respectively.



Figure K4-15. Number 6 rebar sample being taken from panel H38

At wall panel H22 a two foot long sample of the following rebar were obtained: 1) A #4 horizontal bar from the west face of the wall, approximately six inches down from the top of the wall 2) A #5 vertical bar from the west face of the wall approximately 74 inches from the south end of the wall pane. 3) A #6 vertical from the west face of the lower end of the wall approximately 16 inches from the south end of the wall panel. These samples were marked and tagged MH22R1, MH22R2 and MH22R3, respectively.

Figure K4-16 shows the wall panel samples, cores, and rebar samples collected on Monday, 12 December 2005. Note that the cores were placed in sealed plastic bags and each core and the 3 rebar samples from each of the two wall panels were placed in individual latching boxes. These samples were transported to a secure area at a warehouse at the Corps of Engineers' New Orleans District Office.



Figure K4-16. Wall panel samples, cores and rebar samples

After the cores, wall panel and rebar samples were obtained the contractor began demolition of the wall panels to expose the top of the sheet piles for extraction. A scissor concrete crusher was used to demolish the upper portion of the wall panels as shown in Fig. K4-17. A hoe ram was then used to remove the lower portion of the of the wall panel around the sheet piling (Reference the wall cross section in Fig. K4-2.) as shown in Fig. K4-18. The same procedure was used for both wall panels H38 and H22.



Figure K4-17. Demolition of top portion of wall panel H38



Figure K4-18. Hoe ram demolishing lower portion of wall panel H38

On Tuesday, 13 December 2005, sheet piles were extracted. The location of the sheet piles extracted at or adjacent to wall panel H38 is schematically shown in Fig. K4-19. Starting from the north end of panel H38, the piles are designated MH38SP1, MH38SP2, ..., MH38SP16 (the last number of the designation is incremented going from north to south).

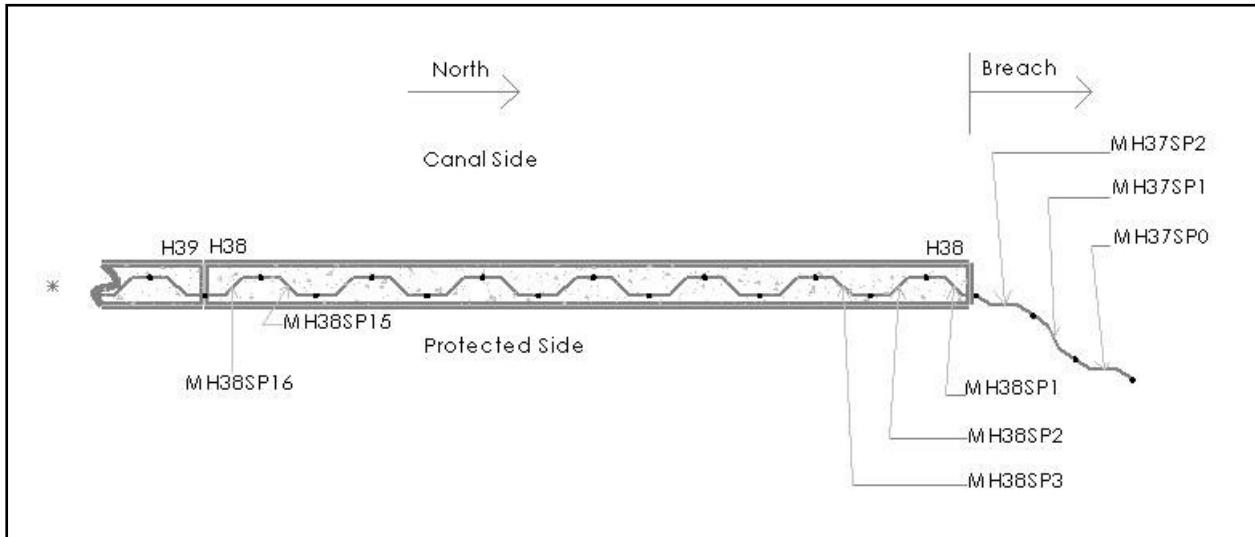


Figure K4-19. Sheet pile designations at wall panel H38

Sheet piles MH38SP2, MH38SP3 were extracted as a pair. Their lengths were approximately 23'-7" and 23'-8", respectively. MH38SP1 and MH37SP2 were then extracted as a pair. Their lengths were approximately 23'-3". The contractor then moved to the south end of wall panel H38 and extracted MH38SP15 and MH38SP16. Their lengths were approximately 23'-5". MH38SP15 and MH38SP16 were at a location corresponding to a soil boring hole where Parallel Seismic tests were conducted in an attempt to determine the length of the sheet pile in situ. The contractor then attempted to extract sheet pile MH37SP1 as a single pile, but MH37SP0 came with it. Their lengths were approximately 23'-6". Extraction of sheet piles at the south end of the breach is shown in Figs. K4-20 and K4-21. The out-of-plumb orientation (from displacement of the piling in the breach) of piles MH37SP1 and MH37SP0 is clearly evident in Fig. K4-21. Figure K4-22 shows measuring and tagging of sheet piling.



Figure K4-20. Extraction of sheet piles MH38SP2 and MH38SP3



Figure K4-21. Extraction of sheet piles MH37SP1 and MH37SP0

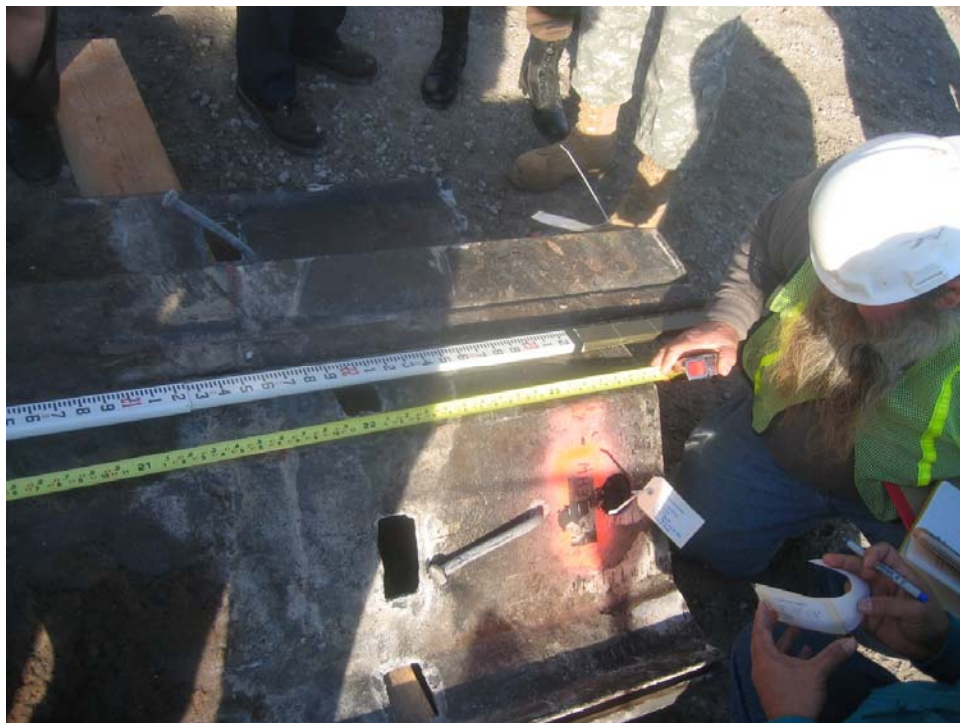


Figure K4-22. Measuring and tagging of sheet piles

Sheet piles were then extracted at the location of wall panel H22, immediately north of the breach. Four sheet piles at the south end of wall panel H22 were designated MH22SP1, MH22SP2, MH22SP3 and MH22SP4. (The last number of the designation was incremented going from south to north.) Sheet piles MH22SP1 and MH22SP2 were extracted as a pair as shown in Fig. K4-23. These piles had a length of approximately 23'-7" and 23'-6", respectively. Sheet piles MH22SP3 and MH22SP4 were extracted as a pair and had a length of approximately 23'-7" and 23'-6", respectively. The contractor then pulled a pair of piles from just north of the north end of wall panel H22 at a location coincident with a boring hole where Parallel Seismic testing had been performed. These piles were designated MH21SP1 and MH21SP2. Both of these sheet piling had a length of approximately 23'-6".



Figure K4-23. Extraction of sheet piling MH22SP1 and MH22SP2

Figures K4-24 and K4-25 show the sheet piling extracted from the south and north ends of the breach, respectively. The sheet piles were loaded on a truck and transported to a secure location within a warehouse at the Corps of Engineers' New Orleans District Office.



Figure K4-24. Sheet piling extracted from south end of breach



Figure K4-25. Sheet piling extracted from north end of breach

Sheet Piling Length and Tip Elevation

The sheet piling extracted from the 17th Street Canal breach site ranged in length from 23'-3" to 23'-8". The top of the pilings were at approximately elevation 6.25 ft. (The pilings adjacent to the expansion joints between wall panels were driven slightly lower as can be seen in Fig. K4-26. This was done to improve the performance and effectiveness of the expansion joint.) A 23'-3"

piling length provides for a tip elevation of -17.0 ft. Obviously, piling driven with a lower top elevation have a correspondingly lower tip elevation.



Figure K4-26. Lower top elevation of sheet piling at expansion joint

Material Testing

On Friday, 16 December 2005, three each, nominally six inch diameter, concrete cores were drilled from the wall panel samples MH22C1 and MH38C1. These cores were marked and tagged MH22C1-01, MH22C1-02, MH22C1-03, MH38C1-01, MH38C1-02, and MH38C1-03. A sample of steel was also flame cut from each of four sheet piling. The six cores, four steel samples and the previously obtained six samples of rebar were transferred to Beta Testing & Inspection, LLC of Gretna, LA (BTI) for testing.

The concrete cores were obtained and tested for compressive strength by BTI in accordance with ASTM C 42 and C 39. As can be seen in Table K4-1, all of the cores had a compressive strength in excess of the specified 3000 psi compressive strength. More comprehensive details of the testing are in BTI's report in Appendix A.

| Table K4-1 Concrete Compressive Strength | | |
|---|---|---|
| Core | Specified Compressive Strength (psi) | Compressive Strength As Tested (psi) |
| MH22C1-01 | 3000 | 4000 |
| MH22C1-02 | 3000 | 3190 |
| MH22C1-03 | 3000 | 3940 |
| MH38C1-01 | 3000 | 3960 |
| MH38C1-02 | 3000 | 4360 |
| MH38C1-03 | 3000 | 4100 |

Tensile tests of the sheet piling material samples were performed, in accordance of ASTM A 370, by a subcontractor to BTI. A summary of the test results and the tensile requirements of the material specification, ASTM A 328 are provided in Table K4-2. More comprehensive details of the testing are in BTI's report in Appendix A.

| Table K4-2 Sheet Piling Tensile Requirements and Tests Results | | | |
|---|-----------------------------|-------------------------------|--------------------------------|
| Sample | Yield Strength (ksi) | Tensile Strength (ksi) | Elongation in 2 in. (%) |
| MH21SP1-01 | 58.5 | 80.9 | 33.0 |
| MH22SP2-01 | 55.4 | 80.1 | 29.9 |
| MH 37SP1-01 | 55.5 | 82.1 | 32.1 |
| MH38SP16-01 | 57.0 | 80.0 | 32.7 |
| ASTM A 328 Tensile Requirements | 39 | 70 | 20 |

Tensile tests of the rebar samples, in accordance of ASTM A 370, were also performed. A summary of the test results and tensile requirements for the specified ASTM A 615 Grade 60 reinforcement is provided in Table K4-3. More comprehensive details are included in BTI's report in Appendix A.

| Table K4-3 Reinforcing Steel Tensile Requirements and Test Results | | | | |
|---|---------------------------------|-----------------------------|-------------------------------|--------------------------------|
| Sample | Bar Size Designation No. | Yield Strength (ksi) | Tensile Strength (ksi) | Elongation in 8 in. (%) |
| MH22R1 | 4 | 65.0 | 107.5 | 11.7 |
| MH22R2 | 5 | 62.9 | 104.5 | 13.2 |
| MH22R3 | 6 | 65.9 | 108.1 | 9.3 |
| MH38R1 | 4 | 91.0 | 107.5 | 16.2 |
| MH38R2 | 5 | 61.3 | 99.7 | 9.8 |
| MH38R3 | 6 | 79.5 | 97.7 | 11.4 |
| ASTM A 615 Grade 60 Tensile Requirements | 3, 4, 5 or 6 | 60 | 90 | 9 |

Appendix A: Test Report from Beta Testing & Inspection, LLC



Beta Testing & Inspection, LLC
Forensic Engineering Division

February 14, 2006

Paul F. Mlakar, Ph.D., P.E.

US Army Corps of Engineers
Engineer Research and Development Center
3909 Halls Ferry Road
Vicksburg, MS 39180

**RE: Testing of 17th Street Canal Floodwall Materials
Final Report
BTI Report No.: 1047-ES121605**

Dear Mr. Mlaker:

On December 16, 2005, specimens were sampled at the US Army Corps of Engineers New Orleans District warehouse and transported to Beta Testing & Inspection, LLC (BTI) laboratory for testing. All specimens were labeled, tagged, and secured prior to transporting. BTI cut a total of six concrete cores from two wall sections. Three cores were cut from each section. Mark Cheek, P.E. of BTI witnessed the removal of 12"x 6" sections from four different sheet piles and assumed responsible possession of six reinforcing bars; two No.4, two No.5, and two No.6. Representatives of BTI were informed by the Corps of Engineers that the material samples provided to BTI or obtained by BTI were portions of existing components taken from the 17th Street Canal Floodwall Project. Also, Mr. Bob Brooks of the USACE provided BTI with material data sheets and project specifications for the sampled materials. BTI has completed testing of concrete cores, steel sheet pile sections, and steel reinforcing bars.

Concrete Cores

Three cores were cut from the west face of sample panel MH22C1 and three from the east face of sample panel MH38C1. The cores were obtained in accordance with procedures defined by ASTM C-42. Prior to compression testing each core was prepared in accordance with ASTM C-42, C-617, and C-39. Each core was then tested in compression to failure and the results recorded in accordance with ASTM C-39. See Tables C.1 and C.2 for results of the concrete core testing.

P.O. Box 2203 • Gretna, LA 70054 • (504) 227-2273 • fax (504) 227-2274
13801 Old Gentilly Road Suite #17 New Orleans, Louisiana 70129

Table C.1

| Sample panel MH38C1 | | | | | | |
|---------------------|----------------------------|---------------|-------------------------|------------------|-------------------|---------------------|
| Core ID | Capped Length (in.) | Diameter (in) | Area (in ²) | l/d | Correction factor | Maximum load (lbs.) |
| MH38C1-01 | 11.9 | 5.67 | 25.25 | 2.09 | 1 | 100,000 |
| | Compressive strength (psi) | Fracture type | Age (days) | Load application | Test date/time | Sample date/time |
| | 3960 | C | NA | vertical | 12/21/05 10:00am | 12/16/05 11:00am |
| Core ID | Capped Length (in.) | Diameter (in) | Area (in ²) | l/d | Correction factor | Maximum load (lbs.) |
| MH38C1-02 | 9.19 | 5.65 | 25.12 | 1.62 | 0.97 | 113,000 |
| | Compressive strength (psi) | Fracture type | Age (days) | Load application | Test date/time | Sample date/time |
| | 4360 | A | NA | vertical | 12/21/05 10:00am | 12/16/05 11:00am |
| Core ID | Capped Length (in.) | Diameter (in) | Area (in ²) | l/d | Correction factor | Maximum load (lbs.) |
| MH38C1-03 | 11.8 | 5.66 | 25.15 | 2.08 | 1 | 103,000 |
| | Compressive strength (psi) | Fracture type | Age (days) | Load application | Test date/time | Sample date/time |
| | 4100 | D | NA | vertical | 12/21/05 10:00am | 12/16/05 11:00am |

Table C.2

| Sample panel MH22C1 | | | | | | |
|---------------------|----------------------------|---------------|-------------------------|------------------|-------------------|---------------------|
| Core ID | Capped Length (in.) | Diameter (in) | Area (in ²) | l/d | Correction factor | Maximum load (lbs.) |
| MH22C1-01 | 11.9 | 5.66 | 25.12 | 2.10 | 1 | 100,500 |
| | Compressive strength (psi) | Fracture type | Age (days) | Load application | Test date/time | Sample date/time |
| | 4000 | D | NA | vertical | 12/21/05 10:00am | 12/16/05 11:00am |
| Core ID | Capped Length (in.) | Diameter (in) | Area (in ²) | l/d | Correction factor | Maximum load (lbs.) |
| MH22C1-02 | 11.8 | 5.66 | 25.22 | 2.08 | 1 | 80,500 |
| | Compressive strength (psi) | Fracture type | Age (days) | Load application | Test date/time | Sample date/time |
| | 3190 | B | NA | vertical | 12/21/05 10:00am | 12/16/05 11:00am |
| Core ID | Capped Length (in.) | Diameter (in) | Area (in ²) | l/d | Correction factor | Maximum load (lbs.) |
| MH22C1-03 | 11.9 | 5.67 | 25.25 | 2.09 | 1 | 99,500 |
| | Compressive strength (psi) | Fracture type | Age (days) | Load application | Test date/time | Sample date/time |
| | 3940 | A | NA | vertical | 12/21/05 10:00am | 12/16/05 11:00am |

The average compressive strength of cores from panel MH38C1 is 4140psi and 3710psi for panel MH22C1. Section C3D-7.2.1 of the provided project specifications requires a minimum compressive strength of 3000psi @ 28 days. The average compressive strength of each set of cores exceeded the project minimum requirements.

Steel Sheet Piling

A welder provided by the Corps of Engineers cut one 12"x 6" specimen from each of the four-sheet pile using an acetylene cutting torch. Mandina's Inspection a subcontractor of BTI then prepared and tested each specimen in tension to failure in accordance with ASTM A-370. The provided material data sheets reference ASTM A328 in which a minimum tensile strength of 70,000psi is required. The average tensile strength of the sheet pile samples was 80,755psi, which exceeds the minimum project requirements. See enclosure SHEET PILE TENSILES for tests results.

Testing of 17th Street Canal
Floodwall Materials

February 14, 2006

Steel Reinforcing Bars

Six pieces of steel reinforcing bars each measuring 2' in length were secured and transported to BTI's laboratory. The steel reinforcing bar samples ranged in size from No. 4 to No. 6 bars. Mandina's Inspection a subcontractor of BTI tested the rebar specimens to failure in accordance with ASTM A-615 & A370. Section C3B-6.1.1 of the project specifications references ASTM A-615. ASTM A-615 requires a minimum tensile strength of 90,000psi for Grade 60 steel. The specimens tested tensile strength exceeds the minimum project requirements. See enclosure STEEL REINFORCING BAR TENSILES for test results.

Upon completion and acceptance of the testing program, all of the materials, tested and untested, will be sealed and returned to the New Orleans District Office of the US Army Corps of Engineers. Enclosed are copies of our laboratory accreditations and equipment calibration reports associated with the test performed. Should you have any questions regarding this letter or require additional information, please do not hesitate to contact us.

Sincerely,

Beta Testing & Inspection, LLC



Mark A. Check, P.E.
Vice-President

Enclosures

SHEET PILE TENSILES

MECHANICAL TESTING LABORATORY DIVISION

MTL JOB NO. _____

TENSILE NO. _____

| SPECIMEN ID | WIDTH INCHES | THICKNESS SQ. IN. | AREA SQ. IN. | YIELD STR. POUNDS | YIELD STR. PSI | TENSILE STR. POUNDS | TENSILE STR. PSI | ELONGATION IN 2" GAGE PERCENT |
|-----------------|--------------|-------------------|--------------|-------------------|----------------|---------------------|------------------|-------------------------------|
| MH 215 P1-01 | .493 | .363 | .188 | 11000 | 53510 | 15200 | 80951 | 2.661 33.0 % |

TENSILE NO. _____

| SPECIMEN ID | WIDTH INCHES | THICKNESS SQ. IN. | AREA SQ. IN. | YIELD STR. POUNDS | YIELD STR. PSI | TENSILE STR. POUNDS | TENSILE STR. PSI | ELONGATION IN 2" GAGE PERCENT |
|-----------------|--------------|-------------------|--------------|-------------------|----------------|---------------------|------------------|-------------------------------|
| MH 225 P2-01 | .500 | .373 | .186 | 10300 | 55370 | 14900 | 80107 | 2.598 29.9 % |

TENSILE NO. _____

| SPECIMEN ID | WIDTH INCHES | THICKNESS SQ. IN. | AREA SQ. IN. | YIELD STR. POUNDS | YIELD STR. PSI | TENSILE STR. POUNDS | TENSILE STR. PSI | ELONGATION IN 2" GAGE PERCENT |
|-----------------|--------------|-------------------|--------------|-------------------|----------------|---------------------|------------------|-------------------------------|
| MH 375 P1-01 | .497 | .371 | .184 | 10200 | 55434 | 15100 | 82065 | 2.642 32.1 % |

TENSILE NO. _____

| SPECIMEN ID | WIDTH INCHES | THICKNESS SQ. IN. | AREA SQ. IN. | YIELD STR. POUNDS | YIELD STR. PSI | TENSILE STR. POUNDS | TENSILE STR. PSI | ELONGATION IN 2" GAGE PERCENT |
|------------------|--------------|-------------------|--------------|-------------------|----------------|---------------------|------------------|-------------------------------|
| MH 385 P16-01 | .493 | .406 | .200 | 11400 | 57000 | 16000 | 80000 | 2.655 32.7 % |

G:\WORDDATA\SI FORMS\TTFY.LAB

STEEL REINFORCING BAR TENSILES MH-22

MH22

MECHANICAL TESTING LABORATORY DIVISION

MTL JOB NO. _____

TENSILE NO. _____

8" Gage

| SPECIMEN ID | DIA. INCHES | AREA SQ. IN. | YIELD LOAD POUNDS | YIELD STR. PSI | ULTIMATE LOAD POUNDS | TENSILE STR. PSI | ELONGATION IN 8" GAGE PERCENT | REDUCTION IN AREA PERCENT |
|-------------|-------------|--------------|-------------------|----------------|----------------------|------------------|-------------------------------|---------------------------|
| R1 | .500 | .20 | 13,000 | 65,000 | 21500 | 107,500 | 8.935 11.68 | .358 .100 50% |

TENSILE NO. _____

| SPECIMEN ID | DIA. INCHES | AREA SQ. IN. | YIELD LOAD POUNDS | YIELD STR. PSI | ULTIMATE LOAD POUNDS | TENSILE STR. PSI | ELONGATION IN 8" GAGE PERCENT | REDUCTION IN AREA PERCENT |
|-------------|-------------|--------------|-------------------|----------------|----------------------|------------------|-------------------------------|---------------------------|
| R2 | .624 | .31 | 19,500 | 62,903 | 32400 | 164516 | 9.052 13.5% | .481 .181 41.6% |

TENSILE NO. _____

| SPECIMEN ID | DIA. INCHES | AREA SQ. IN. | YIELD LOAD POUNDS | YIELD STR. PSI | ULTIMATE LOAD POUNDS | TENSILE STR. PSI | ELONGATION IN 8" GAGE PERCENT | REDUCTION IN AREA PERCENT |
|-------------|-------------|--------------|-------------------|----------------|----------------------|------------------|-------------------------------|---------------------------|
| R3 | .750 | .44 | 29,000 | 65,909 | 45800 | 104,090 | 8.746 9.25% | .626 .307 30.2% |

TENSILE NO. _____

| SPECIMEN ID | DIA. INCHES | AREA SQ. IN. | YIELD LOAD POUNDS | YIELD STR. PSI | ULTIMATE LOAD POUNDS | TENSILE STR. PSI | ELONGATION IN 8" GAGE PERCENT | REDUCTION IN AREA PERCENT |
|-------------|-------------|--------------|-------------------|----------------|----------------------|------------------|-------------------------------|---------------------------|
| | | | | | | | | |

G:\WORD\DATA\MSIFORMS\TT505.LAB

p-2

8891961888

David Mandina

Steel Reinforcing Bar Tensiles MH-38

MH 38

MECHANICAL TESTING LABORATORY DIVISION

MTL JOB NO. _____

TENSILE NO. _____

8" Gage

| SPECIMEN ID | DIA. INCHES | AREA SQ. IN. | YIELD LOAD POUNDS | YIELD STR. PSI | ULTIMATE LOAD POUNDS | TENSILE STR. PSI | ELONGATION IN 8" GAGE PERCENT | REDUCTION IN AREA PERCENT |
|-------------|-------------|--------------|-------------------|----------------|----------------------|------------------|-------------------------------|---------------------------|
| R-1 | .500 | .20 | 18,200 | 91,000 | 21,500 | 107,500 | 9.292 16.15% | .377 .111 44.5% |

TENSILE NO. _____

| SPECIMEN ID | DIA. INCHES | AREA SQ. IN. | YIELD LOAD POUNDS | YIELD STR. PSI | ULTIMATE LOAD POUNDS | TENSILE STR. PSI | ELONGATION IN 8" GAGE PERCENT | REDUCTION IN AREA PERCENT |
|-------------|-------------|--------------|-------------------|----------------|----------------------|------------------|-------------------------------|---------------------------|
| R-2 | .624 | .31 | 19,000 | 61,240 | 30,200 | 99,677 | 9.785 9.81% | .443 .154 50.3% |

TENSILE NO. _____

| SPECIMEN ID | DIA. INCHES | AREA SQ. IN. | YIELD LOAD POUNDS | YIELD STR. PSI | ULTIMATE LOAD POUNDS | TENSILE STR. PSI | ELONGATION IN 8" GAGE PERCENT | REDUCTION IN AREA PERCENT |
|-------------|-------------|--------------|-------------------|----------------|----------------------|------------------|-------------------------------|---------------------------|
| R-3 | .750 | .44 | 35,000 | 79,545 | 43,000 | 97,725 | 8.912 11.4% | .539 .228 48.18% |

TENSILE NO. _____

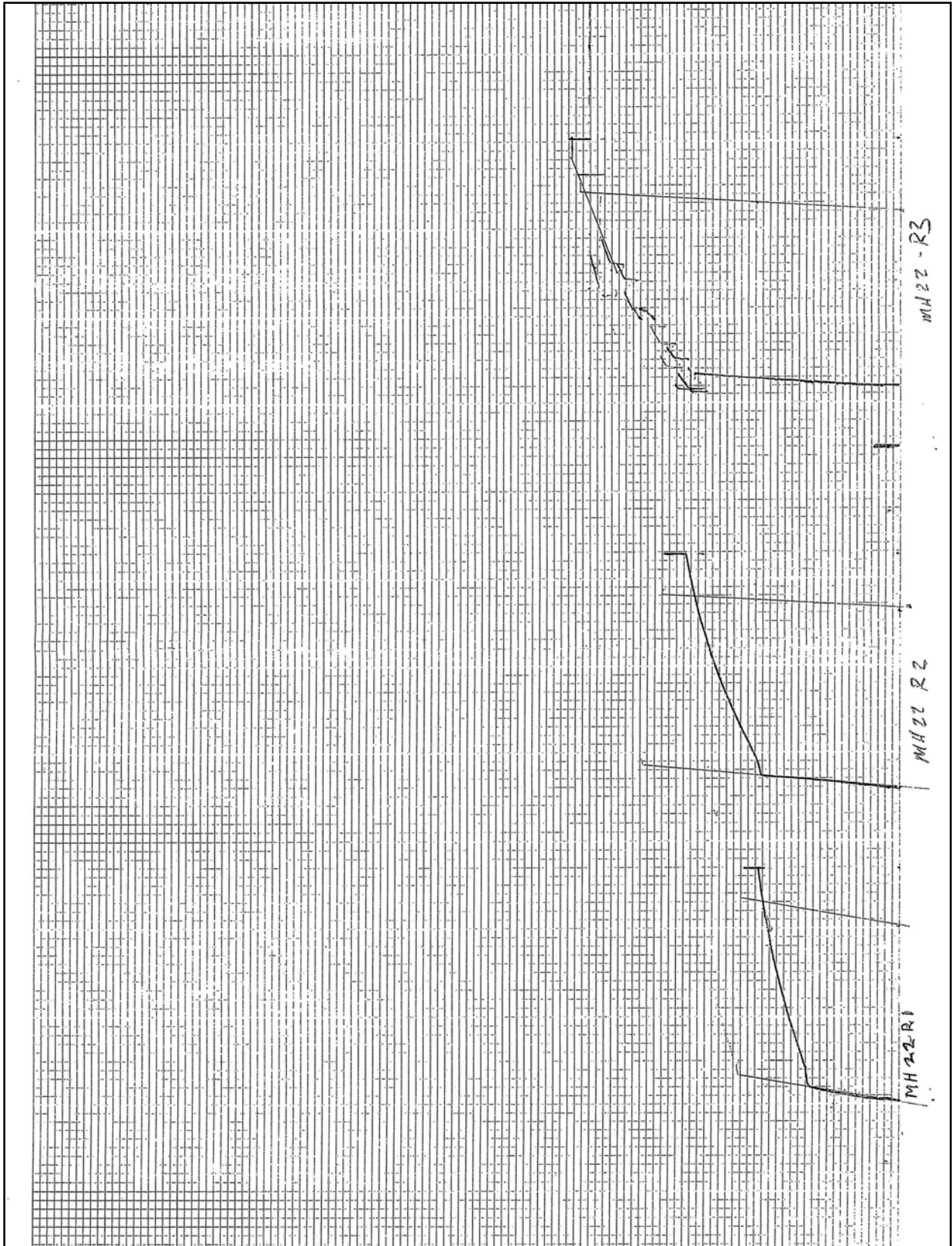
| SPECIMEN ID | DIA. INCHES | AREA SQ. IN. | YIELD LOAD POUNDS | YIELD STR. PSI | ULTIMATE LOAD POUNDS | TENSILE STR. PSI | ELONGATION IN 8" GAGE PERCENT | REDUCTION IN AREA PERCENT |
|-------------|-------------|--------------|-------------------|----------------|----------------------|------------------|-------------------------------|---------------------------|
| | | | | | | | | |

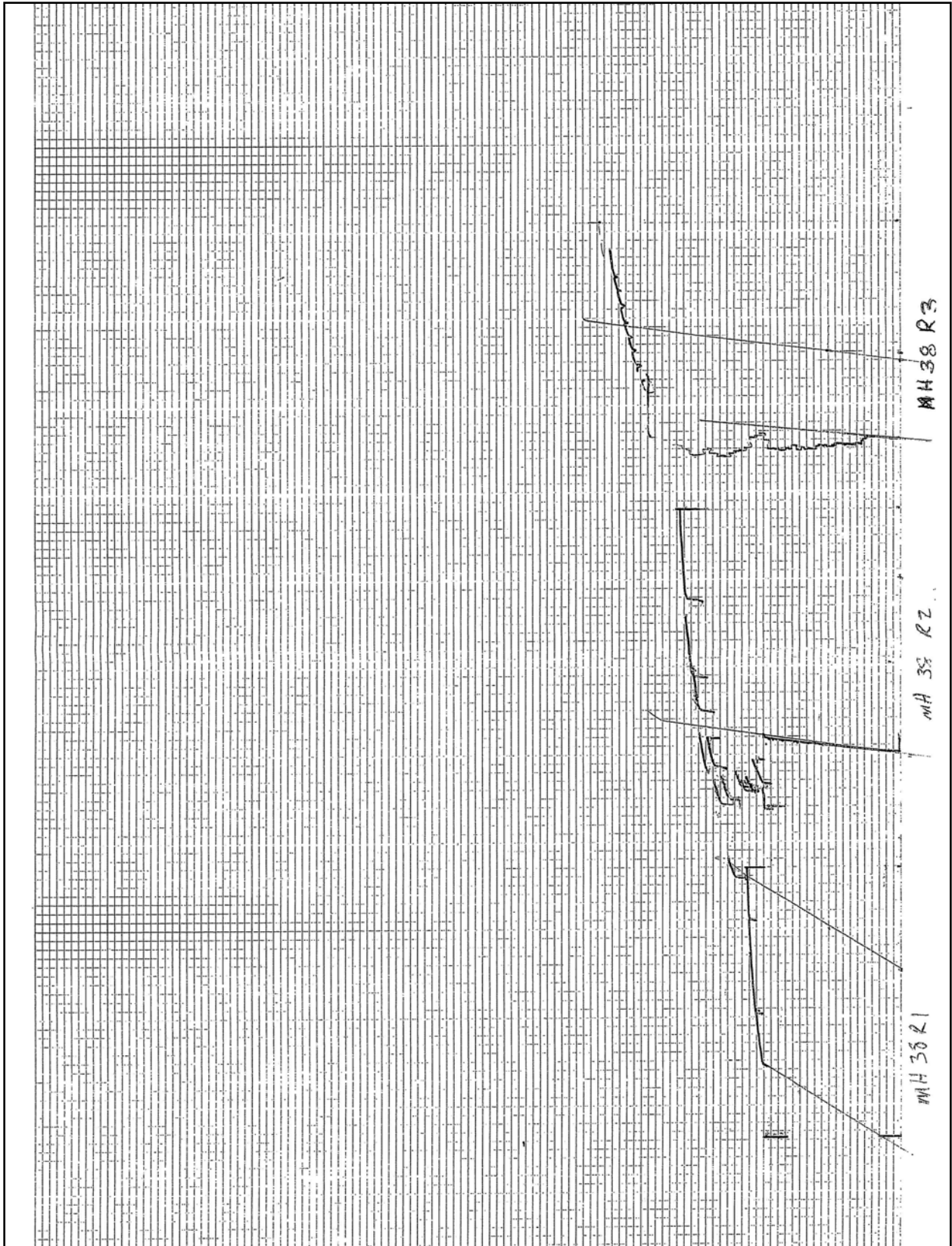
G:\WORDDATA\MSFORMS\TT505.LAB

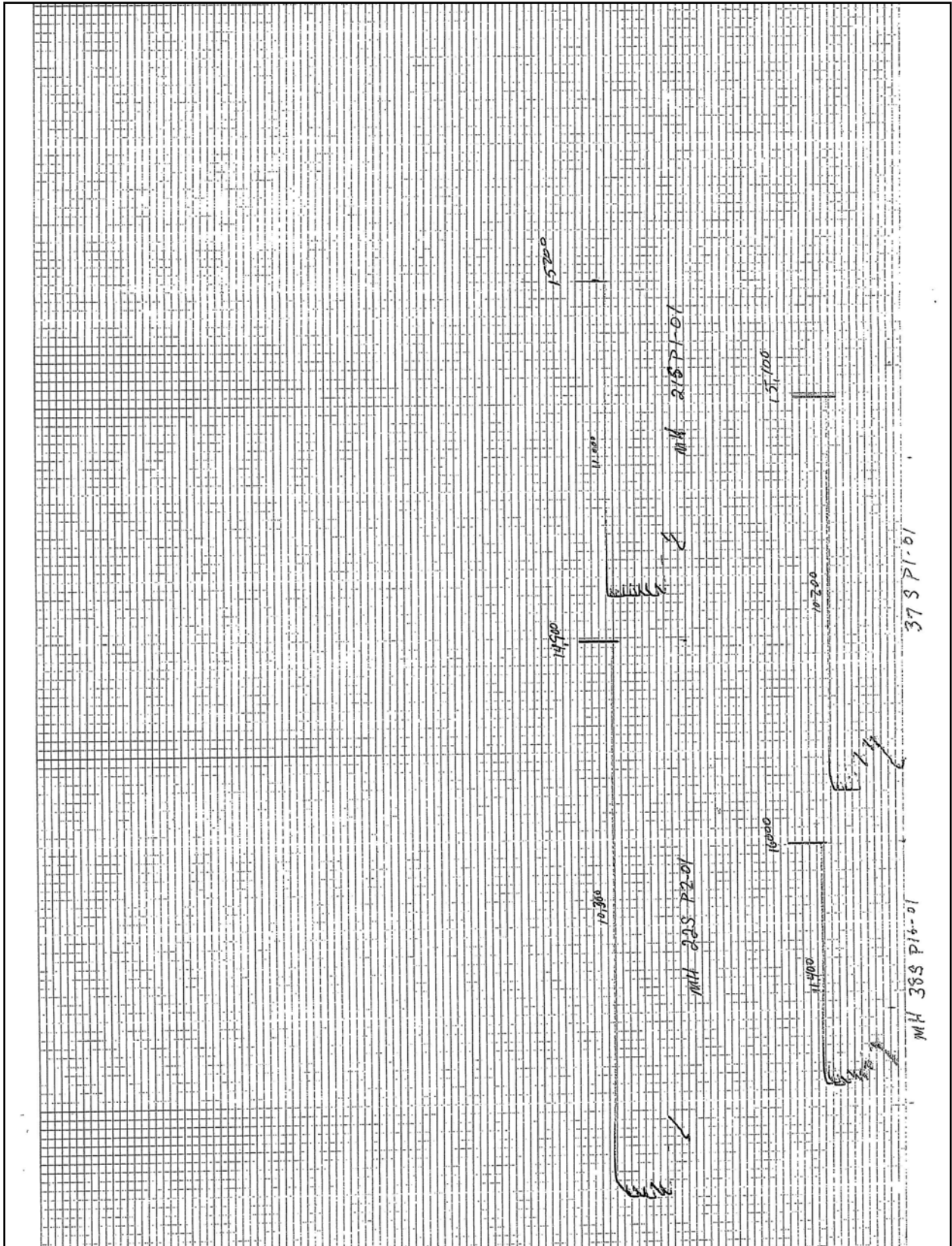
P. 1

5043661688

David Mandina







**American Association of State Highway and Transportation Officials
AASHTO Accreditation Program - Certificate of Accreditation**

This is to signify that

Beta Testing & Inspection, LLC

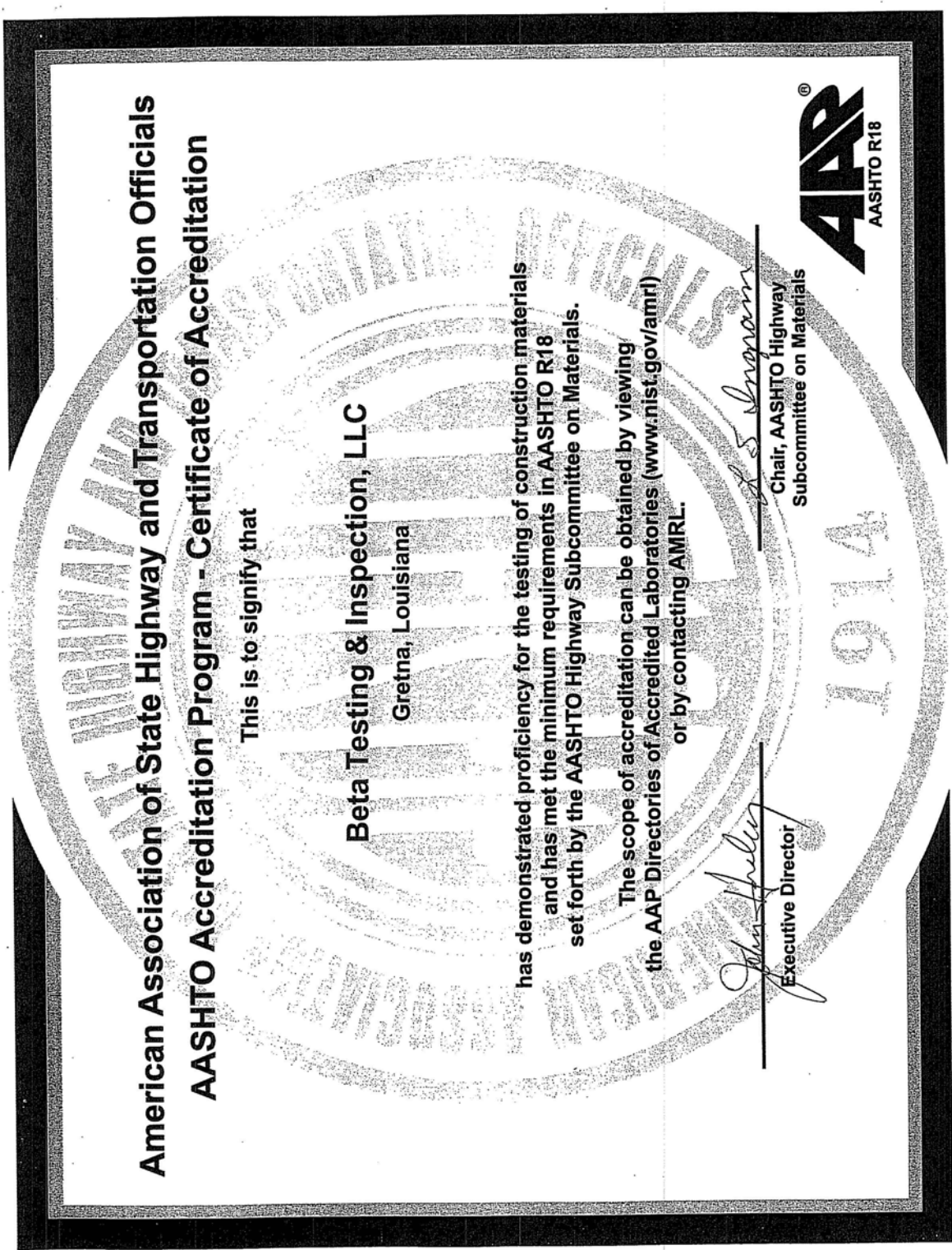
Gretna, Louisiana

has demonstrated proficiency for the testing of construction materials and has met the minimum requirements in AASHTO R18 set forth by the AASHTO Highway Subcommittee on Materials.

The scope of accreditation can be obtained by viewing the AAP Directories of Accredited Laboratories (www.nist.gov/amrl) or by contacting AMRL.


Executive Director


Chair, AASHTO Highway
Subcommittee on Materials





DEPARTMENT OF THE ARMY
ENGINEER RESEARCH AND DEVELOPMENT CENTER, CORPS OF ENGINEERS
GEOTECHNICAL AND STRUCTURES LABORATORY
WATERWAYS EXPERIMENT STATION, 3909 HALLS FERRY ROAD
VICKSBURG, MISSISSIPPI 39180-6199

REPLY TO
ATTENTION OF:

CEERD-GS-E (1110-1-8000c)

22 Aug 05

Memorandum For Commander, USAE District, New Orleans, ATTN: CEMVN-CD-QS/Mr. Geoff Laird,
PO Box 60267, New Orleans, LA 70160-0267

SUBJECT: Validation of Beta Testing and Inspection, LLC, Gretna, LA

1. In reference to Military Interdepartmental Purchase Request No. W42HEM51322885, dated 13 May 05, an inspection of the materials testing laboratory of Beta Testing and Inspection, Gretna, LA was performed on 13 Jun 05. The results of that inspection were reported to the Commander, USAE District, New Orleans on 20 Jun 05. The laboratory reported their deficiency corrections to the Materials Testing Center (MTC) on 19 Jul and 09 Aug 05. These corrections were compared to the ASTM Standards for compliance and were found to be satisfactory. We also examined AMRL Inspection Report No. 994F, Dated 01 Jul 04, CCRL Inspection Report No. J-71, dated 18 Aug 04, and the AASHTO Accredited Laboratory List dated 18 Aug 05.

2. The Quality System of the laboratory is satisfactory and we are granting a validation of the lab to perform material tests for the U.S. Army Corps of Engineers. The material test methods that the laboratory is validated to perform are:

a. **Aggregate Tests:** ASTM C40, C117, C127, C128, C136, C29, C88, C131, C535, C566, C702, D75, and D4791.

b. **Bituminous Tests:** ASTM D2726 and D3666.

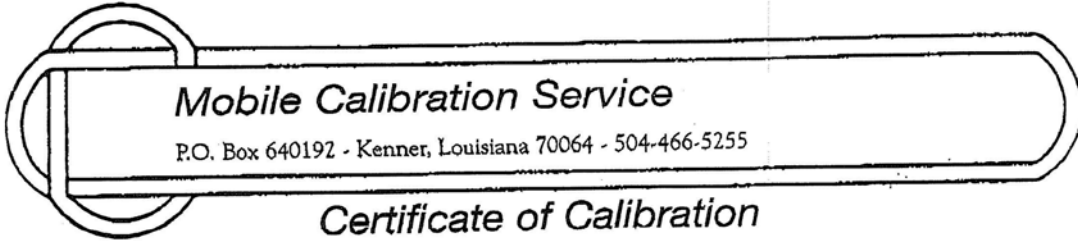
c. **Concrete Tests:** ASTM C31, C39, C138, C143, C172, C173, C231, C1064, C42, C78, C157, C174, C192, C293, C470, C511, C617, C1077, and C1231.

d. **Soil Tests:** ASTM D421, D422, D558, D698, D1140, D1556, D1557, D2168, D2216, D2217, D2487, D2488, D2922, D3017, D3740, and D4318.

3. We will add Beta Testing and Inspection, Gretna, LA to the list of commercial laboratories qualified to conduct material tests for the U.S. Army Corps of Engineers, see the MTC homepage at <http://www.wes.army.mil/SL/MTC/mtc.htm>. All Corps offices will be notified of this decision and will have the opportunity to use their services. The laboratory will remain on our list of laboratories qualified to conduct material tests until **13 Jun 08**, three (3) years from the date of the inspection.

DANIEL A. LEAVELL
Director, Materials Testing Center

CF:
Mr. Mark Cheek / Beta Testing and Inspection, Gretna, LA



Certificate of Calibration

This is to certify that the following described testing machine has been calibrated in accordance with ASTM E4 and found to be within a tolerance of 1%. Method of verification and pertinent data are in accordance with ASTM E-4. The testing device(s) used have been verified per ASTM E 74 and are traceable to the National Institute of Standards & Technology (N.B.S.)

CLIENT: Beta Testing & Inspection Co.
P.O.Box 203
Gretna, Louisiana 70054

DATE: August 1, 2005
Recal: August, 2006
Last Cal: August, 2004

MACHINE IDENTIFICATION: Soiltest Concrete Tester #9003

MACHINE RANGE: 0-250000 Pounds
0-30000 Pounds

CALIBRATED RANGE: 25000-250000 Pounds
3000-30000 Pounds

CALIBRATION APPARATUS
Strainsense Load Cell 860916A
Strainsense Load Cell 880305A

CLASS A RANGE
8400-500000 Pounds
960-12000 Pounds

CALIBRATED TO NIST
8-04
10-04

CALIBRATION RESULTS

| MACHINE READING | ACTUAL LOAD LBS RUN #1 | DIFFERENCE POUNDS | PERCENT ERROR | ACTUAL LOAD LBS | DIFFERENCE POUNDS RUN #2 | PERCENT ERROR |
|----------------------------|---------------------------|-------------------|---------------|-----------------|-----------------------------|---------------|
| LOW PRESSURE GAUGE | | | | | | |
| 3000 | 2985 | 15 | +0.50 | 2990 | 10 | +0.33 |
| 5000 | 4980 | 20 | +0.40 | 4975 | 25 | +0.50 |
| 10000 | 9965 | 35 | +0.35 | 9970 | 30 | +0.30 |
| 15000 | 14955 | 45 | +0.30 | 14945 | 55 | +0.37 |
| 20000 | 19930 | 70 | +0.35 | 19940 | 60 | +0.30 |
| 25000 | 24920 | 80 | +0.32 | 24910 | 90 | +0.36 |
| 30000 | 29880 | 120 | +0.40 | 29900 | 100 | +0.33 |
| HIGH PRESSURE GAUGE | | | | | | |
| 25000 | 25100 | 100 | -0.40 | 25050 | 50 | -0.20 |
| 50000 | 50150 | 150 | -0.30 | 50200 | 200 | -0.40 |
| 75000 | 75190 | 190 | -0.26 | 75270 | 270 | -0.36 |
| 100000 | 100230 | 230 | -0.23 | 100280 | 280 | -0.28 |
| 125000 | 125210 | 210 | -0.17 | 125220 | 220 | -0.18 |
| 150000 | 149840 | 160 | +0.11 | 149790 | 210 | +0.14 |
| 175000 | 174610 | 390 | +0.22 | 174670 | 330 | +0.19 |
| 200000 | 199480 | 520 | +0.26 | 199350 | 650 | +0.33 |
| 250000 | 249260 | 740 | +0.30 | 249060 | 940 | +0.38 |

The above are as found readings.

MOBILE CALIBRATION SERVICE

Warren A. Meyn Jr.
Warren A. Meyn Jr.

Certificate of Calibration

and Traceability to the

United States National Institute of Standards & Technology

MODEL: SS504C
STRAINSENSE LOAD CELL, SERIAL NO. 860916A/M-8/96(LO)
50,000 LBF CAPACITY, COMPRESSION
ADMET-DC-16 INDICATOR, SERIAL NO. P16-0008081

The above identified instrument was calibrated in accordance with section 7 of the American Society for Testing and Materials (ASTM) Specification E74-02, entitled "Standard Practice of Calibration of Force-Measuring Instruments...". This calibration is in conformance with the requirements of Morehouse QAM Rev. 7, dated 12/04/00.

Calibration was performed at the following indicator settings:

Load Cell 1
Channel 1

The result of this calibration as determined by statistical analysis according to section 8 of ASTM E74-02, is as follows:

| <u>Uncertainty</u> | <u>Resolution</u> |
|--------------------|-------------------|
| 20.4 Lbf | 12.0 Lbf |

Class A Loading Range according to ASTM E74-02:

8,160.0 Lbf to 50,000 Lbf

Calibration was performed for a temperature of 23 degrees C.

This calibration is certified traceable to the United States National Institute of Standards & Technology according to the following documentation and calibration apparatus used:

Dead Weight Force Machine S/N M-7471 NIST Lab No. 822/268391-03

Uncertainty of Force Standard used did not exceed +/-0.002% of applied load

Calibrated by:

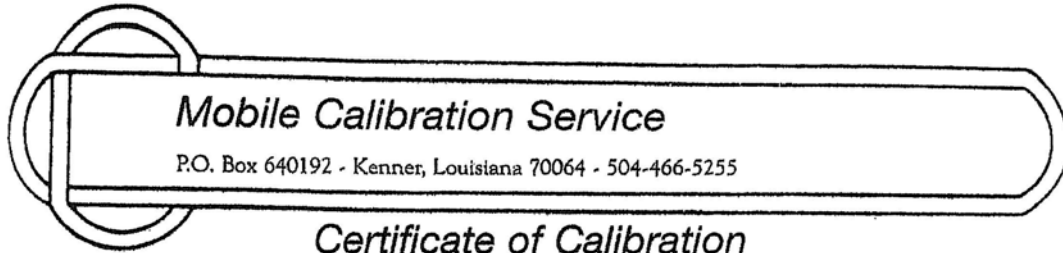


Date Calibrated:
August 18, 2004

Report No:860916A/M-8/96(LO)H1804

MOREHOUSE INSTRUMENT COMPANY, INC.
FORCE CALIBRATION LABORATORY
1742 SIXTH AVENUE
YORK, PA 17403-2675 U.S.A.
PHONE: 717 / 843-0081
FAX: 717 / 846-4193
WEB: www.morehouseinst.com

This Certificate shall not be reproduced except in full, without written approval from Morehouse Instrument Company, Inc.
PAGE 04 12/16/2005 14:48 5044662826 WMEYN MOBILE CAL



Certificate of Calibration

This is to certify that the following described testing machine has been calibrated in accordance with ASTM E4 and found to be within a tolerance of 1%. Method of verification and pertinent data are in accordance with ASTM E-4. The testing device(s) used have been verified per ASTM E 74 and are traceable to the National Institute of Standards & Technology (N.B.S.)

CLIENT: Mandina Inspection Service
 3861 Peters Road
 Harvey, La.

DATE: June 9, 2005

MACHINE IDENTIFICATION: Tinius Olsen Universal Testing Machine

MACHINE RANGE: 0-120000 Pounds

CALIBRATED RANGE: 10000-120000 Pounds

CALIBRATION APPARATUS

Strainsense Load Cell 050106
 Morehouse Ring 5-4537

CLASS A RANGE

5000-50000 Pounds
 25000-250000 Pounds

CALIBRATED TO NIST

1-05
 5-04

| CALIBRATION RESULTS | | | | | | |
|---------------------|-----------------|-------------------|---------------|-----------------|-------------------|---------------|
| MACHINE READING | ACTUAL LOAD LBS | DIFFERENCE POUNDS | PERCENT ERROR | ACTUAL LOAD LBS | DIFFERENCE POUNDS | PERCENT ERROR |
| | RUN #1 | | | RUN #2 | | |
| 10000 | 10030 | 30 | -0.30 | 10025 | 25 | -0.25 |
| 20000 | 20060 | 60 | -0.30 | 20050 | 50 | -0.25 |
| 40000 | 40100 | 100 | -0.25 | 40060 | 60 | -0.15 |
| 60000 | 60120 | 120 | -0.20 | 60150 | 150 | -0.25 |
| 80000 | 80190 | 190 | -0.24 | 80160 | 160 | -0.20 |
| 100000 | 100290 | 290 | -0.29 | 100220 | 220 | -0.22 |
| 120000 | 120330 | 330 | -0.28 | 120290 | 290 | -0.24 |

The above are as found readings. No calibration adjustments required.

MOBILE CALIBRATION SERVICE


 Kevin Wehr
 TECHNICIAN



**OLSON
ENGINEERING, Inc.**

SPECIALIZING IN CONDITION EVALUATION OF THE
CIVIL STRUCTURE & INFRASTRUCTURE



www.olsonengineering.com

January 6, 2006

U. S. Army Corps of Engineers
Engineering Research and Development Center
3909 Halls Ferry Rd.
Vicksburg, MS. 39180

Attn: Mr. Richard W. Haskins, ERDC-ITL-MS
Ofc: (601)634-2931
Fax: (601)634-2873
E-Mail: Richard.W.Haskins@erdc.usace.army.mil

Re: Nondestructive Testing Investigation Report No. 2
Parallel Seismic Re-Testing Results for Sheet Pile Lengths
New Orleans 17th Street and IHNC Levees
New Orleans, LA
Olson Engineering Job No. 1875C

Dear Sirs,

We are pleased to report herein the results of re-testing with the Parallel Seismic method of one sheet pile location at each of the 17th Street and Inner Harbor Navigational Canal (IHNC) levees. This additional work was conducted as a result of the initial incorrect prediction of sheet pile lengths at the North and South ends of the break at the 17th Street Levee (report dated December 5, 2005, Olson Job No. 1875). Actual sheet pile lengths were revealed to be about 23.5 ft in USACE excavations of sheet piles conducted on December 13, 2005 (the sheet piles were incorrectly predicted to be about 7 ft shorter in our initial report).

Discussion of Initial Sheet Pile Depth Predictions

When we learned that the USACE removal of sheet piles at the North and South ends of the 17th Street Levee breach for revealed actual total sheet pile lengths of about 23.5 ft, we immediately reviewed the PS data for ground-truthing purposes to examine the data and see if there was an indication of the actual sheet pile tips in the data or not. Our review of the data found that there was evidence of possible weaker diffraction events in the bottom 3 ft or so of the initial PS data that corresponded to the actual sheet pile tip depths.

As discussed in our draft report addendum letter of December 13th, 2005 which was



transmitted to the USACE at that time, we attribute our mis-interpretation of the data to the following three factors:

1. the PS data sets contained misleading apparent ground/tube vibrations that showed apparent slower velocity and weaker signals at the incorrectly predicted 7ft short sheet pile depths. This energy is now attributed to strong energy emitting from the concrete walls in to the ground due to the horizontal impacts to the concrete walls just below the chamfers;
2. the different shape of the now apparent sheet pile diffraction events due to the spreading out of energy for the wall-shaped steel sheet piles versus our experience with previous arrowhead diffraction events measured for rod-shaped steel H-piles in research and consulting by our firm; and,
3. the single biggest problem that led to the misinterpretation of the initial data was the lack of data available to clearly identify the weak diffraction of wave energy emitting from the pile tips. This was due to the fact that the borehole casings only extended a few feet beyond the actual pile tip depths. The desired typical cased borehole depth would extend 10-15 ft beyond the suspected/hoped for maximum sheet pile depths and this was recommended in our proposal of October 22, 2005 (Olson Proposal No. 2005169.1) for the project.

Borings were also recommended to be drilled as close as practical to the foundation to be tested preferably within 3-5 ft or less horizontally of the foundation, but generally no more than 10 ft away from a foundation to be tested with the PS method. We understand that the USACE borings were initially drilled in to the levees for geotechnical sampling purposes only and that PS testing was decided upon after the borings were drilled. The 4 inch diameter PVC casings that were subsequently grouted in-place in the boreholes for the PS tests were shorter than the drilled boreholes and extended only to depths of 25 ft below the levee ground surface. Such borehole casing depths would have been deep enough for successful PS tests if the sheet piles were around 16 ft in length, but the 25 ft long casings resulted in there only being about 3 feet of casing at or below the 23.5 ft long sheet pile tips. Thus there were only 3-4 PS test records from which hydrophone PS data could be obtained at or below the pile tips. As discussed above and in the report addendum, we feel that the limited PS data from below the sheet pile tips contributed significantly to our incorrect interpretation of the weak diffraction events.

A conference call about the PS results and our draft report addendum was held with Messrs. Richard Haskins and Paul Mlakar of the USACE and Larry Olson and Dennis Sack of Olson Engineering, Inc. on December 16th. As requested by Mr. Mlakar at that time, we have updated the draft addendum letter to include not only a review of the data from the PS tests at the 17th Street Levee, but also the PS data from the London Avenue and IHNC levees that was also presented in our initial report. The final report addendum is being provided as a separate letter.

Parallel Seismic Re-Test Field Investigation Overview

We were quite concerned about the initial incorrect sheet pile length predictions and this led to our decision to gather more data on the weak diffraction events that were apparently indicative of the actual sheet pile tips for the two USACE cased boreholes at the 17th Street Levee North and South breach ends. Consequently, we decided to conduct additional PS tests at the South End of the breach at Station 20+78 which was only about 7 ft from the USACE PS boring in this area. The testing was also at the South End of the 17th Street levee breach immediately adjacent to the area where the USACE excavated sheet piles and found their total lengths to be nominally 23.5 ft on December 13, 2005. We also conducted tests at the IHNC levee adjacent to the North end of the south breach at Station 17+11 within about 10 ft north of where a cased borehole PS test had been done earlier.

This additional nondestructive investigation was conducted at no cost by Olson Engineering to the USACE with the field support of Southern Earth Sciences, Inc. (SESI) of Baton Rouge, Louisiana who also provided their services at no cost. SESI had used their Seismic Cone Penetrometer (SCPT) Geoprobe rig with a biaxial geophone to investigate sheet pile tests in PS/SCPT tests of the 17th Street and London Avenue Levees for the state of Louisiana levee investigation team and their field tests were conducted after our initial field PS tests. A photograph of the Geoprobe rig is shown in Photo 1 and the SCPT tool is shown in Photo 2.



Photo 1 - Geoprobe Rig for PS/SCPT testing at South End of Breach of 17th Street Levee at Station 17+78 where sheet piles were exposed by USACE PS Cased Borehole (white PVC cap visible)



Photo 2 - Seismic Cone Penetrometer Tool with Bearing pressure at tip followed by pore pressure ring followed by skin friction sleeve followed by bi-axial horizontal geophones

The initial SESI PS/SCPT tests were able to be conducted to greater depths and much closer horizontally (typically within 3 ft of the concrete walls) without drilling borings. As discussed with USACE, we also provided consulting services to SESI in the analysis of their initial PS/SCPT results. Analyses of their initial bi-axial geophone results showed similar sheet pile depths to our initial hydrophone PS results with their findings presented in the SESI report to the State of Louisiana.

In our joint efforts with SESI at the IHNC and 17th Street Levees on December 21 and 22, 2005, respectively, SESI conducted PS/SCPT tests with their bi-axial (two perpendicular, horizontal geophones) seismic cone penetrometer tool (Photo 2). For our comparison PS testing with a small diameter hydrophone receiver, they pushed a non-retrievable dummy tip into the levee soils. Next, SESI installed a temporary 1 inch PVC casing inside the Geoprobe hollow steel push rods which were then retrieved to leave the PVC casing in the ground. Then the hole annulus and inside of the PVC casing were filled with water so we could conduct hydrophone-based Parallel Seismic (PS) tests.

The joint effort with SESI allowed for a comparison of the data obtained from the two different types of PS test transducers, ie., the more omni-directional hydrophone receiver vs. the bi-axial horizontal geophones. In our National Cooperative Highway Research Program 21-5 and 21-5(2) research projects for Determination of Unknown Bridge Foundation Depths for scour safety studies, we compared hydrophones and tri-axial geophones in Parallels Seismic tests. Generally, the hydrophone was found to be the more sensitive receiver to the arrival of initial weak direct energy in PS tests of bridge foundations, particularly for diffraction events due to its more all-around or "omni-directional" response to wave energy emitting from the impacted bridge substructure foundation system.

Parallel Seismic Re-Test Results

The joint Olson/SESI PS re-test program was planned to evaluate both bi-axial geophones (results to be reported by SESI) and hydrophone receivers and investigate PS data results quality for impacts applied directly to sheet piles, and from horizontal to vertical impacts to the concrete walls in which the levee sheet piles are embedded. The PS re-test results of the 17th Street re-tests are presented first below followed by the IHNC results. The field effort was also made possible by USACE personnel and their subcontractors who also contributed significantly to the re-test program and assisted in the field by providing site access, excavation assistance to expose sheet piles, and testing assistance. The State of Louisiana levee investigation team also contributed their input to the re-test program and observed the field PS re-test effort as well.

17th Street PS Re-Test Results at South End of Breach - Station 20+78

Based on the stickup of the sheet piles of about 1.25 ft above the levee ground surface, the 23.5 ft long sheet piles extend to about 22.25 ft below existing grade at the south end of the 17th Street levee breach at Station 20 +78 where the 1 inch PVC casing was installed to about 30

ft deep by SESI at about 2.5 ft from the wall edge on the protected side. The locations of the impacts with a 3-lb impulse hammer with a black hard plastic tip to the sheet pile and concrete levee wall at various positions are shown in Photos 3-7 and the PVC casing is shown in Photo 8.



Photo 3 (Fig. 1) - Horizontal impact to sheet pile at 0.5 ft below concrete wall - protected levee side



Photo 4 (Fig. 2) - Horizontal impact to side of concrete wall at el. 5 about 0.5 ft below chamfer



Photo 5 (Fig. 3) - Angled downward impact to chamfer of wall at ~ el. 5.75



Photo 6 (Fig. 4) - Vertical downward impact to top of wall



Photo 7 (Fig. 5) - Angled impact to 1 inch diameter, 6 ft long steel rod held at an angle on sheet pile side at 0.5 ft below concrete - protected levee side

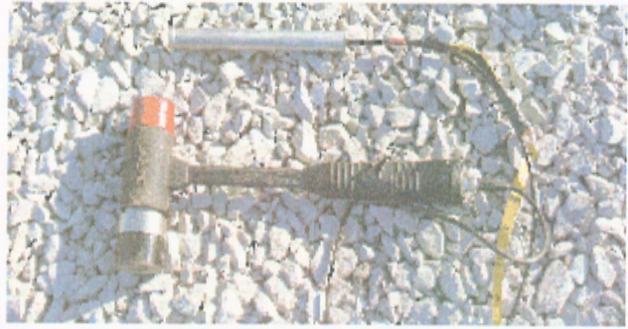


Photo 8 - 3-lb Impulse Hammer with black hard plastic tip and small diameter hydrophone used in PS re-tests

The PS re-test results for the impact positions shown in Photos 3-7 are respectively presented in Figures 1-5 below. The expected diffraction event should occur at a depth of about 22.25 ft from the sheet pile tip in these hydrophone-based PS results. Review of the figures shows that the weak diffraction events are now clearly evident for all of the impact locations. This is due to the increase in PS test depth 30 ft for the 1 inch diameter casing installed by the geoprobe vs. the initial grouted casing depth of only 25 ft.

The PS data presented in Figures 1-5 were produced by 5 impacts which were averaged at each 1 ft test depth interval, filtered and normalized to the largest signal strength (global maximum display) to optimize the display of the diffraction events. Review of Figure 1 shows the diffraction event at 23.0 ft deep due to direct horizontal sheet pile impacts. There is also some energy occurring in advance of the diffraction event at shallower depths. In Figure 2 the horizontal impacts to the concrete wall also show a diffraction event at 22.7 ft deep, but a little less clear with more energy emitting from the concrete wall. By comparison, the diffraction event is clear at 21.8 ft deep for the angled downward impact to the chamfer in Figure 3. Apparently the more vertical impact to the chamfer put more energy down the sheet pile with less energy emitting from the wall. In Figure 4, the impacts to the top of the wall were further away from the ground and the sheet pile, so the diffraction event is quite clear at 21.5 ft. The impacts to the angled steel rod also produced a diffraction event at 22.6 ft as shown in Figure 5, but it was comparatively weaker, likelier due to less energy being imparted by the rod impacts.

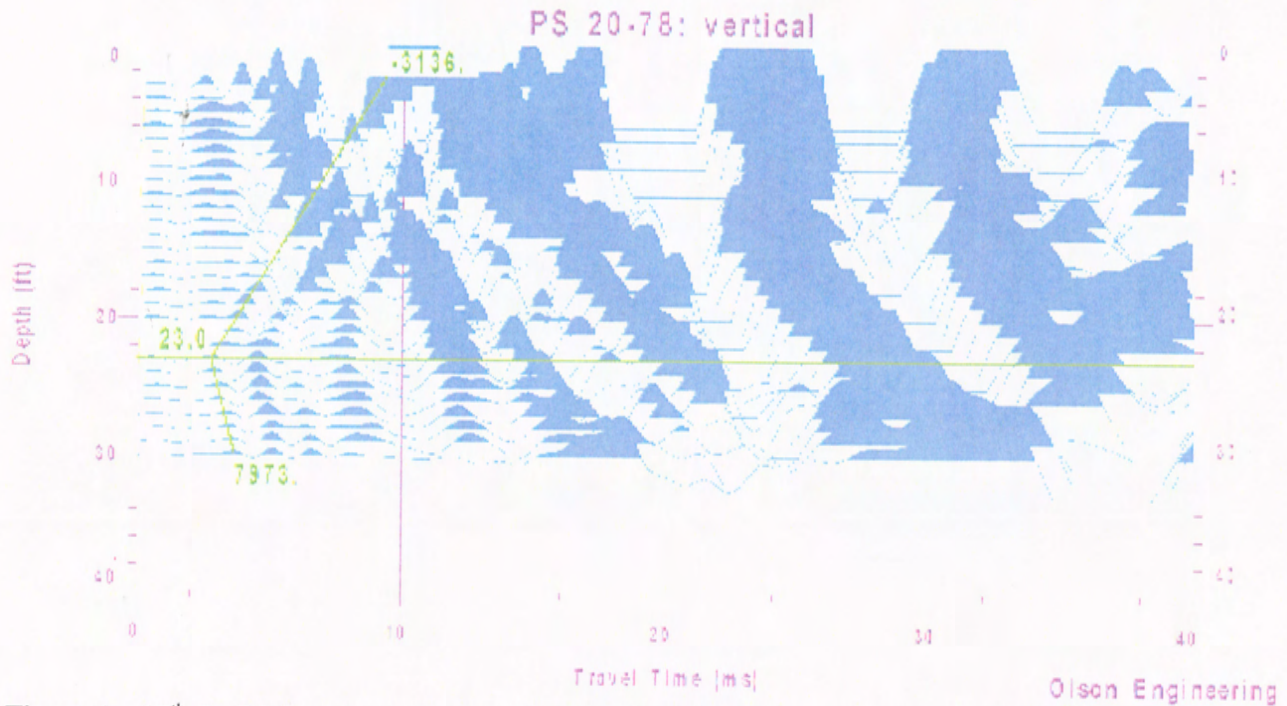


Figure 1 - 17th St. PS Results at Station 20+78 - Sheet Pile impacted at ~ el. 1.5 (0.5 ft below bottom of levee concrete wall on protected side)

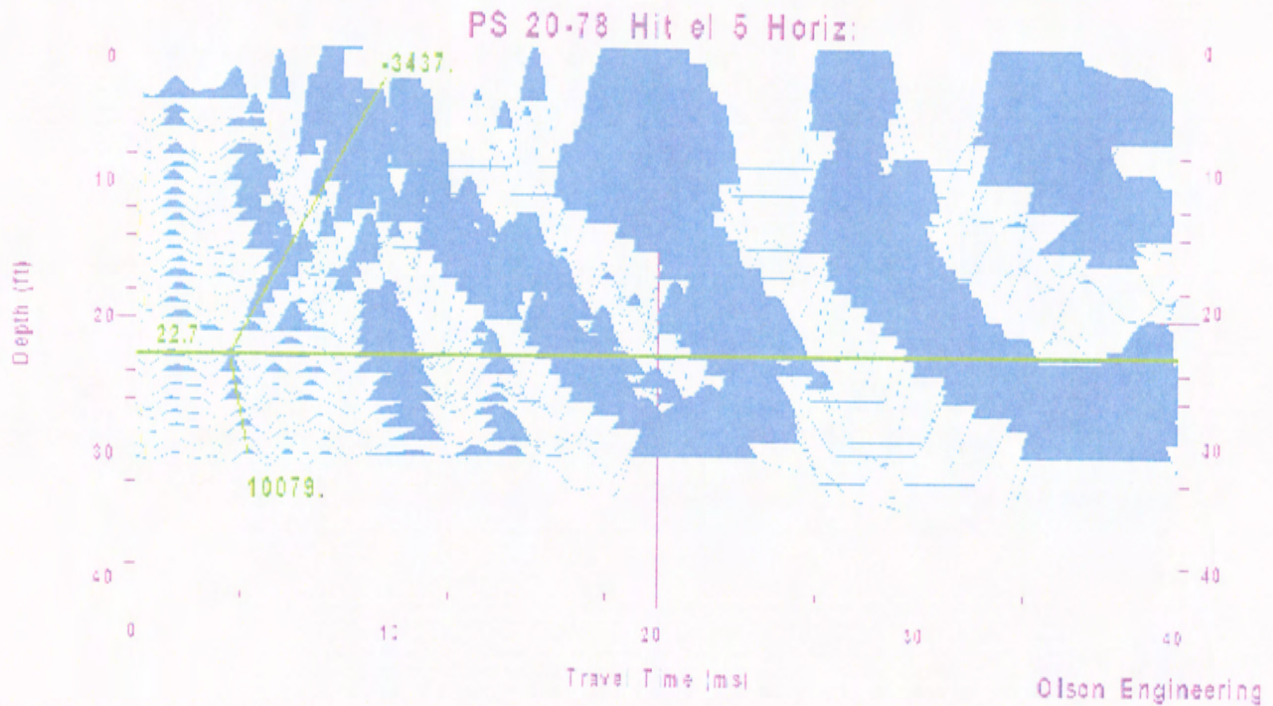


Figure 2 - 17th St. PS Results at Station 20+78 - Concrete Wall impacted horizontally at ~ el. 5 (~0.5 ft below chamfer edge on protected side)

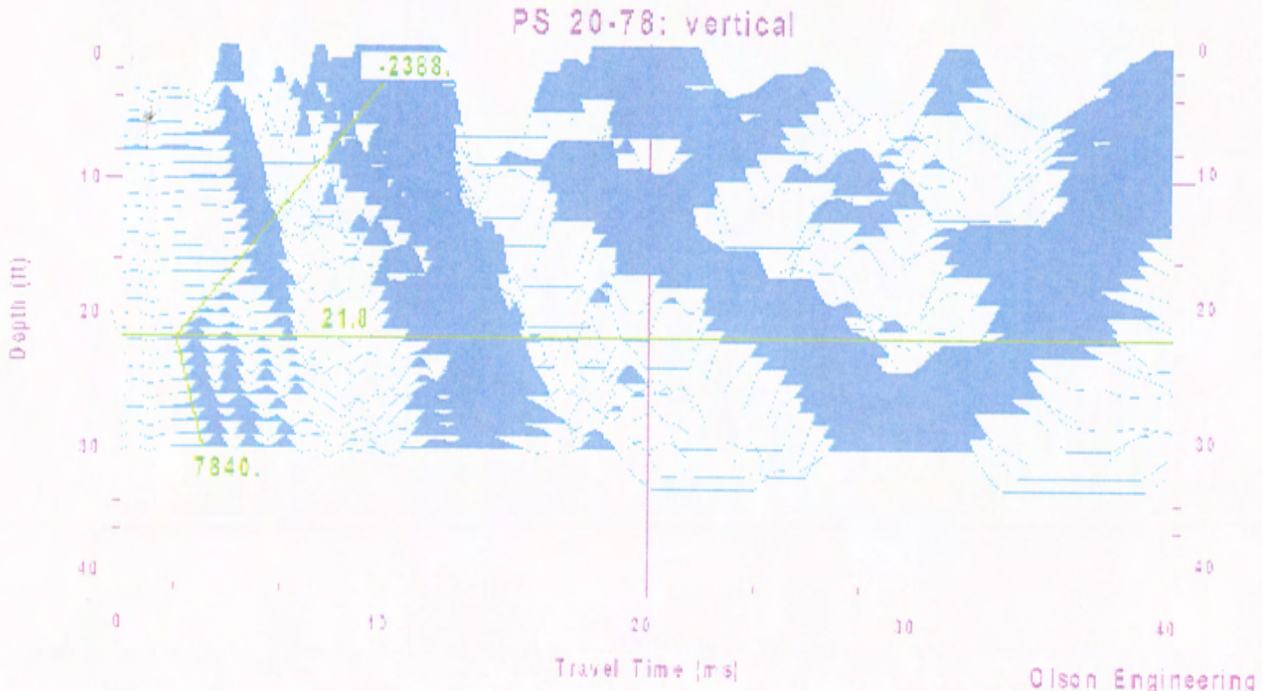


Figure 3 - 17th St. PS Results at Sta. 20+78 - Angled Impacts to Chamfer of Concrete Wall at Sta. 20+78 (~el. 5.75 on protected side)

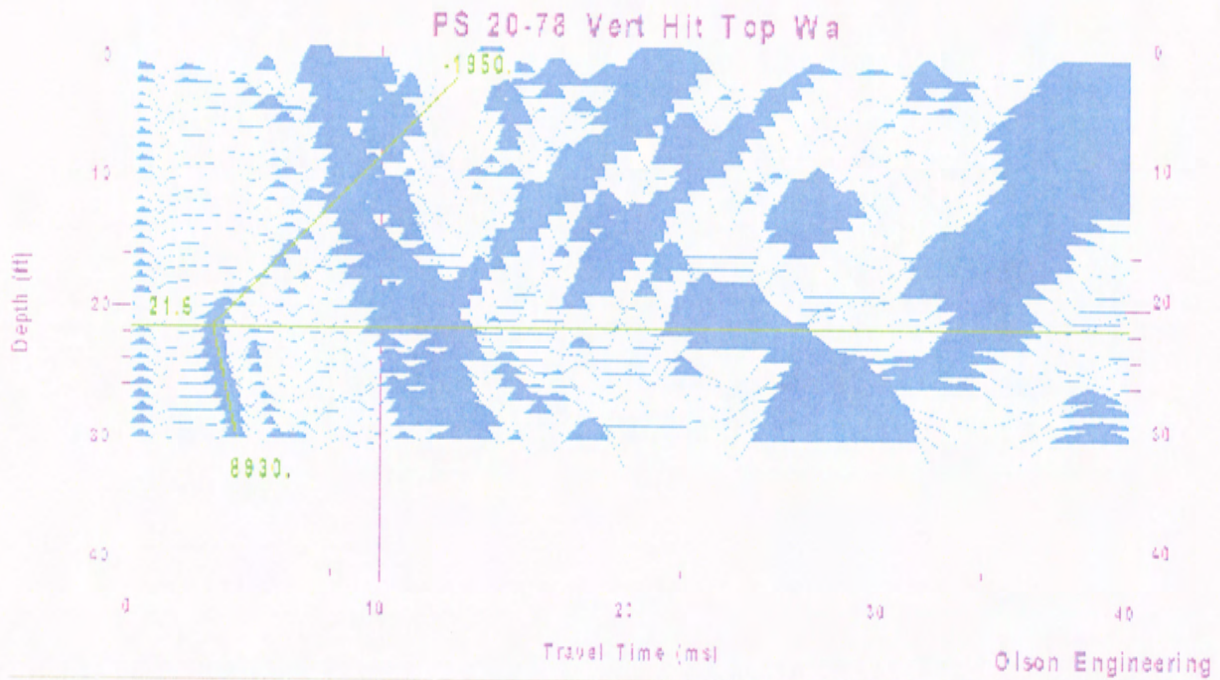


Figure 4 - 17th St. PS Results at Sta. 20+78 - Vertical Impacts to Top of Concrete Wall at Sta. 20+78

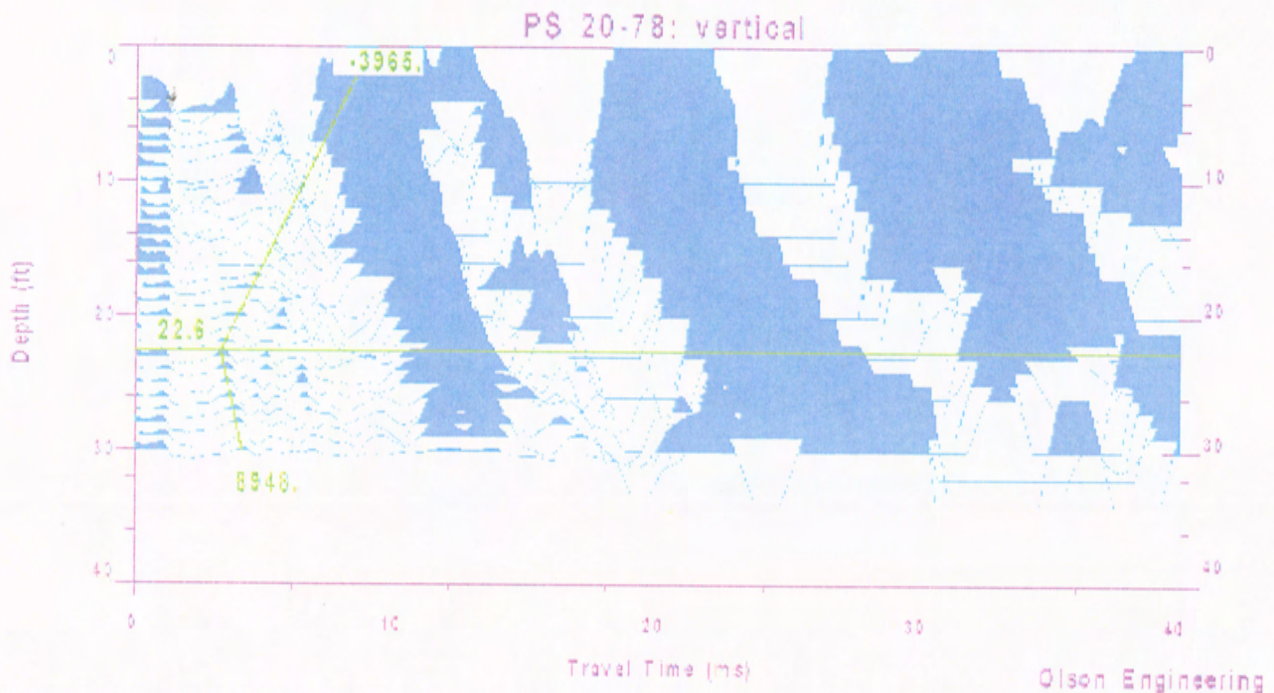


Figure 5 - 17th St. PS Results at Sta. 20+78 - Angled Impacts to 1 inch diameter, 6 ft long rod held against steel sheet pile at ~ el. 1.5 at 0.5 ft below concrete wall

IHNC PS Re-test Results at North End of South Breach - Station 17+11

The IHNC re-tests were performed in an area of the wall that had been pushed back and the levee soils dropped down to expose a sheet pile on the canal side at Station 17+11 which was about 10 ft north of the USACE cased boring in this area. Shovels were used to expose enough of the sheet pile to impact it with the 3 lb impulse hammer as shown in Photo 9. The PS tests were done using a hydrophone in the 1 inch PVC casing installed by SESI with the Geoprobe rig as shown in Photo 10.



Photo 9 - IHNC 3-lb Impulse hammer impacts to sheet pile on canal side at Station 17+11



Photo 10 - Small Hydrophone receiver on tape in 1 inch PVC casing installed by Geoprobe Rig at IHNC

Sonic Echo testing was conducted from end to end of a nearby exposed sheet pile and a compression wave velocity of about 17,000 ft/second was measured which is essentially the theoretical velocity of a steel rod of 16,600 ft/s. The Sonic Echo results did show a single clear echo from the pile tip in air, but not the multiple echoes normally measured on H-piles in air. Impulse Response analyses in the frequency did not show clear resonant echo peaks from the exposed pile tip. This is due to the spreading out of the energy in to the rest of the interlocked sheet pile wall and the lack of a resonant, rod-like shape for a sheet pile wall. When similar Sonic Echo/Impulse response tests were attempted from the exposed top of an embedded 23.5 ft long sheet pile at the South end of the 17th Street breach, no echo from the pile tip was apparent. This result was expected as the attenuation of the compression wave energy is high due to the large surface area of a steel sheet pile.

The exposed sheet pile at the north end of the south IHNC breach showed a total length of 19 ft - 6.5 inches. Of this, about 4 ft - 7 inches of the piles had been embedded in the 8 ft tall concrete wall. Thus, about 15 ft of the sheet piles are typically embedded in the levee soils. Given the 1 ft higher elevation of the top of the PVC casing on the levee soils versus the bottom of the concrete wall, the sheet pile tip is expected to be at a depth of about 16 ft in the PS hydrophone signal versus depth results which are presented below in Figures 6-8. Horizontal impacts were applied just below the concrete wall to the canal side of the exposed sheet pile (Fig. 6) and to the concrete wall at 6.5 ft below the top of the wall (Fig. 7) which was 1.5 ft above the bottom of the concrete wall while vertical impacts were applied to the top of the wall (Fig. 8).

Review of Figure 6 for the case of direct horizontal impacts to the sheet pile shows a weak direct arrival wave front that is slower below the 16 ft depth of the sheet pile. However, no diffraction events are evident in this PS-based hydrophone test data. This may be due to the evident separation of the levee soil from the canal side of the wall due to the wall being pushed back by the breach forces. This apparent lack of tight contact between the sheet pile and the levee soils may have resulted in the diffraction event energy not being well coupled into the surrounding saturated soils.

Review of Figures 7 and 8 for horizontal and vertical impacts to the concrete wall does not show clear direct arrivals when the apparent weak energy was picked as shown in the figures. No diffraction events are clearly evident in the figures either. These results further support the possibility that there is poor soil contact to the sheet pile on the canal side that diminished the diffraction effect in the IHNC re-tests.

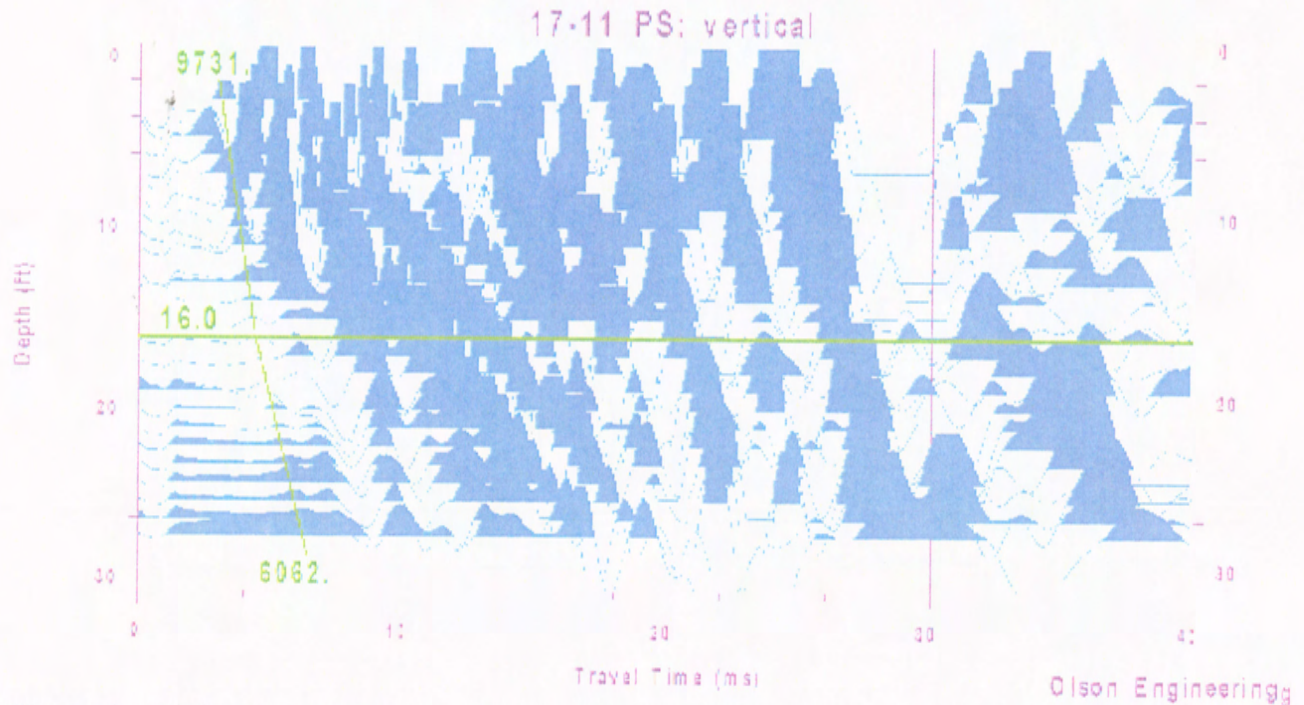


Figure 6 - PS Results at IHNC Sta. 17+11 - Impact to Sheet Pile at ~ 0.5 ft below bottom of Concrete Wall on Canal Side

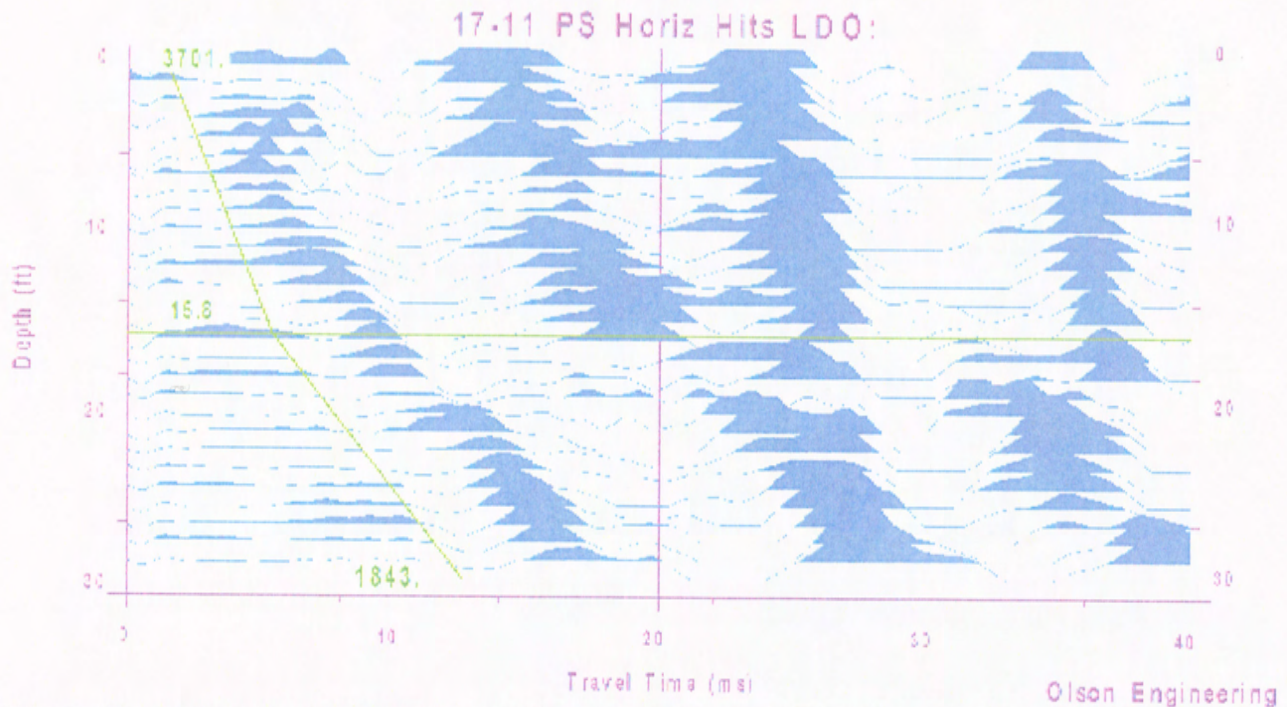


Figure 7 - PS Results at IHNC Sta. 17+11 - Horizontal Impact to Concrete Wall at ~ 6.5 ft below top of Wall on Canal Side

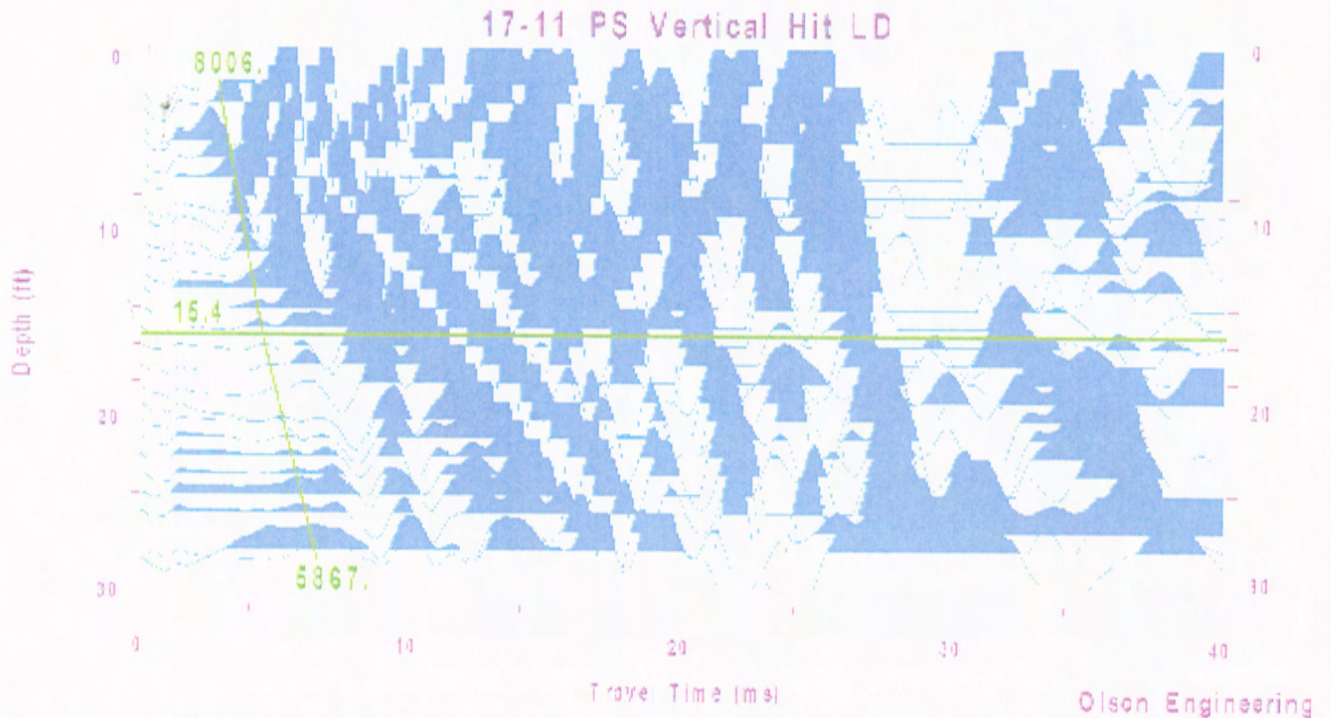


Figure 8 - PS Results for IHNC at Sta. 17+11 for Vertical Impacts to top of 8 ft tall Concrete Wall

Summary of Conclusions and Findings

17th Street Parallel Seismic (PS) Re-Test Results at Station 20+78. The hydrophone-based PS re-test results at the South End of the 17th Street breach clearly identified the pile tips within about 1 ft of the actual sheet pile depth of ~22.25 ft based on clear diffraction events at the sheet pile tip for impacts to the pile side, wall side, chamfer, wall top and even a rod held against the pile side. The results were clearest for the vertical hits on top of the wall, chamfer impacts and direct sheet pile impacts.

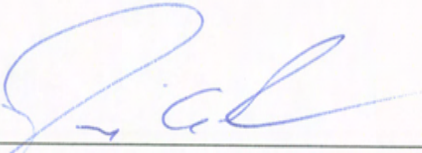
IHNC PS Re-Test Results at Station 17+11. The hydrophone-based PS re-test results at the North End of the south IHNC breach showed a weak direct arrival for impacts directly to the sheet pile that predicted the actual depth of 16 ft. However, only very tentative identifications of such direct arrivals were evident in PS results for either horizontal or vertical impacts to the levee concrete wall. None of the PS results at IHNC showed the clear diffraction arrival events at the pile tip depth found in all of the 17th Street PS re-test results. The lack of the diffraction arrival events may be due to the apparent lack of tight soil contact between the IHNC wall on the canal side as a result of the breach force pushing the wall back. Clear separation of the soil and wall was still evident at the surface in this area. Such lack of contact may have diminished the coupling of energy in to the soils from the diffraction event at the pile tip.

CLOSURE

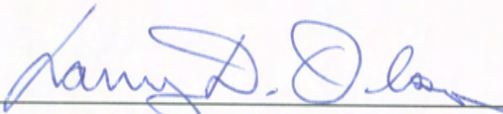
The field NDT investigation was performed in accordance with generally accepted testing procedures. If there are any questions, or further information is required, please do not hesitate to call. If any additional information is developed pertinent to this study, please contact our office.

Respectfully submitted,

OLSON ENGINEERING, INC.



Dennis A. Sack
Associate Engineer



Larry D. Olson, P.E.
Principal Engineer

(1 copy e-mailed and 2 copies mailed)

e-mail cc: Mr. Paul F. Mlakar (Paul.F.Mlakar@erdc.usace.army.mil)



**OLSON
ENGINEERING, Inc.**

**SPECIALIZING IN CONDITION EVALUATION OF THE
CIVIL STRUCTURE & INFRASTRUCTURE**



www.olsonengineering.com

**NONDESTRUCTIVE TESTING INVESTIGATION
SHEET PILE FOUNDATION LENGTHS
NEW ORLEANS LEVEES
NEW ORLEANS, LOUISIANA**

Prepared for:

U. S. Army Corp of Engineers
Engineering Research and Development Center
3909 Halls Ferry Rd.
Vicksburg, MS. 39180

Attn: Mr. Richard W. Haskins, ERDC-ITL-MS
Ofc: (601)634-2931
Fax: (601)634-2873
E-Mail: Richard.W.Haskins@erdc.usace.army.mil

Olson Engineering Job No. 1875

December 5, 2005

This is a preliminary report subject to revision; it does not contain final conclusions of the United States Army Corps of Engineers.

K-226

12401 W. 49th Ave., Wheat Ridge, CO 80033-1927 USA

PHONE: 303.423.1212



FAX: 303.423.6071

TABLE OF CONTENTS

| | |
|---|---|
| 1.0 INVESTIGATION SCOPE AND SUMMARY OF FINDINGS | 1 |
| 2.0 PARALLEL SEISMIC METHOD | 2 |
| 3.0 INVESTIGATION RESULTS AND SUMMARY | 4 |
| 4.0 CLOSURE | 6 |

Table I: Summary of Sheet Pile Tip Depths and Elevations
From Parallel Seismic Testing of New Orleans Levees

Appendix A - Parallel Seismic (PS) Data

1.0 INVESTIGATION SCOPE AND SUMMARY OF FINDINGS

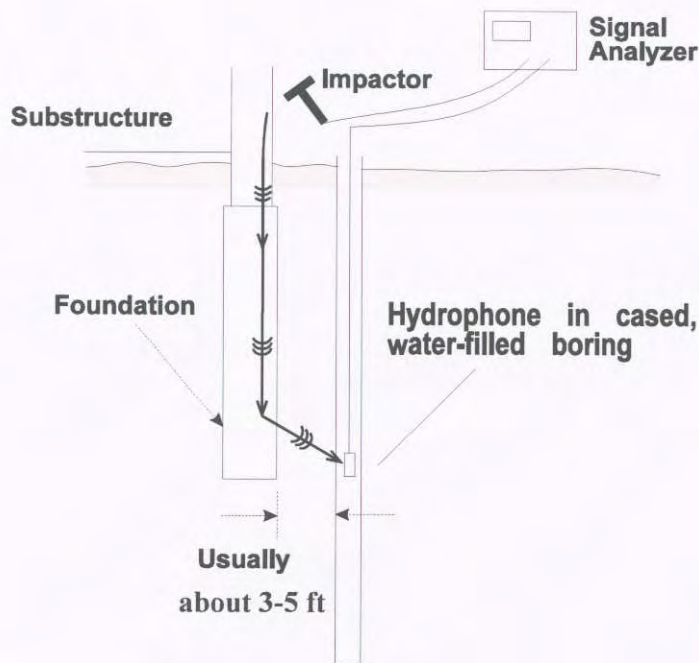
This report presents the Nondestructive Testing (NDT) investigation results for the determination of the unknown lengths of sheet piles below concrete walls of the New Orleans levee system. The levee sheet piles were tested with the Parallel Seismic (PS) method to determine their depths. The PS tests were conducted at the 17th Street, London Avenue, and the Inner Harbor Navigational Canal (IHNC) levees in 8 cased borehole locations at undamaged levee wall locations next to breaches.

The PS results indicate the presence of piles under the concrete wall, and showed that they extended to approximately 13-15 ft below the casing top for all of the sites tested as summarized in Table I. These sheet pile depths translate to elevations of approximately 10 feet below mean sea level (range of 9.3 to 11.8 feet below mean sea level). A discussion of the PS method and the investigation results are presented below.

2.0 PARALLEL SEISMIC METHOD

The Parallel Seismic (PS) method was used to estimate the depth of the foundations. The PS test equipment used in this investigation included a 3-lb instrumented impulse hammer, single hydrophone receiver, and a dynamic signal analyzer (Olson Instruments Freedom Data PC), as illustrated in Fig. 1. When the instrumented hammer directly impacted the supported concrete wall, it (or a nearby accelerometer) triggered the PC-based signal analyzer to capture the time records. A 16-channel National Instruments digital card was used to acquire the data in an Olson Instruments portable Freedom Data PC. Photographs of the field testing are shown in Figure 2.

The PS method involves impacting the exposed portion of the foundation or substructure attached to the foundation or a location which when impacted couples sufficient energy to the pile to generate a sound or stress wave which travels down the foundation. The wave energy is tracked by a hydrophone receiver suspended in a water-filled, cased and sometimes grouted borehole drilled



**Foundation Depth Determination
with the Parallel Seismic Test**
Figure 1 - PS test schematic

typically within 3-5 feet of the foundation edge. Note that for this investigation, the boreholes were found to be located as far as 21.1 feet from the levee wall, resulting in poorer quality data for some tests. The PS tests typically involve lowering the hydrophone(s) to the bottom of the borehole, impacting the exposed portion of the foundation structure and recording the hydrophone(s) responses. Then the hydrophone receiver(s) is raised to the next test elevation. This test sequence is repeated until the top of the casing (or the top of the water level in the casing) is reached. The pile depth is determined by plotting the hydrophone(s) response from all depths on a single display or page. For soils of constant velocity surrounding the piles, a break in the slope of the line occurs below the bottom of the piles indicating the pile depth. For soils with varying velocities, a break often cannot be identified from the slope of the lines, but the bottom of the piles can be identified by observing the traces of the hydrophone plot to identify changes in the response, such as a reduction in signal amplitude, change in signal frequency, or diffraction/reflection of tube wave energy from the foundation bottom.



Figure 2 - Photographs of impacting Wall of IHNC Levee at South Borehole of South Breach and Freedom Data PC at Cased Borehole with Hydrophone Receiver Downhole

3.0 INVESTIGATION RESULTS AND SUMMARY

The investigation was performed on October 27, 2005 and October 28, 2005 using the Parallel Seismic (PS) method by Mr. Larry D. Olson and Ms. Hunter Yarbrough of Olson Engineering, Inc., with assistance from U. S. Army Corps of Engineers personnel Mr. Richard Haskins and Mr. Don Yule. The 3 levee locations tested were at the 17th Street, London Avenue, and Inner Harbor Navigational Channel (IHNC). The PS test site at each test area was designated by the breach location and the position of the borehole. Hammer impacting was done horizontally on the levee wall face and vertically on the wall top where possible. The Parallel Seismic tests were performed with 5 impacts (horizontal and/or vertical) to the concrete walls at each of the hydrophone receiver depth intervals of nominally 1 ft for the entire water-filled length of the boreholes, starting typically 25 ft below the top of the borehole and continuing up to the top of the borehole casing at each site.

The Parallel Seismic tests were performed using a 3-lb hard-plastic tipped instrumented impulse hammer as a source and a single Olson Instruments hydrophone as a receiver. The pile locations were chosen to obtain a length measurement at the locations adjacent to levee breaks which occurred following Hurricane Katrina. Note that the reported data in Appendix A are pile tip depths measured from top of casing and that the PS predicted pile tip depths in true elevation as well as from the bottom wall chamfer can be found in Table I. Review of this table indicates sheet pile depths of 13-15 ft below the tops of the cased boreholes which corresponds to about 10 ft below mean sea level. Given the 1 ft hydrophone receiver measurement depth intervals, the PS results are believed to be accurate to within about 1 ft of the reported depths where data quality is high.

The Parallel Seismic data and results for the 17th Street Site can be found in Figures A-1 and A-2 in the Appendix. The Parallel Seismic data and results for the London Avenue Sites can be found in Figures A-3 to A-5, where Figures A-3 and A-4 are from the North breach and Figure A-5 is from the South breach. The Parallel Seismic data and results for the IHNC can be found in Figures A-6 to A-8, where Figure A-6 is from the breach near Florida Street and Figures A-7 and A-8 are

from the South breach. The exposed parts of all locations consisted of concrete retaining walls which had embedded sheet piles underneath. For the eight tested sites, PS tests were performed to a depth of 25 feet below the top of the grouted, 5 inch PVC casings which were filled with water.

The PS results presented in Appendix A are from typically horizontal hammer hits (data quality was better in one location using a vertical hammer hit as presented in Figure A-3). The horizontal hammer hits were located on the thicker wall sections just below the bottommost chamfer corner and the vertical hammer hits were located on top of the approximately 7 foot concrete retaining wall. The vertical axis in Figures A-1 and A-2 represents depth below casing top, with each waveform at 1 foot intervals starting at 25 feet at the bottom of each casing. The horizontal axis represents acoustic wave travel time in milliseconds (ms).

The generally faster compressional wave velocities of the sheet piles are represented by the shallow, usually more negatively sloped data in the figures at depths near the apparent pile tips. The more gentle, usually less negatively sloped data of the first breaks of the deeper traces represent the slower soil velocities below the pile tips. This is not the case in several of the data sets due to higher soil layer velocities at depth, likely associated with the presence of ground water which results in velocities of about 5,000 ft/second. Where the boreholes could be drilled less than ten feet away from the wall/pile (preferred), such saturated faster soil layers did not have as significant of an impact on data quality.

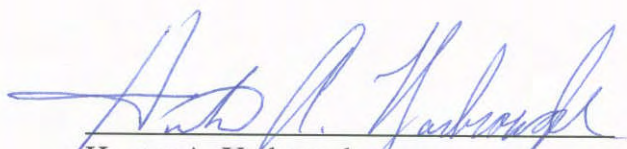
The PS measured pile tip depths for the eight locations indicate that there are piles present underneath the concrete retaining walls. Some of the results are of lower quality data due to a significant distance (17 to 22 ft) between the wall impact points to the boreholes as indicated in Table I. This is evidenced by the relatively weak signals from the piles compared to the signals from the impacted concrete walls on top of the piles, and from the relatively great depth at which the high-velocity pile signals finally start to arrive sooner than the low velocity signals being carried down the water-filled boreholes (tube waves). Accordingly, data quality was rated as high, medium and low (H, M and L) in Table I based on the distance between the wall-borehole and the signal quality.

4.0 CLOSURE

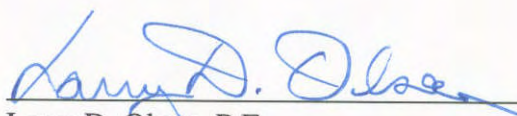
The field NDT investigation was performed in accordance with generally accepted testing procedures. If there are any questions, or further information is required, please do not hesitate to call. If any additional information is developed pertinent to this study, please contact our office.

Respectfully submitted,

OLSON ENGINEERING, INC.



Hunter A. Yarbrough
Geophysical Project Engineer



Larry D. Olson, P.E.
Principal Engineer

(1 copy faxed and 2 copies mailed)

**Table I: Summary of Sheet Pile Tip Depths and Elevations
From Parallel Seismic Testing of New Orleans Levees**

| Levee Site | Sheet Pile Tip Depth From Top of Casing (ft) – (Data Quality) | Sheet Pile Tip Depth From Bottom Concrete Wall Chamfer (ft) | Sheet Pile Tip Elevation (ft above sea level)* | Distance Between Borehole and Levee Wall |
|-------------------------------------|---|---|--|--|
| 17 th Street North End | 14.4 - H | 15.5 | -10.6 | 5.5 ft |
| 17 th Street South End | 14.0 - H | 15.0 | -9.3 | 6.2 ft |
| London Avenue North Break North End | 14.6 - L | 16.1 | -11.2 | 17.8 ft |
| London Avenue North Break South End | 13.1 - M | 14.9 | -9.7 | 7 ft |
| London Avenue South Break | 14.3 - M | 15.3 | -10.6 | 17.2 ft |
| IHNC Florida Street Break | 14.8 - M | 16.5 | -10.3 | 21 ft |
| IHNC South Break North End | 13.7 – H | 16.6 | -10.4 | 9.5 ft |
| IHNC South Break South End | 14.4 – M | 16.1 | -11.8 | 21.1 ft |

H – Indicates areas where the data quality is high and the borehole is positioned within 10 feet of the sheet pile.

M – Indicates areas where the data quality is medium and/or the borehole is positioned greater than 10 feet away from the sheet pile.

L – Indicates areas where the data quality is low and/or the bore hole is positioned greater than 10 feet away from the sheet pile.

* The elevations of the borehole casing tops were provided by the US Army Corps of Engineers and are NAVD 88 Format.

**APPENDIX A
PS DATA AND RESULTS**

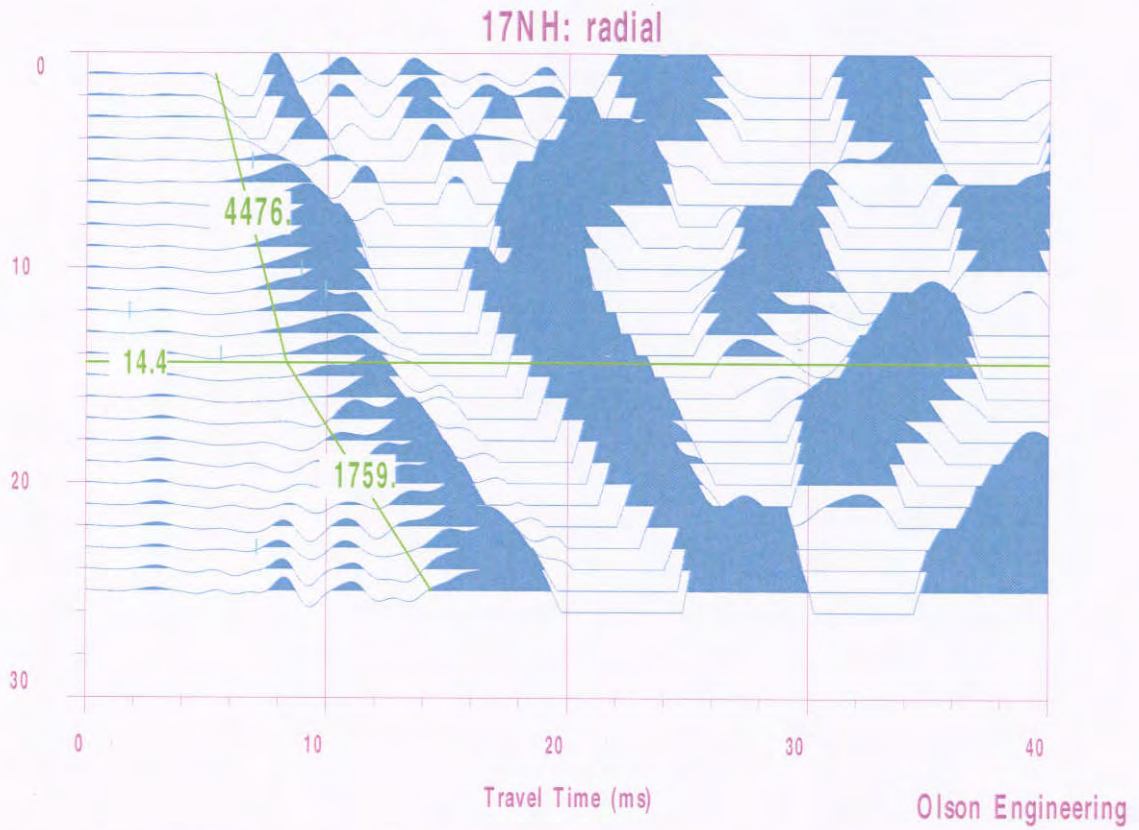


Figure A-1: 17th Street site, North borehole, depth is referenced to top of casing

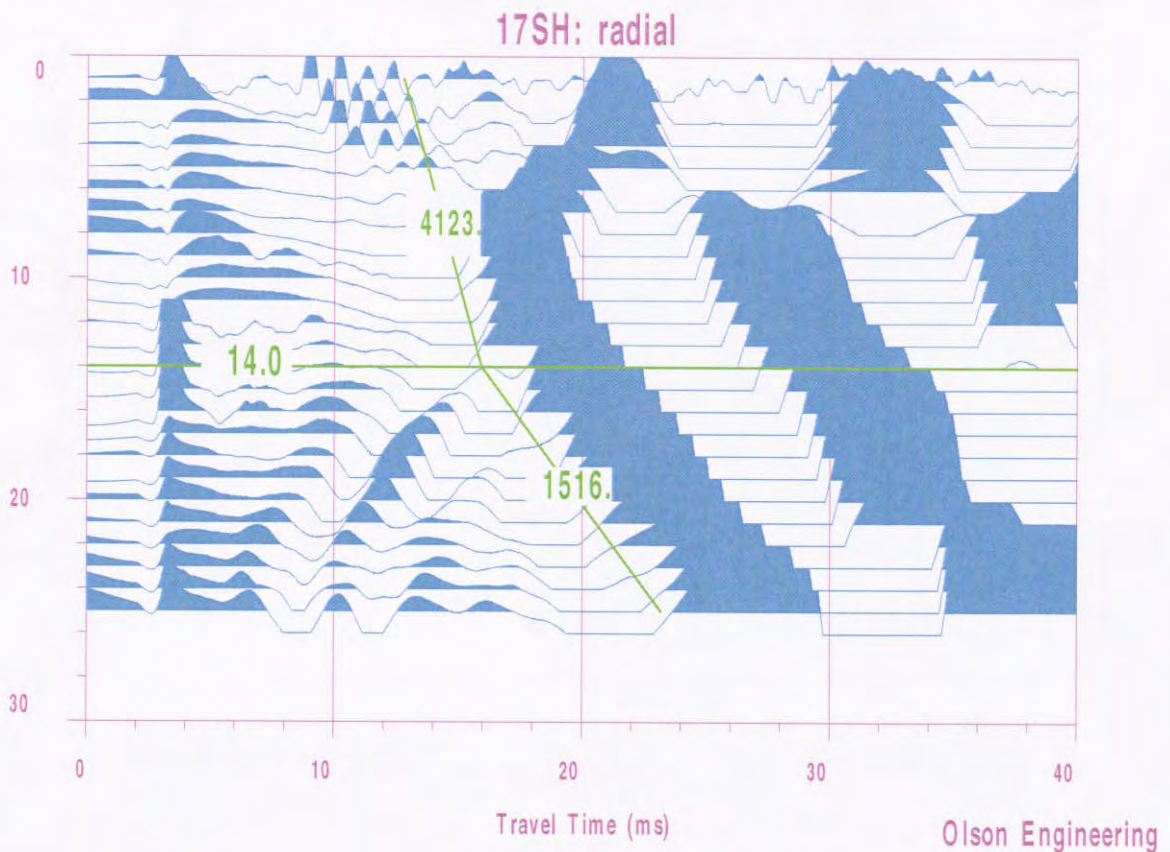


Figure A-2: 17th Street Site, South borehole, depth is referenced to top of casing

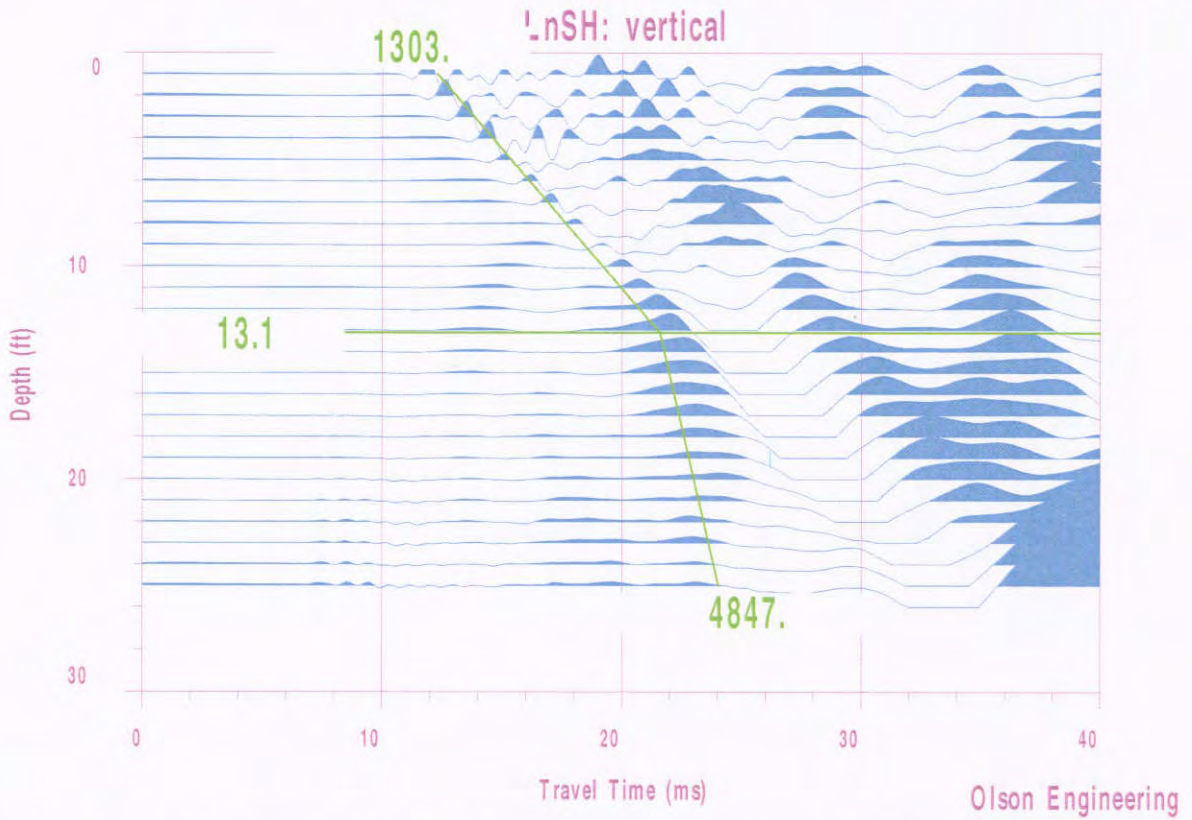


Figure A-3: London Avenue North site, North borehole, depth is referenced to top of casing

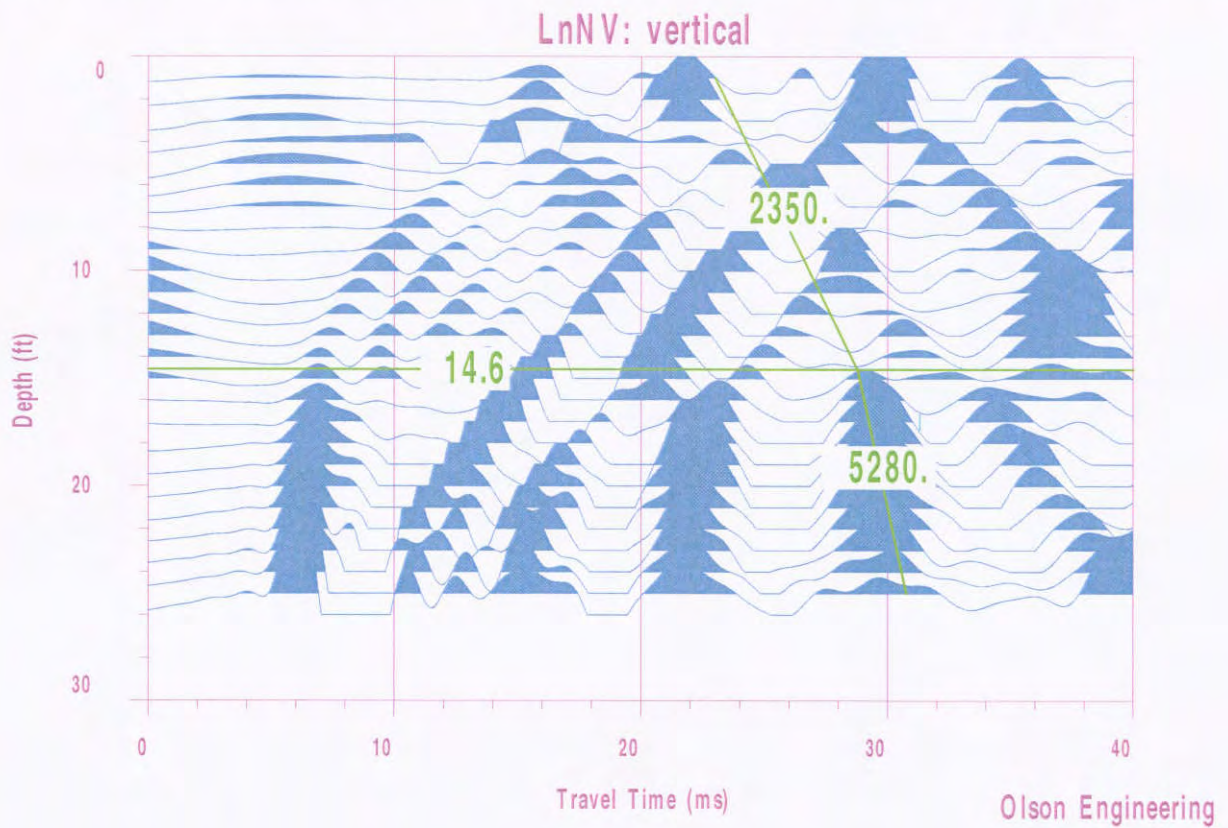


Figure A-4: London Avenue North site, South borehole, depth is referenced to top of casing K-237
 This is a preliminary report subject to revision; it does not contain final conclusions of the United States Army Corps of Engineers.

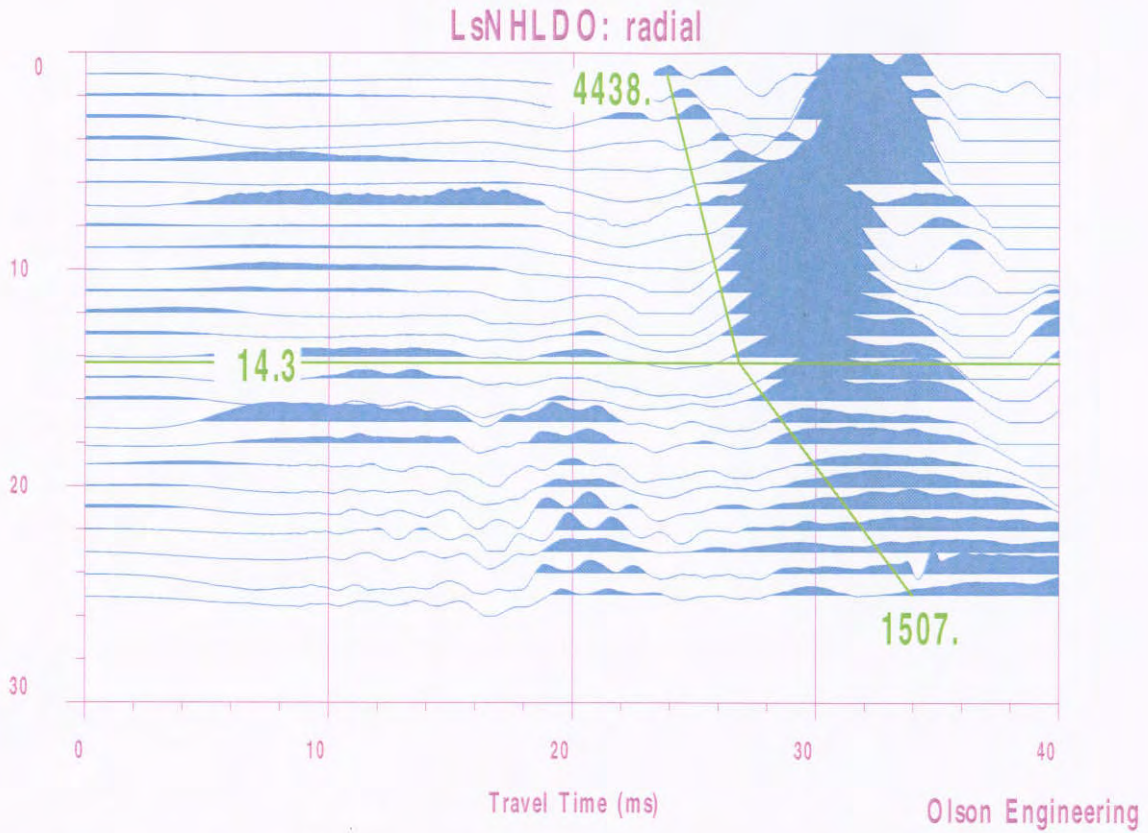


Figure A-5: London Avenue South site, North borehole, depth is referenced to top of casing

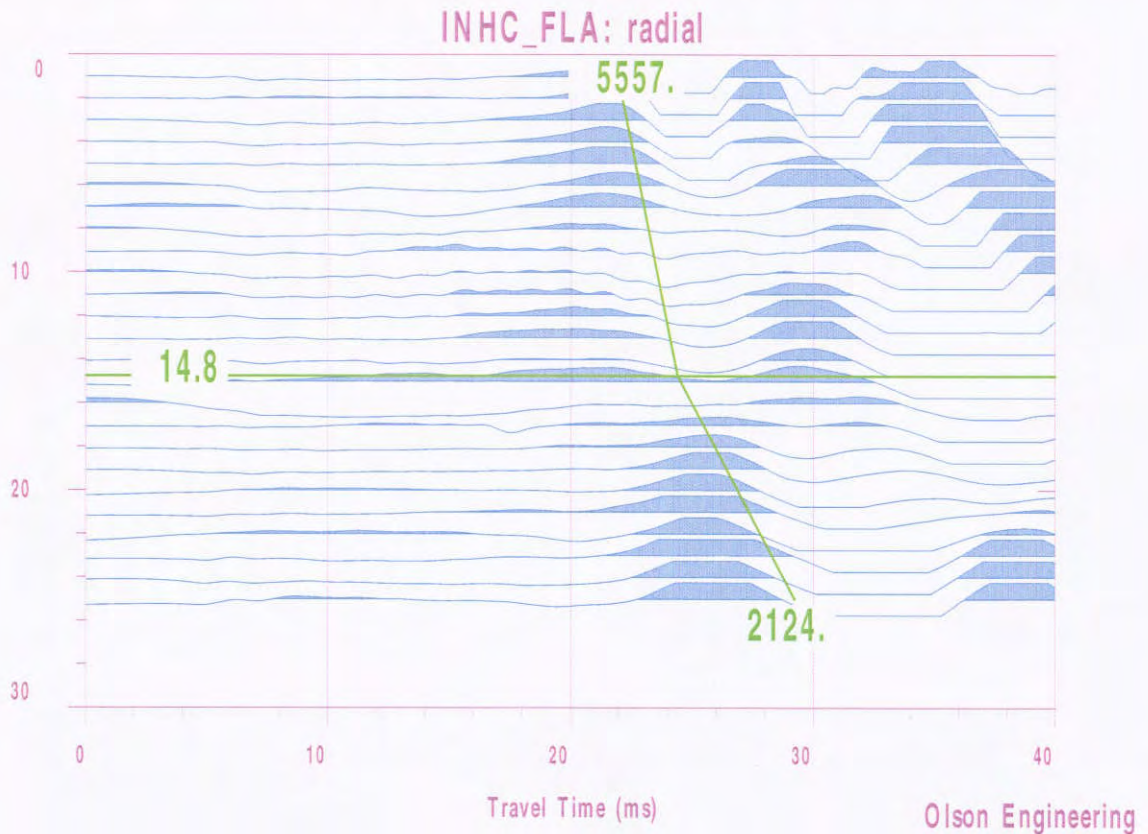


Figure A-6: IHNC Florida Street site, depth is referenced to top of casing

This is a preliminary report subject to revision; it does not contain final conclusions of the United States Army Corps of Engineers.

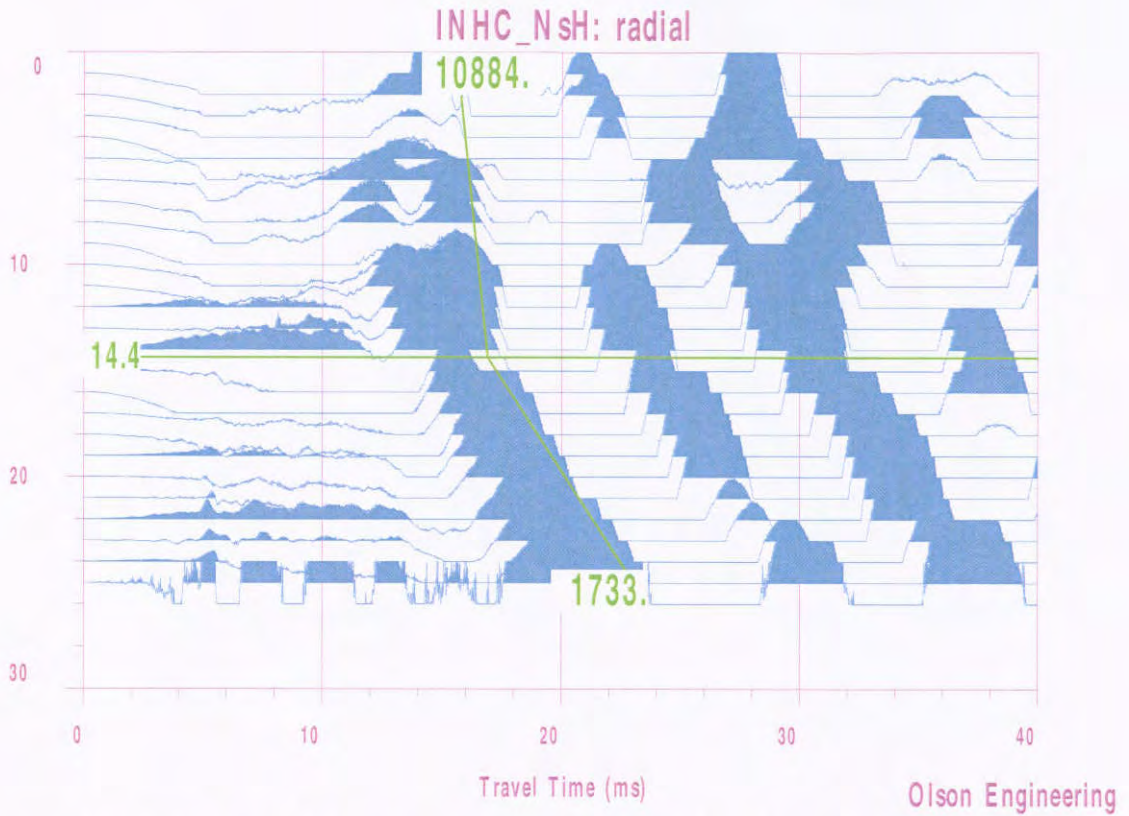


Figure A-7: IHNC South site, North borehole, depth is referenced to top of casing

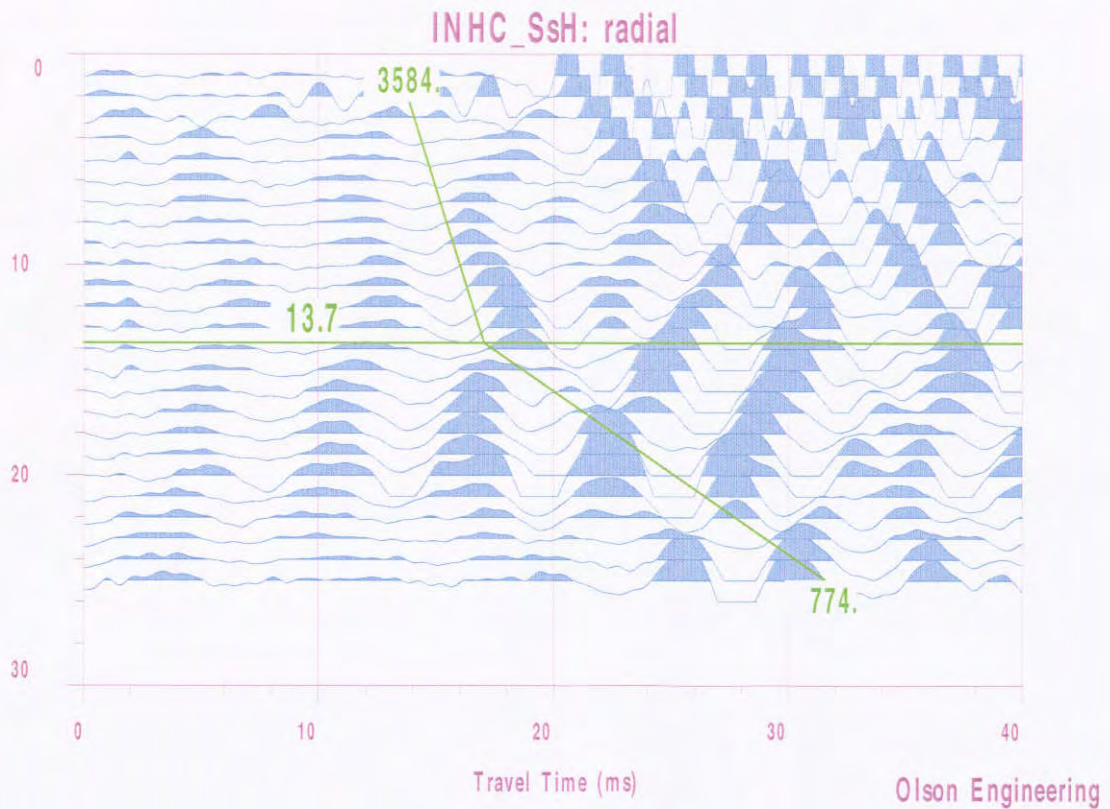


Figure A-8: IHNC South site, South borehole, depth is referenced to top of casing

This is a preliminary report subject to revision; it does not contain final conclusions of the United States Army Corps of Engineers.



**OLSON
ENGINEERING, Inc.**

**SPECIALIZING IN CONDITION EVALUATION OF THE
CIVIL STRUCTURE & INFRASTRUCTURE**



www.olsonengineering.com

January 9, 2006

U. S. Army Corp of Engineers
Engineering Research and Development Center
3909 Halls Ferry Rd.
Vicksburg, MS. 39180
Attn: Mr. Richard W. Haskins, ERDC-ITL-MS
Ofc: (601)634-2931
Fax: (601)634-2873
E-Mail: Richard.W.Haskins@erdc.usace.army.mil

Re: Addendum to Nondestructive Testing Investigation Report
Sheet Pile Lengths
New Orleans Levees
New Orleans, LA
Olson Engineering Job No. 1875

Dear Sirs:

This letter is being sent as an addendum to a report issued to the USACE by our office on December 5, 2005 (Olson Job No. 1875) which reported the results of an investigation conducted by our firm into the determination of the unknown length of steel sheet piles which were located beneath concrete walls and formed part of the levee structure at a number of locations in the New Orleans area. The levee sheet piles were tested with the Parallel Seismic (PS) method to determine their depths. The PS tests were conducted at the 17th Street, London Avenue, and the Inner Harbor Navigational Canal (IHNC) levees in 8 cased borehole locations at undamaged levee wall locations next to breaches.

The initially reported PS test results indicated the presence of piles under the concrete wall, and were interpreted by our firm to show that they extended to approximately 13-15 ft below the casing top for all of the sites tested. These sheet pile depths translated to elevations of approximately 10 feet below mean sea level (range of 9.3 to 11.8 feet below mean sea level).

It is our understanding that four sheet piles at the north end and 4 sheet piles at the south end of the 17th Street levee breach area have been pulled, and that our data interpretation of nearby PS results in north and south cased borings was shown to be incorrect. The actual embedded lengths were found to be approximately 17 feet below mean sea level (20-22 feet below the casing top elevation used in our investigation) with total sheet pile lengths of 23.5 ft.



This addendum to our initial report discusses our review of the initial analyses in light of the ground-truth findings for the pulled sheet pile. It also includes our recommendations for any future nondestructive test programs to determine the unknown sheet pile lengths.

Results of PS Data Review

Since our initial data interpretation is apparently incorrect for PS tests near the north and south ends of the 17th Street levee breach, we decided to re-analyze the data to try to determine why. We used the reported actual sheet pile tip elevations of about -17 ft below mean sea level and the 23.5 foot nominal excavated total pile lengths reported to us by Mr. Haskins of the USACE as a known quantity, and reviewed both the raw data as well as the processed data plots presented in our initial report for all sites tested. What we found was that the error was not due to problems with the actual test method, but rather due to a misinterpretation of the data on our part as discussed below.

17th Street Site PS Data Review

Figure 1 presents the data plot presented in our initial report for the north side location at the 17th Street site. As seen, our interpretation indicated a pile tip depth of about 14 feet, based on the typical "break" in the slope of the lower-frequency signal arrivals at that depth. For most foundations, this would indicate the tip depth quite well, and thus this break was selected as the indicated pile tip depth. However, as seen in both this plot in Fig. 1 and in Fig. 2, which is a re-processed plot of the same data set, there is also a clear set of faster signal arrivals apparent at an earlier time which start to appear at about 20-21 feet deep. These signals are apparently diffracting (reflecting up and transmitting down) from the tip of the sheet pile wall acting as a signal source. Data from the south side of the 17th Street site is presented in Fig. 3 (from the original report) and Fig. 4 (re-processed plot) and these figures also show the high-frequency energy emitted from the apparent sheet pile tip at 21 feet below top of casing. The 21 ft depth corresponds to a mean sea level elevation of about -17 ft for the sheet pile depths.

Our misinterpretation resulted at least partly from the fact that the sheet pile did not emit any significant energy from the side at shallower depths, but rather acted as a point source of energy from the tip. This type of response is unusual, but not unheard of as we have observed it in PS tests of steel H-piles below pilecaps with left-pointing "arrowheads" indicating the H-pile tips in front of the larger wave energy emitting from impacting footings/pilecaps/columns/walls of bridge substructure. The interpretation was also made more difficult in hindsight in that apparently due to the wall shape of the sheet piles, the normally expected arrowhead shape indicating a tip diffraction was bent back to near-vertical (vs. an H-pile with a full arrowhead shape). The interpretation was particularly complicated by there only being about 3 ft of data that could be obtained below the sheet pile tips due to the casing depth of 25 ft. Normally a casing depth of 10 to 15 ft below the expected pile tip depth is recommended for PS tests in order to obtain a clearer pile tip identification.

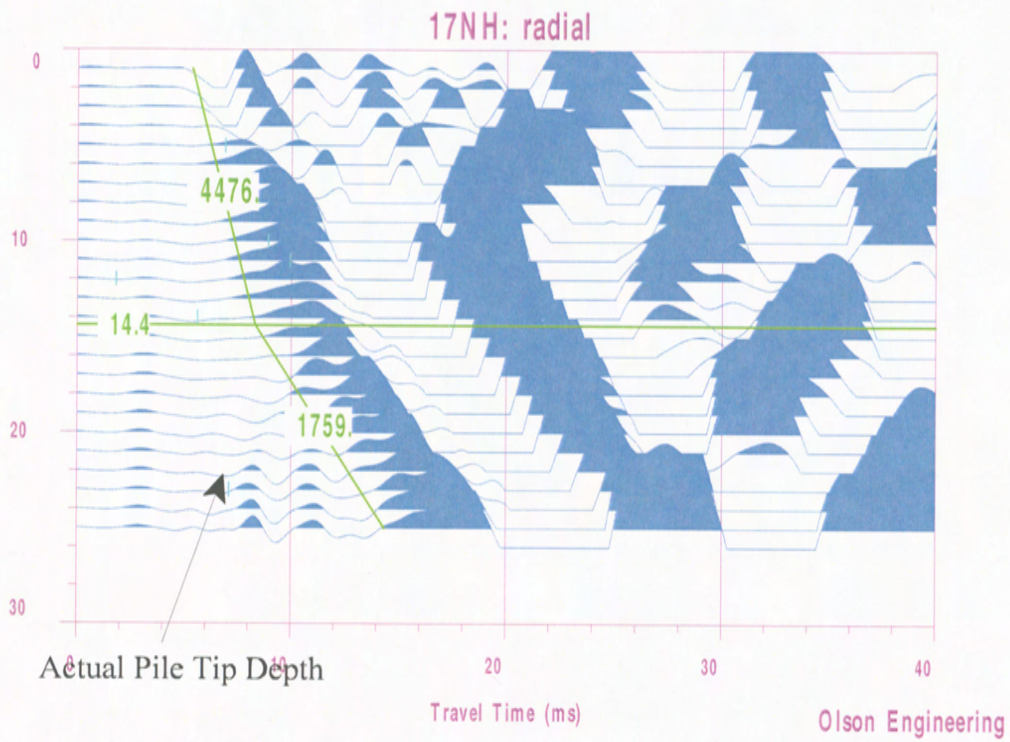


Figure 1 17th Street Levee North Site, Initial PS Data Interpretation

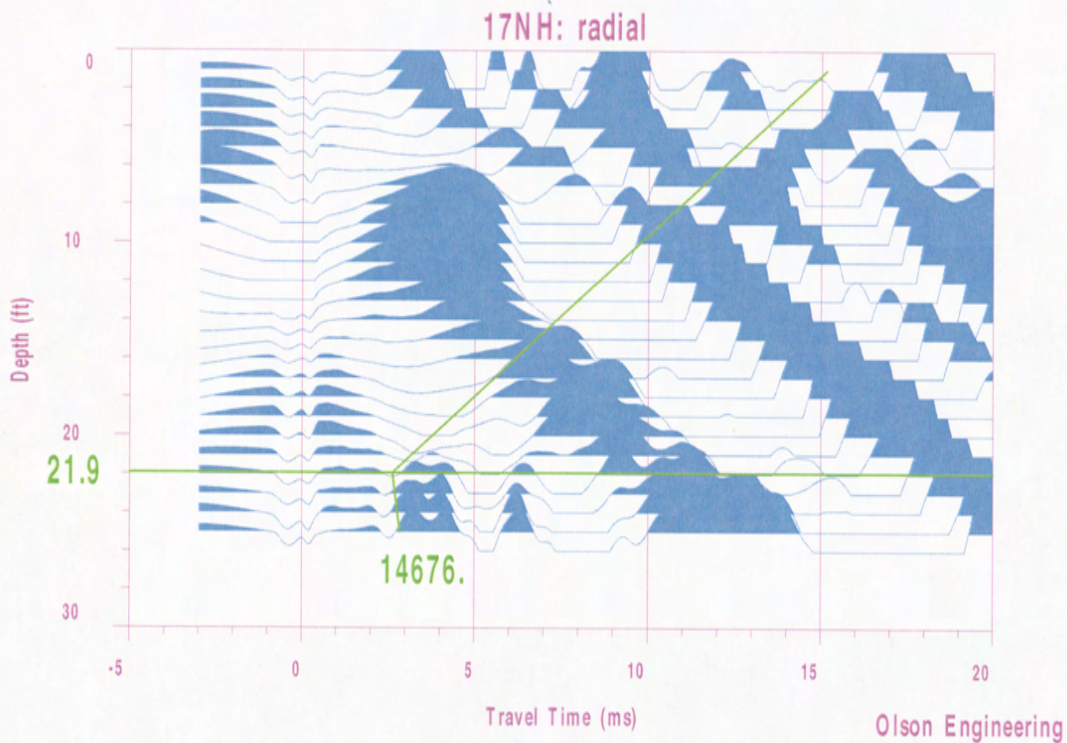


Figure 2 17th Street Levee North Site, Re-interpretation of PS Results

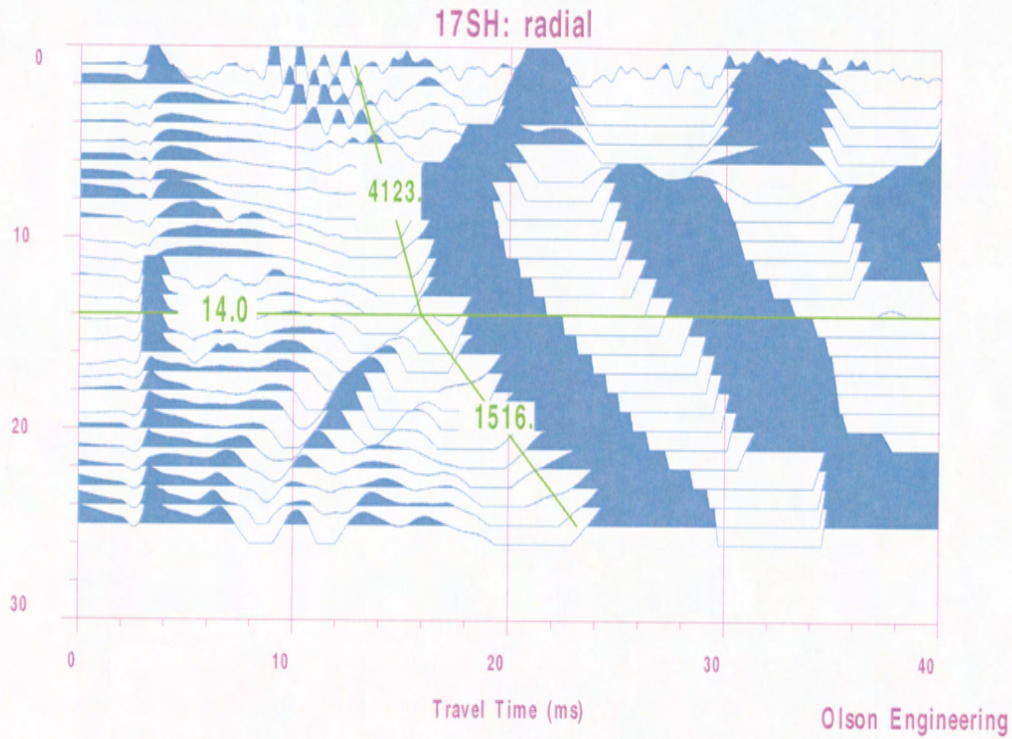


Figure 3 17th Street Levee South Site, Initial PS Data Interpretation

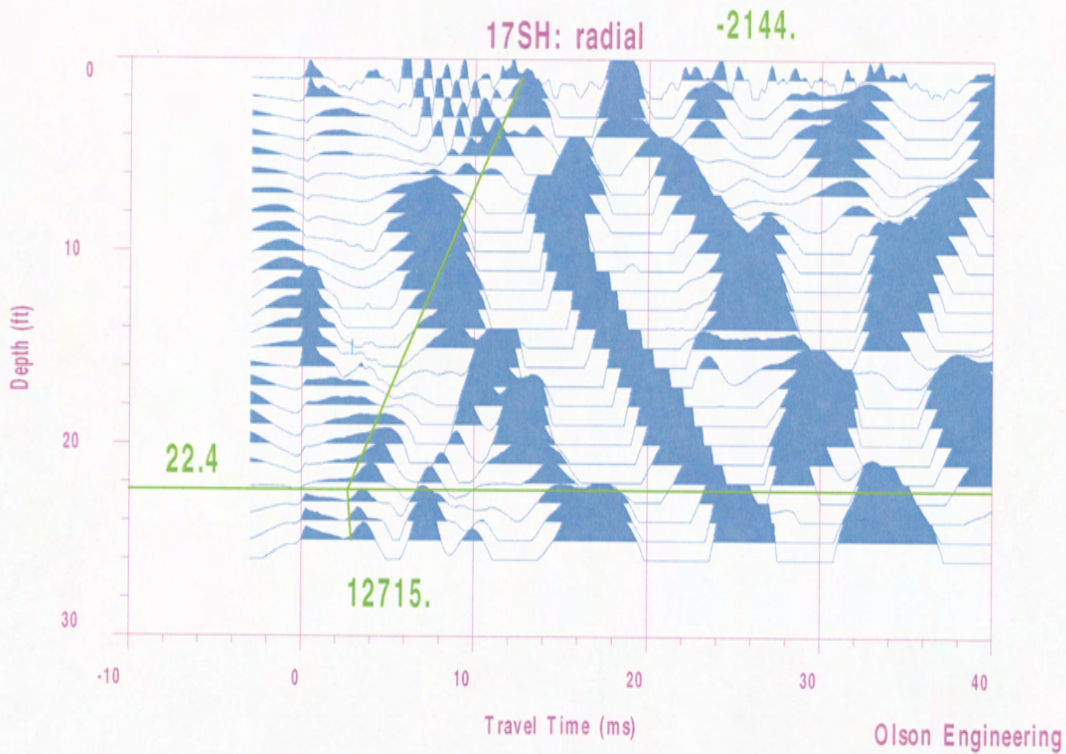


Figure 4 17th Street Levee South Site, Re-interpretation of PS Results

London Avenue North Break Data Review

The data collected from the London Ave. North site was reexamined to look for tip diffraction events similar to those seen for the 17th Street site data sets. Close examination of the data sets (Figs. A-3 and A-4 in our original report on this testing) show that there is a clear but vertical diffraction event for data at the South borehole, which was located at about 7 feet from the levee wall. The diffraction event in this figure, however, appears as a near-vertical line, with no clear "break" in the slope which would be indicative of a tip depth. It would appear likely that a break would have been seen if the casing went down the recommended 10-15 feet deeper than the expected pile tip depth, since there is a small possible indication of a break visible in the very bottom data trace for this location (at about 24 feet below casing top).

The data set from the North borehole shows a very weak set of possible diffraction events, with a similar shape as the south borehole. The diffraction events in the data from this borehole, however, are very weak. This is presumably due to the almost 18 ft horizontal separation between the borehole and the levee wall at this site. This large separation would attenuate the high-frequency diffraction energy, as well as decrease the resolution of the data that is seen.

London Avenue South Break Data Review

The data set from the South Break site borehole (Fig. A-5 in our original report) shows a very weak and distorted set of possible diffraction events, but with no clear slope change in the data indicative of a tip depth. Close examination of the data shows the first arrivals of the possible diffraction energy to be nearly vertical versus depth down to the last recorded record. Again, this is likely due to the limited depth of the casing in the borehole, which limited the test range to just a few feet deeper than the pile tip. In addition, this borehole was located 17.2 feet from the levee wall, which results in attenuated, distorted, low resolution diffraction energy from the pile tip.

IHNC Florida Street Break Data Review

The data set from the IHNC Florida Street Break site borehole (Fig. A-6 in our original report) shows no indication of tip diffraction energy. Note that this borehole was located about 21 feet from the levee wall, which is a distance greater than the expected pile tip depth. This large separation would be expected to greatly distort and attenuate any energy radiating from the pile tip. Thus, it is not unexpected that there is no visible tip diffraction energy in this data set.

IHNC South Break Data Review

The data set from the two tests conducted at the IHNC South Break site were presented in Figs. A-7 and A-8 in our original report. Figure A-7 is from the north borehole, which was located 9.5 feet from the levee wall. Figure A-8 is from the south borehole, which was located 21.1 feet from the levee wall. Examination of both data sets shows no clear indication of diffraction energy from the pile tip. This may be due to the distances between the boreholes and the wall, as well as possible separation between the sheet piles and the soil in the areas near the break.

Recommendations for Future Nondestructive Testing of Sheet Pile Lengths

The data presented in our original report does show the energy emitted by the sheet pile tips for most of the tests done in boreholes close to the levee walls, and can be made even clearer by re-processing the data from the 17th Street site to emphasize the higher frequency energy from the sheet piles as presented in Figs. 2 and 4 above. Based on this knowledge of how the PS test data behaves when testing these types of sheet piles in this environment, we have prepared these recommendations for any future NDT investigations of sheet pile lengths.

1. Drill Cased Borings Closer to Walls and Deeper. In our opinion, the PS method can be effectively used to measure unknown sheet pile depths with good confidence, as long as the boreholes are located and at least within 7 feet or less of the edge of the levee wall. Even closer borings will further improve the accuracy of the PS results. The borings should also be drilled and cased with PVC casings to at least 10 and preferably 15 ft below the expected pile tip depths.
2. Impact Sheet Pile Sides Directly. The PS data quality would be further enhanced by impacting the sheet piles at their exposed top just below the concrete wall directly. This will input significantly more energy in to the sheet pile and less into the concrete wall that was impacted in the initial investigation. This could be done with shallow excavations with a small backhoe in advance of the NDT. Alternatively, we have found that vertical impacts on the wall top or on the chamfer produce clearer diffraction energy traces than do horizontal impacts as discussed in our Report No. 2 for the re-test results.
3. Confirmation with complimentary NDT Methods. Magnetic metal detectors for boreholes may also be able to detect the sheet pile presence if borings are cased with plastic and able to be drilled close enough for this approach to be effective. The practicality of this can be further explored, if desired. We have already gathered some information on available equipment.

CLOSURE

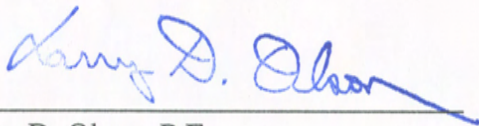
The field NDT investigation was performed in accordance with generally accepted testing procedures. If there are any questions, or further information is required, please do not hesitate to call. If any additional information is developed pertinent to this study, please contact our office.

Respectfully submitted,

OLSON ENGINEERING, INC.



Dennis A. Sack
Associate Engineer



Larry D. Olson, P.E.
Principal Engineer

(1 copy e-mailed and 2 copies mailed)

e-mail cc: Mr. Paul F. Mlakar (Paul.F.Mlakar@erdc.usace.army.mil)